Doctoral Dissertation

A Study of Flame Stabilization in Meso-scale Tube Combustors with Heat Recirculation

March, 2016

Fudhail Bin Abdul Munir

Graduate School of Science and Engineering
Yamaguchi University

TABLE OF CONTENTS

TITLE

PAGE

ABSTRACT

Dwindling energy resources and strong demand for better power sources as compared to conventional batteries have sparked research interest in micro power generation. The invention of state-of-the-art electronic devices requires more energy capacity, shorter charging period and light in weight, characteristics of which batteries lack. Meso and micro combustors can be considered as the most important component in micro power generation. However, stabilizing a flame inside a micro combustor poses a great challenge to researchers. This difficulty is mainly related to the substantial heat losses due to large surface area to volume ratio. This research focuses mainly on the determining factors that affect the flame stabilization in meso-scale tube cylindrical tube combustors with stainless steel wire mesh. There are three main stages involves in this research. At the first stage, the effect of pre-heating of the unburned gas on the flame stabilization is experimentally examined. The lengths of unburned gas (L_u) and burned gas region (L_b) were set to be one of the experimental variables. A part of the tube was heated by an external source to simulate the heat recirculation from the burned gas to the unburned gas. The flame stabilization limits were obtained. Flame stabilization limits in this case is defined as limits in which the flame stabilizes near the wire mesh of the tube combustor. Beyond these limits, two phenomena exist, namely blowout and extinction. Blowout occurs when the flame propagates towards the tube end with an increase of the cross-sectional flow velocity (U). Meanwhile, extinction is a condition where the flame ceases to exist with the decrease of U. The results show that the flame blowout limits especially in the lean and rich region can be greatly improved with the elevation of the ambient air temperature. Nevertheless, there is only a modest change in the extinction limits. In the second stage of the research, the effect of combustor wall thermal conductivity *(k)* on the flame stabilization limits were numerically and experimentally examined. An axisymmetric two-dimensional (2-D) steady-state numerical simulation of propane-air combustion in meso-scale cylindrical tube combustors with concentric rings was conducted. The concentric rings are placed between the unburned and burned gas region. The main function of these rings is to act as a flame holder where a stable flame can be easily established. The wall thermal conductivity in the unburned (k_u) and burned gas region *(k_b)* is varied from 1 W/m/K to 1000 W/m/K and the results in terms of gas, inner wall, outer wall temperature

distributions, the blowout limits and combustion efficiency are analyzed and presented. Experiments with tube combustors that are made of different materials were also performed to compare the trend pattern obtained from numerical results. The main conclusion that can be derived from the second stage of research work is higher wall thermal conductivity in the burned gas region contributes to better flame stabilization limits. Meanwhile, the utilization of materials with wall thermal conductivity higher than 100 W/m/K has insignificant effect on the flame stability. The third stage of research involves the investigation of the effect of exhaust gas recirculation on the flame stabilization. Experiments were conducted where combustors made of quartz and brass tube were inserted into a quartz glass tube and flame stabilization limits were established. The results suggest that the utilization of exhaust gas to improve the flame stabilization limits is only effective for the quartz tube combustor. A three-dimensional (3-D) numerical model was developed to investigate vital factors that might affect the experimental results. The effective role of wire mesh in distributing heat from the burned to the unburned gas region was demonstrated by using the developed 3-D model. The results from the experiments and numerical simulations are utilized to propose a combustor that can be used for both gaseous and liquid fuels.

LIST OF FIGURES

CHAPTER ONE

CHAPTER TWO

CHAPTER THREE

CHAPTER FOUR

CHAPTER FIVE

LIST OF TABLES

LIST OF ABBREVIATIONS

1-D	One-dimensional
2-D	Two-dimensional
3-D	Three-dimensional
CFD	Computational Fluid Dynamics
TPV	micro thermo-photovoltaic
d	Inner diameter of combustor
Da_h	Damkohler number
E_a	Activation energy
F_x	External force in x-direction
F_r	External force in r-direction
h	Convective heat transfer coefficient
k	Wall thermal conductivity
k_b	Wall thermal conductivity in the burned gas region
k_u	Wall thermal conductivity in the unburned gas region
L	Heater length
L_{in}	Insertion length
L_b	Length of the burned gas region
L_u	Length of the unburned gas region
$\dot{m}$	Mass flow rate
mm	Millimeter
p	Pressure

q''	Heat flux
R	Gas constant
T	Temperature
T_{amb}	Ambient temperature
T_h	Setting temperature of heater
T_w	Temperature of wall combustor
U	Flow velocity
u_x	Flow velocity in x-direction
u_r	Flow velocity in r-direction
μ	Fluid viscosity
ϕ	Equivalence ratio
ρ	Density
ε	External emissivity
σ	Stefan-Boltzmann constant
$\tau_{residence}$	Residence time
$\tau_{chemical}$	Chemical time scale

CHAPTER ONE

Introduction

1.1 Overview

Dwindling energy resources and strong demand for better power sources as compared to conventional batteries have sparked research interest in micro power generation [1]. The invention of state of the art electronics devices requires more energy capacity, shorter charging period and lightweight, characteristics which batteries lack. Therefore, in recent years, micro power generation systems have been seen as potential alternatives to batteries owing to obvious advantages that it possesses. One of the advantages is the high-energy storage per unit mass and power generation per unit volume. As shown in Fig.1.1, the energy density of hydrocarbon fuels is approximately 100 times larger than the lithium ion batteries. Even with only 10% of efficiency, the total energy harvested is still by far outnumbering the conventional batteries. In addition, the use of the hydrocarbons fuel as the source substantially reduces the operational cost and improves the voltage stability [2].

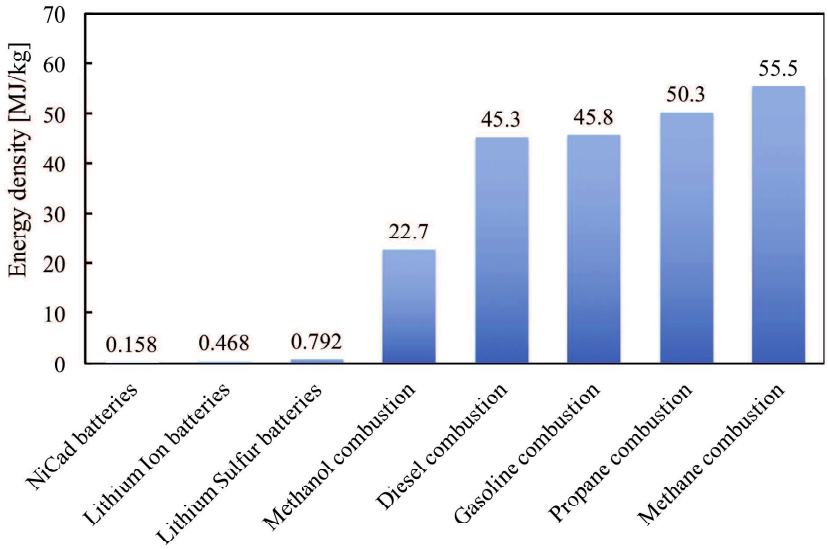

Figure 1.1 Energy density of conventional batteries and hydrocarbons fuels [3]

The process of developing feasible micro power generators is indeed a formidable task since it involves complex flow, transport and thermodynamics phenomena [4]. The

invention of micro electro-mechanical system (MEMS) has become the trigger factor to the development of more practical micro power generation systems. In an MEMS system, the conventional liquid fuels like gasoline or diesel cannot be used due to the instability of the fuel properties [5]. Diesel or gasoline tends to degrade if they are kept for a long period of time. Therefore, liquefied gaseous hydrocarbons such as propane and butane which are suitable for long term storage is the most preferred fuel in MEMS [5]

Meanwhile, significant efforts have been made to develop micro engines, which have the similar mechanism as in the conventional internal combustion engines. Research teams from Massachusetts Institute of Technology (MIT) have developed a silicone gas-turbine engine that utilizes hydrogen as the fuel source [6]. The schematic of the gas turbine engine is shown in Fig.1.2.

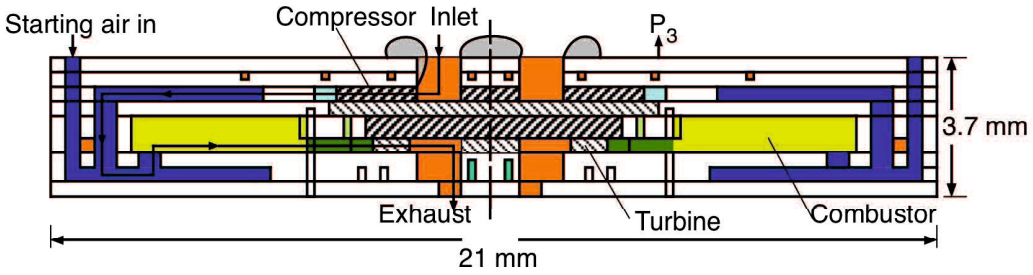

Figure 1.2 Schematic diagram of the MIT micro gas turbine [6]

A rotary meso-scale engine with 78 mm^3 has been successfully developed and tested by Kelvin et al [7]. The engine uses hydrogen mixture as the fuel source as shown in Fig.1.3(a). It has the capacity to generate 3 W of power [7]. The same research group has also developed a rotary engine that is able to combust liquid methanol-nitro methane fuel. Nonetheless, the reduction of the scale has led to severe heat loss and friction sealing problem. Moreover, the complexity of the geometries makes them difficult to be fabricated [8].

The alternative to micro engines is thermoelectric generators that can be considered as more technologically feasible. The development of micro thermo-photovoltaic (TPV) system has been on the rise over the past decades. Unlike the conventional internal combustion engines, the basic principle of micro TPV system is direct conversion of thermal energy into electricity without using any moving parts [9]. The elimination of these moving parts makes TPV system quieter and cleaner source for electrical power than the conventional system. Apart from that, TPV systems are also onsidered as simple

and easy to be fabricated. All these listed advantages makes TPV systems the preferred choice against conventional batteries [10].

(a) MN30 engine with gaseous fuel (b) MN50 with liquid fuel

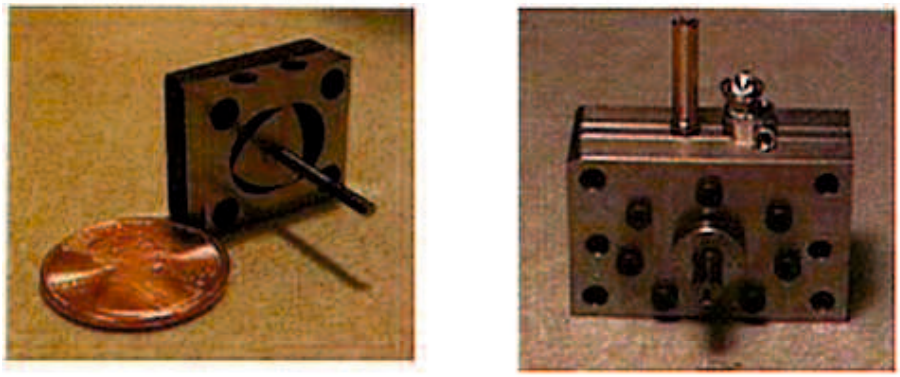

Figure 1.3 Meso-scale rotary engines [7]

The most important component in a TPV system is of course the combustor. In 2002, Weinberg et al. [11] have proposed a system where electricity is generated from the combustion in a heat recirculating combustor. This system consists of a combustor and converter. The converter comprises a large number of flat annular washers and the alternate *n*-type and *p*-type thermoelectric materials are connected in series. Due to limitation of the thermoelectric materials, the allowable maximum flame temperature is 1500 K.

There are four important sections in a TPV system. These sections are the combustor, emitter, filter and the low band gap photovoltaic array [12]. When the emitter is heated up to a certain temperature, it emits photons. The emission of photons of which impinges on the photovoltaic cells causes free electrons to be generated. As a result, electricity is produced. The schematic of a TPV system is shown in Fig.1.4. Generally, a TPV device is applied in military applications where portable electronics for soldiers require minimal weight and charging time [13].

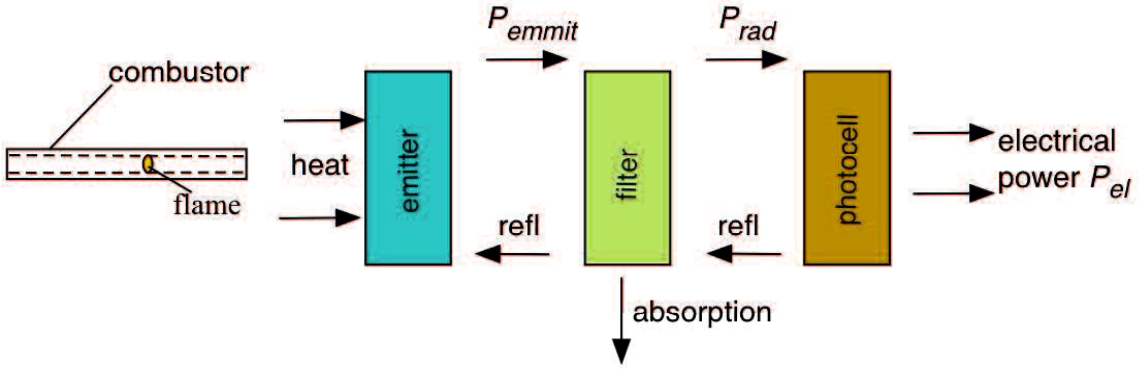

Figure 1.4 Schematic of a micro-thermo photovoltaic unit [12]

As seen in Fig.1.4, the heat energy produced from the combustor is converted into electrical energy. This heat energy can also be converted into various forms of useful energies as illustrated in Fig.1.5. It is practically important for the combustor to generate a high and uniform temperature along the wall [14]. A cylindrical tube combustor is favorable since the coupling with different parts in the system, especially the emitter, can be easily performed [15].

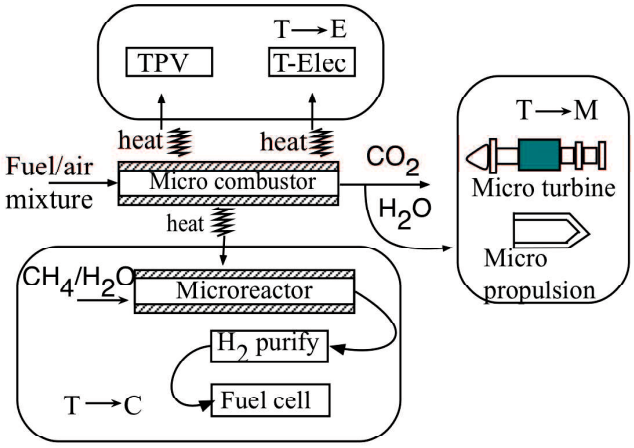

Figure 1.5 Utilization of micro combustor [3]

1.2 Research Background

The ability of a given fuel to be combusted in narrow channels is at first, assumed to be impossible. However, the recent progress in micro power generation has shown that combustion within a confined space, even in sub-millimeter scale is achievable. Despite this positive advancement, there are fundamental issues that need to be addressed and solved. There are many factors that influence micro scale combustion, which generally can be divided into physical and chemical processes. The examples of

these factors are convection, radiation, gas-phase and surface reactions, molecular transport, thermal and mass diffusion [16]. There are several time and length scales involved during combustion process in narrow channel combustors. The length scale is defined as the characteristic size of combustor inner diameter and combustor structure scale [17].

Generally, the difficulty to sustain combustion in micro-scale devices is related to the substantial heat losses due to large surface area to volume ratio and physical time available for the combustion to occur. For any combustion process to take place, the residence time should be larger than the combustion time [18]. However, in micro-scale combustors, the length scale is tremendously reduced. Consequently, the flow becomes laminar due to the decrease of Reynolds number [19]. This laminar flow causes the diffusion time to increase, which lowers the residence time. In such condition, combustion might cease to exist.

The behavior of fluids in micro scale devices can be assumed as the same as in macro scale. However, a few micro combustion features are distinctively different from macro scale combustion. Maruta et al. [20] defines the micro-scale combustion as a condition where combustion occurs in a space that has the characteristic length scales approaching to the quenching distance. On the other hand, combustion that occurs in a space with the characteristic length larger than 1 mm, but features the same features as micro-scale combustion is defined as meso-scale combustion.

Strong thermal and chemical coupling between the flame and combustor structure is also exhibited in micro combustor. In such combustor, the flame quenching is greatly depending on the flame-wall thermal coupling [21]. Therefore, it is essentially important to fully understand the underlying factors that contribute to the flame stabilization in micro combustors so that high-energy conversion can be achieved. Examples of these factors are thermal heat loss, excess enthalpy, wall-flame thermal and chemical coupling, fuel-air mixing, liquid vaporization, flow field, burning rate and flame temperature [22]. Since the combustion of hydrocarbon fuels in micro scale devices is not as efficient as in larger conventional devices, it is also vital to address the issue of fractional production of unburned species and high amount of carbon monoxide (CO). Overall, it is vital for an efficient micro combustor to have features as follows [23];

i. Wide flame stability limits

ii. Versatility in terms of combustion modes for different use of application
iii. Considerably good combustion efficiency
iv. Minimum hazardous gas emission
v. Simple in geometry for easier coupling with energy conversion module

A single channel combustor (SC) can also be considered as a heat recirculation combustor since the heat from the burned gas region is distributed to the unburned gas region via the combustor wall.

1.3 Problem Statement

Combustion in meso and micro-scale channels is possible. However, stabilizing flame in such narrow channel combustors is relatively difficult due to large heat losses. Thus, a proper thermal management is required. Many approaches can be applied to enhance the flame stability. The use of flame holders, catalysts and modification of combustor geometry are the examples of these approaches. Depositing catalysts on micro combustors involves complex and costly process. One of the effective but less complex techniques to improve the flame stabilization limits is by pre-heating the incoming reactants. The increase of reactants temperature prior to combustion leads to the elevation of flame burning velocity. Consequently, a larger flame blowout limit can be achieved. In general, there are two types of pre-heating methods, namely direct and indirect method. A direct method is a condition where the pre-heating is performed by using high combustor wall thermal conductivity. On the other hand, using the heat from the exhaust gas to pre-heat the incoming reactants is the example of indirect pre-heating method. Swiss-roll combustor is one of the micro combustors that utilizes the heat from the exhaust gas to increase the reactants temperature. Nevertheless, the geometry of such a combustor is relatively complicated, which makes it difficult to be numerically and experimentally investigated. Hence, a combustor with simpler in design is preferred. It is desirable that both liquid and gaseous hydrocarbon fuels can be used in the proposed combustor.

1.4 Objectives of the research

The main purpose of this study is to propose a meso-scale non-catalytic cylindrical tube combustor that utilizes heat recirculation mechanism. Both liquid and gaseous fuels can be used. The following approaches are conducted:

i. To initially fabricate a meso-scale cylindrical tube combustor with a flame holder. This combustor is then used as a reference model for the next numerical and experimental work.
ii. To experimentally investigate the effect of ambient air temperature on the flame stabilization.
iii. To numerically and experimentally examine the effect of wall thermal conductivity of combustor on the flame stabilization limits. Numerical simulations are also utilized to provide the detailed insight and basic understanding of the problem.
iv. To investigate the effect of exhaust gas heat recirculation on the flame stability. Experiments with tube combustors made of different materials are conducted. Numerical simulations are also employed to examine the important parameters that contribute to the changes of experimental results.
v. To propose a conceptual design of combustor that utilizes heat recirculation mechanism based on inputs derived from the numerical simulations and experiments.

CHAPTER TWO

Literature Review

This chapter summarizes the previous well-known experimental and numerical works that have been performed in the field of micro power generation. Majority of the work are related to the use of hydrocarbon fuels as the fuel source. It is important to stabilize the flame inside a micro combustor. The various methods and mechanisms of stabilizing flame in a narrow channel combustor are presented in this chapter. In addition, important terminologies in the field of micro combustion are also explained.

2.1 Flame stabilization in micro combustors

Even though combustion in micro combustors is possible, stabilizing the flame inside such narrow channel is a challenging task. Generally, in a micro combustor, the flame can be stabilized within certain limits. These limit are named as the flammability limits. The definition of flammability limits is given as a range of mixture strengths of which a particular flame propagates within these limits [24]. Any fuel-air mixture has a certain propagation speed. When the fuel-air mixture is ignited, the flame propagates towards the fresh unburned mixture with a velocity approximately near the propagation speed. For micro power applications, stationary or also known as stable flame is preferred. In theory, a flame can be made stable by adjusting the mean flow velocity of the unburned mixture to match the flame propagation speed. However, in practice, it is difficult to stabilize flame in narrow channel combustors. This difficulty is mainly due to the complexity of interaction between the combustor wall and the flame. At the gas-wall interface, a highly intensified heat loss from the combustor wall and radical destruction occurs [25].

To stabilize the flame in micro combustors, various methods have been introduced. Generally, a proper thermal management is essentially required to overcome the flame quenching. The utilization of heat recirculation mechanism can significantly enhance the flame stabilization limits [26-28]. In these types of combustors, the excess enthalpy from the combusted products is utilized to pre-heat the fuel and air mixtures. Examples of these combustors are shown in Fig.2.1. Since the flow in micro combustor is

categorized as laminar, the mixing process of fuel and air is relatively slow. As such, the mixing process is performed by the molecular diffusion and chaotic advection [29]. To improve the mixing process that can possibly enhance flame stabilization, a mixer can be introduced [30]. A static mixer improves the molecular diffusion by increasing the surface area that is in contact with the two incoming fluids [31].

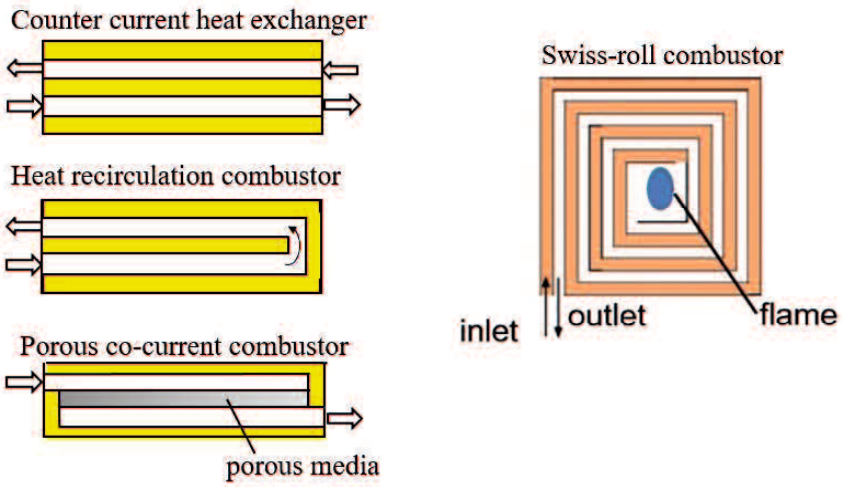

Figure 2.1 Various geometries of heat recirculation micro combustors [3]

Meanwhile, through the modification of laminar flow pattern inside the micro combustor, the chaotic mixing can be enhanced. One of the ways to alter the flow pattern is by having obstacles in the combustor. For instance, a bluff body can be put in the middle of the combustor [32]. Apart from that, the irregularity of the combustor wall can also improve the chaotic mixing. A combustor with backward-facing step can significantly improve the mixing of the fuel mixture and prolonge the residence time, which subsequently increases the flame stabilization limits [33].

The utilization of catalysts in micro combustors can also improve the flame stabilization limits through enhanced mass transfer [34]. In a catalytic combustor, combustion of reactants generates significant lower flame temperature than non-catalytic combustors. This low combustion temperature leads to the reduction of thermal stress related problems [34]. Catalytic materials consist of three major components, which are the catalyst, support and substrate. Metals with specific compositions such as Pt, Pd and Rh are the most widely used in catalytic combustion. There are many techniques to deposit catalysts in micro burners. The use of catalytic wires in micro combustors is probably the easiest way to introduce catalysts in combustors [35]. A thin-

film coated with catalyst can also be implanted in a micro combustor as presented in Fig.2.2. Nevertheless, there are a few drawbacks of using catalysts in micro combustors. Firstly, the interaction between the heterogeneous and homogeneous combustion is very complex [36]. As a result, conducting experiments can be difficult since there could be many variables to be controlled. Apart from that catalysts deposition is relatively expensive [3] and the problem of storing hydrogen gas, which is the main fuel source for catalytic combustion makes catalytic micro combustors relatively impractical.

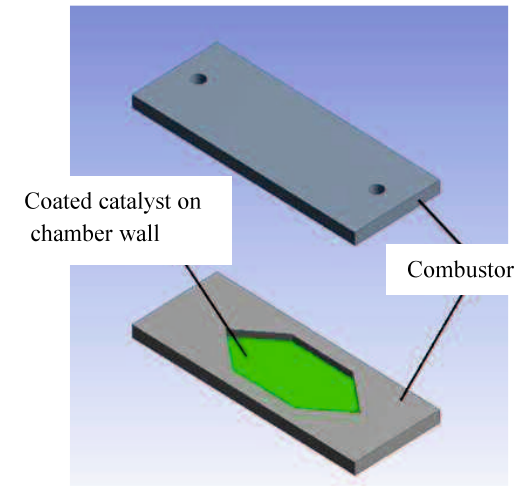

Figure 2.2 Schematics of micro-catalytic combustor with thin-film coated

2.2 Flame quenching

One of the major challenges in designing a reliable micro combustor is the phenomenon of incomplete combustion due to the flame quenching [37]. The classical definition of flame quenching is a condition where flame extinguishes upon entering a small channel. There are two types of mechanisms, namely thermal and radical quenching that cause flame quenching. The thermal quenching occurs when the heat generated by the combustion process is not sustainable due to heat losses to the ambient. In micro scale combustors, heat losses is not only due to the radiation, but it is largely contributed by the convection and conduction heat losses [1]. Meanwhile, radical quenching occurs when radicals from the flame are diffused to the walls, resulting to radical species depletion [38]. The radical recombination leads to the loss of active combustion carriers that eventually results to a flame quenching.

The critical distance of a channel in which a flame extinguishes is defined as the quenching distance. Both radical and thermal quenching play an important role in determining this distance. In general, this quenching distance depends on the reaction rate, temperature, species and radical concentration. The importance of knowing the quenching distance is for mainly for designing a fire-resistant device or system. To experimentally determine the quenching distance, a visual observation on a particular flame at the end of a circular tube is conducted. As long as the stable flame does not flashback to the upstream of the circular tube when the reactant is disconnected, the diameter of the tube is considered larger than the quenching distance.

The effect of thermal and radical quenching on flame propagation is dominant in meso and micro-scale combustion [39, 40]. In order to minimize or eliminate quenching problem, selection of proper operating conditions and optimization of combustor design are required [41]. Miesse and co-workers [42] have performed outstanding experimental works to show the possibility of combustion of gaseous hydrocarbon fuels in their designed micro scale combustor, which is shown in Fig.2.3. The results show that the combustion of methane and propane-air mixture is achievable even in tubes with 0.75 mm diameter. Combustion is made possible by minimizing heat losses to the ambient. Heat losses is reduced by insulating the combustor wall. In the meantime, the use of material that is susceptible to radical quenching as the combustor wall makes the combustion sustainable.

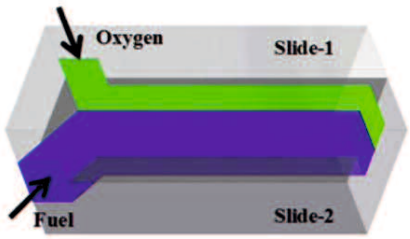

Figure 2.3 Schematic diagram of the designed combustor by Miesse et al. [42]

2.3 Residence and chemical reaction time

Residence time can be defined as the physical time available for the reactants to combust. A combustor residence time is given by the formula below;

$$\tau_{residence} = \frac{volume}{volume\ flow\ rate} = \frac{VP}{\dot{m}RT} \tag{2-1}$$

while the chemical time reaction can be approximated as follows [24];

$$\tau_{chemical\ reaction} = \frac{[fuel]_o}{A[fuel]^o[O_2]^b e^{\frac{-E_a}{RT_o}}} \quad (2\text{-}2)$$

From the above equations, it is known that the residence time has an indirect relationship with the mass flow rate. On the other hand, chemical reaction time depends on the fuel type, temperature and pressure of the mixture. In order to sustain combustion in any combustors, residence time should be larger than chemical reaction time [43]. A specific term, named as Damkohler number (Da_h), quantify this time limitation. Da_h is defined as the ratio between the residence time to the characteristic chemical reaction time.

$$Da_h = \frac{\tau_{residence}}{\tau_{chemical}} \quad (2\text{-}3)$$

The value of Da_h should be greater than one to ensure combustion in micro combustor [44]. The increase of residence time by enlarging the volume of combustion chamber is not an option in micro combustion. Thus, the only way to elevate the residence time in micro combustors is by reducing the mass flow rate. Nevertheless, the reduction of flow rate can significantly decrease the power density for energy conversion. Considering all these constraints, the best possible way to achieve Da_h that is greater than one is by reducing the chemical reaction time. To decrease the chemical reaction time, high combustion temperature is required [45]. However, the greatest limitation of having high temperature combustion is the ability of combustor material to withstand high flame temperature.

2.4 Methods of flame stabilization for micro combustors

2.4.1 Excess enthalpy combustors

Stable flame in narrow channel combustors can be achieved by recirculating the heat produced from the combusted products to the incoming fuel mixture. In conventional combustor devices like the internal combustion engine, a portion of the burned product gases is re-circulated and injected into the fuel-air mixture to reduce the amount of oxides of nitrogen (NO_X) [24].

On the other hand, in micro combustion applications, the purpose of heat recirculation is to minimize heat loss and to expand the flame stabilization limits. This heat recirculation concept was first proposed by Weinberg in 1971 [46]. The schematic diagram of the combustor is shown in Fig.2.4. The enthalpy from the hot burned gas is utilized to pre-heat the incoming fuel and air mixtures, which results to the enhancement of combustion reaction.

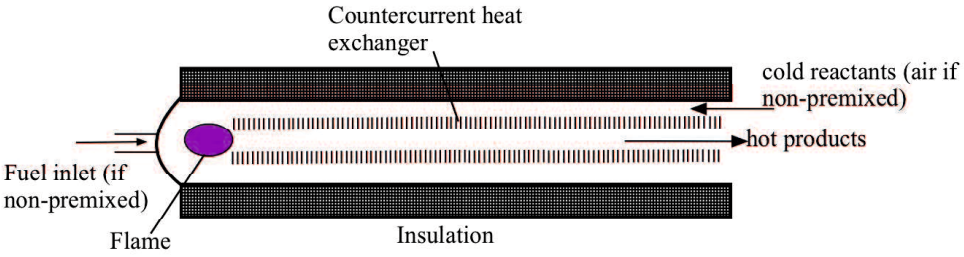

Figure 2.4 Schematic of a heat recirculation burner system [11]

This mechanism of flame stabilization is also called as excess enthalpy principle [47]. Generally, in an excess enthalpy micro combustor, the flow of the reactants and combustion products occurs in the adjacent channel and in an opposite direction. This condition causes the unburned mixture being preheated by the high-temperature exhaust gas. Consequently, the total enthalpy is greatly increased [48].

There are two types of pre-heating methods [49]. Direct method is a condition where the heat is transferred through conduction and radiation from the burned gas to the unburned gas region. This direct method is normally applied in a single channel (SC) micro combustor. In such combustor, the heat from the burned gas region is axially transferred to the unburned gas region through the solid structure, resulting to better flame stabilization limits. On the other hand, the burned gas can be reversed to pre-heat the unburned reactants coming into the combustor inlet. This method is named as indirect pre-heating and mainly utilized in counter-current heat recirculation combustors.

Swiss-roll (SR) combustor is probably the most popular configuration for combustors with heat recirculation. This type of combustor employs indirect pre-heating mechanism. A typical diagram of SR combustor is depicted in Fig.2.5. The combustion zone is located in the center where flame stabilizes there. Both inlet and outlet are in the form of spiral shape so that the heat can be exchanged. The inlet channel is flanked with solid structures, which provides large surface area for heat exchange. To vary this

surface area, the number of turns can be changed without affecting the diameter of the combustion zone.

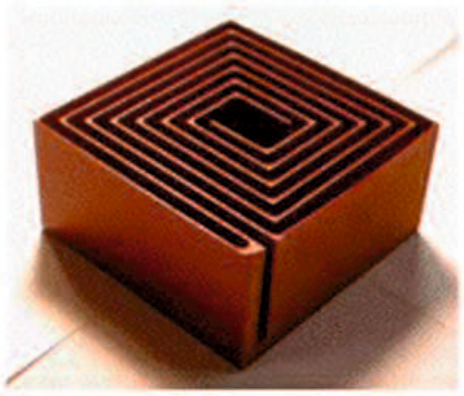

Figure 2.5 Image of a typical Swiss-roll combustor [50]

There are substantial experimental works that have been conducted on various types of Swiss-roll combustors. Most of these studies focus on the flame behaviours and responses [48, 51, 52]. Combustion of both propane and butane-air mixture in a toroidal Swiss-roll meso-scale combustor has been demonstrated by Sitzki et al. [47]. Flameless mode was observed even without the use of catalysts. It was also reported that flame could even be stabilized at a very low Reynolds number and highly lean mixtures. Meanwhile, a disk-shape SR was precisely fabricated by Kim et al. [51] using an electro-discharge machining (EDM) technique. The combustor is made of stainless steel and has a maximum of four channel turns. The inner diameter of the combustion chamber is fixed at 3.5 mm. Propane premixed with air is used as the fuel source. The results show that a wide range of flame stabilization limits can be achieved with the use of the combustor. Apart from that, the thermal efficiency is significantly increased. Although the emission of NOx is decreased, the amount of carbon monoxide is likely to rise. This is one of the drawbacks of small-scale combustion. Nevertheless, by incorporating catalysts at the exhaust outlet, the emission of carbon monoxide (CO) could be eliminated. Despite of the many advantages of Swiss-roll combustors, their complexity in terms of geometry and design parameters has made them difficult to be analytically and experimentally investigated.

A counter-current heat recirculation combustor that also utilizes the concept of indirect pre-heating method has been proposed. In a numerical study conducted by Ronney [45], a meso-scale counter current heat exchanger combustor was modeled and analyzed. The heat exchanger is modeled as a divider between the reactants and product stream as depicted in Fig.2.6. The combustion of the unburned gas occurs in a well-stirred reactor. The hot burned gas then flows through the exhaust outlet where the unburned gas on the other side is pre-heated by mean of conduction on both sides of the wall. This analysis is a simplified version of the complex phenomenon that occurs in a Swiss-roll combustor. Ju et al. [53] suggested a more comprehensive excess enthalpy-micro combustor model in which two flames propagate in opposite directions. However, the analysis is only limited to analytical solutions.

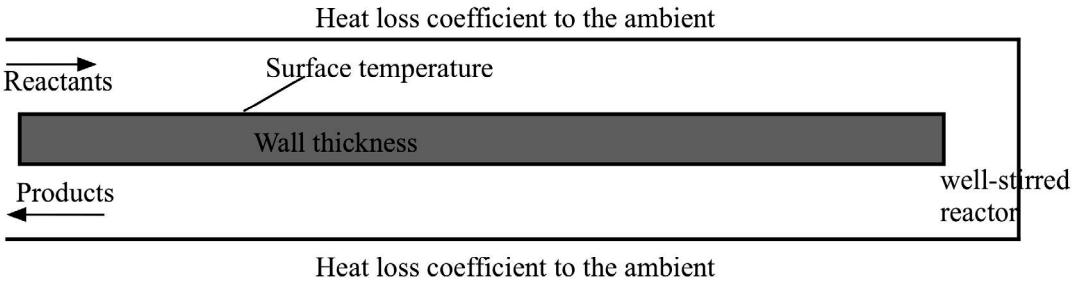

Figure 2.6 Counter-current heat recirculation combustor [45]

The experimental investigations on flame stabilization and characteristics of homogeneous (without catalysts) micro combustor with indirect pre-heating principle have been successfully demonstrated [54, 55]. Maruta et al. [27] showed that the flame stabilization limits of methane-air mixture in an 2-mm inner diameter U-shaped channel can be significantly increased with the elevation of wall temperature. The results also suggest that the flame can be stabilized even with an equivalence ratio as low as 0.05 and mixture velocities up to 150 cm/sec. This equivalence ratio and mixture velocities are beyond the theoretical flammability limits of methane and air mixtures. Nonetheless, the demerit of this system is the dependence of external heating.

Heat recuperation is also one of the indirect methods of preheating the unburned reactants. Heat recuperation is defined as temporal thermal coupling between the hot product and cold reactant streams. This coupling can be done via the periodic flow reversal in reverse-flow (RF) reactors as shown by Kaisare et al. [56]. In the meantime, micro combustors with heat recuperation mechanism for micro-thermophotovoltaic (TPV) system has been experimentally investigated [57, 58]. In this type of system, the

exhaust gas produced from the combustion of hydrogen-air mixture is re-circulated to pre-heat the outer wall of the combustor. Simultaneously, the incoming inlet feed is also pre-heated. From the results, the mean wall temperature shows an increase between 70 to 110 K while the useful radiation energy improves up to 83% [58].

2.4.2 Combustor geometry

There are substantial experimental works that have been performed to examine the effect of combustor geometry on the flame stability and efficiency [59-62]. In the early progress of micro power generation systems, straight cylindrical tube combustors without catalysts were preferred, owing to the simple geometry [11]. Generally, for a micro combustor, the wall thickness, gap width or also known as inner diameter, and combustor length are the geometrical parameters that can be changed. The combustor wall plays an important role in the thermal management and power conversion. By having a relatively high and uniform temperature along the wall, high electrical power output can be obtained [14]. However, the high surface to volume ratio of a micro combustor leads to numerous heat losses through the wall. Therefore, to improve the flame stabilization limits, reduction of this heat losses is necessary.

According to Kaisare and Vlachos [63], smaller gap width leads to higher heat losses that negatively affects the flame stabilization limits. They also stated that in order to design an efficient micro combustor, it is important to set the gap width between 0.6 mm to 1.2 mm. This range is deemed as an optimum range for a micro combustor. Nevertheless, vital factors like material type and operational flow velocity also need to be considered before determining the gap width.

Junwei and Beijing [64] experimentally demonstrated combustion in micro tube combustors made of two different materials, namely ceramic and steel. It was found that the ceramic combustor significantly reduces the axial heat transfer. As a result, lower flame stabilization limits were obtained. They concluded that an ideal micro combustor should be made of material with high wall thermal conductivity, but low emissivity.

Meanwhile, the effect of combustor length on the operational limits was reported in [65]. The fuels utilized were propane and methane-air mixture while the combustor is made of straight cylindrical tubes. The results indicate that by using longer tube length,

the flame stabilization limits become lower. The main drawback of using a straight tube as the combustor is the difficulty to control the position of the flame. In such tubes, the flame consistently changes its position. Apart from that, flame could not be sustained at high flow rates. Due to these difficulties, improvements on the design of combustor have been suggested.

A backward facing step combustor were first proposed by Yang et al. [66] as shown in Fig.2.7. The backward facing step combustor is considered as the best practical alternative to straight cylindrical tube shape combustors [67]. By having sudden steps, the mixing process of the fuel and air can be enhanced. Consequently, residence time increases, which leads to better flame stabilization. Moreover, the flame position can be easily controlled in the proposed combustor. The extended research of backward facing step combustors was performed by Wenming et al. [68]. They reported that the wall thickness is significantly affected by the wall temperature. However, no information was provided pertaining to the flame stability limits.

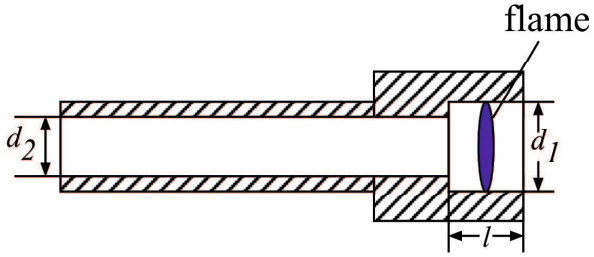

Figure 2.7 Backward facing step combustor [66]

2.4.3 Utilization of porous media

Flame stability in narrow channel combustors can also be improved by utilizing porous media [69, 70]. The use of porous material reduces the emission of pollutants such as NO_x and CO. Chou et al.[70] have successfully simulated the combustion of hydrogen fuel in a narrow channel backward-facing step combustor packed with porous media. The results suggest that the wall temperature can be greatly elevated. As mentioned before, higher wall temperature is one of the characteristics of an efficient micro combustor.

In 2009, Jiang et al. [71] presented a novel miniature cylindrical combustor with the chamber wall made of porous material. The fuel used is methane-air mixture. The combustor is designed in such a way that the heat losses through the wall can be

minimized. A thin unburned film is placed between the flame and porous wall. The proposed technique leads to the increase of residence time, which results to the enhancement of flame stabilization limits.

2.4.4 Combustors with flame holders

Flame can also be stabilized by inserting a bluff body in the combustion chamber of micro combustor [32]. A simple yet effective way of extending flame stabilization limits has been demonstrated by Wan et al.[32, 72]. In their work, a bluff body is inserted into a planar micro channel combustor. The experimental result shows that blow off limits are greatly extended with the presence of the bluff body.

The idea of using a flame holder in meso-scale cylindrical quartz tube combustors was first proposed by Mikami et al. [73]. In their experimental work, a stainless steel wire mesh is placed between the burned and unburned gas region. The experimental results show that flame can be stabilized for both gas and liquid fuel. In fact, it was also reported that the flame could even be stabilized in a tube combustor with an inner diameter below than the classical quenching distance. The wire mesh improves the heat transfer from the hot burned gas to the unburned gas region, resulting to better flame stabilization limits. Interestingly, no external heating is required to sustain the flame.

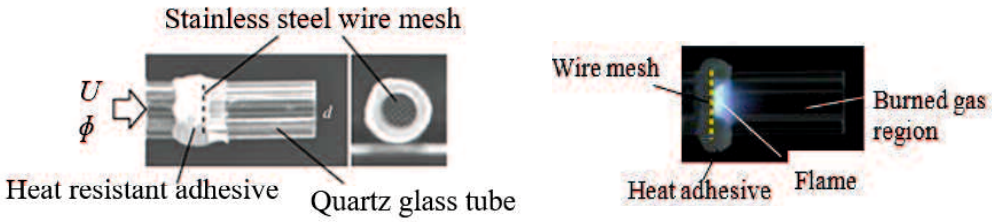

Figure 2.8 Meso-scale quartz tube combustor with stainless steel wire mesh [73]

The tube combustor with wire mesh can also be considered as the combustor with heat recirculation since the wire mesh effectively re-distributes the heat from the burned gas to the unburned gas region as illustrated in Fig.2.9.

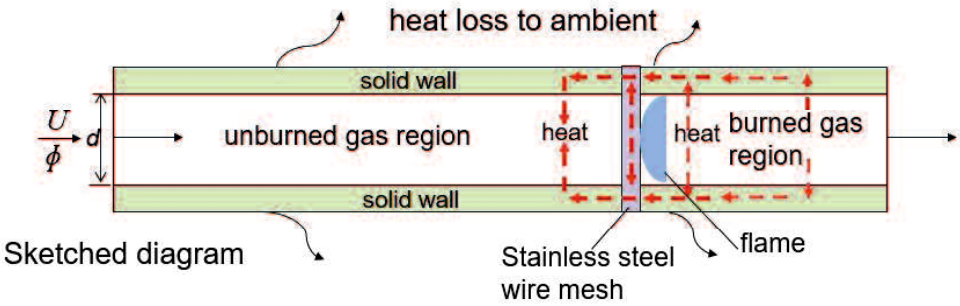

Figure 2.9 Illustrated diagram of a single channel combustor with wire mesh

2.4.5 Combustors with catalysts

The combustion stability and efficiency in micro combustors can be improved by depositing catalysts into combustors [74, 75]. The main function of catalysts is to drive and enhance the endothermic reactions that can possibly improve the combustion efficiency [76]. Combustion with catalysts also requires lower activation energy. Moreover, radical depletion on the combustor wall can be effectively eliminated, which leads to the reduction of radical quenching [77]. The other benefits of catalytic combustion are immobility of heat release zone, no quenching limits, emission free and moderate reactions [78, 79].

Experimental works have been conducted to investigate the catalytic combustion in micro combustors. Generally, the flame stability limits for micro combustor with catalysts are wider than the homogeneous combustors for both liquid and gaseous hydrocarbons fuel [80-82]. Flame can also be stabilized even in a combustor that is made from material with low wall thermal conductivities. Hydrogen is favored against hydrocarbon fuels in catalytic combustion. One of the reasons for this preference is that hydrogen can catalytically react with air even without an ignition source [83]. Nonetheless, the main problem with catalytic micro combustors is the catalysts deactivation. This deactivation is caused by the thermal control related to hot spots, traveling heat waves and wrong way behaviors [84].

2.5 Combustors with liquid fuels

Liquefied gaseous fuels like propane and butane are suitable fuels for micro combustor since they are designed for long shelf life [85]. Methane might not be suitable to be used as the primary fuel source for micro combustors since it requires large storage requirements and high ignition temperature [86]. On the other hand, hydrogen is also one of the preferred fuels for micro combustors. Hydrogen has high burning velocity, short reaction time, fast vaporization rate and high heating value [87]. Nevertheless, the practicality of gaseous fuels is questionable. This doubt is mainly contributed by the storage and mobility problem [88].

The utilization of liquid fuels eliminates the problem of mobility and storage [89, 90]. However, the primary challenge in liquid fuel combustion is to establish a clean and efficient combustion [91]. Kyritsis et al.[92, 93] introduced a catalytic combustor that utilized JP8 as the fuel. The fuel is atomized and dispersed into the combustion chamber by using an electro-sprayed system.

The use of porous medium to generate combustible liquid film in meso-scale combustors has been successfully demonstrated by Li et al. [94]. In their work, heptane fuel is injected into the combustor using a syringe pump. The injected fuel passes through porous media, which is made of stainless steel and bronze. These porous media induce a thin-liquid film to be generated. In addition to that, the metallic characteristic of the porous media enhances heat conduction from the flame. This heat is then utilized to vaporize the liquid film for sustainable combustion.

In 2009, Sadasivuni and Agrawal [95] proposed a flow-blurring injector to generate fine kerosene fuel droplets in a counter-flow micro combustor. Flat flame is generated with a considerably low emission. The results also show that 94% of the heat released can be retained.

Recently, Lilis and co-workers [96] experimentally demonstrated the flame stabilization in meso-scale quartz tube combustors with stainless steel wire mesh. The schematic diagram of the combustor is shown in Fig.2.10. Heptane with a mixture of ethanol was injected into the combustors. A single capillary-ring extractor and mesh collector electrode configuration was proposed to generate fine fuel droplets. The results

show that the combustion of heptane fuel is possible. Furthermore, there is no need for external heating or expensive catalysts deposition process.

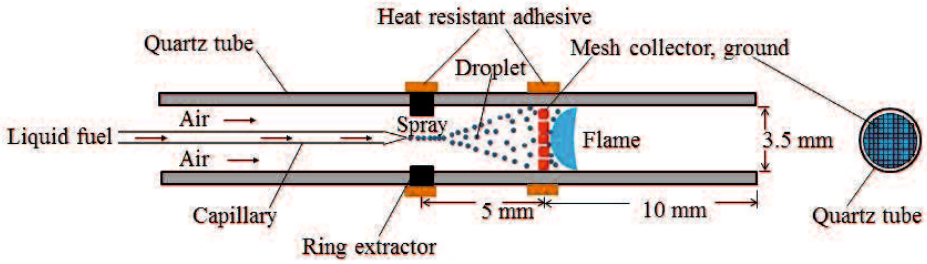

Figure 2.10 Quartz tube combustor with heptane fuel [96]

2.6 Numerical simulations of combustion in narrow channel combustors

Due to the advancement of computing technologies, numerical simulations have been proposed to examine the combustion feasibility in meso and micro-scale channel combustors. The use of numerical simulations can significantly reduce development cost of micro combustors. By performing numerical validations, any newly designed micro combustors can be thoroughly studied and optimized [97].

Computational Fluid Dynamics (CFD) has been utilized to numerically investigate the flame characteristic in micro-combustors with hydrocarbon fuels [98-100]. Raimondeau et al.[49] demonstrated the combustion of methane-air in a two-dimensional tubular micro combustor. A detailed multi-component transport and gas chemistry was employed in the numerical model. The results show that the effect of reactants pre-heating and insulations allows the flame to propagate even in micro channel combustors. Furthermore, initial heat losses and wall radical quenching are the main parameters that determine the flame propagation in micro combustors.

In 2004, numerical codes were used to model two dimensional (2-D) combustion in a Swiss-roll combustor [101]. Nevertheless, the model is simplified to reduce the complexity of the geometry. Sanz [102] conducted a numerical study to investigate flame extinctions in narrow channels with and without heat recirculation. It was found out that the calculated maximum flame temperature exceeds the adiabatic flame temperature due to the effect of heat recirculation.

Meanwhile, Ju et. al [103] applied numerical codes with one dimensional (1-D) model to examine the effect of transport properties and chemical kinetics on the flame

propagation in meso-scale straight quartz tube. A detailed chemistry of propane (C_3H_8) was presented and GRI was used to numerically model the flame. Two notable flame regimes, namely fast and slow burning regime occur as the channel height decreases. In order to provide better understanding to the underlying fundamentals of the combustion of gaseous hydrocarbon fuels in micro-burners, numerical simulations using more sophisticated commercial softwares were conducted [98]. Norton and Vlachos [104, 105] employed FLUENT to investigate the effect of wall conductivities, burner dimensions and external heat losses on combustion characteristics in parallel plates meso-scale combustors. The computational domain is shown in Fig.2.11. Combustion chemistry with one-step irreversible reaction mechanism was employed. This chemistry is deemed sufficient to demonstrate the flame dynamics behavior. The results suggest that propane-air micro-flames are more stable than methane-air flames. The lower ignition temperature of propane fuel contributes to this flame stability enhancement.

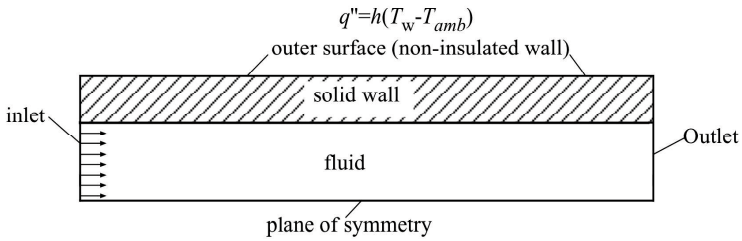

Figure 2.11 Computational domain employed in [105]

Li et al. [106] presented their findings on methane-air combustion using detailed combustion chemistry with 25-reversible reaction mechanism in two-dimensional (2-D) cylindrical tubes and parallel plates. The partial oxidation that is involved in the reaction process can be well represented by the detailed mechanism. The results show that proper material selections can be performed if the flame temperature is known.

Numerical simulations are also conducted to predict the premixed flame temperature and flame dynamics of micro combustion with hydrogen fuel [107-110]. The effects of various heat transfer conditions on hydrogen fuel combustion have been demonstrated by Hua et al. [37, 111]. In their work, a detailed reaction mechanism with 19-reversible reaction mechanisms was employed to study the flame stability with and without the presence of wall conduction. As seen in the results, lower wall thermal conductivity can tremendously reduce the heat losses. Consequently, the flame stabilization limits are enhanced. Nevertheless, such combustors have the problem of

hot spots. It is a well-known fact that the presence of hot spots on the combustor wall could possibly decrease the combustor lifespan.

More complex numerical simulations of micro combustion with catalysts have also been performed [112, 113]. A two dimensional (2-D) full-elliptic model for both gas and solid phases is used. The main objective of the simulations is to examine the mechanism of hetero and homogeneous combustion in micro combustors. Flame stability maps were also established with respect to the dependent parameters [114].

Table 2.1 shows the numerical simulation models that were previously employed by researchers in meso and micro scale combustion. Hydrocarbon fuels were utilized and the governing equations were solved by employing FLUENT software.

Table 2.1 Summary of previous numerical simulation with gaseous hydrocarbon fuels

Researchers	Combustor geometry	Fuel type	Reaction mechanism	Objectives of research
Raimondeau et al.[49]	Cylindrical tubes (2-D), steady-state	CH_4 +air	Detailed gas phase reactions	To investigate the effect of pre-heated gas mixture
Norton and Vlachos [104]	Parallel plates (2D), steady-state	CH_4 +air	One-step global reaction	To determine flame stability factors
Norton and Vlachos [105]	Parallel plates (2D), steady-state	C_3H_8+air	One-step global reaction	To determine flame stability factors
Lee and Kwon [98]	Cylindrical micro tube (2D), transient state	CH_4 +air	Reduced mechanism with 25 steps	To investigate flame structure at elevated temperature and pressure
Federeci and Vlachos [115]	Parallel plates (2D) steady-state	C_3H_8+air	One-step global reaction	To investigate the flame stability with heat recirculation combustor
Choi et al. [116]	3D micro cyclone combustor, steady-state	CH_4 +air	2 step global reaction	To determine flame stability of the designed combustor
Li et al.[106]	Cylindrical tube (2-D),steady-state	CH_4 +air	Reduced kinetic mechanism (25 steps)	To investigate flame temperature with different combustor geometry

2.7 Summary

Several mechanisms adopted by previous researchers in order to stabilize the flame in micro combustors have been discussed. Experiments and computational fluid dynamics (CFD) simulations are fully utilized to examine the multiple factors that affects the flame stabilization in narrow channel combustors. Due to large heat losses, a proper thermal management is required in order to stabilize flame in a micro combustor.

A micro combustor with heat recirculation is one of the well-known approaches in enhancing the flame stability. Apart from that, the use of flame holders, porous media and catalysts also improves the flame stabilization limits. Hydrocarbon gaseous fuels namely methane and propane are preferred as the fuel source in micro combustor due to the high energy density. However, liquid hydrocarbon fuels are favored over gaseous fuel since the problem of mobility can be eliminated.

The rapid progress of computing technologies allows for numerical simulations to be widely employed to simulate combustion in micro combustors. Numerical simulations also provide detailed insight of the problem. However, most of the simulations model used are two-dimensional (2-D). This 2-D model could not be utilized in a case where there is a bluff body inside a cylindrical tube combustor. Therefore, a three-dimensional (3-D) numerical model is required.

CHAPTER THREE

Effects of Ambient Temperature on Flame Stabilization

This chapter presents the effects of ambient temperature on the flame stabilization of meso-scale tube combustors with stainless wire mesh. Experiments were performed in which the ambient air temperature is specifically controlled. In order to control the ambient air temperature, a specific heater was utilized. Tube combustors made of quartz were inserted into the heater. These tube combustors have different set of length. Flame stabilization limits for each experimental condition were then established and analyzed.

3.1 Experimental setup

In this experimental work, narrow cylindrical quartz tubes with stainless steel wire mesh were used. The mesh type was 60 mesh/in with wire diameter of 0.14 mm. The inner diameter of the tube was 3.5 mm with wall thickness of 0.7 mm. The length from the mesh to the upstream part of the tube was varied at 10 mm, 30 mm and 160 mm. This length can be defined as the unburned gas region length L_u. On the other hand, L_b is defined as the burned gas region length, which is the length between the mesh to the downstream part of the tube. L_b was varied at 5 mm, 10 mm and 30 mm in this investigation. The ambient temperature was 295 K which was maintained at 100 mm away horizontally from the combustor wall. Propane (C_3H_8) and air was mixed and supplied into the tube with equivalence ratio (ϕ)and the cross-sectional-area mean flow velocity U. Each flow rate of air and propane was controlled by a mass flow controller.

A ceramic heater (WATLOW 220W) was used to heat up the unburned mixture region of the com bustor. This condition simulates the excess enthalpy combustors such as Swiss-roll burner where heat recirculation mechanism exists. The heater inner temperature T_h was set to 673 K during experiment. A thermocouple of Type-K was used to measure the heater inner temperature. It was placed as near as possible to the heater inner wall. A Proportional-Integral-Derivative (PID) controller was employed in order to control the temperature. In addition, this temperature setting of T_h is determined based on the measured exhaust gas temperature at the downstream area of the tube. Meanwhile, the narrow quartz tube was set up horizontally and connected to a copper tube with 4.5

mm inner diameter and 0.90 mm wall thickness which supplied propane/air mixture. The connection was done using a thermal- resistant cellophane tape.

Since the outer diameter of the quartz tube is smaller than the copper tube outer diameter, it was necessary for the connecting part of the quartz tube to be covered by cellophane tape. This is to ensure that both quartz and copper tube can be perfectly fitted together. By doing this, gas leaking0 can also be avoided. The width of the tape on the quartz tube was fixed to 4 mm.

The quartz tube was inserted L_{in} into the heater using a traverse system. L_{in} is defined as the insertion length which was measured between the downstream of the quartz tube to the heater opened end. L_{in} was consecutively varied at 26 mm and 36 mm in this experiment. Figure 3.1 and 3.2 summarizes all the parameters involved in the experiment.

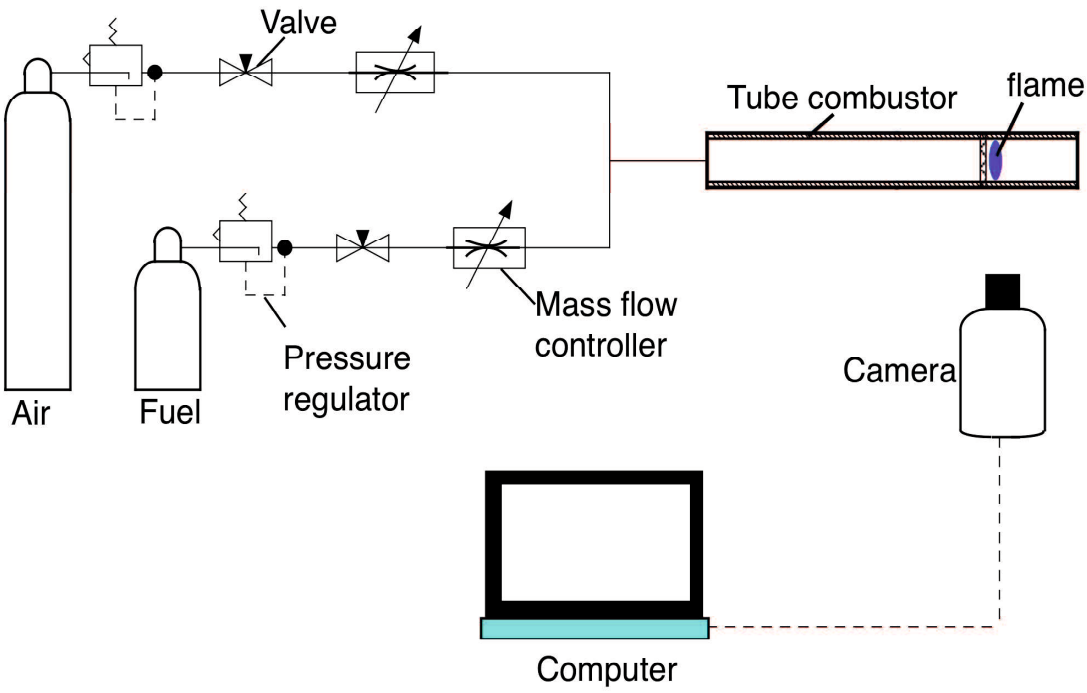

Figure 3.1 Schematic diagram of experiment without a heater

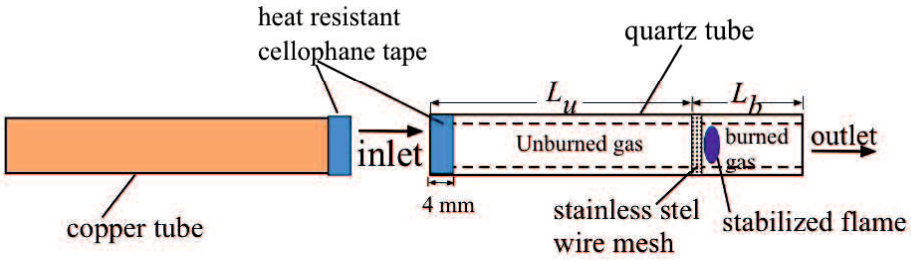

Magnified diagram of copper and quartz tube

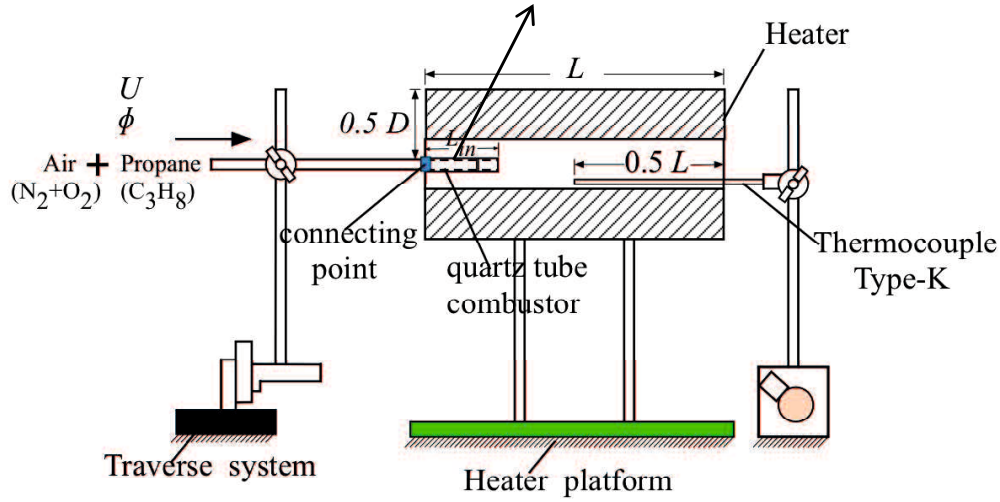

Figure 3.2 Experimental setup with a heater

3.2 Results and Discussion

Before the quartz tube was inserted into the heater, the temperature inside the heater was measured with respect to the axial distance. A thermocouple type-K, which was placed at the center of heater, was used for this purpose. Figure 3.3 depicts the temperature distribution of the heater inner area with respect to the axial distance. Due to heat losses at both ends of the heater, there were temperature variations along the axial distance. Therefore, to reduce the heat losses to the ambient, fiberglass insulator sheets were placed at the heater opened end where the quartz tube was inserted as shown in Fig.3.4. In order to observe flame stabilization inside the tube, no fiber glass insulator sheet was placed at the other heater end. As illustrated in Fig.3.3, with the presence of

the fiber glass insulator, heat loss to the ambient can be reduced. Consequently, higher surrounding temperature can be achieved with the same corresponding distance.

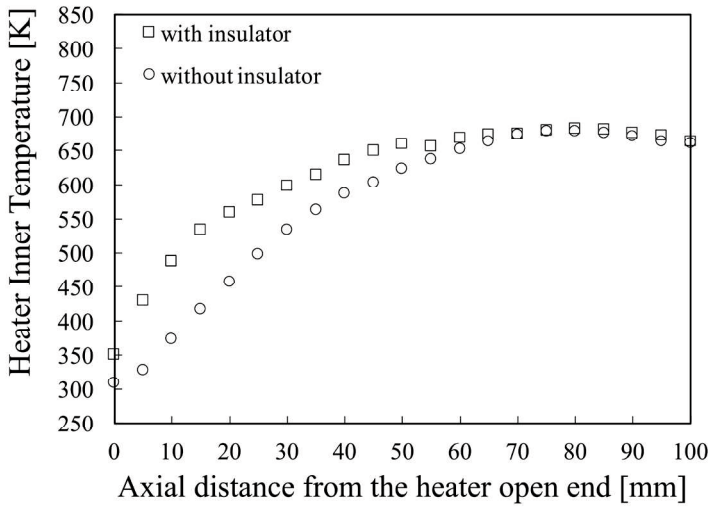

Figure 3.3 Temperature distribution inside the heater for setting temperature of T_h=673 K

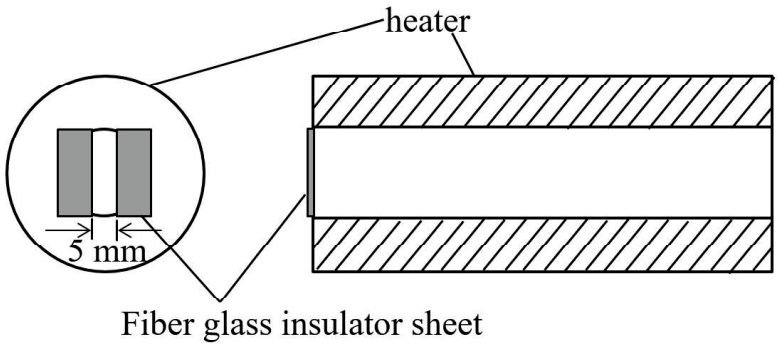

Figure 3.4 Location of the fiberglass insulator sheet

3.2.1 Effects of tube lengths on flame stabilization limits

At the initial stage of the experiment, the effect of tube lengths with respect to the unburned and burned gas region on the flame stabilization was investigated. In this investigation, the tube was not inserted into the heater. At first, the burned gas region lengths were varied at 5 mm, 10 mm and 30 mm whereas the unburned gas region length L_u was maintained at 10 mm. The results in term of flame stabilization limit for different burned gas region lengths L_b are presented in Fig.3.5.

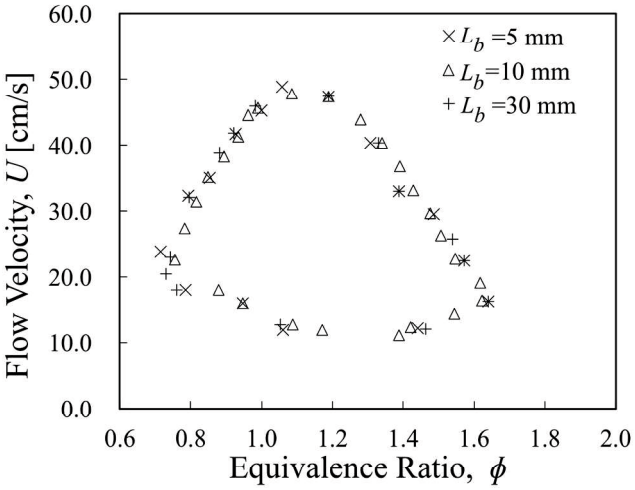

Figure 3.5 Flame stabilization limit in narrow tubes with wire mesh with L_u=10 mm for different burned gas region lengths L_b(without heating effect)

The flame stabilization limit in this work is defined as limit where the flame is stabilized near the mesh inside the combustor. Beyond these limits, the phenomenon of blow off or quenching may occur. As seen in Fig.3.5, for the tube with L_b of 10 mm and equivalence ratio of unity, the maximum mean flow velocity is 46 cm/s just before the flame is blown off. As for the minimum mean flow velocity, the flame starts to quench when the velocity is 12 cm/s. There is no significant change in term of flame stabilization limits for all the three types of tube. This suggests that the burned gas region length does not influence these limits for narrow quartz tubes with wire mesh combustor.

Next, Fig.3.6 demonstrates the flame stabilization limit for tube with different unburned gas region lengths. The burned gas region length L_b was fixed to 10 mm. On the same graph, flame stabilization limit obtained from the previous research [117] for tube with L_u=10 mm was plotted as well. The results show that the longer the unburned gas region length is, the smaller the flame stabilization limit is. For instance, the flammability limit for tube with L_u=160 mm is the smallest as compared to the other two tubes. The reduction is considerable especially in lean and rich conditions. This significant change indicates that the unburned gas region lengths might affect the flame stabilization. The possible cause for this behavior is explained in the wall temperature section.

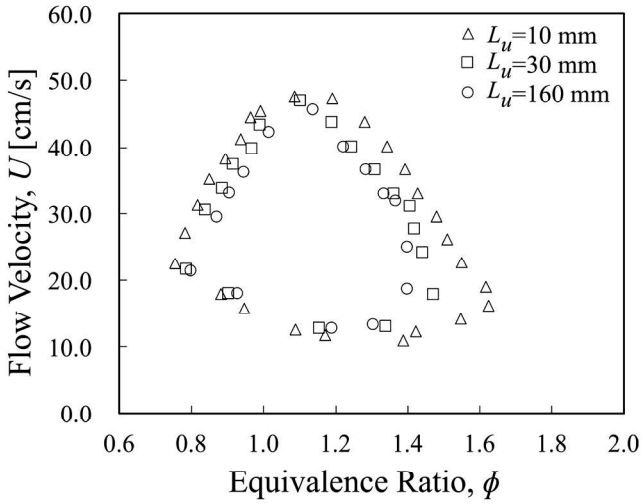

Figure 3.6 Flame stabilization limit in narrow tubes with wire mesh with L_b=10 mm for different unburned gas region lengths L_u (without heating effect)

3.2.2 Heating effect on the flame stabilization limits

It is predicted that the flame stabilization limits can be effectively enhanced by utilizing the heat generated from the combustion products. In a heat recirculation type of combustor, heat is transferred from the burned gas to the unburned gas region to preheat the incoming cold reactants. As a result, the total reactant enthalpy of the cold reactants is escalated. This excess enthalpy combustion leads to better flame stabilization. In this experiment, the same mechanism was implemented. The temperature inside the heater was intentionally set to 673 K. This value is determined based on the results obtained in an experiment where the temperature of the exhaust gas was measured using a thermocouple type-R as shown in Fig.3.7.

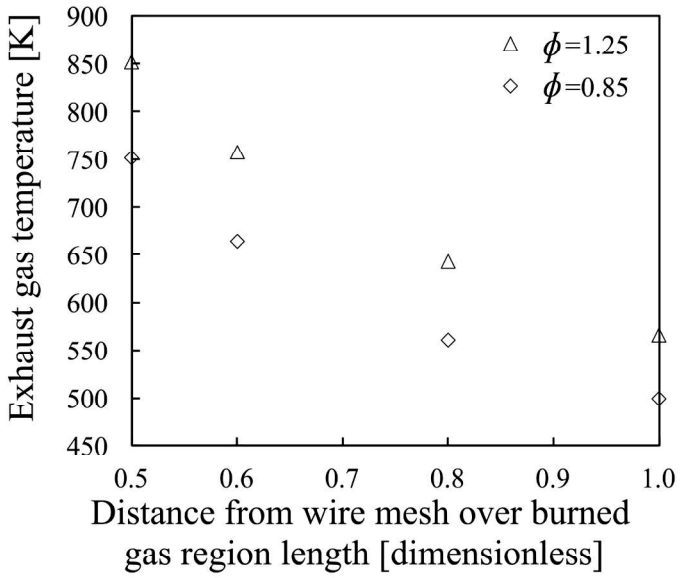

Figure 3.7 Exhaust gas temperature distribution in the burned gas region with L_b=30 mm (for lean and rich condition)

For lean condition of which the equivalence ratio (ϕ) is 0.85, the minimum exhaust gas temperature was 500 K. On the other hand, for rich condition (ϕ=1.25), the minimum temperature measured was 565 K. Both of these minimum temperatures were measured at the quartz tube end. Thus, by considering heat losses, the setting temperature of heater was set to 673 K in order to sufficiently simulate the condition of a heat recirculation combustor. Next, Fig.3.8 illustrates the flame stabilization limit for tube with heating effect and with different insertion lengths L_{in}. The results suggest that the flame stabilization limit is significantly expanded with the presence of heating especially in lean and rich conditions. However, there is only small change in term of minimum flow velocity for all tubes. Apart from that, the flammability limit for the tube with L_{in}=36 mm is wider than the tube with L_{in}=26 mm. This is possibly due to the temperature variation at different axial distance inside the heater, which was previously measured. For instance, at L_{in}=26 mm, the maximum temperature surrounding the tube unburned gas region was 503 K. As the tube was inserted 10 mm further into the heater, the maximum temperature for the same condition was recorded to be 553 K. Hence, it is likely that this increase in temperature leads to a better flame stabilization limit.

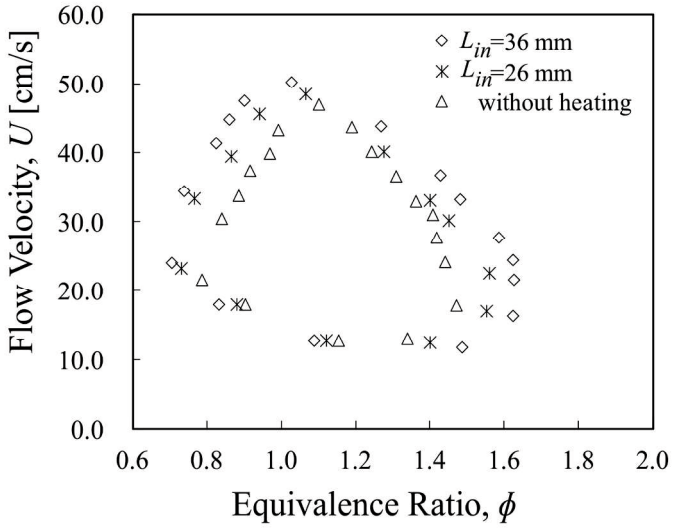

Figure 3.8 Flame stabilization limit in a narrow tube with wire mesh for tube with L_u=30 mm and L_b=10 mm for different insertion lengths L_{in}

3.2.3 Combustors wall temperature

The wall temperature for the tube with unburned gas region length of L_u=30 mm with and without heating effect is shown in Fig.3.9. The wall temperature at the area of the unburned gas region for the tube with heating effect is higher than the tube without heating effect. Clearly, this finding provides evidence of the positive effect of heating to the enhancement of flame stabilization limit.

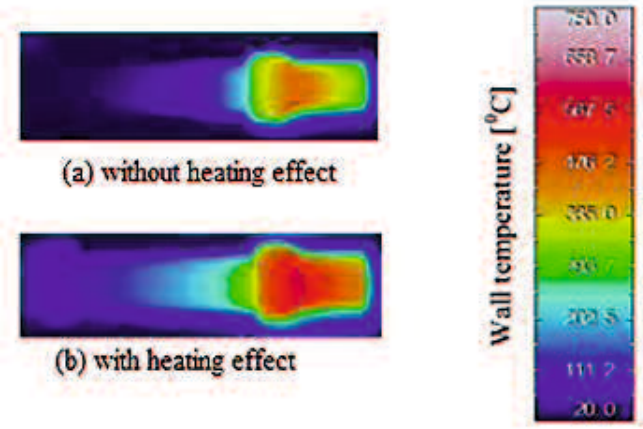

Figure 3.9 Wall temperatures for tube with L_u=30 mm, L_b=10 mm and L_{in}=36 mm

Next, the wall temperature of tubes without heating effect and for different unburned gas region lengths L_u is depicted in Fig.3.10. The maximum wall temperature recorded for the tube with L_u=10 mm was 791 K. For the tube with L_u=30 mm, on the other hand, the maximum wall temperature was 749 K. Since this maximum wall temperature was recorded near the flame location, this indicates that the flame temperature for the tube with L_u=10 mm is higher than the tube with L_u=30 mm. One of the potential causes for this wall temperature difference is heat losses from the tube non-insulated wall to the ambient. These heat losses occurred through convection and radiation. Nonetheless, since there is similarity in term of experimental conditions and type of tube used, the amount of heat losses to surrounding might be the same for both tubes. In other words, the value of convective heat transfer coefficient and the emissivity was made constant for all conditions. Therefore, this suggests that the potential cause for better flame stabilization limit in the tube with L_u=10 mm is the effect of heat recirculation.

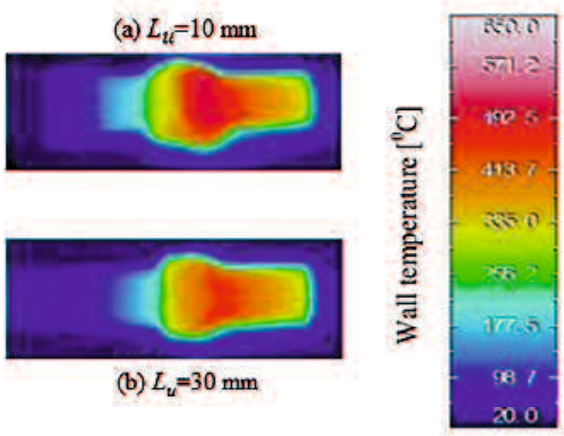

Figure 3.10 Wall temperatures for tube with L_b=10 mm and for different unburned gas region lengths L_u (without heating effect)

Even if the tube is not surrounded by the burned gas, heat recirculation occurs from the burned gas to the unburned gas by thermal conduction in the wall and the mesh. In Fig.3.10, it appears that heat recirculation is better for the tube with shorter unburned gas region length. This fact is supported by the minimum wall temperature recorded at the area of the unburned gas region. The minimum wall temperature at the unburned gas region for the tube with L_u=10 mm is higher than the tube with L_u=30 mm. This suggests that in the tube with L_u=10 mm, more heat was transferred from the burned gas region to the unburned gas region. This enhancement of heat recirculation may be partly

contributed by the distance from the mesh to the copper tube which has higher thermal conductivity than quartz.

3.3 Summary

Obviously, the tube with L_u=10 mm has shorter distance from the flame to the connecting point (point where the quartz and copper tube were connected). Therefore, there is strong possibility that higher amount of heat is conducted from the burned gas to the copper tube through the quartz tube wall and then from the copper tube to the unburned gas region. As a result, there is wider range of distance where the incoming reactants are heated up before being combusted. Hence, better flame stabilization is achieved as demonstrated in the results.

The results also show that the flame stabilization limits can be significantly improved, which the enhancement is higher in lean and rich conditions. However, there is almost no change in term of minimum flow velocity recorded. Apart from that, there is strong possibility that the unburned gas region length (L_u) influence flame stabilization limits of the combustors. There is an inverse relationship between L_u and these limits. On the other hand, there is no indicator that the burned gas region length (L_b) has any significant effect on flame stabilization.

As for the effect of the unburned gas region length, there is possibility that the use of copper tube that was connected to the quartz tube in the unburned gas region enhanced the effect of heat recirculation from the burned to the unburned gas by thermal conduction in the wall. Thus, by replacing the copper with a quartz tube, any effect due to differences in thermal conductivity between the quartz and the copper tube can be eliminated.

CHAPTER FOUR

Effects of Wall Thermal Conductivity on Flame Stabilization

This chapter explains the approach taken and outcomes obtained in the investigation of the effect of wall thermal conductivity on the flame stabilization. As mentioned in Chapter Two, there are two types of pre-heating method that can be applied to improve the flame stabilization in tube combustors with wire mesh. The first method is named as direct pre-heating method while the second is defined as indirect pre-heating. Increasing the combustor wall thermal conductivity to allow for more heat being recirculated from the burned gas to the unburned gas region is the example of a direct pre-heating method. Both numerical simulations and experiments were performed to examine the effect of wall thermal conductivity. The results are then analyzed and presented in this particular chapter.

4.1 Two dimensional (2-D) numerical setup

A two-dimensional (2-D) steady-state numerical simulation was performed using ANSYS Release 14.0 with Fluent 6.3 [118]. Fluent employs a finite-volume approach in solving the governing equations. The inner diameter of the combustor is 3.5 mm and the wall is 0.7 mm thick. The wall thickness is modeled as a solid phase where only the energy equation is solved. The total length of the combustor is set to 40 mm. The combustor is divided into two parts namely the unburned and burned gas region.

The concentric rings are modeled as square rectangles with 0.14 mm in length and placed side by side where the location is set to be 30 mm from the inlet. This value is chosen to ensure that the flow will be fully developed before passing the rings. The gap between the rectangles is set to 0.10 mm. The fuel type used is propane (C_3H_8)-air mixture.

The schematic of the computational domain for this simulation is illustrated in Fig.4.1. In this work, Dufour, gas radiation effects and the work done by pressure and viscous force are assumed to be negligible. Norton and Vlachos [104] have shown that the gas phase radiation has minimal effect on the combustion reactions. Ideal gas law

is assumed for the gas density and the specific heat for all the species is calculated using a piecewise polynomial fit of temperature.

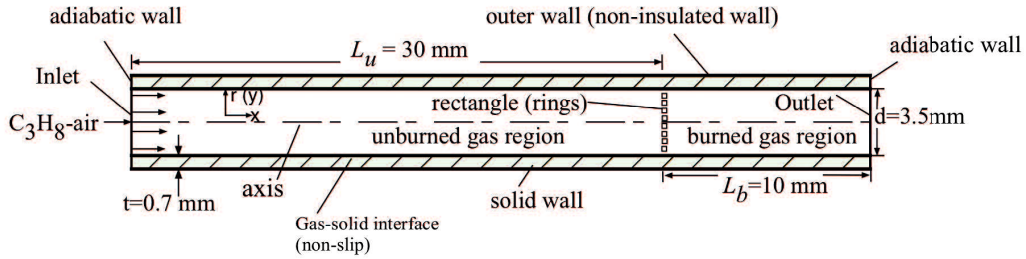

Figure 4.1 Schematic of the computational domain

Meanwhile, reduced one-step propane combustion with five species as suggested by Westbrook and Dryer [119] is employed as the combustion chemistry,

$$C_3H_8 + 5O_2 \rightarrow 3CO_2 + 4H_2O \quad (4\text{-}1)$$

The species involved are C_3H_8, O_2, N_2, CO_2 and H_2O.

It should be noted that a detail kinetics mechanism is compulsory if simulations are performed to evaluate flame or emission characteristics. However, since the focus this study is to examine the trend pattern of the effect of wall thermal conductivity on the flame stabilization, the single step mechanism is sufficient. Radical quenching due to material surface reaction is excluded in the study since material that is resistant to radical quenching is now available. A total number of elements of 19482 is employed for all cases.

Boundary conditions are specified as proposed by Norton and Vlachos (2004), Li et al. (2009) and Jalal et al. (2012). No-slip boundary type condition is applied at the interface between the fluid and the solid wall. The heat flux at this interface is calculated using Fourier's law. A wall thermal conductivity of 20 W/m/K is applied on the wall boundary of the concentric rings. Heat transfer by means of convection at the outer surface of the wall is given by:

$$q'' = h\,(T_W - T_{amb}) \quad (4\text{-}2)$$

where h is the convective heat transfer coefficient, T_W is the wall temperature and T_{amb} is the ambient temperature which is set to 300 K for all cases.

The convective heat transfer coefficient (*h)* is fixed to be at 5 W/m^{2}K, which represent a weak natural convection (Li, et al., 2009). A thermal insulation (zero flux boundary) is applied at both left and right wall edge. The emissivity value is fixed to 0.90. The wall thermal conductivity for both the unburned gas region (k_u) and the burned gas region (k_b) of the solid wall is varied from 1.0 W/m/K to 1000 W/m/K. The

solid zone of k_u and k_b can be established by defining two separate cell zones of the solid wall in the ANSYS-Fluent. In a practical application, this region can be separated by using two composite tubes for the unburned and burned gas region. These tubes can be adhered together using special ceramic adhesive as demonstrated by Mikami et al. (2013). For the outlet boundary condition, a far-field pressure condition is assumed. An axis boundary condition is established at the centerline so that the calculation can be performed only in the half of the domain. Table 4.1 summarizes the numerical model setup.

Table 4.1 Summary of the model setup

Parameters	Model setup
Solver	Pressure-based, steady-state and axisymmetric
Species model	Laminar finite-rate with stiff chemistry solver
Pressure-velocity coupling	SIMPLE
Spatial discretization	First -order upwind scheme
Density	Ideal gas law
Mixture specific heat	Mixing law
Species specific heat	Piecewise polynomial
Convergence criteria values	1×10^{-3} for continuity, 1×10^{-3} for velocity 1×10^{-6} for energy and 1×10^{-3} for species equation

A laminar flow of U with a flat velocity profile is applied at the inlet while the inlet feed temperature is maintained at 300 K. A technique called “cold flow” is employed where the momentum and continuity equation is solved first. Then, by patching an initial temperature around the patch zone, the energy and species equations are solved. This patching zone is located at 2 mm from the outlet. A sufficiently high temperature of 1700 K is applied in the patching zone to ensure that the fuel- air mixture can be ignited. Once the flame has been stabilized near the rings, the value of U and the equivalence ratio of ϕ are varied. To obtain the blowout limit, the value of ϕ is first fixed and the value of U is gradually stepped up. The corresponding U value of which causes the flame to propagate away from the rings and subsequently blown off the tube is considered as the blowout limit. By employing a first-order upwind scheme, the governing equations are solved. In addition to that, the pressure-velocity coupling

is handled by SIMPLE algorithm. The results in term of temperature contours, outer wall surface temperature and blowout limits are analyzed and presented.

The governing equations involved for this steady state axisymmetric simulation are as follow;

The mass conservation equation (continuity);

$$\frac{\partial}{\partial x}(\rho u_x) + \frac{\partial}{\partial r}(\rho u_r) + \frac{\rho u_r}{r} = S_m \tag{4-3}$$

This general form valid for incompressible and compressible flows. The source S_m is the mass added to the continuous phase from the dispersed second phase (eg. due to vaporization of liquid droplets) and any user-defined source.

Momentum conservation equations;

In x-coordinate;

$$\frac{1}{r}\frac{\partial}{\partial x}(r\rho u_x u_x) + \frac{1}{r}\frac{\partial}{\partial r}(r\rho u_r u_x) = -\frac{\partial p}{\partial x} + \frac{1}{r}\frac{\partial}{\partial x}\left[r\mu\left(2\frac{\partial u_x}{\partial x} - \frac{2}{3}(\nabla\cdot\vec{u})\right)\right] + \frac{1}{r}\frac{\partial}{\partial r}\left[r\mu\left(2\frac{\partial u_x}{\partial r} + \frac{\partial u_r}{\partial x}\right)\right] + F_x \tag{4-4}$$

In radial (r) coordinate;

$$\frac{1}{r}\frac{\partial}{\partial x}(r\rho u_x u_r) + \frac{1}{r}\frac{\partial}{\partial r}(r\rho u_r u_r) = -\frac{\partial p}{\partial r} + \frac{1}{r}\frac{\partial}{\partial x}\left[r\mu\left(\frac{\partial u_r}{\partial x} + \frac{\partial u_x}{\partial r}\right)\right] + \frac{1}{r}\frac{\partial}{\partial r}\left[r\mu\left(2\frac{\partial u_r}{\partial r} - \frac{2}{3}(\nabla\cdot\vec{u})\right)\right] - 2\mu\frac{u_r}{r^2} + \frac{2}{3}\frac{\mu}{r}(\nabla\cdot\vec{u}) + F_r \tag{4-5}$$

Where

$$\nabla\cdot\vec{u} = \frac{\partial u_x}{\partial x} + \frac{\partial u_r}{\partial r} + \frac{u_r}{r} \tag{4-6}$$

x is the axial coordinate, r is the radial coordinate, u_x is the axial velocity, and u_r is the term for the radial velocity.

F_x=external force in x-direction

F_r=external force in r- direction

p=static pressure

μ= fluid viscosity

For the energy equation is given as:

$$\nabla \cdot (\vec{u}(\rho E + p)) = \nabla \cdot \left(k\nabla \mathrm{T} - \sum_i h_i \vec{J}_i + (\bar{\bar{\tau}} \cdot \vec{u})\right) + S_h \quad (4\text{-}7)$$

Where

$E = h - \frac{p}{\rho} + \frac{v^2}{2}$ and h is sensible enthalpy and is defined for ideal gases as $h = \sum_j Y_j h_j$and for incompressible flow given as $h = \sum_i Y_i h_i + \frac{p}{\rho}$

Y_i= mass fraction of species *i* and $h_i = \int_{T_{ref}}^{T} c_{p,i}\, dT$ where $T_{ref} = 298.15\ K$

Meanwhile, the energy equation in the solid region is given as:

$$\nabla \cdot (\vec{u}\rho h) = \nabla \cdot (k\nabla \mathrm{T}) + S_h \quad (4\text{-}8)$$

k= thermal conductivity

$\vec{J}_i$= diffusion flux of species *i*

$\bar{\bar{\tau}}$= stress tensor

S_h= heat of chemical reaction or any other volumetric heat sources added by the user

For the species transport equation is defined as:

$$\nabla \cdot (\rho \vec{u} Y_i) = -\nabla \cdot \vec{J}_i + R_i + S_i \quad (4\text{-}9)$$

R_i= net rate of production of species *i* by chemical reaction

S_i= rate of creation by addition from the dispersed phase plus any user-defined sources

Y_i=mass fraction of species *i*

For the mass diffusion in laminar flows, ANSYS Fluent employs the dilute approximation which also known as Fick's law to model the mass diffusion due to concentration gradients

$$\vec{J}_i = -\rho D_{i,m} \nabla Y_i - D_{T,i} \frac{\nabla T}{T} \quad (4\text{-}10)$$

$D_{i,m}$=mass diffusion coefficient for species i

$D_{T,i}$=thermal diffusion coefficient

The sample calculation of mass fraction at equivalence ratio (ϕ=0.90) for the input

of equations above is as follow:

It is assumed that air is assumed to be a mixture of 21 mol% oxygen and 79 mol% nitrogen. Using the given chemical reaction of one-step propane combustion;

$$C_xH_y + a(O_2 + 3.76N_2) \rightarrow xCO_2 + \frac{y}{2}H_2O + 3.76aN_2$$

$$C_3H_8 + a(O_2 + 3.76N_2) \rightarrow 3CO_2 + 4H_2O + 3.76aN_2$$

$$a = \frac{x+\frac{y}{4}}{\phi} = \frac{3+2}{0.90} = 5.5556$$

$$C_3H_8 + 5.5556(O_2 + 3.76N_2) \rightarrow 3CO_2 + 4H_2O + 3.76(5.5556)N_2$$

Finding the molar fraction (χ) of each species;

$$N_{C_3H_8} = 1;\ \chi_{C_3H_8} = \frac{N_{C_3H_8}}{N_{Total}} = \frac{1}{1+5.5556+(3.76)(5.5556)} = \frac{1}{27.444656} = 0.03644$$

$$N_{O_2} = 5.5556;\ \chi_{O_2} = \frac{N_{O_2}}{N_{Total}} = \frac{5.5556}{1+5.5556+(3.76)(5.5556)} = \frac{5.5556}{27.444656} = 0.2024$$

$$N_{N_2} = 20.8891;\ \chi_{N_2} = \frac{N_{N_2}}{N_{Total}} = \frac{20.8891}{1+5.5556+(3.76)(5.5556)} = \frac{20.8891}{27.444656} = 0.7611$$

Calculating the mixture molecular weight (MW_{mix})

$$MW_{mix} = \sum \chi_i MW_i;$$

$$MW_{mix} = \chi_{C_3H_8}MW_{C_3H_8} + \chi_{O_2}MW_{O_2} + \chi_{N_2}MW_{N_2};$$

$$MW_{mix} = 0.03644(44.06) + 0.2024(32) + 0.7611(28.013);$$

$$MW_{mix} = 29.4048\ kg/kmole$$

Thus, the species mass fraction for C_3H_8 and O_2 can be determined by;

$$Y_{C_3H_8} = \frac{\chi_{C_3H_8}MW_{C_3H_8}}{MW_{mix}} = \frac{0.03644(44.06)}{29.4048} = 0.05460$$

$$Y_{O_2} = \frac{\chi_{O_2}MW_{O_2}}{MW_{mix}} = \frac{0.2024(32)}{29.4048} = 0.2203$$

These values of species mass fraction are then being the input to the Fluent.

A grid dependent was first performed and the result is shown in Fig.4.2. There is no significant change in term of the gas temperature with respect to the total number of elements.

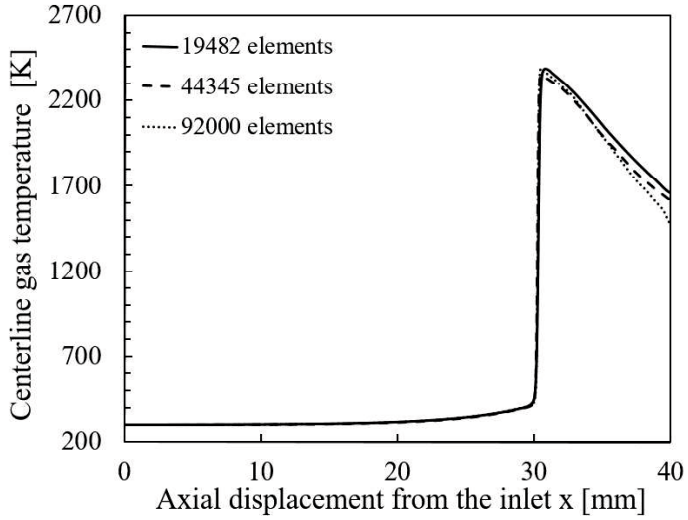

Figure 4.2 Centerline gas temperature distribution along the axial displacement with different number of elements with k_u=1 W/m/K and k_b=1 W/m/K for U=30 cm/s and ϕ=1.0

4.1.1 Flame propagation and stabilization

Flame propagation in a narrow channel is a broad subject matter. Investigation of flame propagation behaviors in a narrow channel tube combustor is indeed a formidable task. There are many factors that affect flame propagation in a narrow channel [120-122]. In order to numerically study the phenomenon of flame propagation inside a meso-scale tube combustor, a detailed kinetics reaction mechanism is required that can lead to a higher computational cost. This investigation is mainly on the effect of various values of wall thermal conductivities on the combustion characteristics. Therefore, results shown in Fig.4.3 are only limited to demonstrate the capability of the concentric rings. The ignition was attained by applying a sufficiently high temperature on the patch zone. This ignition method replicates the experimental condition reported by Mikami et al. [73]. The inlet velocity was set to U=20 cm/s while the equivalence ratio (ϕ) was fixed to 1.0. Since the flame burning velocity is faster than the inlet velocity, the flame propagated towards the inlet once it was ignited. As shown in Fig.4.3, the flame stopped to propagate when it reached the rings and stabilized there until a converged solution

was achieved. This condition is defined as a stable flame. The concentric rings act as a flame holder by which the flame can be stabilized at a fixed location.

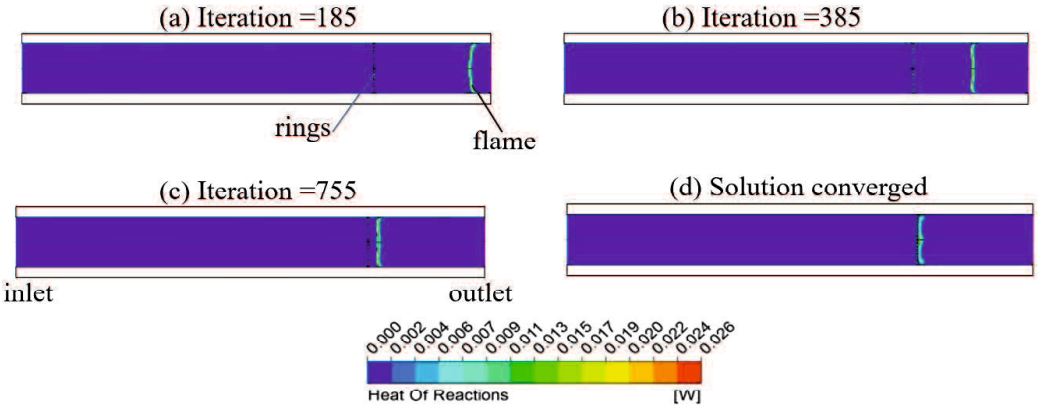

Figure 4.3 Heat of reaction contours with different values of iteration number for k_u=1 W/m/K and k_b=1 W/m/K, ϕ=1.0 and U=20 cm/s, (not to scale; for easier visualization, reflection of axis is used in all figures

4.1.2 Flame, gas and wall surface temperature profile

In micro combustors, flame, inner and outer wall temperatures are interdependent to each other. These features are essentially important in a micro power generation research. Yang et al. [58] suggest that a good combustor for micro power generation application should have a sufficiently high and uniform outer wall surface temperature. As for this simulation study, the wall thermal conductivity values for both the unburned (k_u) and burned *(k_b)* gas region were varied at 1 W/m/K, 10 W/m/K, 100 W/m/K and 1000 W/m/K. The effect of wall thermal conductivity on the temperature contours of the combustor is shown in Fig.4.4 while Fig.4.5 illustrates the corresponding gas centerline temperature distribution. The flame temperature can be defined as the highest gas temperature recorded along the axial displacement. Figure 4.4 suggests that the variation of the wall thermal conductivity has a minimal effect on the flame temperature. As the value of k_u and k_b is increased to 10 W/m/K, 100 W/m/K and 1000 W/m/K respectively, there is notably better uniformity of gas temperature.

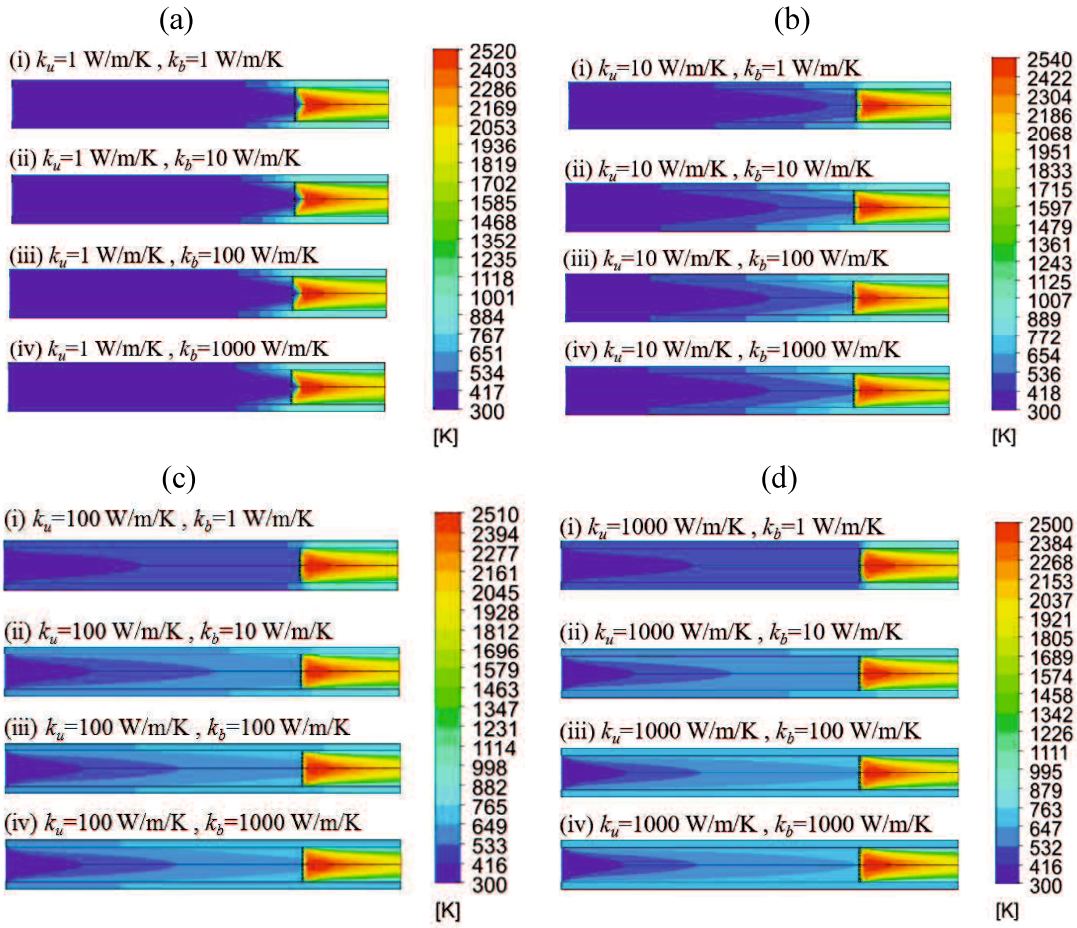

Figure 4.4 (a)-(d) Temperature contours with different values of k_u and k_b for U=30 cm/s and ϕ=1.0 (not to scale; for easier visualization, a reflection of the axis is used in all figures)

Meanwhile, Fig.4.5 shows that there is a direct relationship between k_u values and the gas temperature in the unburned gas region particularly from x=3 mm onwards. This change is due to the role of the combustor wall as a heat conductor. The main method of transferring the heat from the hot burned gas to the unburned reactants in this type of combustor is by the wall conduction. The process of heating up the unburned gas prior to the combustion starts from the inner wall. Thus, the intensity of this process depends on the value of k_u.

Figure 4.6 presents the temperature distribution of inner wall and gas inside the combustor with two different values of k_u and a fixed k_b value. For k_u=10 W/m/K, higher inner wall temperature is obtained in the unburned gas region up to 29.0mm as more heat energy is distributed to the unburned gas region. Generally, this trend is repeated with a further increment of the k_u value. Nonetheless, using k_u=1000W/m/K is no longer effective in boosting up the unburned gas temperature.

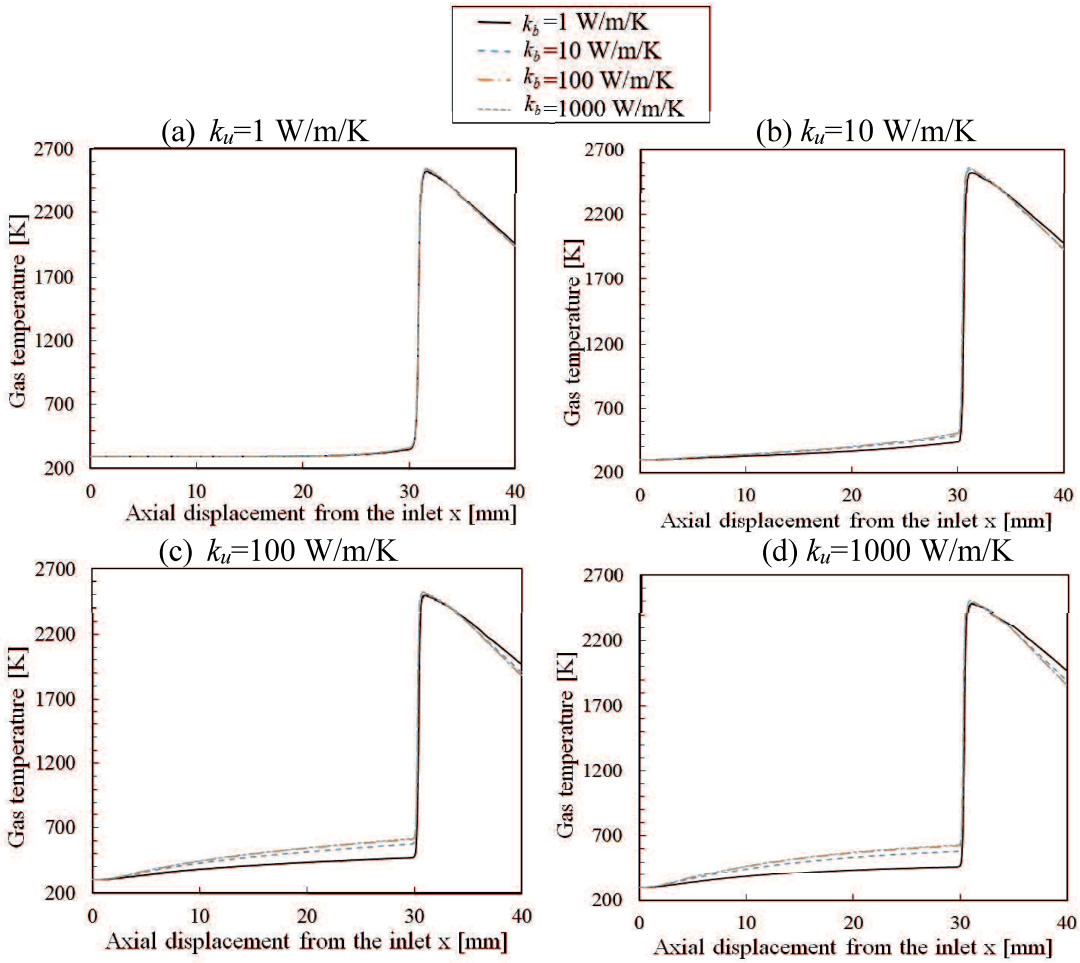

Figure 4.5 Temperature distribution of gas at the centerline along the axial displacement with different values of k_u and k_b for U=30 cm/s and ϕ=1.0

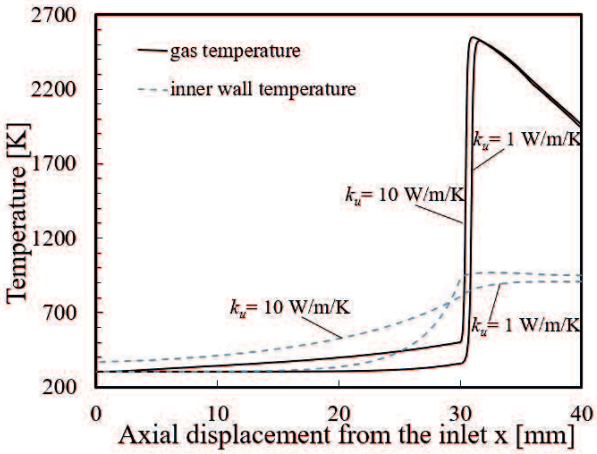

Figure 4.6 Temperature distribution of the inner wall and gas at the centerline along the axial displacement from the inlet with k_u=1 W/m/K and k_u=10 W/m/K for k_b=10 W/m/K, U=30 cm/s and ϕ=1.0

The next important criterion for meso and micro scale combustion is the outer wall temperature distribution, which is presented in Fig.4.7. Obviously, it is shown in the figure that the combination of low wall thermal conductivities in the unburned and burned gas region leads to steeper temperature gradients.

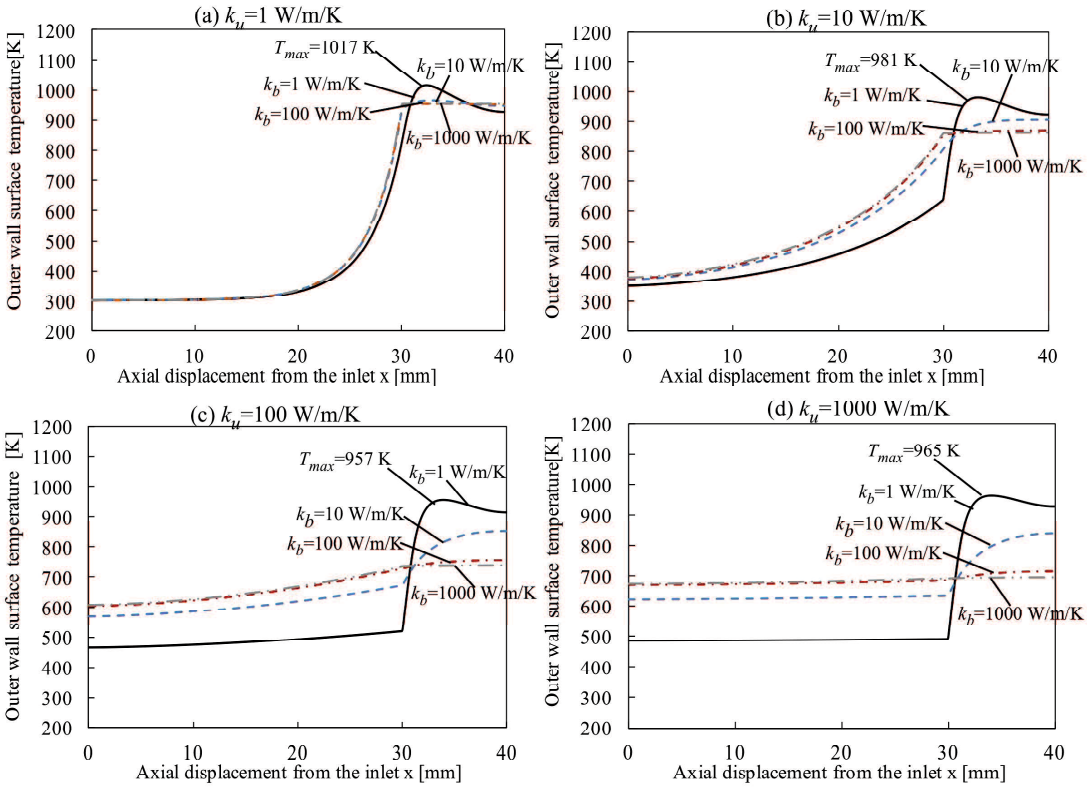

Figure 4.7 Outer wall surface temperature distribution along the axial displacement from the inlet with different values of k_u and k_b for U=30 cm/and ϕ =1.0

According to Norton and Vlachos [104], such large temperature gradients can significantly reduce the material lifespan. In severe cases, melting of the combustor material might occur. Therefore, to avoid such a problem, a uniform outer wall temperature distribution is desired. This uniform temperature can be achieved by using a high wall thermal conductivity in the unburned (k_u) and burned gas region (k_b). However, it is noted that by utilizing a high value of k_u and k_b, the maximum wall temperature is dramatically reduced. For instance, with k_u=1000 W/m/K and k_b=1000 W/m/K, the maximum wall temperature is only at 694.7 K. This reduction is mainly due to the heat energy being distributed to a wider range of area. A lower wall temperature means a reduction of the combustor efficiency in converting heat to electrical energy. As such, a proper consideration is necessary in order to balance between the need of a high performance combustor and a durable combustor.

4.1.3 Effects of the inlet velocity and equivalence ratio

Park et al. [88] stated that the efficiency of a micro combustor in converting the heat produced from combustion to electrical energy is significantly affected by the inlet velocity. This fact is due to the temperature variation with respect to the inlet velocity. With the elevation of the inlet velocity, more reactant mixture is delivered to the burned region that eventually escalates the reaction rate. Consequently, there is a surge of flame temperature that results to a greater outer wall surface temperature distribution.

Figure 4.8 depicts the outer wall temperature distribution along the axial displacement with different values of inlet velocity (U) and equivalence ratio (ϕ). As shown in Fig.4.8 (a), the increment of the inlet velocity escalates the wall temperature particularly in the burned gas region. This pattern is also valid for larger values of k_u where the increase of wall temperature is more noticeable in the unburned gas region. It is important to note that the process of obtaining a higher outer wall temperature distribution by applying a higher inlet velocity should be prudently performed as blowout might occur. The other way to elevate the wall temperature without adjusting the inlet velocity is by increasing the equivalence ratio (ϕ). Figure 4.8(b) clearly shows that a richer fuel-air ratio can result to an increase in the wall temperature due to greater reaction rate. Nevertheless, considering the environment where micro power generators are utilized, combustion of fuel mixture with below the stoichiometric ratio is preferred.

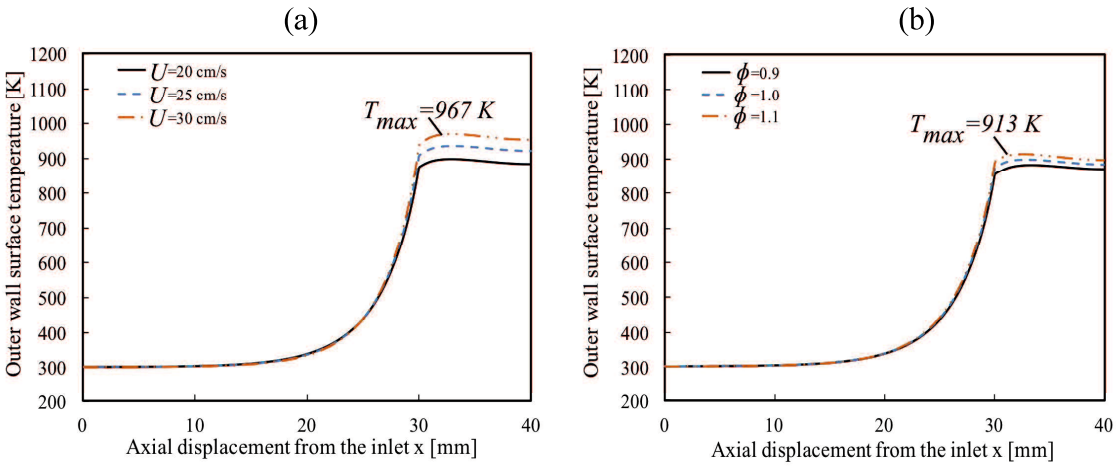

Figure 4.8 Outer wall surface temperature distribution along the axial displacement from the inlet with different U and ϕ for k_u=1 W/m/K and k_b=10 W/m/K: (a) for different values of U with constant ϕ=1.0; (b) for different values of ϕ with constant U=20 cm/s

4.1.4 Effects of the wall thermal conductivity on the flame stability and combustion efficiency

In meso and micro-scale combustors, the wall thermal conductivity plays a significant role in determining the flame stability. The axial heat conduction from the burned gas region promotes the pre-heating of the unburned gas that eventually enhances the flame stability. One of the indicators of flame instability in a micro combustor is blowout. In general, blowout occurs when the combustor exit velocity is higher than flame burning velocity [24]. It is important to determine the blowout limits for meso and micro-scale combustors so that the operative range can be ascertained.

In this study, the determination of blowout limits is as follow. Firstly, a stable flame is established in the combustor. For all cases, a stable flame can be achieved with the inlet velocity (U) of 20 cm/s regardless of the equivalence ratio (ϕ) value. Then, the value of U is gradually stepped up with 1 cm/s interval and further calculation is conducted until a converged solution is achieved. For instance, if increasing the value of U from 25 cm/s to 26 cm/s causes the flame to propagate away from the rings toward the outlet, then U=25 cm/s is considered as the blowout limit. This step is repeated for each case of ϕ and both wall thermal conductivities (k_u and k_b). Figure 4.9 shows the flame image with a blowout condition while Fig.4.10 summarizes the blowout limits with respect to all variable parameters. As depicted in Fig.4.9, with the value of U increased to 42 cm/s, the flame is blown out to the tube end resulting to the flame extinction.

Meanwhile, Fig.4.10 indicates that as k_b is increased from 1 W/m/K to 100 W/m/K, the flame stability is enhanced. In overall, the combustion of mixture that is rich in fuel significantly improves the blowout limits as Mikami et al. [73] experimentally showed for meso-scale quartz tube combustors with wire mesh. However, there is only a slight improvement in the limit with the use of k_b=1000 W/m/K. It is also shown that there is an inverse relationship between the value of k_u and the blowout limits except for ϕ=0.90 as indicated in Fig.4.10 (b) to (d). This reduction of limit is probably due to the variation of pre-heating effect that occurs in the unburned gas region.

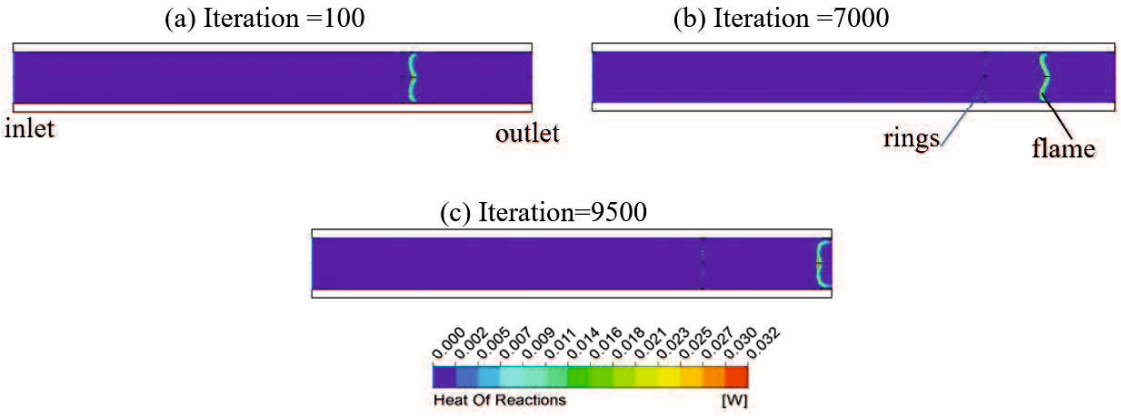

Figure 4.9 Heat of reaction contours in near blowout condition for k_u=100 W/m/K, k_b=100 W/m/K, ϕ=1.0 when U was increased from 41 cm/s to 42 cm/s

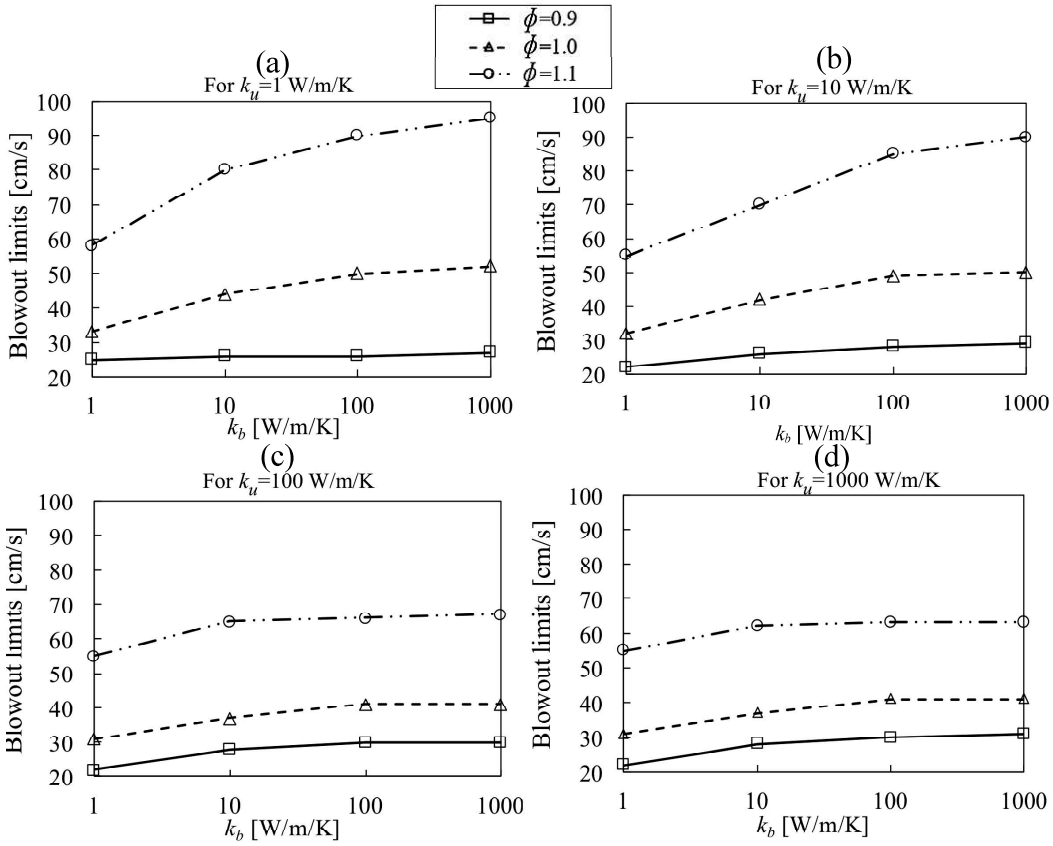

Figure 4.10 Blowout limits with different values of k_u, k_b and ϕ

Figure 4.11 presents the temperature distribution along the inner wall with different values of k_u and k_b. It can be seen from the figure that the inner wall temperature at x=29.5 mm for k_u=1 W/m/K is the highest. This maximum inner wall temperature is still within the unburned gas region. Figure 4.12 (a) depicts the numerical value of inner wall temperature at x=29.5 mm while Fig 4.12 (b) shows the blowout limits for ϕ=1.0. The highest inner wall temperature is recorded to be 848.7 K while the maximum blowout

limit is 52 cm/s. Clearly from the figure, it is suggested that the blowout limits are affected by the inner wall temperature, particularly in the small area just before the ring position. The increased inner wall temperature at such a position conceivably increases the local burning velocity at the flame attachment region. The use of a bigger k_u value can result to a lower temperature in this area.

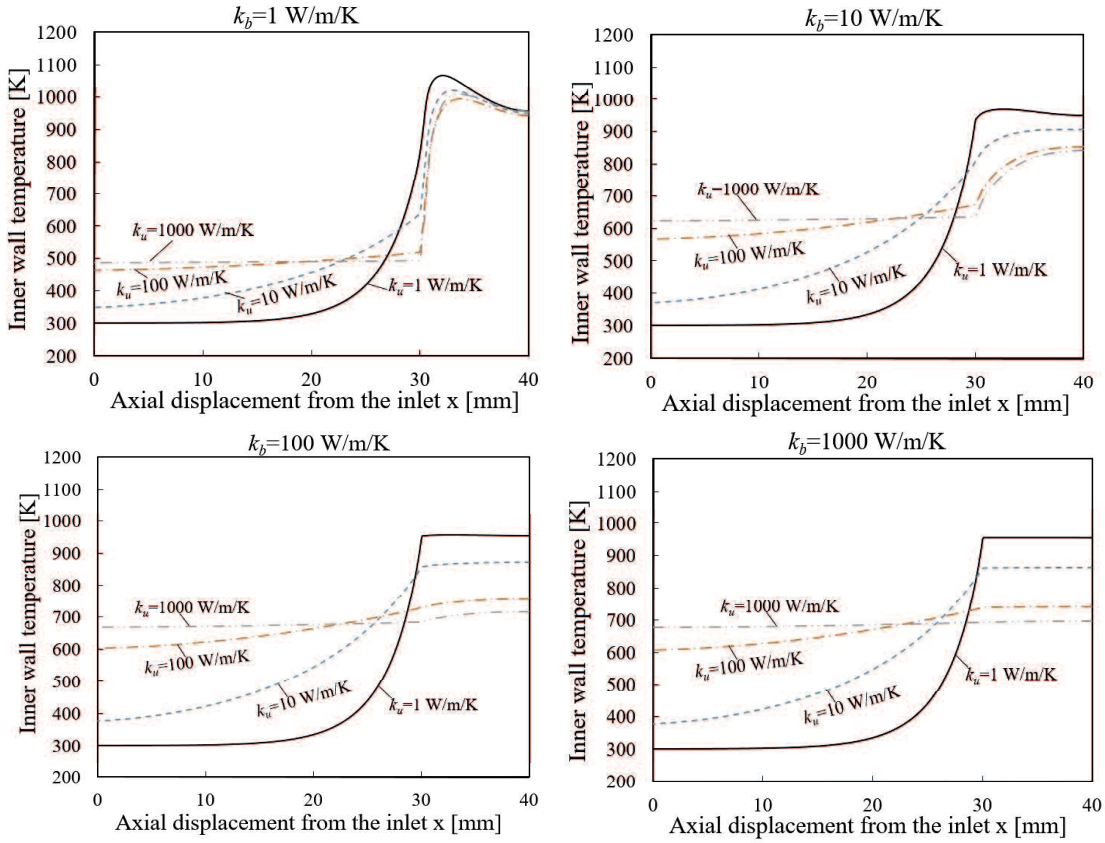

Figure 4.11 Inner wall temperature with different values of k_u for U=30 cm/s and ϕ=1.0

Consequently, the blowout limit is decreased. However, it is observed from the results that for the combustor with k_b=1 W/m/K, the blowout limit does not change dramatically with the increase of k_u. It is important to note that at near blowout conditions, the flame is slightly displaced towards the downstream. For the combustor with k_u=1 W/m/K and k_b=1 W/m/K, the flame is located at 32.2 mm from the inlet when U is increased to 32 cm/s (the blowout limit is 33 cm/s). There is possibility that the elevation of the inner wall temperature has no effect on the flame stability at this near blowout condition.

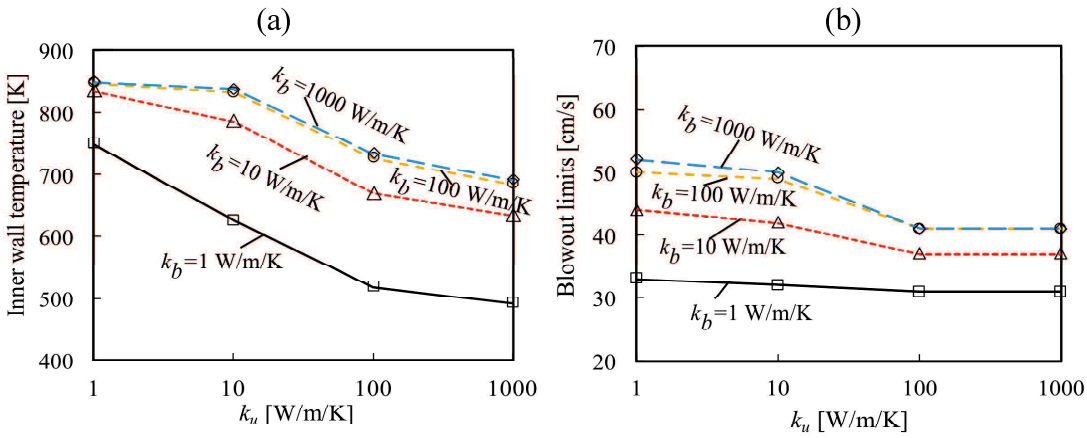

Figure 4.12 Inner wall temperature with different values of k_b at x=29.5 mm for U=30 cm/s and ϕ=1.0 (b) Blowout limits with different values of k_b for ϕ=1.0.

Meanwhile, the combustion efficiency with respect to the wall thermal conductivity is presented in Fig.4.13. Since there are limited number of species in a numerical model with one-step combustion chemistry, the only way to calculate the combustion efficiency is by determining the ratio between the mass fractions of propane at the outlet and at the inlet. This method has also been proposed by Jianlong et al.[123].

$$\text{Combustion efficiency} = 1 - \frac{mass\ fractions\ of\ C_3H_8\ at\ the\ outlet}{mass\ fractions\ of\ C_3H_8\ at\ the\ inlet} \tag{4-11}$$

The combustion efficiency for the combustor with wall thermal conductivity k_b of 1000 W/m/K is not shown in the graph as it has the same tendency as the combustor with k_b=100 W/m/K. It can be seen from the figure that there is an inverse relationship between the wall thermal conductivity k_u and the efficiency. Jianlong et al. [32] demonstrated that the combustion efficiency for a micro combustor depends on the inlet velocity, heat losses and flame temperature. Thus, this variation of combustion efficiency is mainly due to the transverse heat loss to the ambient air with the use of higher wall thermal conductivity. Nevertheless, the efficiency change is relatively small.

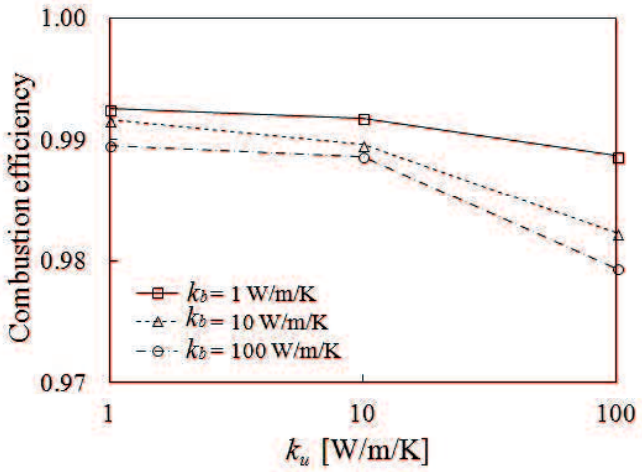

Figure 4.13 Combustion efficiency with different values of k_u and k_b for U=20 cm/s and ϕ=0.90

4.2 Experimental setup

In the experiment, meso-scale combustors made of straight cylindrical tube were used. Each type of combustor was made of two-piece tubes. A stainless steel wire mesh was placed in between the two-piece tube dividing between the upstream and the downstream area (shown in Fig.4.14).

The mesh type was 60 mesh/in with wire diameter of 0.14 mm. In order to adhere the parts together, a heat resistant ceramic adhesive (Ceramabond 569, Aremco Product Inc.) was used. The inner diameter of the tube was 3.5 mm with wall thickness of 0.7 mm. The length from the mesh to the upstream part of the tube is defined as the unburned gas region length L_u. On the other hand, L_b is defined as the burned gas region length, which is the length between the mesh to the downstream part of the tube. The other parameter involved was the wall thermal conductivity in the unburned gas region. This wall thermal conductivity is assigned to be k_u. On the other hand, the material used for the burned gas region was fixed to quartz. The ambient temperature was 295 K, which was maintained at 100 mm horizontally away from the combustor wall. Propane (C_3H_8) and air were mixed and supplied into the combustor with an equivalence ratio of ϕ and a corresponding cross-sectional-area mean flow velocity of U. A mass flow controller (SEC-E440J, HORIBASTEC) was used to precisely control each flow rate of air and fuel.

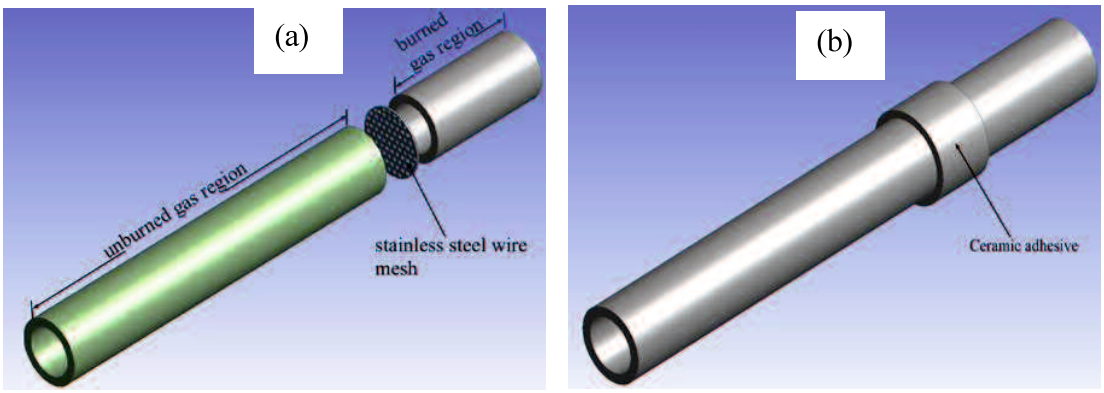

Figure 4.14 Sketch diagram of the combustor (a) exploded view (b) assembly view

The ignition of the flame inside the combustor was done by introducing spark at the exhaust outlet. Once ignited, the flame propagated to the upstream and flame stabilization limits were recorded. For this experiment, a stable flame is defined as the flame that stabilizes near the wire mesh. Wall temperatures in the unburned and burned gas region were measured using an infra-red thermal camera (AVIO InfReC R300R). All combustors have the same unburned gas region length L_u, which is 30 mm. This length is adequate for the flow to be fully developed. In addition to that, since the combustor is connected to a copper tube (fuel supply line), it is important to have a reasonable length from the mesh to the connecting point. If the distance is too close, there is possibility that the heat from the wire mesh is conducted via the burner wall all the way to the copper tube. This leads to the undesirable effects of reactants being pre-heated before flowing into the combustor. Consequently, inaccuracies of results may occur. The value of L_b for all combustors is maintained to be at 10 mm. This value is appropriate considering the practical geometry of a meso-scale combustor. Moreover, varying the value L_b has no significant effect to the flame stabilization limits as demonstrated by Munir et al. [124].

In general, for this type of combustor, blow-off occurs at lean and rich regions. The extinction and the blow-off regions for this type of combustor have been well discussed in details by Mikami et al. [125]. For hydrocarbon gaseous combustion, there are two options of fuel type namely methane (CH_4) and propane (C_3H_8). Propane is preferred since it gives better flame stabilization limits than methane as shown in Fig.4.15.

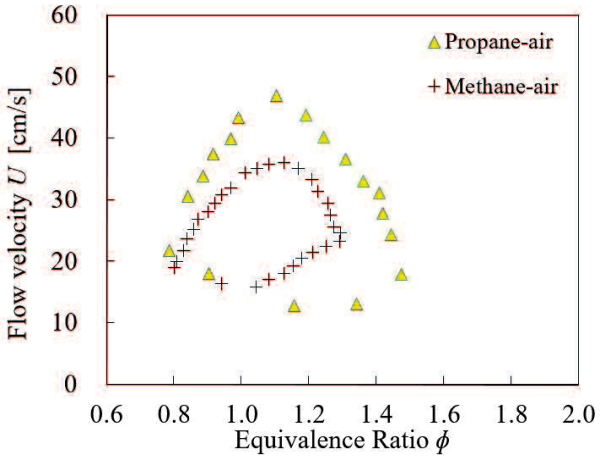

Figure 4.15 Flame stabilization limits with different types of fuel

4.2.1 Effects of wall thermal conductivity in the unburned gas region

The value of the wall thermal conductivity (k_u) in the unburned region was varied. This variation can be achieved by changing the material of that particular region. Type A combustor utilizes quartz as the material in the unburned gas region while Type B and C use brass and copper respectively. All combustors have the same values of L_u and L_b that is 30 mm and 10 mm respectively. The wall thickness and the inner diameter were also made constant. The typical value of thermal conductivity (k_u) for quartz, brass and copper is 1.6 W/m/K, 100 W/m/K and 400 W/m/K respectively [126]. Figure 4.16 shows an image of one of the combustors that is Type B. No parts of the combustors were insulated.

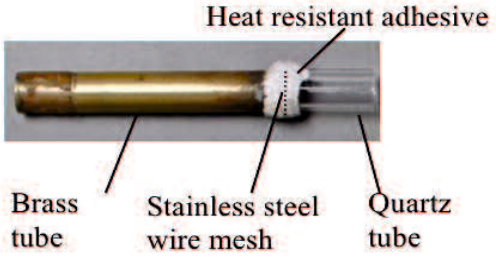

Figure 4.16 The image of Type B (brass) combustor

The flame stabilization limits are presented in Fig.4.17. Type A combustor has the widest flame stabilization limits while Type B has the narrowest limits. In meso-scale combustor, the axial heat transfer via the wall is considered as the primary mechanism of flame stabilization [127]. In other words, heat is re-circulated from the hot burned gas to the unburned gas region, which enables the incoming reactants to be pre-heated and flame stability can be significantly improved. Thus, increasing the wall conductivity

should have resulted in better flame stabilization limits. This is a possible reason why Type C has better flammability limits than Type B. However, this condition is not necessarily true for Type A, which has low wall thermal conductivity. In Type A combustor, the flame stability limits are wider than those of the other two combustors. This phenomenon suggests that the steel wire mesh inside the combustor plays a vital role in contributing to this better flame stability. The wire mesh helps to transfer much of the heat from the burned gas to the unburned gas region. Figure 4.17 also shows that at high wall thermal conductivity, transverse heat transfer across the burner wall is likely to be more dominant than the axial heat transfer to the upstream.

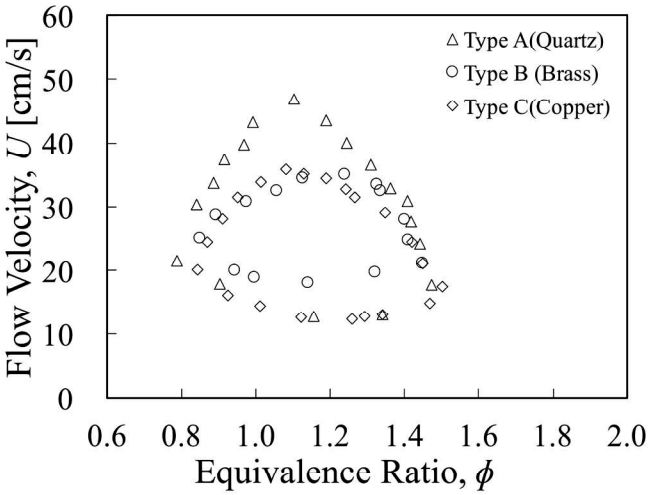

Figure 4.17 Flame stabilization limits for Type A, B and C combustor

The wall surface temperature along the unburned gas region for each combustor was measured using an infrared thermal camera. For this purpose, combustor Type A and Type B were chosen as the samples. The corresponding emissivity used for Type A and Type B is 0.90 and 0.64 respectively. The average wall surface temperature distribution along the axial distance in the unburned gas region for each combustor is plotted in the graph as depicted in Fig.4.18. This distance starts 4 mm from the inlet considering the clearance needed between the fuel supply connecting point and the combustor inlet. As shown in the figure, the temperature gradient for Type A combustor is steeper than that for Type B. This suggests that there is potentially a higher number of hot spots in combustor Type A than Type B despite its better flame stability limits.

Next, insulators were installed in the unburned gas region for all combustors. The type of insulator used was of fiberglass sheet (AS ONE 6-9773-01). The thickness of the insulator was made constant at 2.0 mm while the length was 24 mm. This insulator was

wrapped around the unburned gas region except for the ceramic adhesive part and the connecting area of the fuel supply line. Experiments were conducted again for all types of combustor.

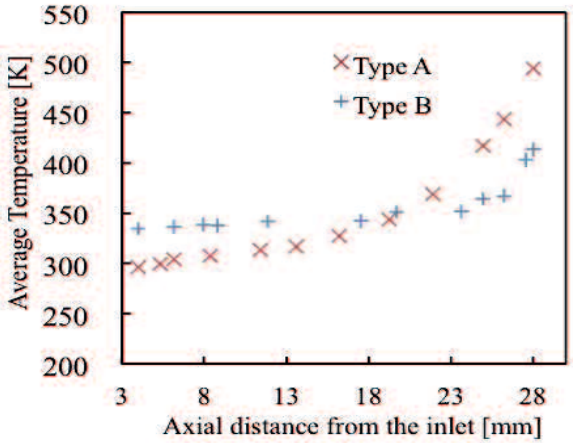

Figure 4.18 Wall surface temperatures distribution in the unburned gas region along the axial distance (centerline) for Type A and Type B

Flame stabilization limits were obtained and shown in Fig.4.19. The results presented in the figure suggest that by insulating the unburned gas region of a combustor with low wall thermal conductivity such as in the Type A combustor, there is little effect on the flame stability (shown in Fig.4.19 (a)). However, in the Type B combustor, there is a sharp increase in the limits, especially in term of the maximum flow velocity attained before the flame is blown out. Moreover, the extension of limits is higher than in Type C, which indicates that the heat loss across the wall in Type B is lower than that in Type C.

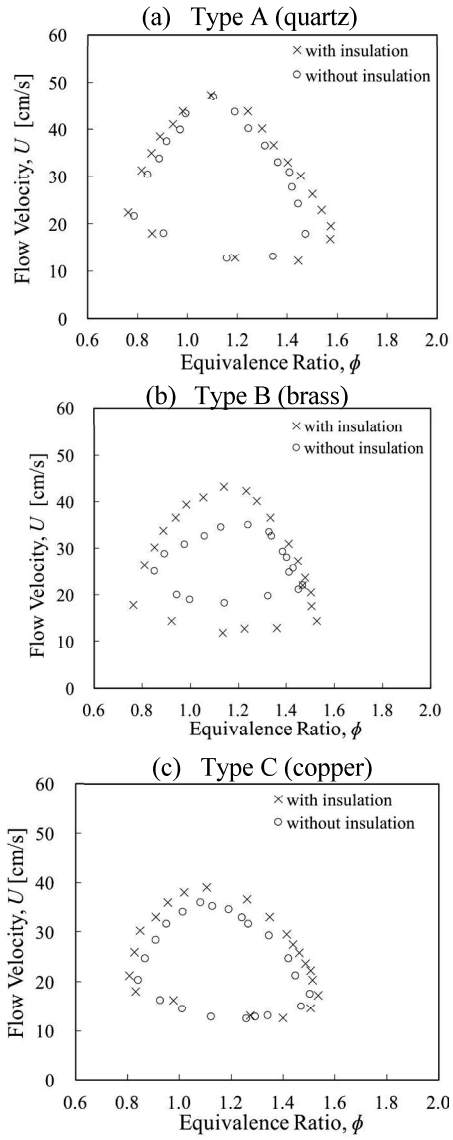

Figure 4.19 Flame stabilization limits for Type A, B and C with insulations effects

4.2.2 Wall surface temperature in the burned region

Wall surface temperature is an important criterion for a meso-scale combustor. A uniform and stable temperature is required for a good combustor. In a combustor with wire mesh, flame stabilizes in the burned gas region. Thus, high a temperature is recorded on the wall surface in this region. Therefore, it is essential to investigate the effects of wall thermal conductivity in the unburned gas region on the wall surface temperature in the burned gas region.

Initially, the effect of inlet velocity on the maximum wall surface temperature was examined. This relationship is important in designing a micro power generation system

that utilizes this type of combustor. For this purpose, the Type A combustor was chosen as the sample. The equivalence ratio was set to stoichiometric because the highest temperature is generally achieved at this particular value. No insulation was installed on any part of the combustor. As depicted in Fig.4.20, there is a direct relationship between the flow velocity and the maximum wall surface temperature. This phenomenon is possibly due to flame interaction with the wire mesh. At high velocity, the distance between the flame and the mesh is likely to increase even though this increment is relatively small. For a meso-scale combustor, even a small increase in this distance could result in significant changes. Since the distance has increased, there is less heat conducted by the wire mesh, which results in a reduction of heat loss. As a result, the flame temperature might increase along with the wall surface temperature.

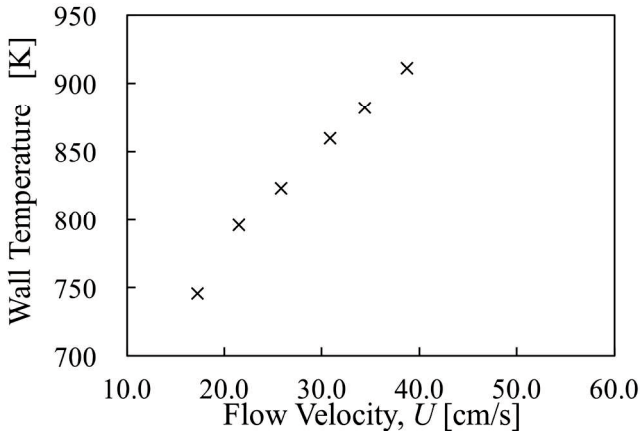

Figure 4.20 Maximum wall surface temperature in the burned region for Type A (ε=0.90 ϕ=1)

Next, the wall surface temperature in the burned region without insulation for each combustor was measured and the results are presented in Fig.4.21. As illustrated in the figure, Type A has the maximum wall surface temperature with a value of 523°C. Meanwhile, the maximum wall surface temperature for Type B and Type C is 476°C and 420°C, respectively. These results indicate that the wall surface temperature in the burned region is also affected by the wall thermal conductivity in the unburned gas region.

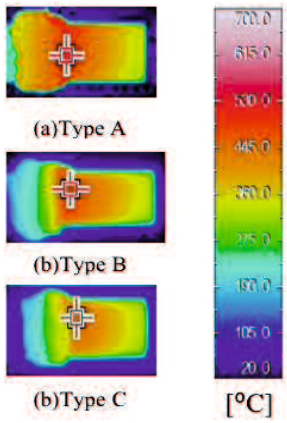

Figure 4.21 Wall surface temperature of the burned gas region for Type A, B and C in Degree Celsius (The cross-mark indicates the location of maximum wall temperature)

4.2.3 Optimization of the combustor performance

Insulation on the outer surface of the unburned gas region might reduce the combustor capability of converting thermal energy. This reduction is possibly due to the fact that there is less hot area available for external heat transfer. In order to satisfy the need for high power devices and a wide range of operational limits, the heat loss across the combustor wall should be minimized without the use of insulators. Type B-1 and C-1 combustors were fabricated while considering this problem. Figure 4.22 shows an image of the Type B-1 combustor. A three- piece tube was combined together using the ceramic heat adhesive.

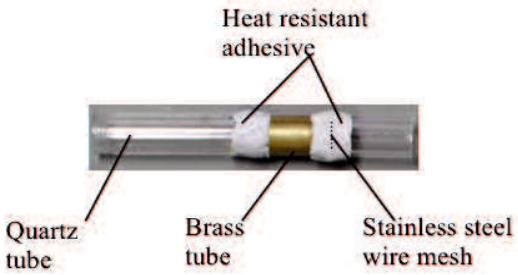

Figure 4.22 The image of Type B-1 combustor

Type B-1 is a combination of quartz, brass and quartz while Type C-1 is a combination of quartz, copper and quartz. A single wire mesh was used. The brass and copper tube length is maintained at 10 mm while the unburned gas region length L_u and L_b are both maintained at 30 mm and 10 mm respectively. The flammability limits of the Type B-1 and C-1 combustors are presented in Fig.4.23. The flame stabilization limits

for Type A are plotted on the same graph for comparison. Both combustors have almost the same flame stability limits. The limits have even increased to be on par with those of the Type A combustor. In fact, there is a slight increase in limits particularly in the rich region. These results indicate that the length reduction has significantly enhanced the flame stability. In other words, the heat loss across the burner wall is minimized.

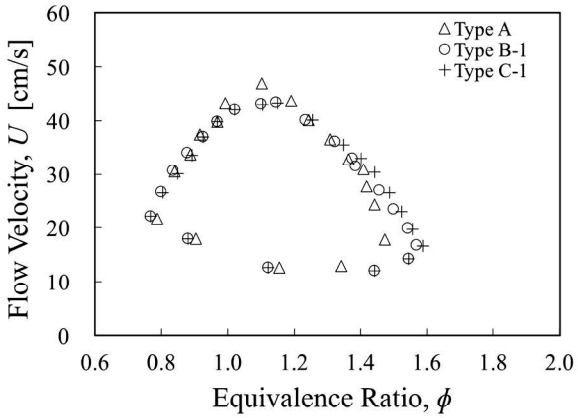

Figure 4.23 Flame stabilizations limit for Type B-1 and C-1 combustor in comparison with Type A

The two-piece type of combustor used in this investigation enabled the wall thermal conductivity in the unburned gas region to be easily varied. Despite the low wall thermal conductivity in the Type A combustor, the flame stability is better compared to that of Type B and Type C. The improvement of the flame stabilization limits is due to the existence of the wire mesh, which plays a vital role in transferring heat from the burned to unburned gas region. However, the experimental results show that the Type A combustor has a high temperature gradient along the wall of the unburned gas region. This might increase the number of hot spots, which can affect the material durability. Type A combustor also exhibits a limited surface area with high a temperature, which is likely to decrease the efficiency of the combustor.

The use of material with high wall thermal conductivity causes the wall surface temperature to be distributed more uniformly. As a result, there is a decrease in the temperature gradient and such condition can enlarge the hot area, which increases the combustor performance. However, the main disadvantage of having high a wall thermal conductivity is the reduction of flame stabilization limits. Although a high thermal conductivity enhances the axial heat transfer to the unburned gas region, the transverse heat transfer offsets this effect. Consequently, the flame stability limits become smaller.

Therefore, in order to have a combustor with considerably wide operational limits but low temperature gradient, modifications are needed in the unburned gas region. The following three-piece types of combustors were fabricated: Type B-1 and Type C-1. The experimental results show that the flame stabilization limits of these combustors is significantly increased. Moreover, these combustors have generally uniform wall temperature distribution in the unburned gas region. In summary, the results obtained in the experiment and simulations allow for optimization of a meso-scale combustor with wire mesh. This vital knowledge can be further used to enhance the flame stabilization of this type of combustor.

4.2.4 Effects of wall thermal conductivity in the burned gas region

The results obtained in the two-dimensional simulation suggest that the use with higher wall thermal conductivity in the burned gas region can enhance the flame stabilization limits. The tube used in the burned gas region is made of brass while quartz is utilized for the unburned gas region. This combustor is specified as quartz-brass tube combustor as shown in Fig 4.24. Meanwhile, the result in terms of flame stabilization limits is illustrated in Fig.4.25.

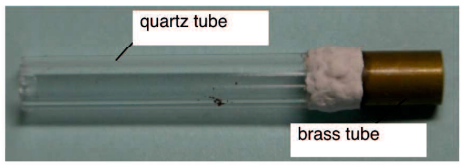

Figure 4.24 Quartz-brass tube combustor

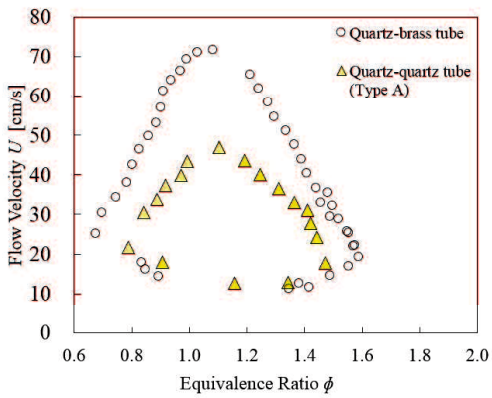

Figure 4.25 Flame stabilizations limit for quartz tube (Type A) and quartz-brass tube combustor

Clearly, it is shown from the figure that there is a significant increase in the limits with the use of higher of wall thermal conductivity in the burned gas region. For further investigation, the material in the unburned gas region is changed from quartz to brass tube as shown in Fig.4.26 and specifed as brass-brass tube combustor. Flame stabilization limits were then determined, which is shown in Fig.4.27. On the same graph, the flame stabilization limits for quartz tube combustor (Type A) and quartz-brass tube combustor are also plotted for the purpose of quantitave comparison.

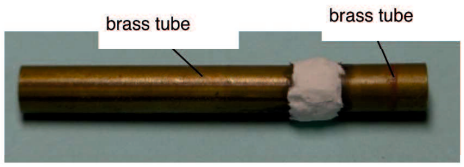

Figure 4.26 Brass-brass tube combustor

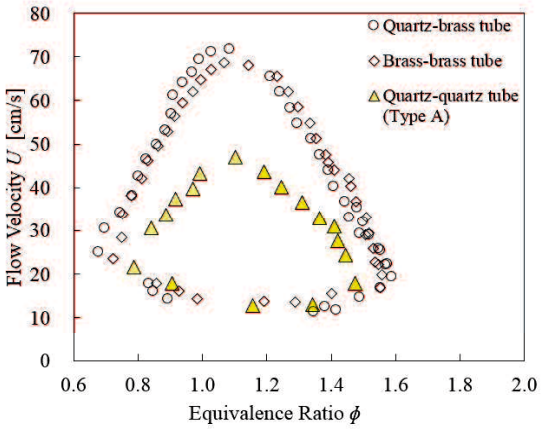

Figure 4.27 Flame stabilizations limit for brass-brass tube combustor in comparison with quartz tube and quartz-brass tube combustor

As depicted in Fig.4.27, it can be deduced that there is only a marginal change of the flame stabilization limits for the brass-brass tube combustor as compared to the quartz-brass tube combustor. Nevertheless, using brass tube combustor in both unburned and burned gas region greatly increases the flame stabilization limits when compared to quartz-quartz tube combustor.

4.3 Summary

The function of the concentric rings is to stabilize the flame at a fixed location. With the use of these rings, it is possible to vary the wall thermal conductivity in the two different regions. In this type of combustor, the wall and gas temperature distribution in the unburned gas region is tremendously affected by the value of wall thermal conductivity. However, the use of a high value of k_u or k_b in which for this case k=1000 W/m/K produces no notable effect on both the wall and gas temperature profile. It is demonstrated that the flame temperature is independent to the wall thermal conductivity. On the other hand, the inlet velocity and the equivalence ratio have a significant impact on the flame temperature, which in turn affects the wall and gas temperature distribution.

It is a well-known fact that the utilization of low wall thermal conductivity values leads to the high temperature gradients that eventually contributes to hot spot related problems. Thus, by establishing the two separate regions of wall thermal conductivity, the problems related to the high thermal stress could be minimized without compromising the combustor efficiency. The blowout limits greatly depend on the wall thermal conductivity. The blowout limits are significantly affected by the inner wall temperature particularly in the area just before the ring position. The increased inner wall temperature at such a position conceivably increases the local burning velocity at the flame attachment region. The use of higher wall thermal conductivity in the unburned gas region brings down the value of the inner wall temperature in the area just before the ring position. As a result, the blowout limits are also reduced. It is also demonstrated that the combustion efficiency is influenced by the variation of the wall thermal conductivity k_u. The use of a combustor with a low value of k_u can improve the combustion efficiency. However, other critical factors such as the outer wall temperature and the blowout limits should also be considered before selecting the appropriate wall thermal conductivity.

Generally, even though there is a different of assumptions in the numerical and experimental setup, the results are relatively in the same tendency. Nonetheless, for further investigation, a three-dimensional (3-D) model should be employed in the numerical simulation. This 3-D numerical model is presented in Chapter Five.

CHAPTER FIVE

Combustors with heat recirculation mechanism

One of the approaches to demonstrate the function of the wire mesh in enhancing heat recirculation is by performing numerical simulations. Even though a two-dimensional (2-D) simulation has been conducted as explained in Chapter Four, a three-dimensional (3-D) numerical simulation is essential. In a 3-D model, the stainless steel wire mesh can be modeled as such that it is inter-connected to each other up to the outer wall of combustor resulting to a three directional of thermal path. The novel 3-D numerical model is shown in this chapter where it was utilized to investigate the effect of wall thermal conductivity on the flame stabilization. Apart from that, experiments were also performed to examine the effect of exhaust gas recirculation on the flame stabilization of tube combustors with wire mesh. Important parameters that are difficult to be established through experiments were determined using the developed 3-D numerical model.

5.1 Three dimensional (3-D) numerical setup

A three-dimensional (3-D) numerical simulation of propane-air combustion in meso-scale cylindrical tubes with stainless steel wire mesh is also performed. A two-dimensional (2-D) model is not accurate, as the conductive heat transfer from the center of the wire mesh to the outer wall of combustor could not be represented. The gas, inner wall and wire mesh temperature were investigated. The flame stabilization limits were also determined. Experiments were performed to compare the flame stability limits obtained by the simulation. The surface reaction is excluded in the analysis since there are materials that can resist radical quenching. The main purpose of this study is to demonstrate the capability of the wire mesh and to investigate its effect on the flame stabilization in a tube combustor.

The steady-state numerical simulation was performed using ANSYS Release 14.0 with Fluent 6.3 [118]. The inner diameter of the combustor is 3.5 mm and the wall is 0.7 mm thick. The wall thickness is modeled as a solid phase where only the energy equation is solved. The total length of the combustor is set to 40.2 mm. The combustor is divided

between two parts namely the unburned and burned gas region by a stainless steel wire mesh. The location of the wire mesh is 30 mm, which is measured from the center of the combustor inlet to the left side of the wire mesh. This value is chosen to ensure that the flow will be fully developed before passing through the wire mesh. Three-dimensional (3-D) conductive heat transfer is assumed on the wire mesh with the value of wall thermal conductivity *(k)* is set to 20 W/m/K, which represent the typical value of *k* for stainless steel [8]. To enable the fluid flows and passes through the wire mesh, a number of square-shaped holes with length of 0.28 mm are created. The fuel type used is propane (C_3H_8)-air mixture. The schematic of the computational domain for this simulation is illustrated in Fig.5.1.

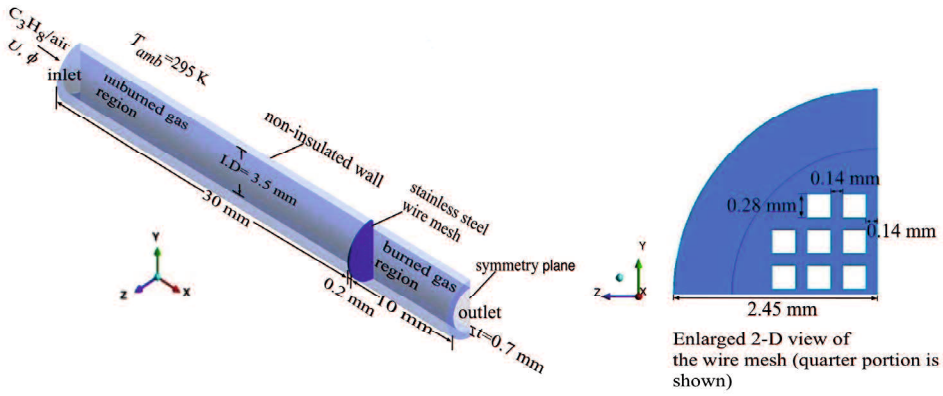

Figure 5.1 Schematic of the computational domain (the figures size is not to scale)

In this work, Dufour, gas radiation effects and the work done by pressure and viscous force are assumed to be negligible. Norton and Vlachos [104, 105] have shown that the gas phase radiation has minimal effect on the combustion reactions. Ideal gas law is assumed for the gas density and the specific heat for all the species is calculated using a piecewise-polynomial fit of temperature. Meanwhile, the specific heat and the thermal diffusion coefficient of the gas mixture are calculated based on the mixing law and kinetic theory. To reduce the computational loads, the gas thermal conductivity, viscosity, and mass diffusivity values of the mixture are assumed to be constant, which are based on Fluent (default values option shown in Table 5.1).

Table 5.1 Values of gas mixture properties by Fluent default option

Thermal Conductivity (W/m.K)	Viscosity (kg/m.s)	Mass Diffusivity (m^2/s)
0.0454	1.72×10^{-5}	2.88×10^{-5}

A reduced one-step propane combustion with five species is employed as the combustion chemistry [119]. The species involved are C_3H_8, O_2, N_2, CO_2 and H_2O. It should be noted that a detail kinetics mechanism is compulsory if simulations are performed to evaluate flame or emission characteristics. However, since the focus this study is to examine the flame stabilization mechanism in this type of combustor, the single step mechanism is sufficient. A non-uniform grid element size is utilized where high grid concentrations are applied in the area surrounding the wire mesh. The total number of elements is 43548 and employed for all cases. A grid dependent test was performed and revealed that greater number of elements yields no significant numerical advantage.

The type governing equations utilized are the typical fluid motion combined with reacting flows. The mass conservation equation (continuity) is given by;

$$\frac{\partial \rho}{\partial t} + \frac{\partial}{\partial x}(\rho u_x) + \frac{\partial}{\partial y}(\rho u_y) + \frac{\partial}{\partial z}(\rho u_z) = S_m \tag{5-1}$$

S_m is the source term (if any). An example of this term is vaporization of liquid or any user-defined source. Nevertheless, in this numerical model, $S_m = 0$. For a steady state condition $\frac{\partial \rho}{\partial t} = 0$. Meanwhile, the momentum conservation equation in x-direction;

$$\frac{\partial \rho u_x}{\partial t} + \frac{\partial (\rho u_x u_x)}{\partial x} + \frac{\partial (\rho u_y u_x)}{\partial y} + \frac{\partial (\rho u_z u_x)}{\partial z} = -\frac{\partial p}{\partial x} - \frac{\partial}{\partial x}\left(\frac{2}{3}\mu(\nabla \cdot \vec{u}) + 2\mu \frac{\partial u_x}{\partial x}\right) + \frac{\partial}{\partial y}\left[\mu\left(\frac{\partial u_y}{\partial x} + \frac{\partial u_x}{\partial y}\right)\right] + \frac{\partial}{\partial z}\left[\mu\left(\frac{\partial u_x}{\partial z} + \frac{\partial u_z}{\partial x}\right)\right] + \rho f_x \tag{5-2}$$

Momentum equation in y-direction is given as;

$$\frac{\partial (\rho u_x u_y)}{\partial x} + \frac{\partial (\rho u_y u_y)}{\partial y} + \frac{\partial (\rho u_z u_y)}{\partial z} = -\frac{\partial p}{\partial y} - \frac{\partial}{\partial x}\left[\mu\left(\frac{\partial u_y}{\partial x} + \frac{\partial u_x}{\partial y}\right)\right] + \frac{\partial}{\partial y}\left(\frac{2}{3}\mu(\nabla \cdot \vec{u}) + 2\mu \frac{\partial u_y}{\partial y}\right) + \frac{\partial}{\partial z}\left[\mu\left(\frac{\partial u_z}{\partial y} + \frac{\partial u_y}{\partial z}\right)\right] + \rho f_y \tag{5-3}$$

Momentum equation in z-direction is given as;

$$\frac{\partial(\rho u_x u_z)}{\partial x}+\frac{\partial(\rho u_y u_z)}{\partial y}+\frac{\partial(\rho u_z u_z)}{\partial z}=-\frac{\partial p}{\partial z}-\frac{\partial}{\partial x}\left[\mu\left(\frac{\partial u_x}{\partial z}+\frac{\partial u_z}{\partial x}\right)\right]+\frac{\partial}{\partial y}\left[\mu\left(\frac{\partial u_z}{\partial y}+\frac{\partial u_y}{\partial z}\right)\right]+$$
$$\frac{\partial}{\partial z}\left(\frac{2}{3}\mu(\nabla\cdot\vec{u})+2\mu\frac{\partial u_y}{\partial z}\right)+\rho f_z \quad (5\text{-}4)$$

where;

$$\nabla\cdot\vec{u}=\frac{\partial u_x}{\partial x}+\frac{\partial u_y}{\partial y}+\frac{\partial u_z}{\partial z}$$

For the energy equation pertaining to the fluid motion, the same equation employed in the Chapter 4, which is Eq. 4.7 is utilized. Energy transfer due to conduction, species diffusion, and viscous dissipation is represented by the energy equation. The source term S_h includes heat of chemical reaction or any other heat sources defined by the user such as gas radiation.

$$\nabla\cdot(\vec{u}(\rho E+p))=\nabla\cdot\left(k\nabla\mathrm{T}-\sum_i h_i\vec{J}_i+(\bar{\bar{\tau}}\cdot\vec{u})\right)+S_h \quad (4\text{-}7)$$

The above Eq.4.7 has already included the pressure work and kinetic energy terms. However, the numerical model is assumed to be incompressible flows and neglects these types of works. Moreover, the selected pressure-based solver by default does not include the pressure work or kinetic energy. For the energy transfer in the solid wall region and the species transport equation, the same equations, which is Eq.4.8 and Eq.4.9 in Chapter Four are employed;

$$\nabla\cdot(\vec{u}\rho h)=\nabla\cdot(k\nabla\mathrm{T})+S_h \quad (4\text{-}8)$$

$$\nabla\cdot(\rho\vec{u}Y_i)=-\nabla\cdot\vec{J}_i+R_i+S_i \quad (4\text{-}9)$$

Boundary conditions that have been successfully demonstrated by the previous researchers are used [106]. No-slip boundary type condition is applied at the interface between the fluid and the solid wall. The heat flux at this interface is calculated using Fourier's law. Heat transfer per unit area by means of convection at the outer surface of the combustor wall is given by:

$$q_{loss}=h_{conv}(T_{wall}-T_{amb})+\varepsilon\sigma(T_{wall}^4-T_{amb}^4) \quad (5\text{-}5)$$

Where h_{conv} is the convective heat transfer coefficient, T_{wall} is the wall temperature of the combustor and T_{amb} is defined as the ambient temperature. The value of T_{amb} is initialized to 295 K. The value of h_{conv} is fixed to be at 5 W/m^{2}K, which represent a

weak natural convection [106]. The external emissivity (ε) for the outer wall of the combustor and the wire mesh is set to 0.90 and 0.70 respectively. The value of Stefan-Boltzmann constant (σ) used is $5.67 \times 10^{-8} \mathrm{W/m^2K^4}$. A thermal insulation (zero heat flux boundary) is applied at both left and right wall edge of the combustor. The value of k for the tube combustor is set to 1.6 W/m/K, which represents the typical value of k for a quartz tube. For the outlet boundary condition, a fixed pressure inlet is applied. A symmetrical boundary condition is established at the origin of z-plane so that the calculation can be performed only in half of the domain. The thermodynamic properties and gas transport data are obtained from Kutz [128] and Fluent internal database [118]. The values of thermodynamics properties for solids used in the numerical model are summarized in Table 5.2.

Table 5. 2 Values of thermodynamic properties for solids used in the model

Material name	Wall thermal conductivity, k (W/m.K)	Specific heat C_p (J/kg.K)	Density, ρ (kg/m^3)
Quartz	1.6	800	2500
Stainless steel	20	510	7900

A laminar flow of U with a flat velocity profile is applied at the inlet while the inlet feed temperature is initialized at 295 K. No swirl flow of velocity is applied. To ignite the propane-air mixture in the combustor, the value of U is first set to 20 cm/s and the equivalence ratio (ϕ) is fixed to 1. A technique that is called as “cold flow” is employed where the momentum and continuity equation is first solved. Then, by patching a high temperature around an area that can be defined as patch zone, the energy and species equations are then solved. This patch zone is located at 2.5 mm from the outlet and should not be placed too close to the outlet since it can result to a reverse gas flow that negatively affects the ignition process. A sufficiently high temperature of 1600 K is applied in the patch zone to ensure that the fuel- air mixture can be ignited. Once ignited, the flame propagated to the upstream and eventually stabilized near the wire mesh. To obtain the blowout limits, the U value is gradually stepped up with 5 cm/s interval. If the new value of U causes the flame to propagate to the outlet, then the process is started again with the previous U value. The increment is then reduced to 1 cm/s interval until the flame is blown out of tube. The maximum value of U before the flame is blown out is considered as the blowout limit. As for determining the extinction limit, the value of

U is gradually reduced with 1 cm/s interval. The lowest value of U before the flame extinct is defined as the extinction limit.

5.1.1 Combustion in tube combustors with stainless steel wire mesh

Flame propagation in a narrow channel is a broad subject matter. Investigation of flame propagation characteristics in a narrow channel tube combustor is indeed a formidable task. In order to numerically study the phenomenon of flame propagation inside a meso-scale tube combustor, a detailed kinetics reaction mechanism is required that can lead to higher computational cost. Therefore, results shown in Fig.5.2 are only limited to demonstrate the capability of the wire mesh.

The ignition was attained by applying a sufficiently high temperature on the patch zone. This ignition method replicates the experimental condition reported by Mikami et al. [73]. Since the flame burning velocity is faster than the inlet velocity, the flame propagated towards the inlet once it was ignited. As shown in Fig.5.3, the flame stopped to propagate when it reached the wire mesh and stabilized there until a converged solution was achieved. This condition is defined as a stable flame. The wire mesh acts as a flame holder by which the flame can be stabilized at a fixed location.

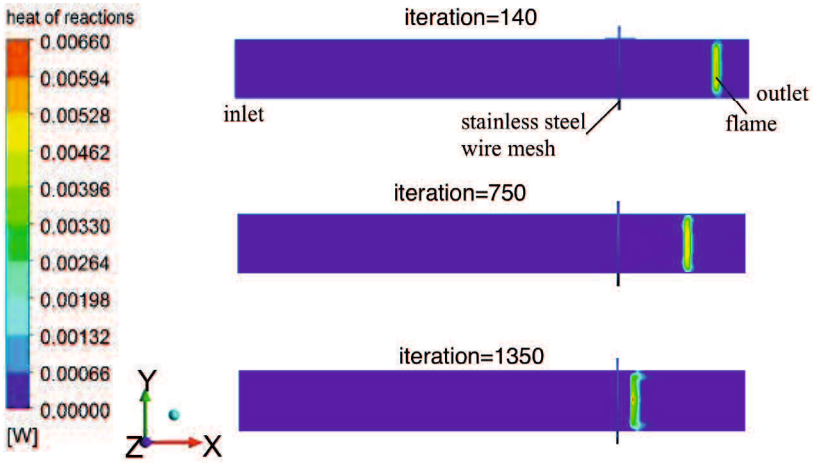

Figure 5.2 Heat of reaction contours with different values of iteration number for ϕ=1.0 and U=20 cm/s, taken at z-plane=0.28 mm

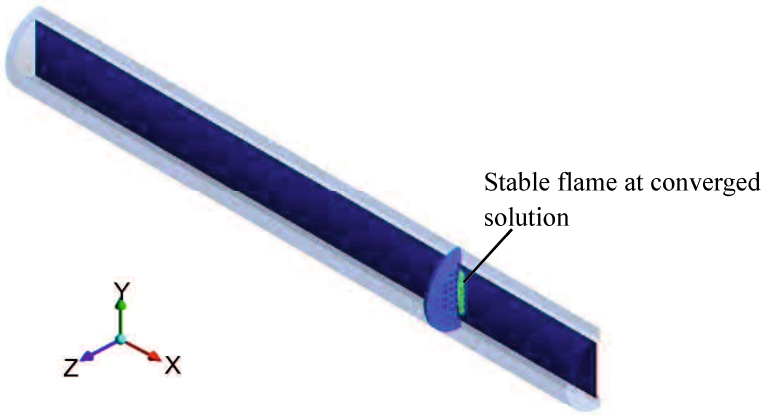

Figure 5.3 Stable flame near the stainless steel wire mesh for ϕ=1.0 and U=20 cm/s

Figure 5.4 shows the temperature of gas and inner wall along the centerline of the combustor. Meanwhile, the temperature contours of the combustor and wire mesh are

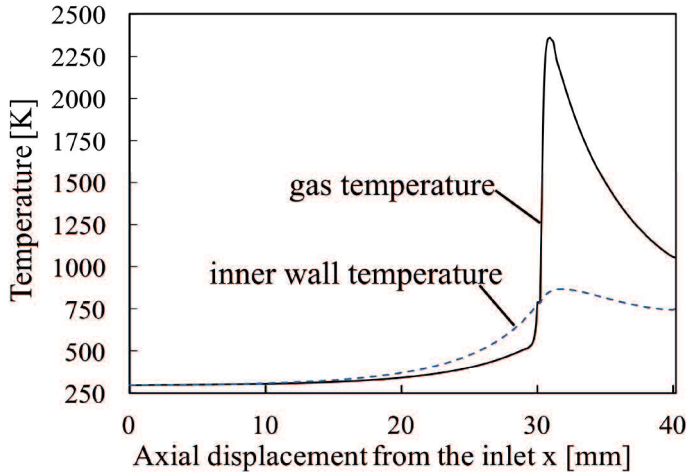

Figure 5.4 Gas and inner wall temperature distributions along the x-axial displacement (coordinate line y=0 mm & 1.75 mm, z= 0 mm & 0.875mm) for ϕ=1.0 and U=20 cm/s

shown in Fig.5.5. It is shown in the figure that the inner wall temperature becomes higher than the gas temperature in the unburned gas region starting from x=20 mm onwards. This elevation suggests that the heat is conducted from the hot burned gas to the unburned gas region via both the inner wall and the wire mesh. The higher temperature at the center of the wire as shown in Fig.5.5(b) indicates that the preheat zone of the flame is in contact with the wire mesh. The corresponding maximum heat release rate for this condition is located at 0.21 mm from the wire mesh. Note that this maximum heat release rate occurs in the reaction zone of the combustion.

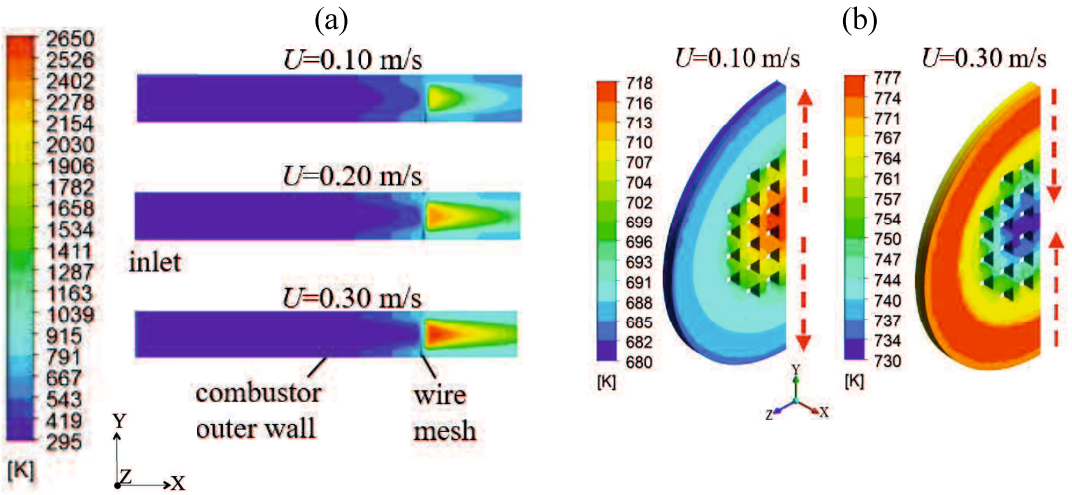

Figure 5.5(a) 2-D view of the temperature contours of the combustor for ϕ=1.0 (b) Surface temperature contours of the wire mesh for ϕ=1.0(the arrows show the thermal path direction)

Flame stabilization limits are also numerically examined. Blowout and extinction limits are the example of flame stabilization indicators in meso and micro-scale tube combustors. Both limits for this type of combustor are presented in Fig.5.6. In order to ensure that the numerical model is credible, experiments were also conducted to determine the stability limits. The similar experimental configuration as explained in Chapter 4 is utilized. The results obtained from the experiment are plotted on the same graph. The predicted value of the blowout limit at ϕ=1.0 is U=46 cm/s, which is higher than the experimental result.

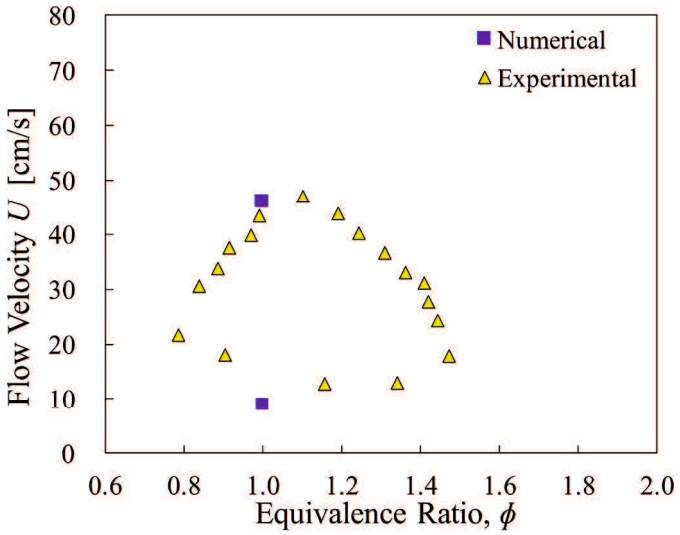

Figure 5.6 Flame stabilization limits for numerical simulation with respect to experimental results

On contrary, a reverse pattern is observed for the extinction limit. These notable differences are mainly due to the reduced one-step propane reaction that has over predicted the flame temperature. Meanwhile, Fig.5.7 illustrates the surface temperature of the wire mesh for different values of *U*. It can be seen from the figure that at *U*=10 cm/s and *U*=20 cm/s, the wall temperature at the center part of the wire mesh is higher than the outer mesh wall. Consequently, the transfer of heat from the hot burned gas to the ambient air via the wire mesh is intensified. A further reduction of *U* could potentially lead to the flame extinction. On the other hand, as the value of *U* is increased to 30 cm/s and 40 cm/s respectively, the opposite trend occurs. A sufficiently high inlet velocity causes the stable flame to slightly displace away from the wire mesh. For instance, for *U*=30 cm/s, the maximum heat reaction rate is located at 0.5 mm from the wire mesh. As a result, the direct heat transferred from the flame to the wire mesh is reduced. At this condition, the inner wall of the combustor plays the effective role of circulating the heat from the burned gas to the wire mesh and unburned gas region.

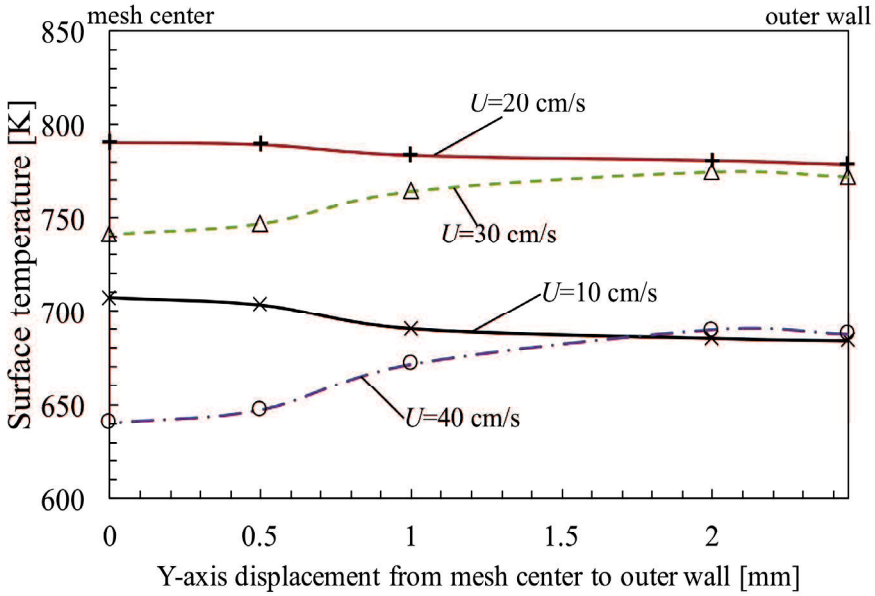

Figure 5.7 Surface temperature of the wire mesh along the y-axis line (coordinate is x=30.2 mm, z=0 mm) for different values of *U* with ϕ =1.0

Meanwhile, Fig.5.8 presents the blowout conditions when the inlet flow velocity was changed from 46 cm/s to 47 cm/s whereas Fig.5.9 shows the phenomenon of extinction at a low flow velocity. As shown in Fig.5.9, the combustion cease to exist at *U*=8 cm/s. The flame extinction occurs mainly due to numerous heat losses to the ambient.

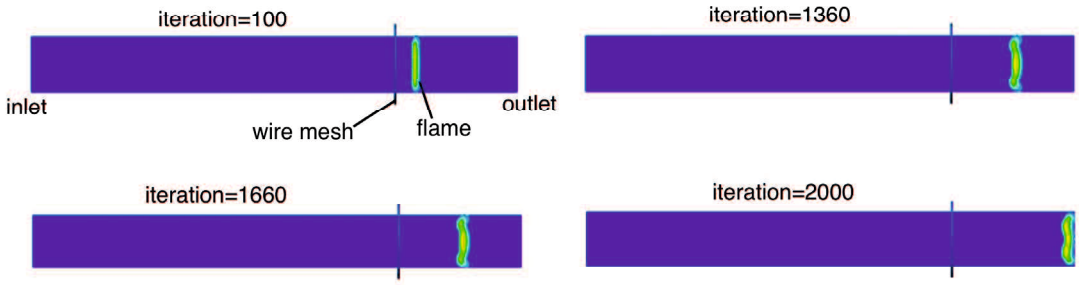

Figure 5.8 Heat of reaction when U is increased from 46 cm/s to 47 cm/s with ϕ=1.0

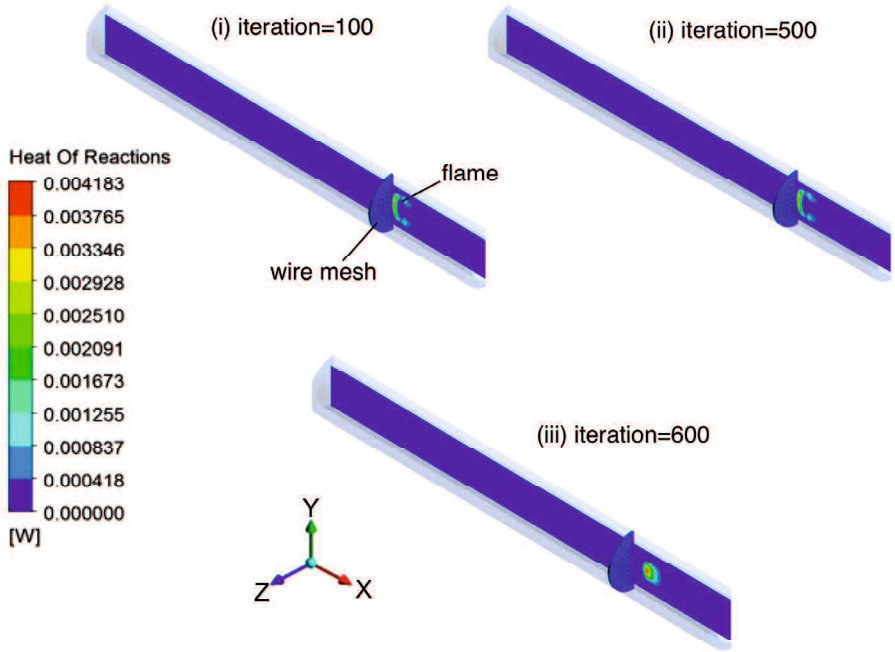

Figure 5.9 Heat of reaction for ϕ=1 when U was changed from 9 cm/s to 8 cm/s

5.1.2 Effect of thermal path between the stainless wire mesh and the inner wall on the blowout limit

In order to investigate the effect of the wire mesh on the blowout limit, the geometry of the wire mesh is modified. The modified wire mesh has a small gap in between the inner wall. This gap is set to 0.20 mm as presented in Fig 5.10. The blowout limit for the modified wire mesh is then numerically determined and shown in Fig.5.11. From the graph, the predicted value of the blowout limit is 34 cm/s. The corresponding wire mesh temperature with and without modification is shown in Fig.5.12. As seen in the figure,

the drop in temperature surrounding the center part of the wire mesh is one of the reasons for this reduction of limit.

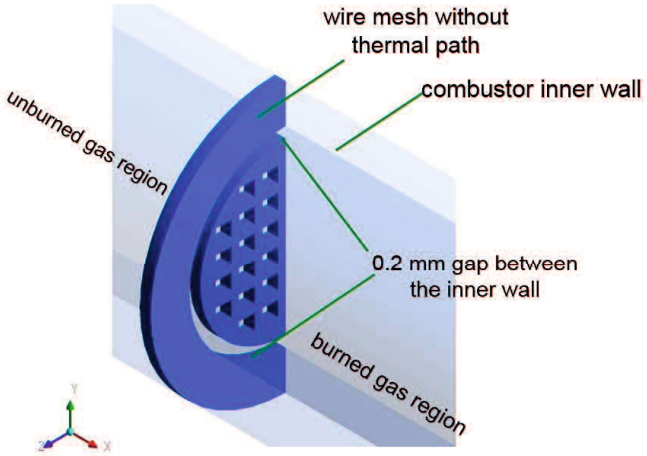

Figure 5.10 Wire mesh without thermal path (enlarged scale)

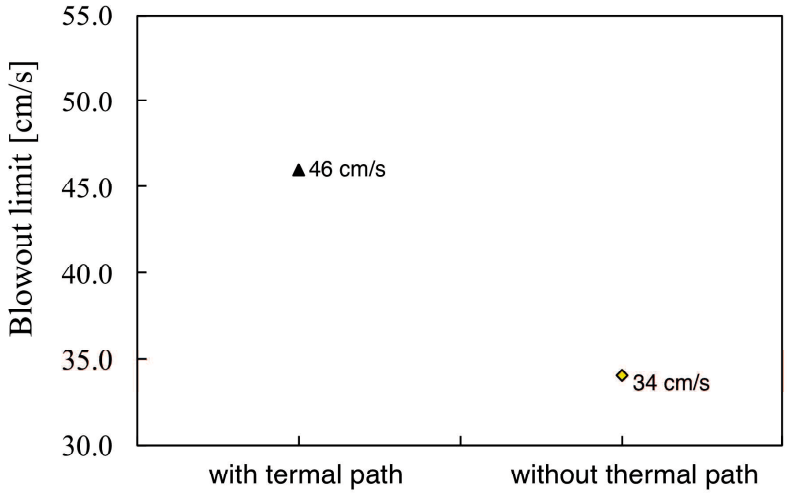

Figure 5.11 Blowout limits of wire mesh with and without thermal path for ϕ=1.0

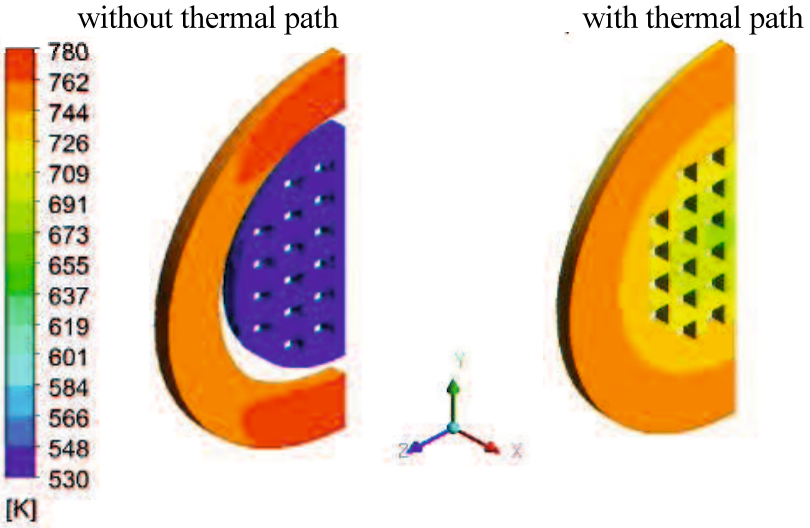

Figure 5.12 Surface temperature contours with and without thermal path with U=34 cm/s and ϕ=1.0

However, by having such a gap, the flow of the gas is also affected as shown in Fig.5.13. The flow changes might affect the results. Thus, to isolate this effect of flow change, the slit area is declared as a solid with a low wall thermal conductivity as depicted in Fig.5.14. The value of thermal conductivity (k) used is 0.0454 W/m/K, which equivalent to the thermal conductivity of propane-air mixture. The blowout limits for this new condition is determined and presented in Fig.5.15.

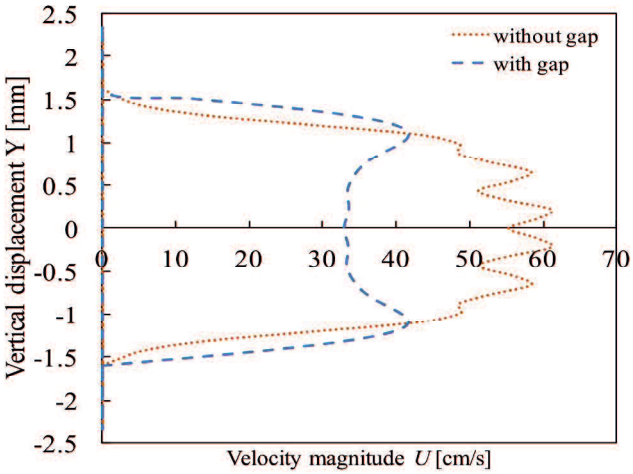

Figure 5.13 Velocity magnitude for cold flow simulation taken at x=31 mm for U=30 cm/s

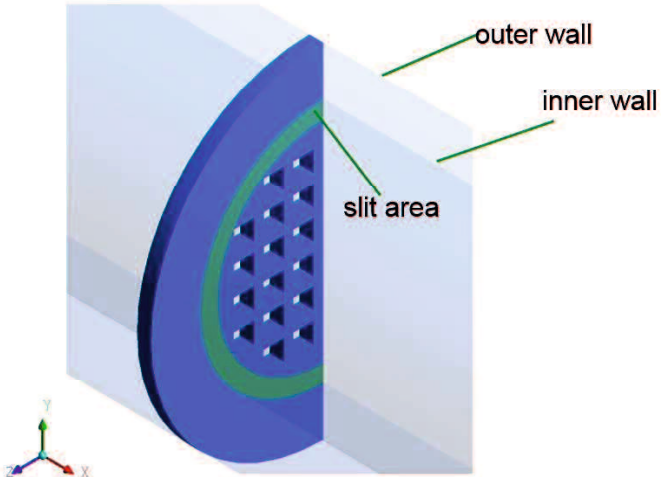

Figure 5.14 The slit or gap is declared as a solid

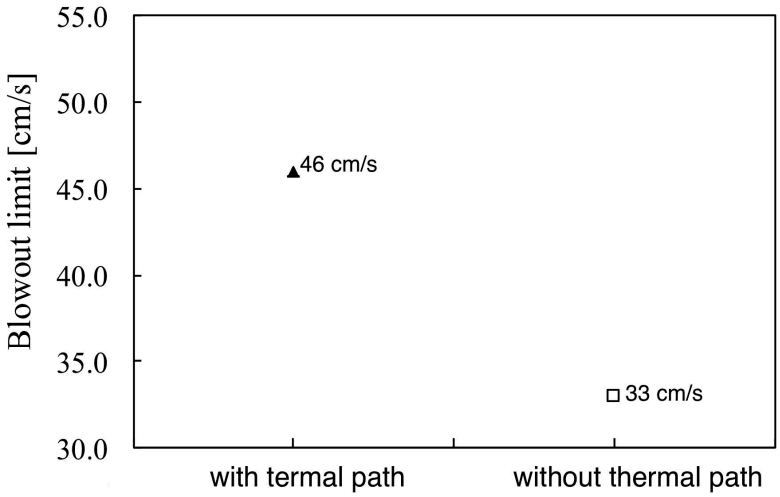

Figure 5.15 Blowout limits with the new condition for ϕ=1.0

With this new condition, the blowout limit is also significantly reduced. The reduction of the limits is mainly due to the decrease of the surface temperature around the center part of the wire mesh as depicted in Fig.5.16. There is a temperature different about 150 K between the center and outer part of the wire mesh.

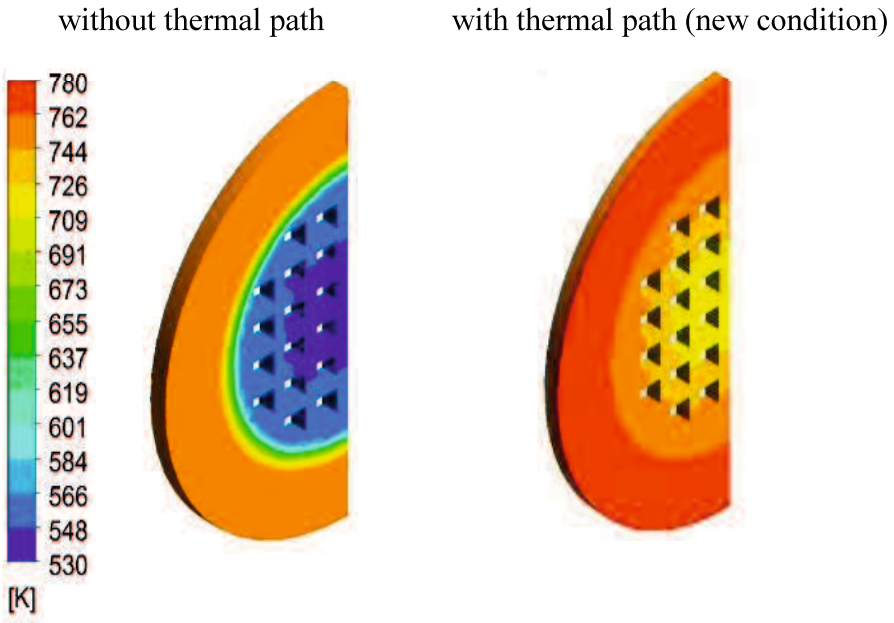

Figure 5.16 Surface temperature contours with and without thermal path with new condition for U=32 cm/s and ϕ=1.0

The presented numerical model can sufficiently represent the propane-air combustion in this type of combustor. At a low inlet velocity, the stabilized flame is located in close proximity to the wire mesh. In fact, the pre-heat zone of the flame is already in contact with the wire mesh. As a result, the transfer of heat from the hot burned gas to the combustor walls and ambient air is intensified. Further reduction of the inlet velocity can potentially lead to the flame extinction.

On the other hand, a sufficiently high inlet velocity but within the blowout limit slightly shifts the stable flame away from the wire mesh. As a result, the pre-heat zone of the flame is no longer in contact with the wire mesh. As such, the inner wall of the combustor dominates the role of recirculating the heat from the hot burned gas to the center part of the wire mesh and the unburned gas region. This heat recirculation enhances the flame stabilization in the combustor. The effect of wire mesh on the flame blowout limit is also numerically investigated. By having a small gap between the inner wall of the combustor and the center part of the wire mesh, the heat from the burned gas region could not be efficiently transferred from the inner wall to the unburned gas region. As a result, the temperature around the center part of the wire mesh decreases. Consequently, the blowout limit is significantly reduced.

5.1.3 Three-dimensional (3-D) numerical investigation of the effect of combustor wall thermal conductivity on the flame stabilization

In the previous section, the significant role of stainless steel wire mesh in enhancing the flame stabilization limits has been shown numerically. In this section, the same three-dimensional (3-D) numerical model is utilized to investigate the effect of combustor wall thermal conductivity on the flame stabilization. The wall thermal conductivity (k) in the unburned (k_u) and burned gas region (k_b) is varied from 1.6 W/m.K, 100 W/m.K and to 400 W/m.K respectively. These are the typical values of k for quartz, brass and copper respectively. The results in term of gas temperature contours, outer wall temperature and wire mesh temperature are presented in Fig.5.17 to 5.20.

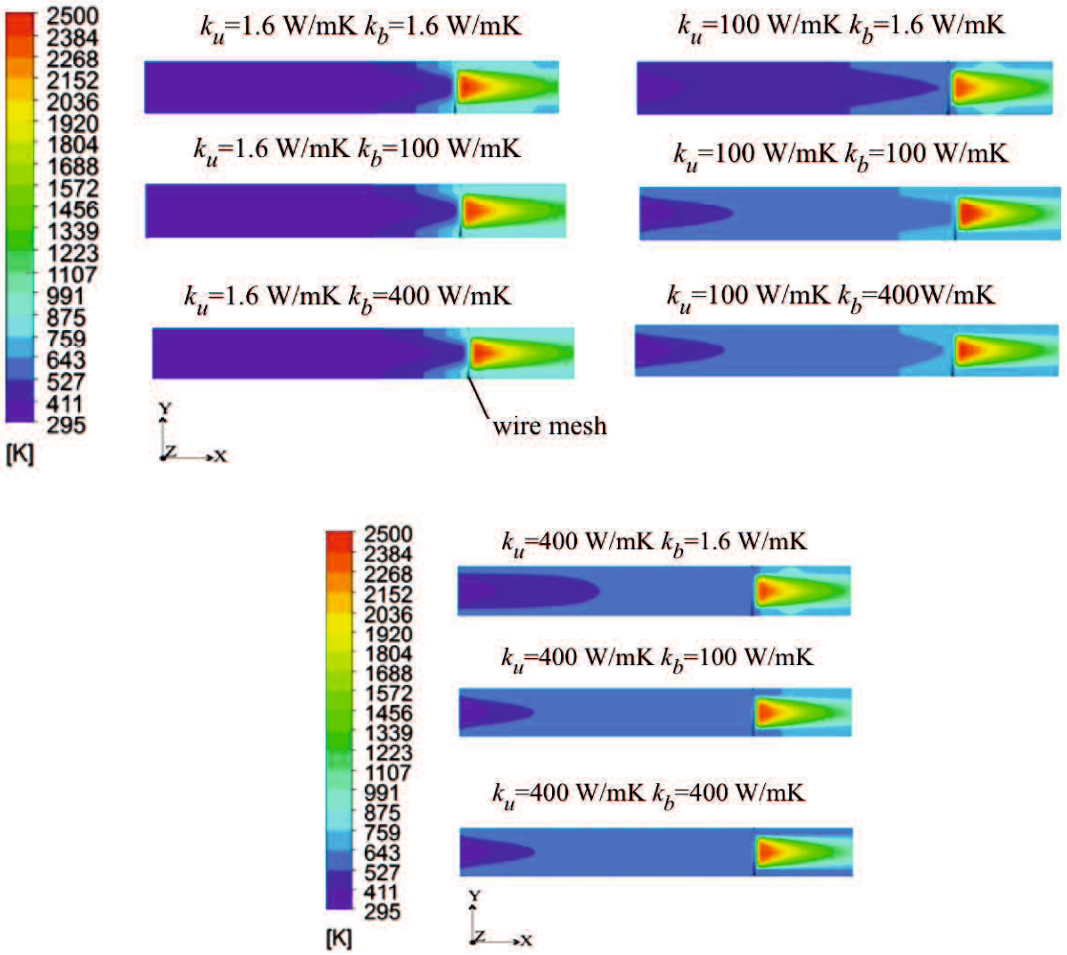

Figure 5.17 Gas temperature contour of the combustor h different values of k_u and k_b for U=20 cm/s and ϕ =1.0

As shown in Fig.5.17 and Fig.5.18, the use of higher wall thermal conductivity in both unburned and burned gas region results to an increase in the unburned gas temperature. However, there is no significant increase of unburned gas temperature if the value of k is shifted from 100 W/m/K to 400 W/m/K.

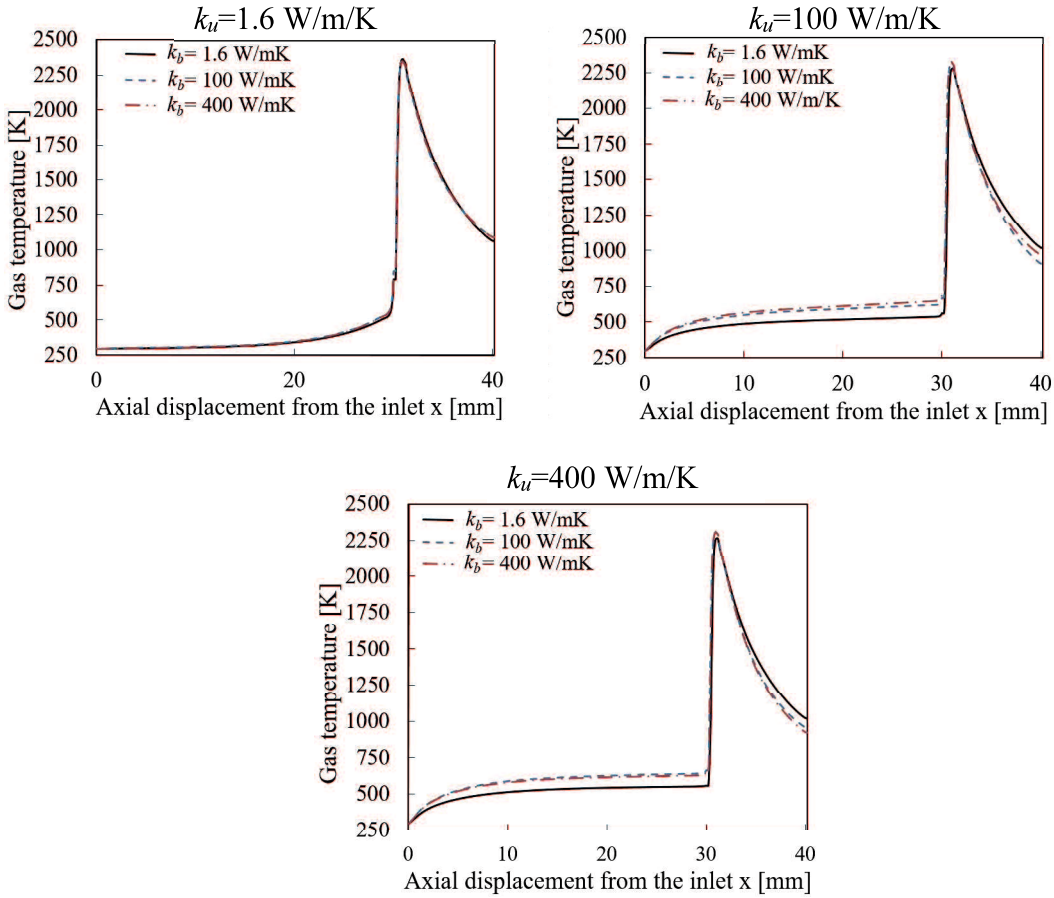

Figure 5.18 Gas temperature along the axial centerline for different values of k_u with U=20 cm/s and ϕ=1.0

Figure 5.19 depicts the outer wall temperature of the combustor while Fig.5.20 shows the wire mesh temperature with different values of k_u and k_b. As indicated in Fig.5.19, higher wall thermal conductivity leads to more uniform temperature along the combustor outer wall. Yang et al. [66] stated that in a micro power generation system, it is essential to ensure a high and uniform temperature along the combustor wall for greater conversion efficiency.

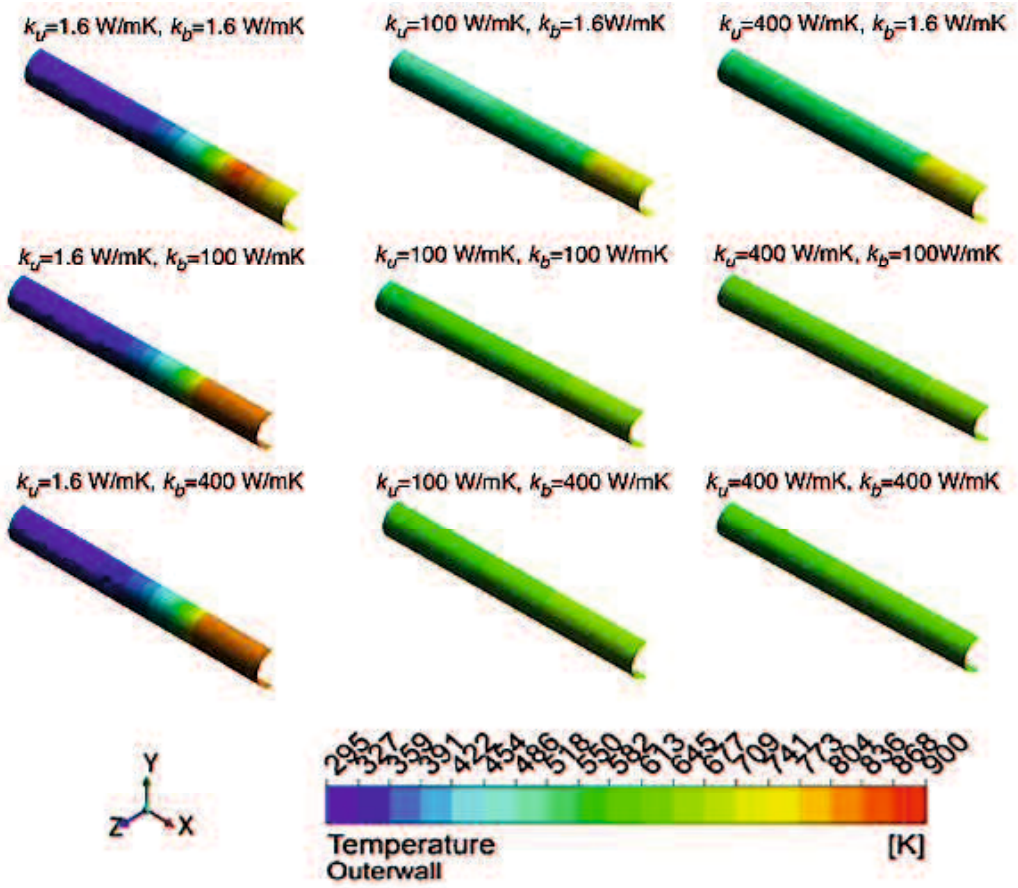

Figure 5.19 Outer wall temperature for U=20 cm/s and ϕ=1.0 with different values of k_u and k_b

The wire mesh temperature contours were also calculated and shown in Figure 5.20. As seen in the figure, higher mesh temperature can be obtained with the use of higher wall thermal conductivity (k_b) in the burned gas region. However, there is an inverse relationship between the wall thermal conductivity in the unburned gas region (k_u) and the wire mesh temperature. A significant decrease of temperature is seen in the results with the use of higher value of k_u. It is very likely that a higher value of k_u leads to much of the heat from the burned gas region being distributed evenly in the unburned gas region.

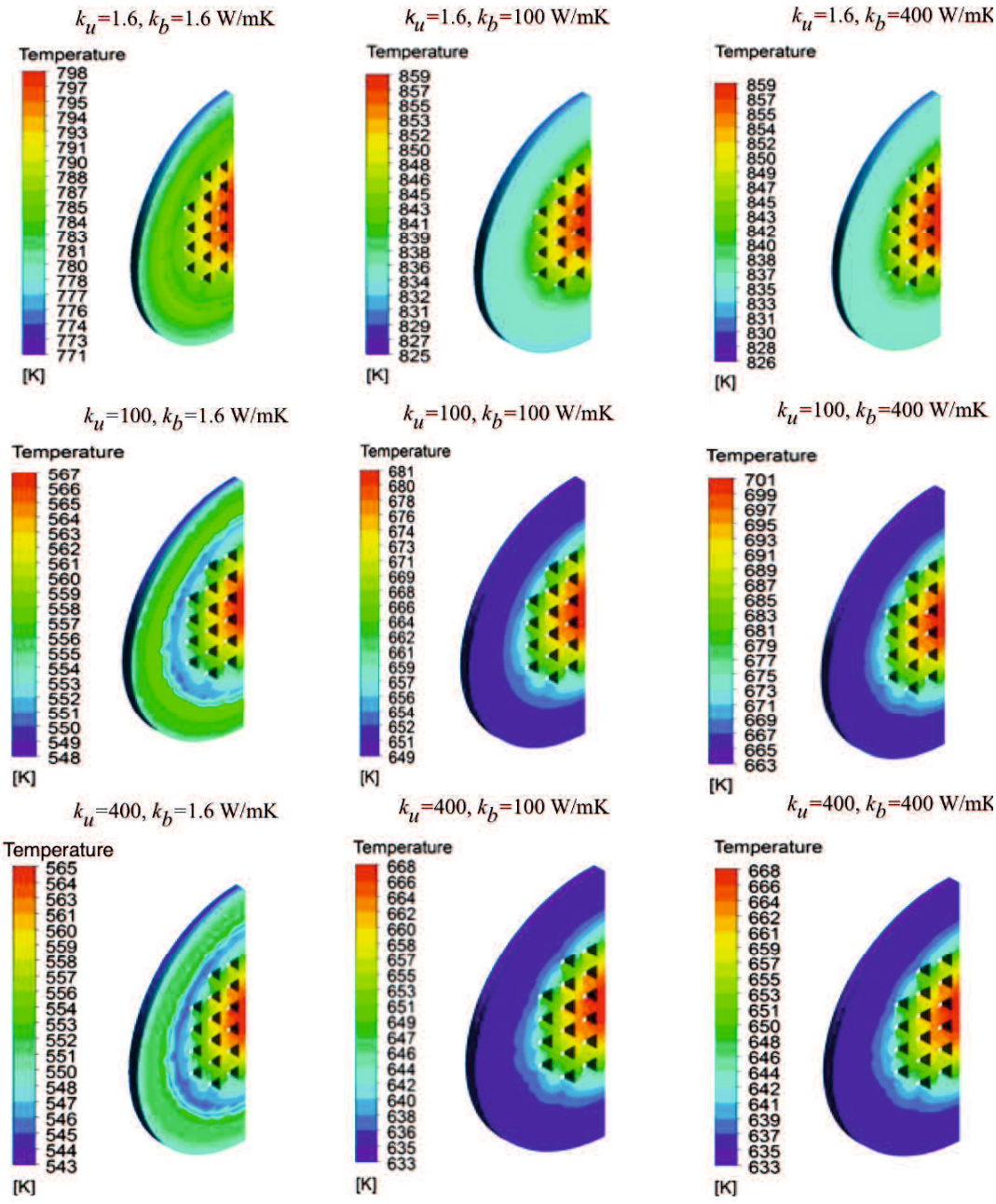

Figure 5.20 Stainless steel wire local mesh temperature contours for U=20 cm/s and ϕ=1.0 with different values of k_u and k_b

Meanwhile, the blowout limits with respect to different values of k_u and k_b were also determined and presented in Fig.5.21. From the figure, it suggested that there is an inverse relationship between k_u and the blowout limit. However, the blowout limits are in proportional to the k_b. The elevation of the blowout limits is mainly due to the increase of the wire mesh surface temperature as shown in Fig.5.22.

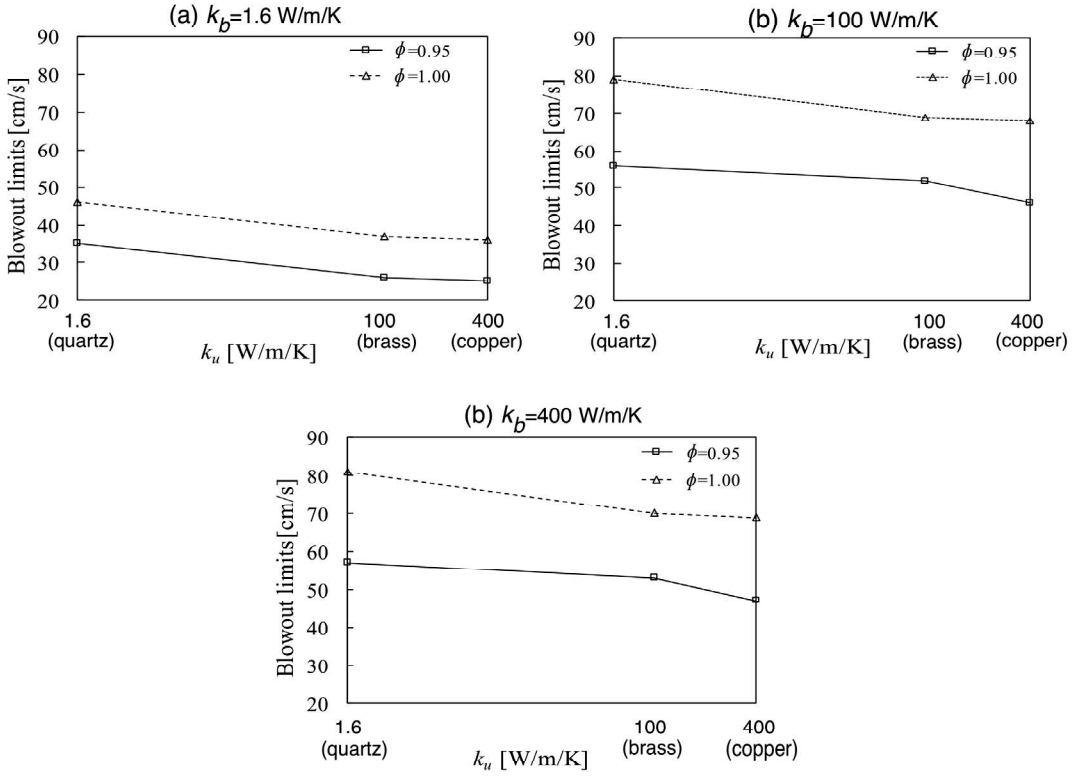

Figure 5.21 Blowout limits for ϕ=0.95 and ϕ=1.0 with different values of k_b

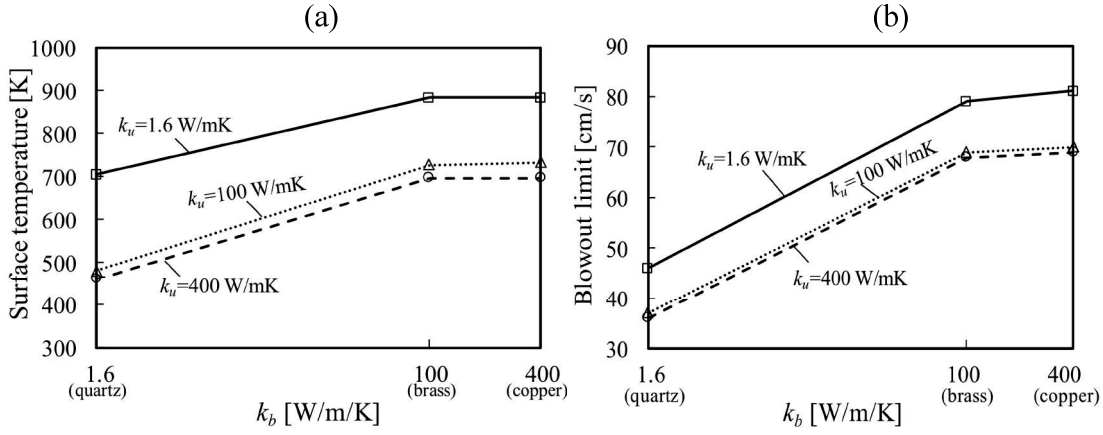

Figure 5.22 (a) Wire mesh center surface average temperature for U=35 cm/s and ϕ=1.0 (b) Blowout limits for ϕ=1.0

In order to show that the 3-D numerical model is acceptable, the blowout limits are compared with the experimental results as depicted in Fig.5.23, Table 5.3 and Table 5.4 respectively. In experiments, quartz, brass and copper tube were used to represent the same value of k as in the simulation. As seen in Table 5.3, the highest percentage of relative error is 19.3%. This large error is mainly due the use of one-step global chemistry reaction, which has over predicted the flame temperature.

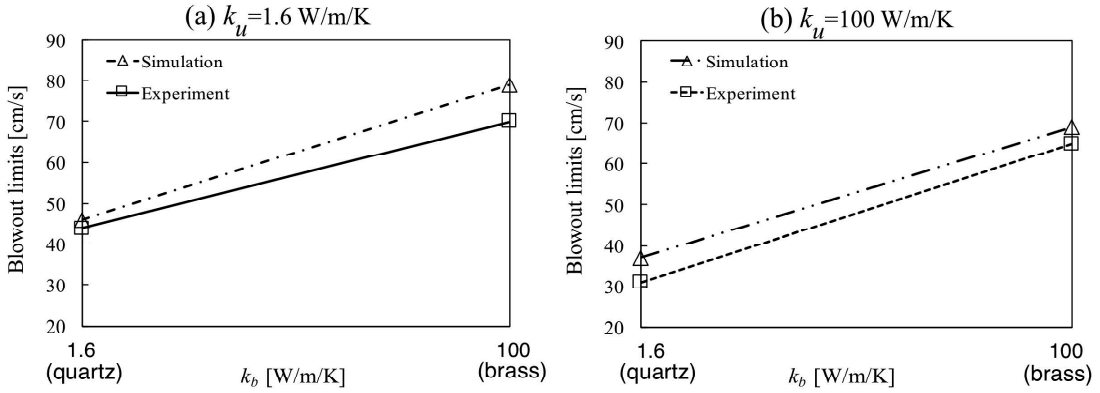

Figure 5.23 Blowout limits with different values of k_b for ϕ=1.0

Table 5.3 Comparison between numerical and experimental blowout limits for ϕ=0.95

k_u (W/m/K)	k_b(W/m/K)	Numerical blowout limits (cm/s)	Experimental blowout limits (cm/s)	Relative error (%)
1.6		35	39	10.3
100	1.6	26	30	13.3
400		25	30	16.7
1.6		56	65	13.8
100	100	52	60	13.3
400		46	NA	NA

Table 5.4 Comparison between numerical and experimental blowout limits for ϕ=1.0

k_u(W/m/K)	k_b(W/m/K)	Numerical blowout limits (cm/s)	Experimental blowout limits (cm/s)	Relative error (%)
1.6		46	44	4.5
100	1.6	37	31	19.3
400		36	33	9.1
1.6		79	70	12.9
100	100	69	65	5.9
400		68	NA	NA

It is generally important for a micro combustor to have a relatively high blowout limits. This is due to the fact that a higher blowout limit leads to an increase of energy input rate. Consequently, a higher power conversion of the heat from the combustion can be achieved. For instance, the calculated energy input rate with flow velocity of 30 cm/s for a cylindrical tube combustor with inner diameter of 3.5 mm is 9.5 W. This

energy input rate can be increased to 22.2 W by applying a flow velocity of 70 cm/s. Thus, combustors with relatively high blowout limits are desireable.

Apart from the blowout limits, the effect of wall thermal conductivity (*k)* and flow velocity *(U)* on the combustion efficiency was also numerically examined. Figure 5.24

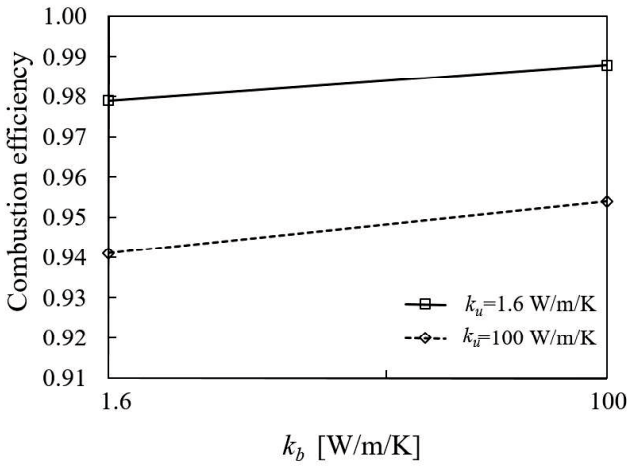

Figure 5.24 Combustion efficiency with different k_u and k_b for U=20 cm/s and ϕ=0.95

depicts the combustion efficiency with respect of different values of k_u and k_b. The figure suggests that the combustion efficiency has a direct relationship with the wall thermal conductivity in the burned gas region (k_b). Meanwhile, Fig.5.25 shows that the combustion efficiency can be increased by applying higher inlet flow velocities. However, such method is only effective for certain range of U values.

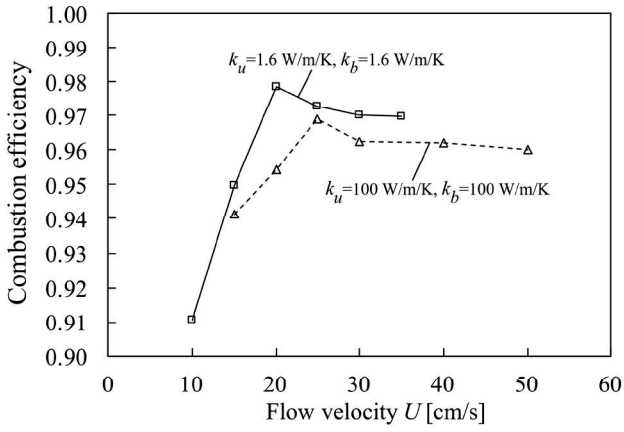

Figure 5.25 Combustion efficiency with different values of flow velocity U for ϕ=0.95

5.1.4 Effects of heat recirculation on the blowout limits

In this sub-section, the effects of heat recirculation on the blowout limits for different combination of tube combustors are numerically studied and presented. Table 5.5 presents the blowout limits for different type of tube combination obtained from the three dimensional (3-D) numerical simulations. To be easily identified, the name of these combustors are based on the combination of the tube types in both the unburned and the burned gas region. For instance, if a brass tube is utilized in the unburned gas region and a quartz tube is used in the burned gas region, the combustor is named as brass-quartz tube. The numerical results show that the blowout limits improve with the use of brass tube in the burned gas region. In fact, this tendency is similar as results obtained from the experiments that are presented in Section 4.2.3.

Table 5. 5 Blowout limits for different tube combustors (from 3-D simulation)

Type of combustor	Blowout limits [cm/s]
Quartz-quartz tube	46
Quartz-brass tube	79
Brass-quartz tube	37
Brass-brass tube	69

As previously discussed in Section 5.1.2, the direction of the wire mesh thermal path is reversed with a higher flow velocity (U). This behavior is due to the variation of flame position with respect to U. Within relatively low values of U, the flame is located very near to the wire mesh. On the other hand, at relatively high values of U, the stable flame is slightly displaced from the wire mesh. This relative flame position can be

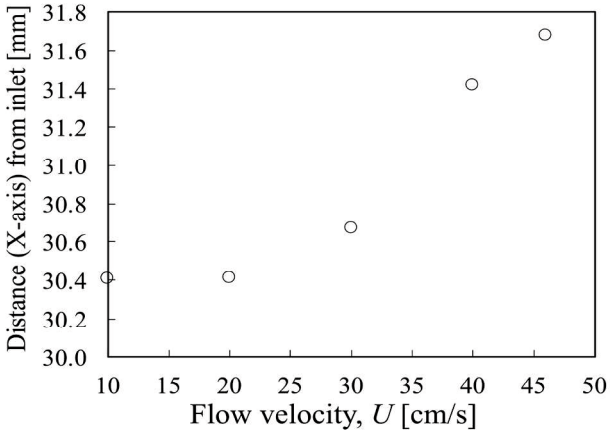

Figure 5.26 Flame position with different values of flow velocity U at ϕ=1.0 for quartz-quartz tube combustor

determined from numerical simulations and results are shown in Fig.5.26. As indicated in the figure, when U=30 cm/s, the flame is located 0.43 mm from the wire mesh. Consequently, the heat from the burned gas region is primarily recirculated via the hot inner wall in the burned gas region to the wire mesh.

It is important to analyze how heat is recirculated in the tube combustor and the developed 3-D numerical model enable such study to be performed. Figure 5.27 illustrates the direction of the heat supplied in near blowout conditions for a tube combustor with wire mesh. The definition of terms in the figure are as follows:

Q_{C1}=heat conducted via the inner wall of the burned gas region

Q_{C2}=heat conducted via the inner wall of the unburned gas region

Q_{RU}= heat recirculated to the unburned gas region

Q_{RM}=heat recirculated to the wire mesh

Q_{LB}=heat loss from the outer wall of the burned gas region to the ambient

Q_{LM}=heat loss from the outer wall of the wire mesh to the ambient

Q_{LU}=heat loss from the outer wall of the unburned gas region to the ambient

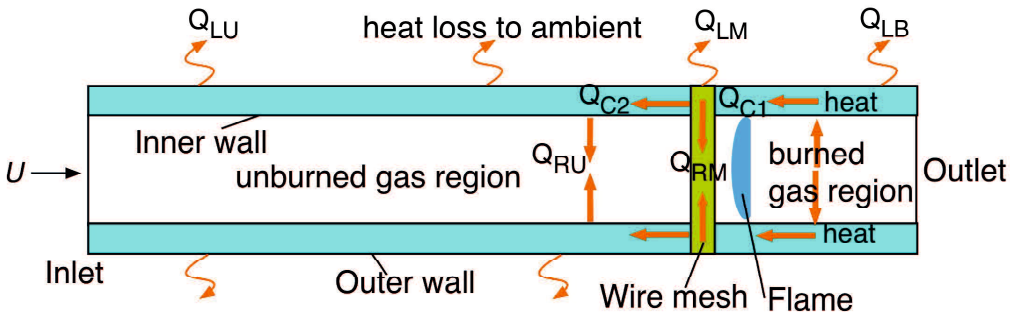

Figure 5.27 Heat recirculated in the combustor near blowout conditions

When the unburned gas flows into the inlet, it is first pre-heated by the heat recirculated to the unburned gas region (Q_{RU}). The flowing gas is further heated by the heat recirculated to the wire mesh (Q_{RM}). Thus, the value of Q_{RU} and Q_{RM} are important as it indicates how much heat is recirculated to pre-heat the unburned gas, which results to the elevation of gas temperature prior to combustion. From Fluent software, the energy balance for each boundary can be calculated. The results of Q_{RU} and Q_{RM} for each type of combustors are shown in Fig.5.28. The negative value of Q_{RM}, which occurs in low flow velocity shows that the heat flows from the wire mesh center to the outer wall. In this condition, the wire mesh acts as flame inhibitor. As seen in Figure 5.28 (a) and (b), with the use of quartz tube in the unburned region, the wire mesh plays more important role in recirculating heat to the unburned gas (Q_{RM}) in near blowout conditions. As such, the wire mesh act as flame enhancer at higher flow velocities. On the other hand, Figure 5.28 (c) and (d) suggest that with the use of brass tube in the unburned region, the wire mesh plays less important role in recirculating the heat. In such conditions, the combustor inner wall in the unburned gas region plays more dominant role in recirculating heat to the unburned gas (Q_{RU}).

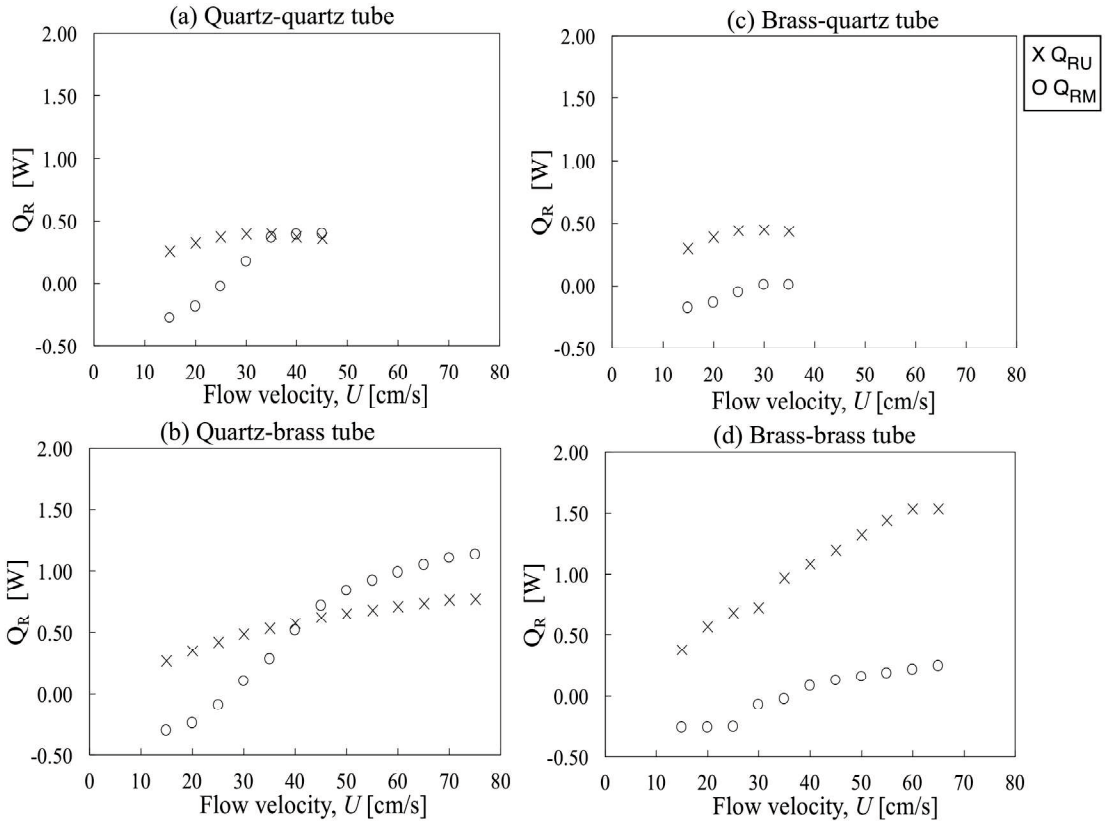

Figure 5.28 Values of Q_{RU} and Q_{RM} with different flow velocities for each of combustor

Meanwhile, Fig.5.29 depicts the value of Q_{RU} and Q_{RM} that are plotted on the same graph for each type of combustor for better comparison. From the figure, it can be deduced that the utilization of brass tube in the burned gas region can significantly improve the total heat recirculated (Q_{RU}+Q_{RM}) to the unburned gas. Figure 5.29 (d) shows 19% of the heat release rate (HRR) is being recirculated to the unburned gas for the brass-brass and quartz-brass tube combustor. This value is considerably high for the tube combustor with wire mesh.

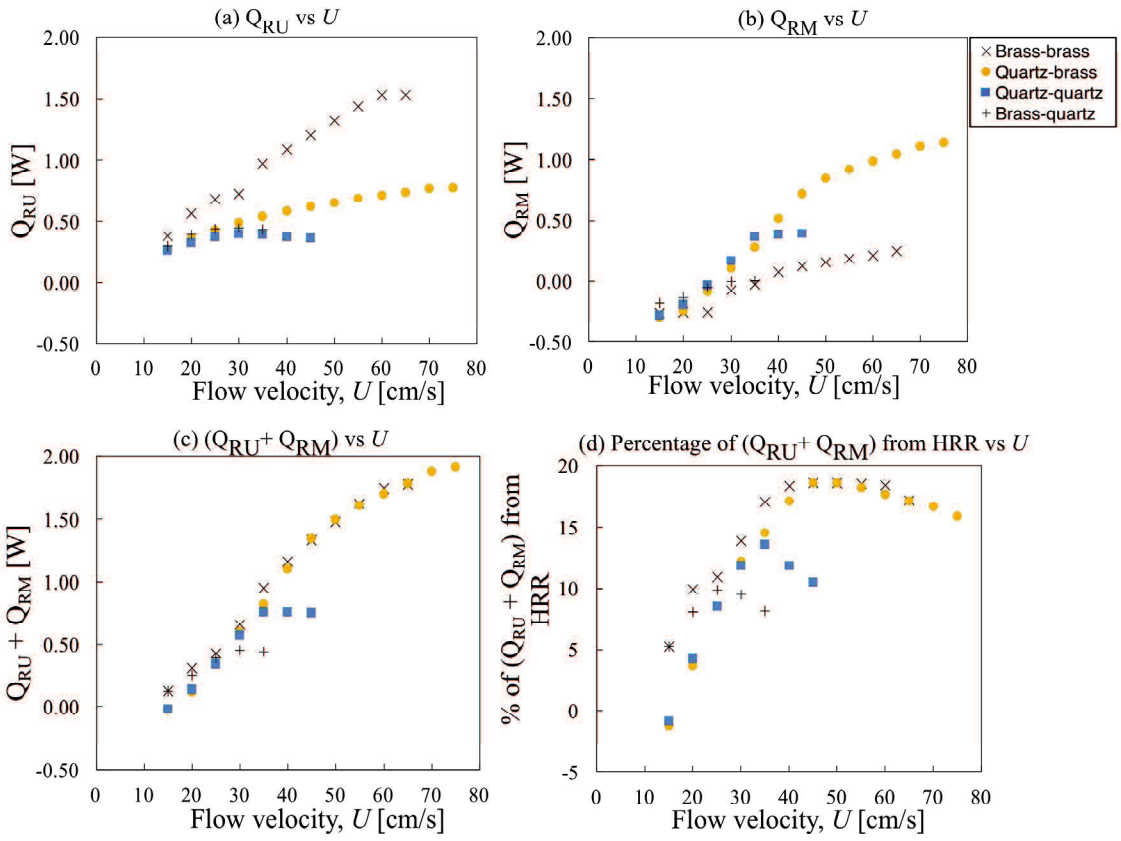

Figure 5.29 Combined values of Q_{RU} and Q_{RM} with different flow velocities for each of combustor

In condition of high flow velocity (U), the heat from the burned gas region is primarily conducted by the solid walls of the tube combustor, which can be represented as Q_{C1} and Q_{C2}. The value of Q_{C1} and Q_{C2} is directly proportional to the wall thermal conductivity *(k)* of the tube. In order to determine these values of Q_{C1} and Q_{C2}, two equations are established. These equations are as follow;

$$Q_{C1}=Q_{C2}+Q_{RM}+Q_{LM} \quad (5\text{-}6)$$

$$Q_{C2}=Q_{RU}+Q_{LU} \quad (5\text{-}7)$$

Since Q_{RU}, Q_{RM}, Q_{LU} and Q_{LM} are already determined with the aid of Fluent software, the value of Q_{C1} and Q_{C2} can be calculated. The results are depicted in Fig.5.30. From the figure, the utilization of brass tube in either side of the region has dramatically increased the value of Q_{C1} and Q_{C2}.This increment is expected since the wall thermal conductivity of the brass tube is much larger than the quartz tube.

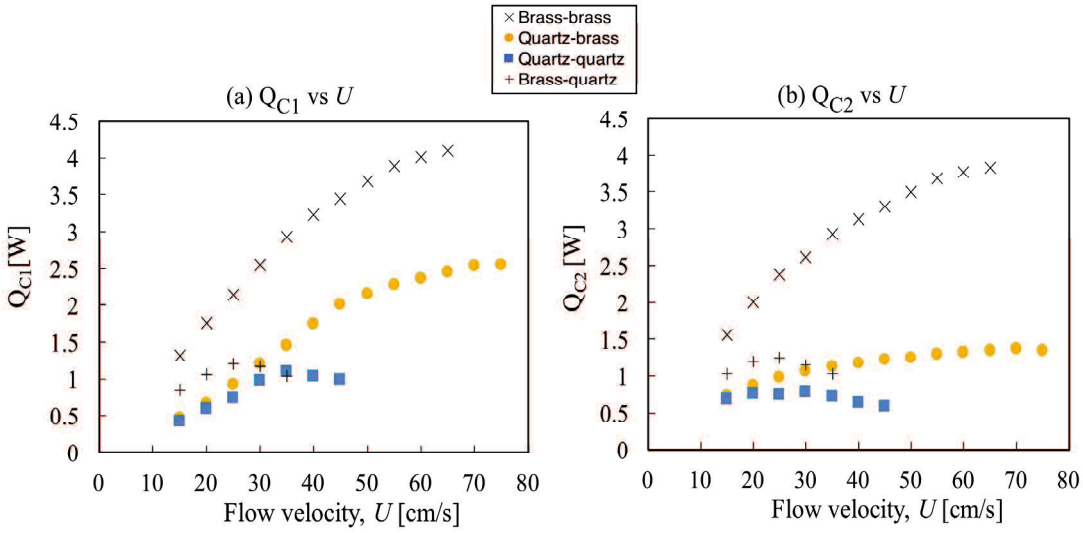

Figure 5.30 Values of Q_{C1} and Q_{C2} with different flow velocities for each of combustor

5.2 Experimental setup for the investigation of heat recirculation effect

In order to examine the effect of exhaust gas on the combustion performance, the combustor was inserted into the glass test tubes with specific dimensions. A traverse system was utilized to precisely insert the combustor. The stable flame was observed by using a digital video camera (PANASONIC HC-750M). Propane (C_3H_8) and air were mixed and supplied into the combustor with an equivalence ratio of ϕ and a corresponding cross-sectional-area mean flow velocity of U. A mass flow controller (SEC-E440J, HORIBASTEC) was used to precisely control each flow rate of air and fuel. The experimental configuration is depicted in Fig.5.31 and 5.32.

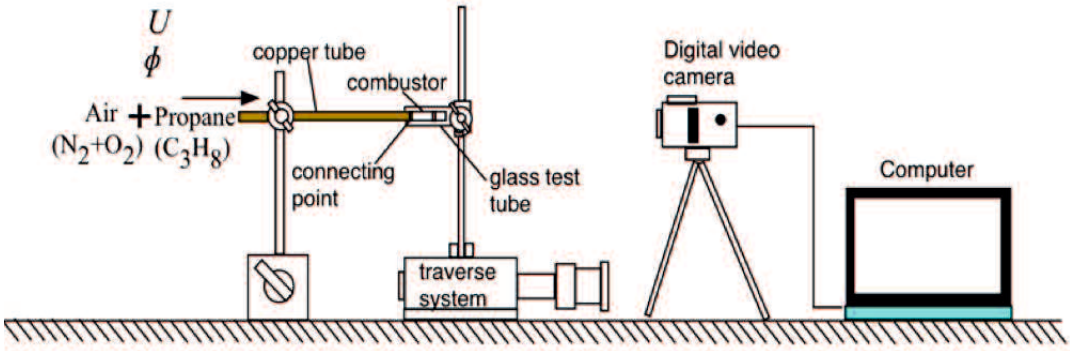

Figure 5.31 Experimental configuration to investigate heat recirculation effect

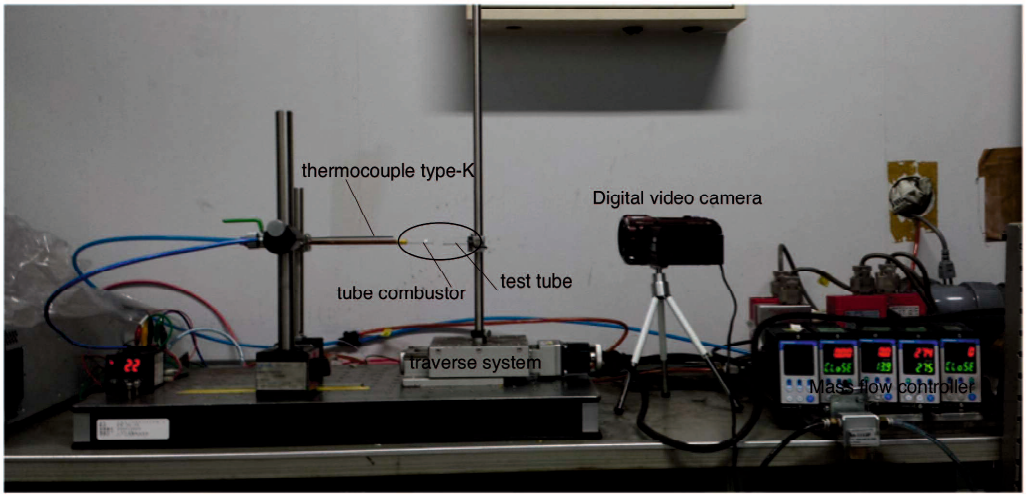

Figure 5.32 Experimental apparatus image

5.2.1 Effects of exhaust gas recirculation on the flame stabilization

There are two types of combustors that were utilized in this experiment. The first type is made of quartz tube and the latter is made of brass tube. Both of the combustors were inserted 48 mm up into the test tube as illustrated in Fig.5.33. The cylindrical test tube is made of quartz glass and has an inner diameter of 8 mm with 1 mm thick. The length of the test tube is 50 mm. This tube dimension is selected considering the scale of the combustor. The flame stabilization limits were established and plotted on a graph as shown in Fig.5.34.

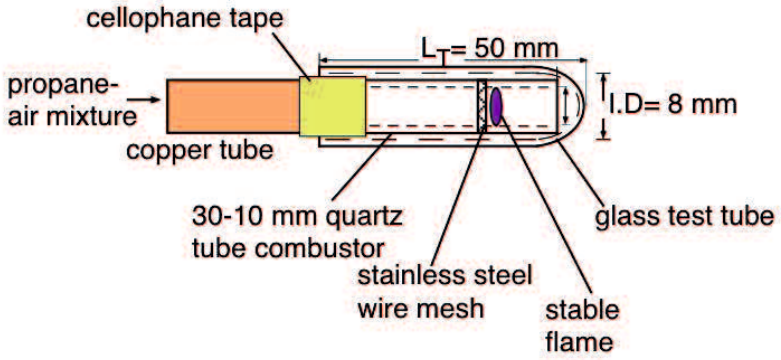

Figure 5.33 Graphic illustration of combustor being inserted into the test tube

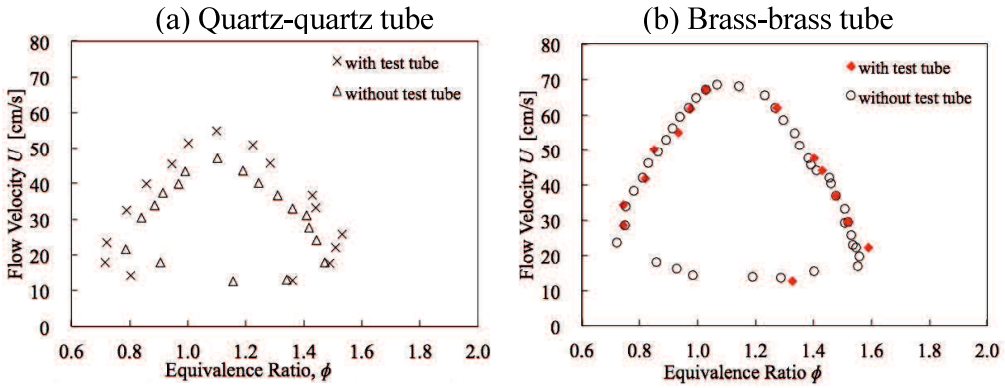

Figure 5.34 Flame stabilizations limits with and without the glass test tube

It is shown in Fig.5.34 that the flame stabilization limit is significantly improved only in quartz tube combustor. On the contrary, there is no notable change of limits for the brass tube combustor. In order to further examine the potential cause for such results to occur, simulations were performed using the same numerical model as explained in Section 5.1. However, for simplicity, the geometry of the outer test tube is not modeled. To generate the same effect as with the use of outer tube, the ambient temperature (T_{amb}) is increased to 600 K as shown in Fig.5.35. The rest of the boundary conditions are maintained as shown in Section 5.1.

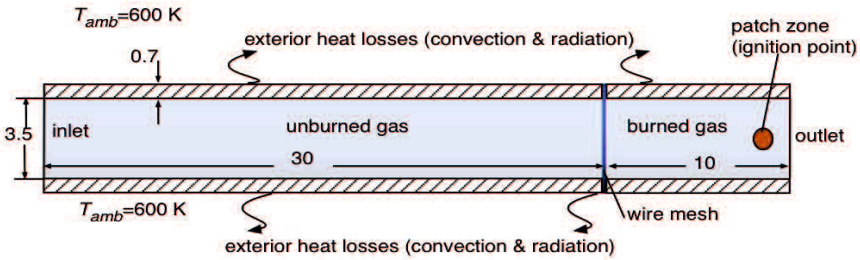

Figure 5.35 Model with increased ambient temperature

With the new boundary condition, the blowout limits for equivalence ratio (ϕ) equal to 1 for each type of combustor were determined and compared with the experimental results. These limits are plotted on the same graph as shown in Fig.5.36 while Table 5.6 depicts the numerical values of blowout limits. Generally, the numerical results are in the same tendency as results obtained from experiments. As seen in Table 5.6, the quartz-quartz tube combustor gives the highest improvement of blowout limit with the increase of T_{amb}. On the contrary, the elevation of T_{amb} does not significantly affect the blowout limit for the brass-brass tube combustor.

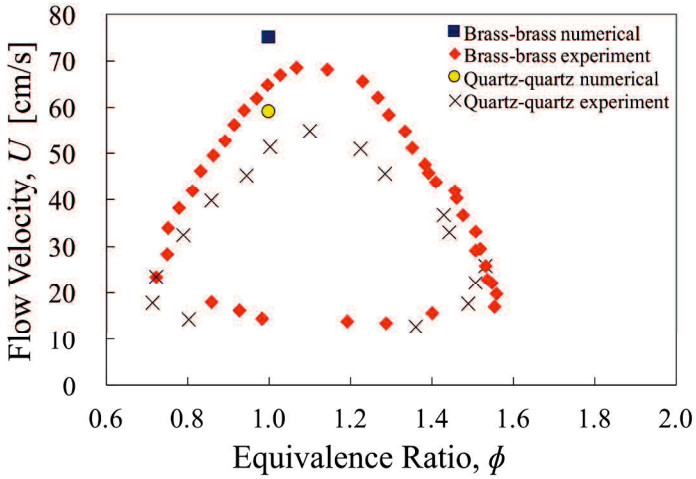

Figure 5.36 Numerical and experimental results of blowout limits with heat recirculation effect

Table 5.6 Numerical results for blowout limits with different ambient temperature (T_{amb}) for ϕ=1

Blowout limits			
Type of combustor	T_{amb}=295 K	T_{amb}=600 K	Percentage change (%)
Quartz-quartz tube	46 cm/s	59 cm/s	28.3
Brass-brass tube	69 cm/s	75 cm/s	8.7

The gas temperature for each condition is also extracted from the numerical simulation and shown in Fig.5.37. Qualitatively, the unburned gas temperature for quartz-quartz tube combustor is dramatically increased with the elevation of the ambient temperature. However, this is not the case for brass-brass tube combustor where the increment is not significant. From the combustion theory perspective, one of the factors that affects the laminar flame speed the unburned gas temperature. Higher unburned gas temperature contributes to a higher laminar flame. The average temperature of the unburned gas region for each type of combustor is calculated and presented in Table 5.7 for a quantitative comparison.

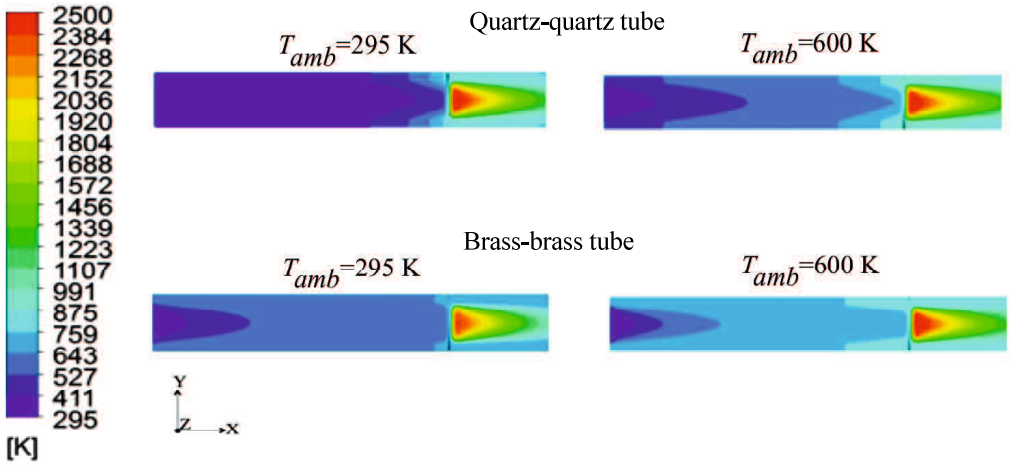

Figure 5.37 Gas temperature for simulated combustors for U=20 cm/s & ϕ=1.0 with different ambient temperature

Table 5.7 Numerically measured of mass-weighted average gas temperature in the unburned gas region measured at U=20 cm/s, ϕ=1.0

Type of combustor	Gas temperature for T_{amb}=295 K	Gas temperature for T_{amb}=600 K	Percentage increase(%)
Quartz-quartz tube	355 K	541 K	52.5 %
Brass-brass tube	561 K	641 K	15.3 %

From Table 5.7, it is clearly seen that larger percentage increase is recorded with quartz tube combustor as compared to brass tube combustor. In other words, there is a direct relationship between the unburned gas temperature with the changes in the

blowout. It can also be deduced that the use of outer tube to increase the flame stabilization limits is only effective for the quartz tube combustor.

Meanwhile, Fig.5.38 presents the combustion efficiency with different values of ambient temperature at a fixed equivalence ratio and flow velocity. The results obviously show that a greater combustion efficiency can be achieved by circulating the heat from the exhaust gas to the unburned mixture.

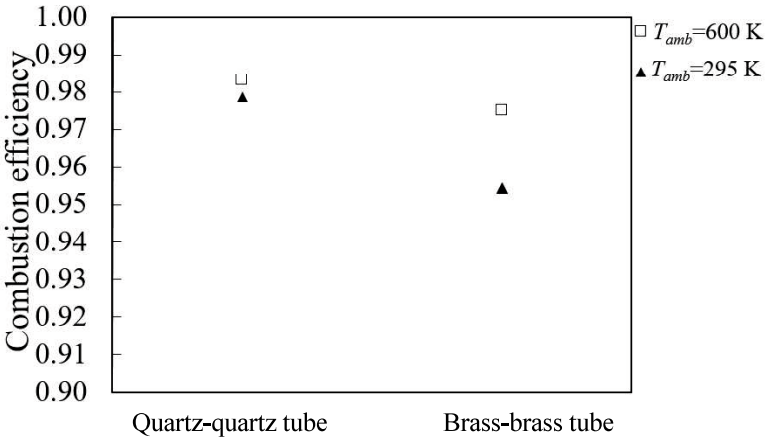

Figure 5.38 Combustion efficiency with different ambient temperature (T_{amb}) for U=20 cm/s and ϕ=0.95

5.3 Improvement on the numerical model

In order to improve the accuracy of the results, enhancement of the numerical model is made. These improvements are explained in the next sub-sections.

5.3.1 Increasing the number of holes of the wire mesh

To improve the accuracy of numerical results, the number of holes on the wire mesh is increased from 16 to 26 holes as presented in Fig.5.39. A steady-state cold flow simulation with U=30 cm/s was first performed to examine the effect on the flow streamlines. The results in terms of flow streamlines are shown in Fig.5.40. As indicated in the figure, the local velocity magnitude of the flow around the wire mesh becomes lower with the use of higher number of holes. This reduction is expected since higher number holes increases the average cross-sectional flow area.

(a) 16 holes model (b) 26 holes model

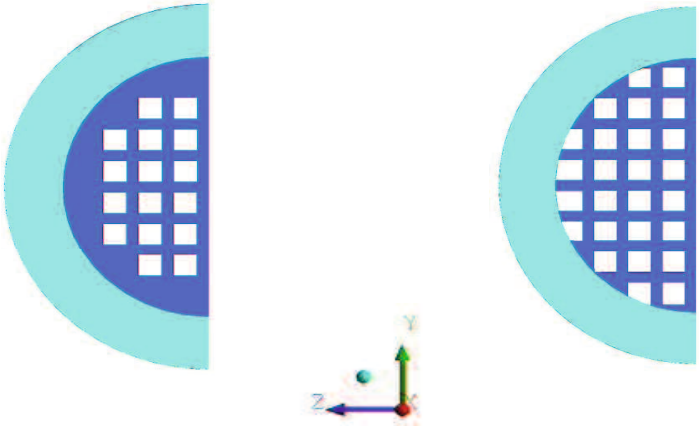

Figure 5.39 Wire mesh with different number of holes

In the meantime, Fig.5.41 illustrates the local velocity magnitude values with respect to the vertical Y displacement for the two different number of holes. The results suggest that a more stable flow can be obtained by increasing the number of holes in the wire mesh.

(a) 16 holes model (b) 26 holes model

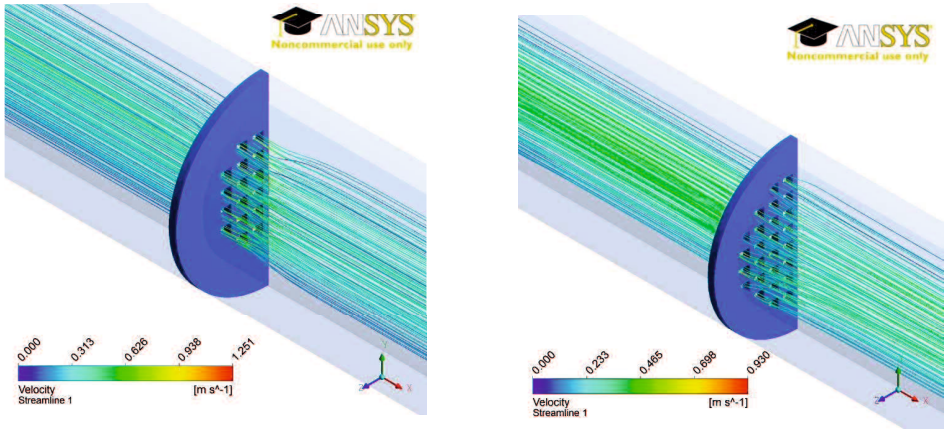

Figure 5.40 Velocity streamline pattern for cold flow simulation with U=30 cm/s

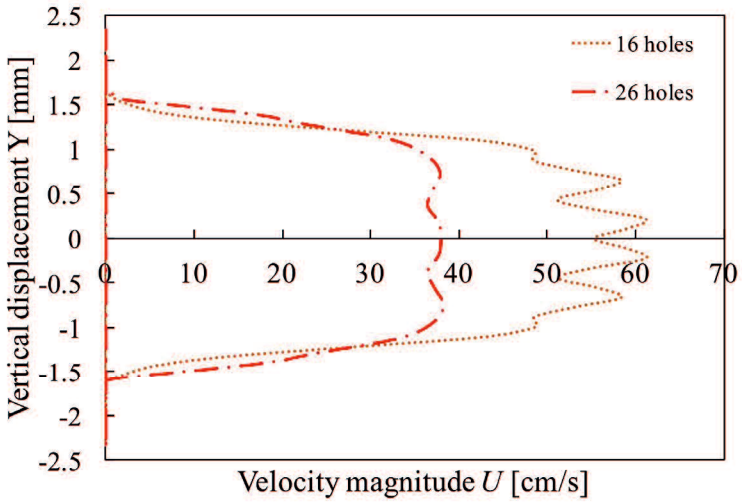

Figure 5.41 Velocity magnitude along the vertical line of x=31 mm for the cold simulation with U=30 cm/s

The gas temperature contours and temperature along the centerline is presented in Fig. 5.42. As depicted in Fig.5.42 (b), the maximum temperature is about 2200 K. This value is 162K lower than the flame temperature for wire mesh with 16 holes. Lower local flow velocity magnitude at the area of the burned gas region might contribute to this reduction of flame temperature.

(a) Gas temperature contours (b) Gas temperature along the centerline

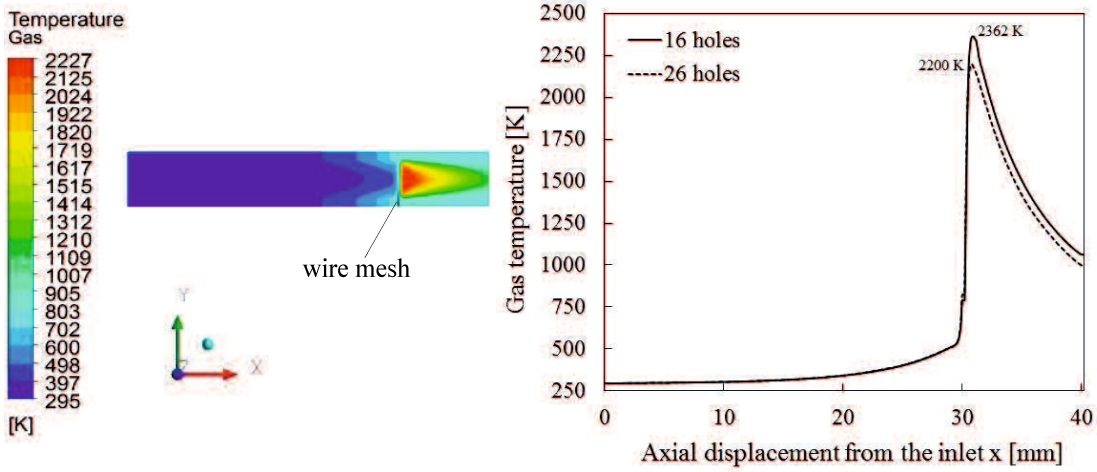

Figure 5.42 Gas temperature for U=20 cm/s, ϕ=1.0 for quartz-quartz tube combustor

Meanwhile, Fig.5.43 illustrates the comparison between the blowout of the wire mesh with 16 holes and 26 holes respectively. As seen in the figure, the values of blowout limits for model with 26 holes are closer to the experimental results. Clearly, these results show that with the higher number of holes passing through the wire mesh, the discrepancy between simulated and experimental results becomes narrower.

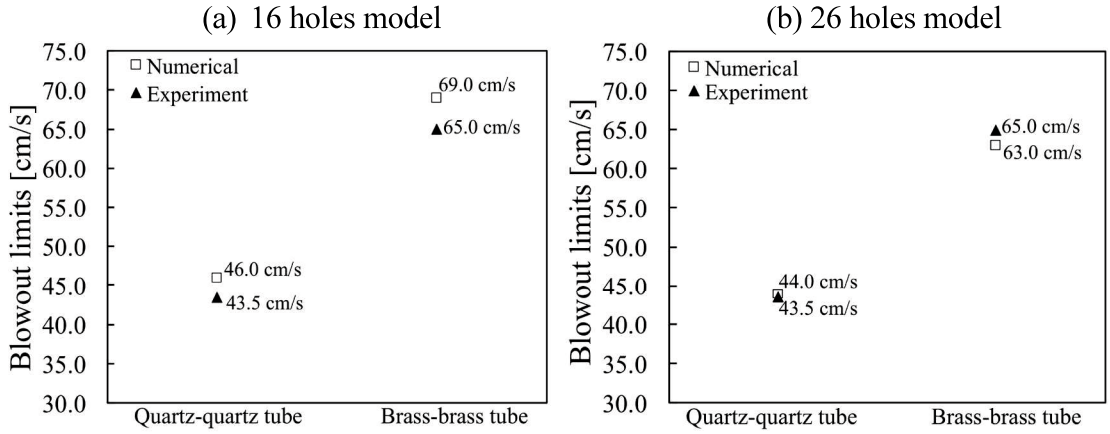

Figure 5.43 Numerically determined blowout limits in comparison with experimental results for 16 holes and 26 holes numerical model with ϕ=1.0

5.3.2 Numerical model with an outer tube

To include an outer tube that encapsulates the combustor requires significantly higher number of grids. In addition, the geometry involved is more complex that might lead to computational errors. However, such model can be done and presented in this sub-section. Figure 5.44 shows the computational domains of the model. The outer tube is assumed to be made of quartz tube. The exterior heat losses through the outer wall are in the form of convection and radiation. The value of the convective heat transfer coefficient (h) is 5 W/m^{2}K while the emissivity is fixed to 0.9. Quartz is assumed to be the material for both the combustor and outer tube. The thickness of the outer tube is set to 1 mm by activating the shell conduction in Fluent. The material for both the combustor and outer tube is assumed to be made of quartz, which means that the k value is fixed to 1.6 W/m/K.

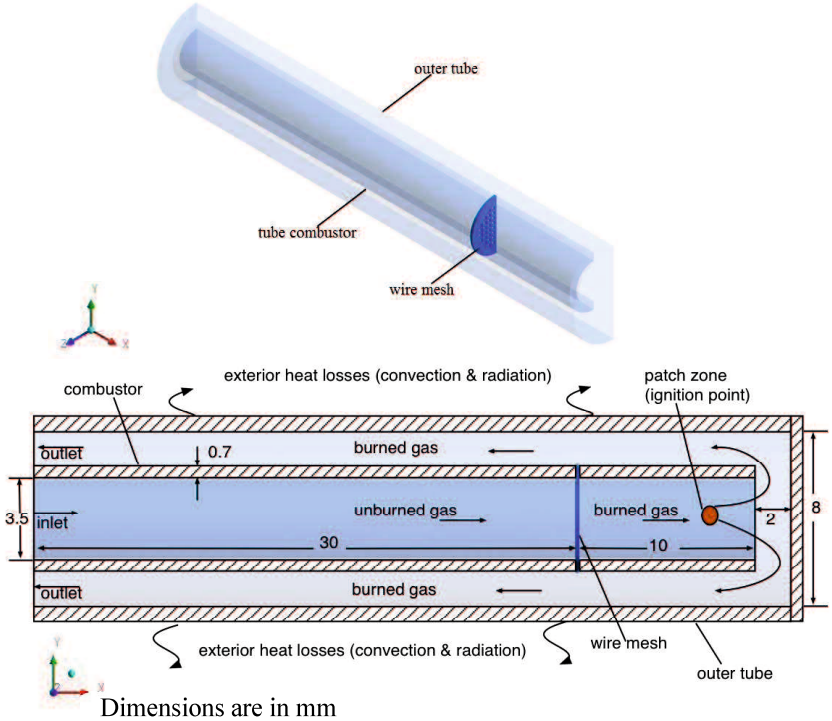

Figure 5.44 Computational domain for combustor with an outer tube

A cold flow simulation condition is first performed in which only the continuity and momentum equations are solved. The results of local velocity magnitude and streamline pattern is depicted in Fig.5.45 while the results with energy and species equations solved are shown in Fig.5.46.

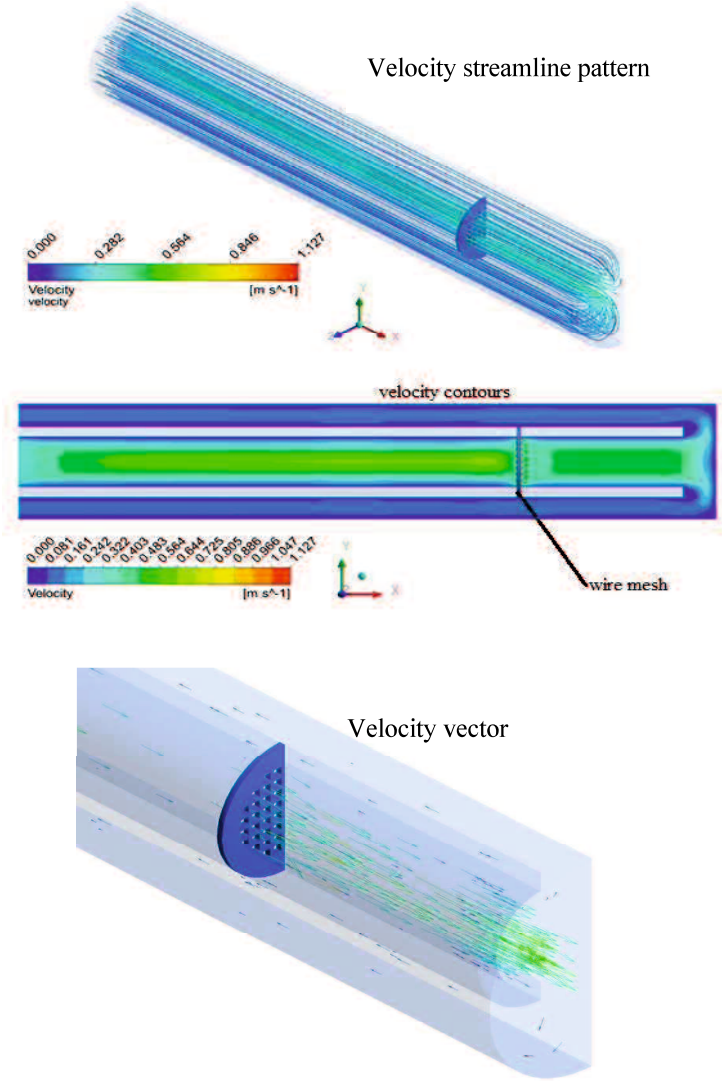

Figure 5.45 Cold flow simulation local velocity results with *U*=35 cm/s

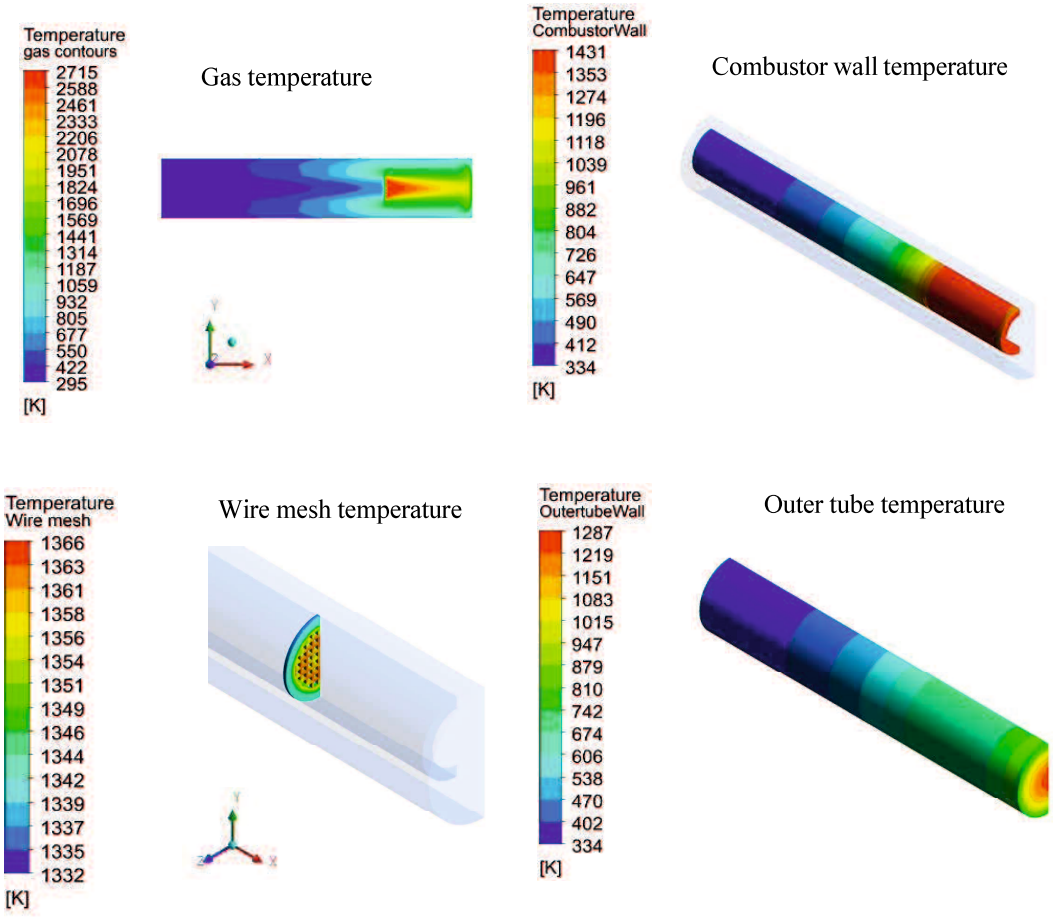

Figure 5.46 Temperature contours for U=35 cm/s and ϕ=1.0

As seen in Fig.5.46, the wire mesh temperature is significantly high. This elevation of temperature is mainly because there is no straight thermal path from the wire mesh to the ambient air. As for the gas, combustor wall and outer tube temperature contours, the results are generally within the expectation. Since the outer tube is assumed to be made of quartz glass, it can be seen that much of the heat is only concentrated within a small area. In other words, there is high thermal stress occurs on the combustor and outer tube wall. It is important to note that in order to include the outer tube in the numerical model, a total of 188043 nodes need to be utilized. This high number of nodes require longer computational time especially in determining the blowout limits.

5.4 Design improvement for combustors with heat recirculation

The findings obtained from the numerical and simulation works are utilized as the guideline to properly design a meso-scale tube combustor with heat recirculation mechanism. It is desirable to have a combustor with high blowout limits as high power output can be achieved with a high flow velocity.

5.4.1 Reduction of the outer tube diameter

To improve the practicality of the combustor, the inner diameter of the outer tube is suggested to be reduced to 6 mm. The effect of the diameter reduction on the combustion characteristics is then numerically examined. The computational domain and results obtained from the simulations are depicted in Fig.5.47. The exterior heat losses through the outer wall are assumed to be in the form of convection and radiation. The value of the convective heat transfer coefficient (h) is fixed to 5 W/m^{2}K while the emissivity is set to 0.9. Quartz is assumed to be the material for both the combustor and outer tube. As seen in Fig.5.47(b), there is a small drop of flame temperature as compared to the outer tube with 8 mm of inner diameter. It is expected that the flame stabilization limits should not be significantly affected. The blowout limit with this new condition is 65 cm/s for equivalence ratio (ϕ) equal to 1.0.

(a) Computational domains (dimensions in mm)

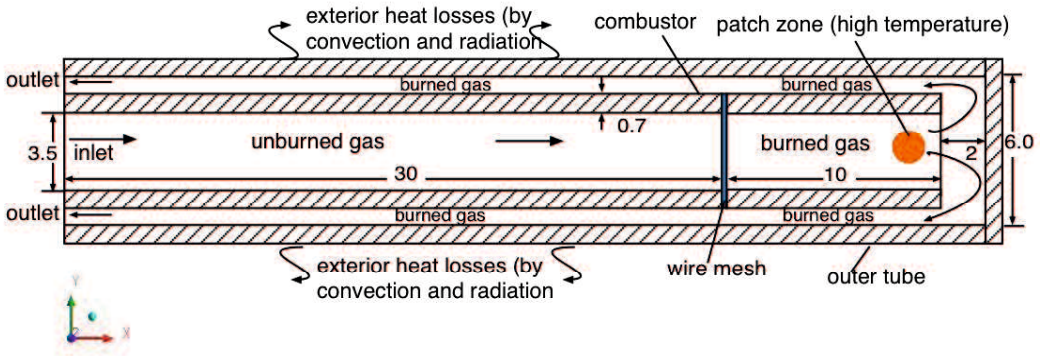

(b) Simulation results for U=35 cm/s and ϕ=1.0

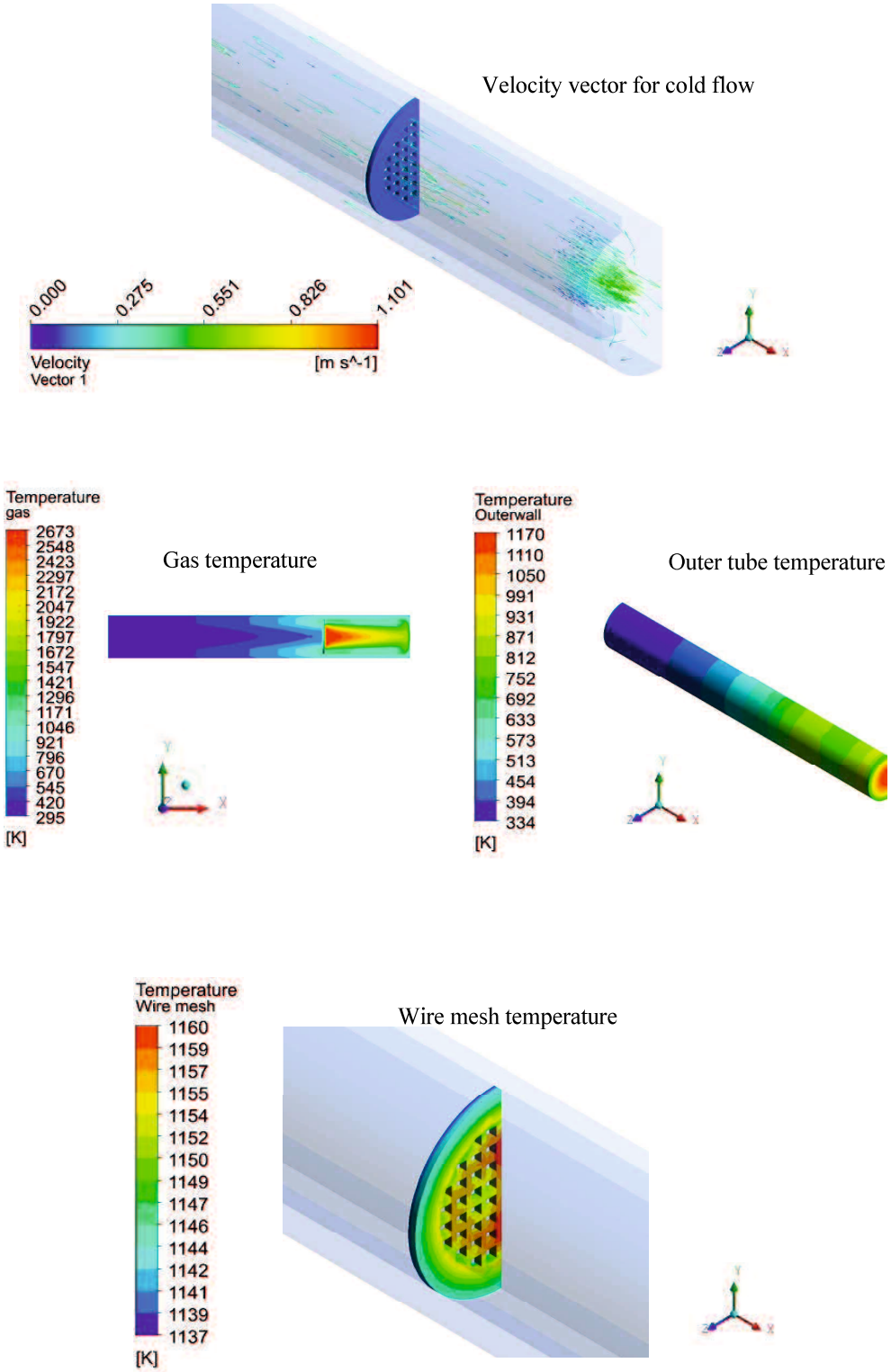

Figure 5.47 Computational domains and simulation results for outer tube with inner diameter of 6 mm

5.4.2 Proposed combustor for the use of gas and liquid fuel

It is desirable that an improved design of combustor can also be used for liquid fuels. The use of liquid fuel eliminates the problem of combustor mobility. Droplets of liquid fuel can be generated with the utilization of electrospray technique as proposed by Lilis et al.[96]. In order to apply the electrospray method on the combustor, a minimal modification needs to be performed. The direction of inlet flow of combustor in Section 5.4.1 needs to be reversed. The gas should be supplied through the small gap between the combustor and the outer tube. The sketched diagram of the proposed combustor is presented in Fig.5.48 (a). The effect of changing the flow of gas is then numerically examined, where the computational domain is shown in Fig.5.48 (b). Both of the combustor and outer tube is assumed to be made of quartz. Results of the numerical simulations are presented in Fig.5.49.

(a) Illustration of the proposed combustor with gas and liquid fuel

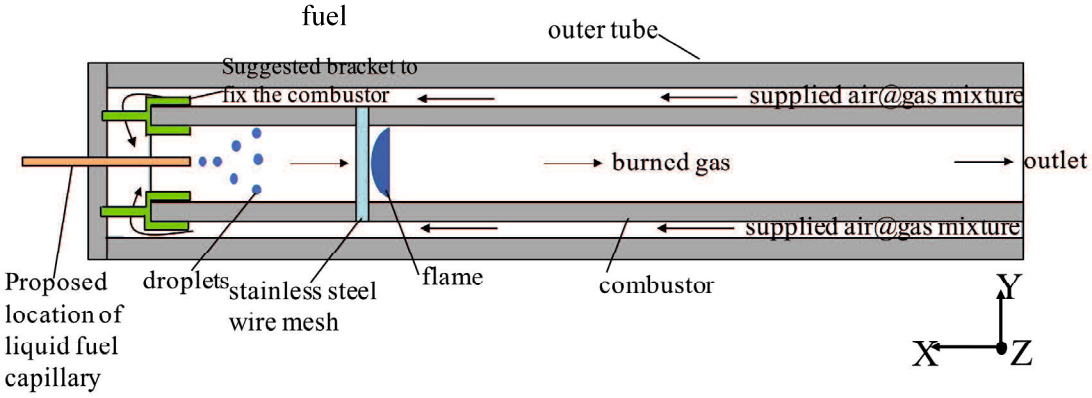

(b) Computational domain for propane-air simulation (unit in mm)

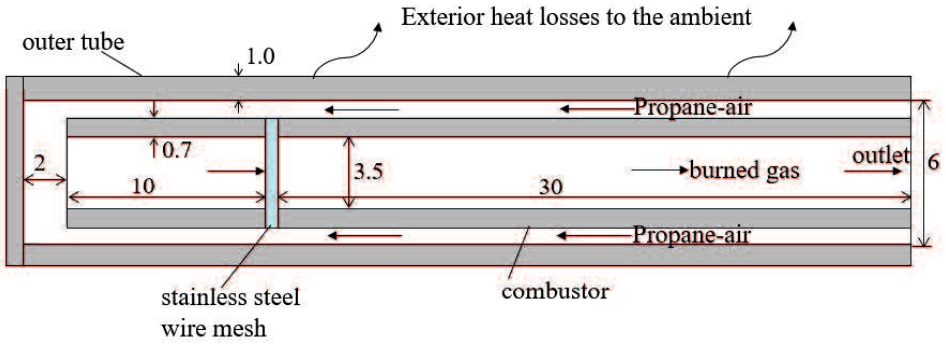

Figure 5.48 Computational domain with a reversed direction of gas flow

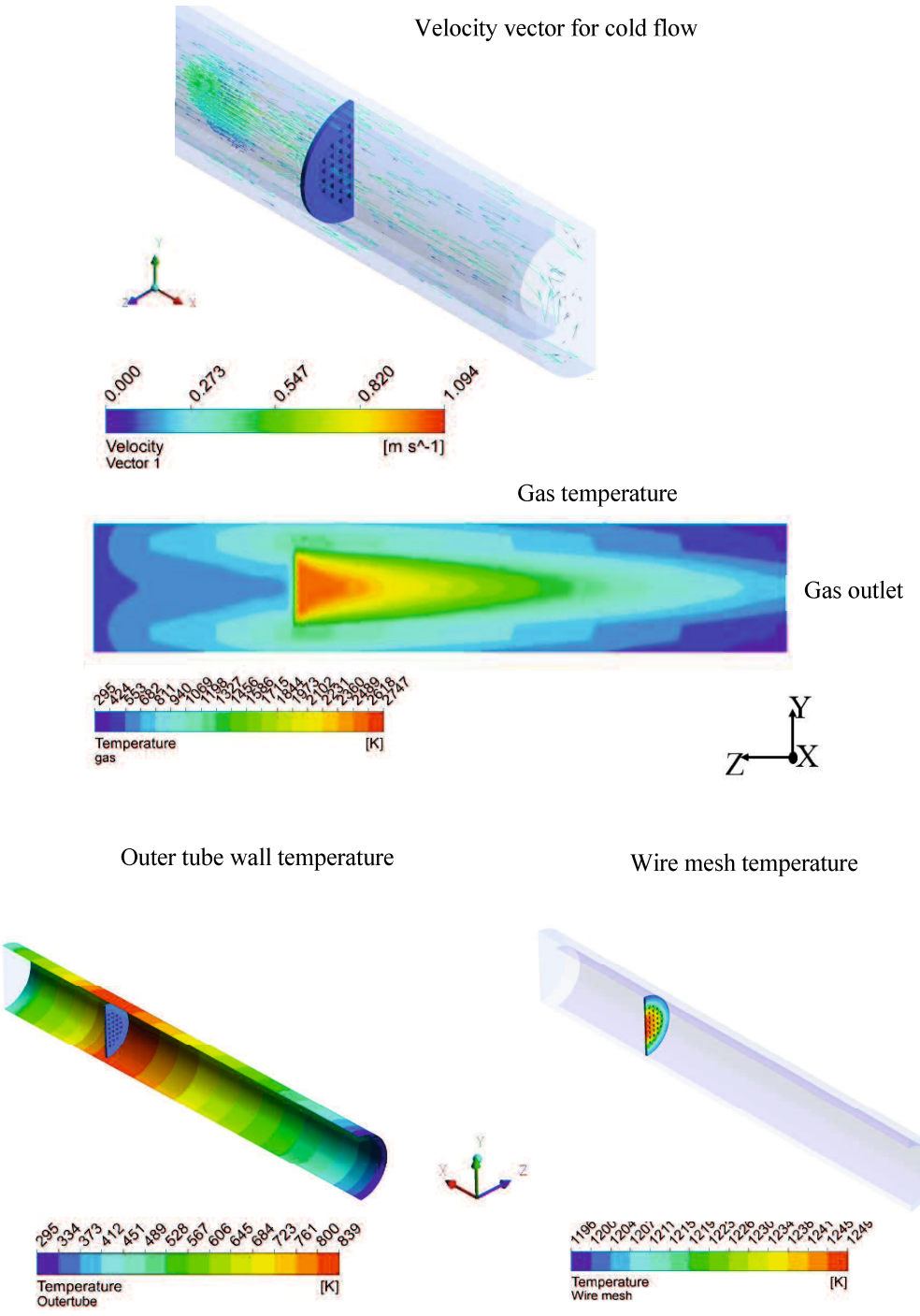

Figure 5.49 Results of simulations with gas flow through the gap for U=35 cm/s and ϕ=1.0

Since the average cross-sectional area of the inlet is the same as average cross-sectional area of the inlet in combustor shown in Section 5.4.1, direct comparison of the flow velocity can be made. As shown in Fig.5.49, the flame temperature is slightly increased as compared to results in Fig.5.47, but the increment can be considered as insignificant. The increase of the flame temperature causes a modest elevation of the outer wall and wire mesh temperature. However, it can be seen from the figure that there is a notable upward change on the unburned gas temperature. This finding is further corroborated from the graph of gas temperature along the centerline of the combustor as depicted in Fig.5.50. The calculated mass-weighted average of the unburned gas temperature for the case of inlet flow through the small gap is given as 711 K. On other hand, the average temperature for the case in Section 5.4.1 is calculated as 641 K. Thus, it is predicted that flame stabilization can be enhanced with the change of the inlet flow direction.

(a) Gas is supplied through the combustor as in 5.4.1

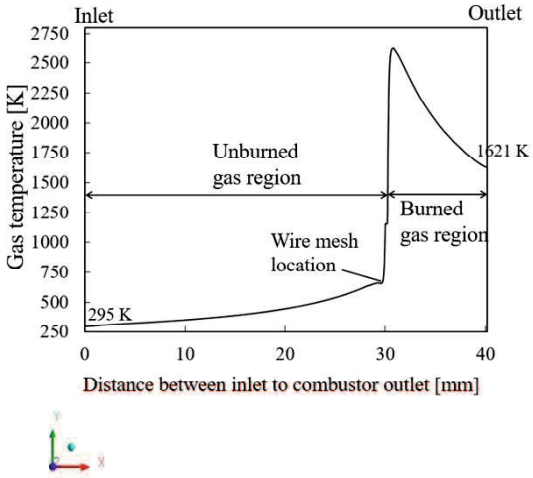

(b) Gas is supplied through the gap between combustor and outer tube

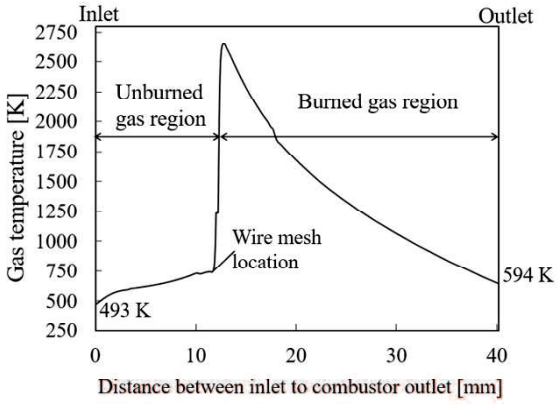

Figure 5.50 Gas temperature along the centerline of combustor for U=35 cm/s and ϕ=1.0

5.5 Summary

In this chapter, experiments to investigate the effect of exhaust gas on the flame stabilization were performed. Apart from that, a credible three dimensional (3-D) numerical model has also been established.

It is important to note that the exhaust gas does not mix up with the unburned reactants. Thus, the experimental method is different from the conventional Exhaust Gas Recirculation (EGR). The results show that the flame stabilization limits of the brass tube combustor could not be significantly increased by pre-heating the unburned gas. In other words, the flame stabilization limits can only be greatly improved in a tube combustor with low wall thermal conductity, which in this case, the quartz tube combustor.

The developed numerical model is used to demonstrate the importance of the wire mesh in enhancing the blowout limits. Essential parameters such as combustion efficiency, gas, wire mesh and wall temperatures can be easily obtained with the use of simulations. The changes in these critical parameters help to explain the experimental results. For instance, the experimental results show that the brass tube combustor has a significant flame blowout limits as compared to the quartz tube combustor. By conducting 3-D numerical simulations, it is then known that the reason of the elevation of the limits is due to the significant increase of the unburned gas temperature near the wire mesh.

The numerical and experimental results obtained in this chapter are then utilized to propose a cylindrical tube combustor with heat recirculation mechanism. The proposed combustor is also equipped with stainless steel wire mesh, which enhances the flame stability. Apart from propane-air mixture, liquid fuel such as heptane can also be used in the proposed combustor.

CHAPTER SIX

Conclusions and Recommendations for Further Work

6.1 Conclusions

The main objective of this study is to investigate the various factors that affect the flame stability in meso-scale tube combustor with stainless steel wire mesh. Both numerical simulations and experiments were performed. Experiments were utilized mainly to determine the flame stabilization limits. Meanwhile, numerical simulations were conducted to provide the detailed understanding of the given problems. The specific findings of the present research are summarized below:

1. For the experiments to examine the effect of ambient air temperature on the flame stabilization.
   a. The blowout limits of a meso-scale cylindrical quartz tube combustor in both lean and rich regions can be enhanced by increasing the ambient air temperature. However, there is no notable change of extinction limits with the elevation of ambient air temperature.
   b. The length of unburned gas region L_u plays a significant role in improving the flame stabilization limits. Shorter length of L_u results in a better flame stabilization limits. On the other hand, the length of burned gas region L_b does not have any significant effect on these limits.

2. For both simulations and experiments performed to investigate the effect of wall thermal conductivity on the flame stabilization
   a. The use of higher wall thermal conductivity *(k)* in the burned gas region improves the blowout limits. However, the utilization of material with wall thermal conductivity higher than 400 W/m/K has no positive effect on the flame stabilization limits.
   b. When the wall thermal conductivity in the burned gas region is elevated, the inner wall temperature especially near the flame holder is also increased. As a result, the local burning velocity at the flame attachment region is also escalated. Consequently, the flame blowout limits are also increased.

c. The use of higher wall thermal conductivity only in the unburned gas region leads to the reduction of blowout limits. This reduction is due to the decrease of the inner wall temperature in the area just before the flame holder position.
d. Better wall temperature uniformity can be obtained with the use of metal tube combustors. It is desirable that the wall of the combustor should have a uniform temperature to avoid thermal stress related problems.

3. For both simulations and experiments to investigate the effect of heat recirculation from exhaust gas to the unburned gas region
   a. It has been numerically shown that the stainless steel wire mesh has a significant role in enhancing the flame blowout limits. At relatively high flow velocities but within the stabilization limits, the wire mesh helps to re-circulate the hot exhaust gas in the burned gas to the unburned gas region. However, at low flow velocities, the close position between the flame and wire mesh causes numerous heat losses to the ambient. As a result, flame extinction occurs.
   b. The experimental results show that the utilization of heat from exhaust gas can significantly enhance the flame stabilization limits of tube combustors with stainless steel wire mesh. However, such method is only effective for the combustor made of quartz.

6.2 Recommendation for Further Research

The recommendations to further improve the present research work are summarized below:

1. Further investigations on the effect of exhaust gas recirculation should be performed on liquid fuels. Heptane is suggested as the fuel.
2. For the numerical simulation model, a detailed kinetic mechanism of propane-air mixture should be employed to examine the emission characteristics. An unsteady state numerical model should also be performed to investigate the flame response.
3. It is recommended that the flame stabilization limits for a reversed flow combustor as suggested in Chapter 5 are experimentally determined.

4. To demonstrate that the combustor is relevant in the real world application, a coupling system to convert the heat energy of the combustor into electrical energy is suggested to be developed.

LIST OF RELATED PAPERS

[1] Fudhail Abdul Munir, Masato Mikami. A Numerical Study of Propane-air Combustion in Meso-scale Tube Combustors with Concentric Rings. Journal of Thermal Science and Technology. Vol. 10 pp.1-12, 2015 (Related to Chapter Four).

[2] Fudhail Abdul Munir, Naoyuki Hatakeda, Takehiko Seo, Masato Mikami. Improvement of Combustion Stability in Narrow Tubes with Wire Mesh, The 24th International Symposium on Transport Phenomena (ISTP). Yamaguchi Japan, 2013 (Related to Chapter Three).

[3] Fudhail Abdul Munir, Masato Mikami. Modeling of Propane-air Combustion in Meso-scale Tubes with Wire Mesh. 10th Asia Pacific Conference on Combustion (ASPACC 2015). Beijing China, 2015 (Related to Chapter Five).

[4] Fudhail Abdul Munir, Tsuyoshi Tokumasa, Takehiko Seo, Masato Mikami. Approaches to Enhance the Combustion Stability in Meso-scale Cylindrical Tube Combustors. The 26th International Symposium on Transport Phenomena (ISTP). Leoben Austria, 2015 (Related to Chapter Five).

Bulletin of the JSME Vol.10, No.1, 2015
Journal of Thermal Science and Technology

A numerical study of propane-air combustion in meso-scale tube combustors with concentric rings

Fudhail Abdul MUNIR* and Masato MIKAMI*
*Graduate School of Science and Engineering, Yamaguchi University
2-16-1 Tokiwadai, Ube, Yamaguchi 755-8611, Japan
E-mail: s505wc@yamaguchi-u.ac.jp

Received 8 January 2015

Abstract

Dwindling energy resources and strong demand for better power sources as compared to conventional batteries have sparked research interest in micro power generation. The invention of state-of-the-art electronic devices requires more energy capacity, shorter charging period and light in weight, characteristics of which batteries lack. Therefore, in recent years micro power generation systems have been seen as a potential alternative to batteries owing to the obvious advantages that it has. It is essential to fully understand the underlying factors that affect the combustion stability in meso and micro-scale combustors. One of the popular methods to examine these factors is by performing numerical simulations. This paper demonstrates an axisymmetric two-dimensional steady state numerical simulation of propane-air combustion in meso-scale cylindrical tube combustors with concentric rings. The inner diameter of the tube is set to 3.5 mm and the wall thickness is specified to 0.7 mm. The concentric rings are placed between the unburned and burned gas region. The main function of these rings is to act as a flame holder where a stable flame can be easily established. The wall thermal conductivity in the unburned and burned gas region is varied from 1 W/m/K to 1000 W/m/K and the results in terms of gas, inner wall, outer wall surface temperature distribution, the blowout limits and combustion efficiency are analyzed and presented. In addition, the effect of the inlet velocity and the equivalence ratio is also investigated. The results show that the inlet velocity and equivalence ratio have significant impacts on the flame temperature, which in turn change the wall temperature distribution. Although the wall thermal conductivity has minimal effect on the flame temperature, both inner and outer wall surface temperature are greatly affected. Consequently, this variation of wall temperature contributes to the significant changes on the blowout limits. It is also shown that the combustion efficiency is influenced by the wall thermal conductivity of the combustors.

Key words: Micro power generation, Micro and meso-scale combustors, Numerical simulations, Blowout limits

1. Introduction

Meso and micro-scale combustion phenomena are the key components in micro power generation. An experimental study has shown that flame stabilization in a confined space or a narrow channel is achievable (Miesse, et al., 2004). However, the difficulty of sustaining a stable flame for a micro combustor due to its high surface to volume ratio is a major issue in micro combustion (Suenaga, et al., 2011; Maruta, 2011). This high ratio causes a large portion of heat loss from the flame to the wall, which leads to thermal quenching (Kaisare, et al., 2012). In recent years, numerical simulations have been utilized as prominent methods to study the combustion feasibility in meso and micro-scale channels. By performing the verification, any newly designed of micro combustors can be thoroughly studied and optimized (Kurdyumov, et al., 2009).

Paper No.15-00029
[DOI: 10.1299/jtst.2015jtst0008]

As early as in 2000s, Computational Fluid Dynamics (CFD) has been utilized to numerically investigate the flame propagation in micro-burners. Raimondeau et al. (2002) demonstrated methane (CH_4) combustion in a two-dimensional tubular micro combustor, which was modeled using a detailed multi-component transport and gas chemistry. The results show that the effect of reactants pre-heating and insulations allows the flame to propagate even in micro channels. Furthermore, initial heat losses and wall radical quenching are the main parameters that determine the flame propagation in such micro burners.

In order to provide a better understanding to the underlying fundamentals of the combustion of gaseous hydrocarbon fuels like propane (C_3H_8) and methane (CH_4) in micro-burners, numerical simulations using commercial software were conducted. For instance, FLUENT software has been used to investigate the effect of wall conductivity, burner dimensions and external heat losses on combustion characteristics in meso-scale burners, which modeled as two parallel plates (Norton and Vlachos, 2003, 2004). In their work, combustion chemistry with one-step irreversible reaction mechanism was employed. This chemistry is deemed sufficient to demonstrate flame dynamics behavior. It was highlighted that propane-air micro-flames are more stable than methane-air flames. The lower ignition temperature of propane fuel contributes to this flame stability enhancement. A similar reaction mechanism is used by Feng et al. (2010) to numerically solve methane-air combustion in a circular tube combustor. Factors affecting the flame temperature like the combustor size, inlet velocity and equivalence ratio were studied. Their results indicate that the equivalence ratio of the mixture and the burner dimension can be considered as important parameters to the flame temperature. Next, Li et al. (2009) presented their findings on methane-air combustion using detailed combustion chemistry with 25-reversible reaction mechanism in two-dimensional (2-D) cylindrical tubes and parallel plates. The partial oxidation that involves in the reaction process can be well represented by the detailed mechanism. Their studies show that proper material selections can be performed if the flame temperature in the combustor is known.

Apart from hydrocarbon fuels, the prediction of premixed flame temperature and flame dynamics in a narrow cylindrical tube with hydrogen as a fuel has been reported by several researchers (Brambilla, et al., 2013; Jejurkar and Mishra, 2011). The effects of various heat transfer conditions on hydrogen combustion have been well discussed by Hua et al. (2005). A detailed reaction mechanism with 19-reversible reaction mechanism was employed to study the combustion stability with and without the presence of wall conduction. Their studies suggest that lower wall thermal conductivity can reduce the heat loss, which results to the enhancement of combustion stability. Nevertheless, the low wall thermal conductivity is likely to cause hot spot on the combustor wall that can decrease the material lifespan.

Numerical simulation was also performed on a more complex combustor geometry like Swiss-roll combustor in order to reduce the occurrence of extinction. Chen and Buckmaster (2004) demonstrated the combustion of the premixed fuel-lean propane–air mixture in a Swiss-roll combustor. The idea of using a flame holder in meso-scale cylindrical tube combustors was first proposed by Mikami et al. (2013). In their experimental work, a stainless steel wire mesh is placed between the burned and unburned gas region. The experimental results show that the flame can be stabilized for both gas and liquid fuel. In fact, it is also demonstrated that flame could be even stabilized in a tube with a diameter below than the classical quenching distance.

In this study, a numerical simulation of propane-air combustion in meso-scale cylindrical tubes with concentric rings is presented. A set of rings is used as a flame holder. The effect of wall thermal conductivities of the unburned and burned regions on flame, inner and outer wall surface temperature distribution was examined. The blowout limits and combustion efficiency with different combination of wall thermal conductivities were also investigated. The surface reaction is excluded in the analysis since materials that can resist radical quenching are now available.

[DOI: 10.1299/jtst.2015jtst0008]

2. Numerical Simulation Setup

A two-dimensional (2-D) steady state numerical simulation was performed using ANSYS Release 14.0 with Fluent 6.3 (ANSYS Inc, 2012). The inner diameter of the combustor is 3.5 mm and the wall is 0.7 mm thick. The wall thickness is modeled as a solid phase where only the energy equation is solved. The total length of the combustor is set to 40 mm. The combustor is divided into two parts namely the unburned and burned gas region by concentric rings.

The concentric rings are modeled as square rectangles with 0.14 mm in length and placed side by side where the location is set to be 30 mm at which is measured from the center of the combustor inlet to the left side of the rings. This value is chosen to ensure that the flow will be fully developed before passing the rings. The wall of the rings is modeled as a thermally thin-wall and its material is stainless steel that has a wall thermal conductivity of 20 W/m/K. One-dimensional (1-D) conductive heat transfer is assumed at the wall of the rings and to model this 1-D heat transfer, a sufficiently small wire thickness is defined to the wall of the rings, which in this case is 0.01 mm. Hence, with this assumption, defining the mesh element inside the rings is not necessary and the total number of mesh element in the computational domain can be reduced. The effect of this thermal conduction is minimal as compared to the thermal conduction via the combustor wall. The main function of the rings is to stabilize the flame before any variation of other

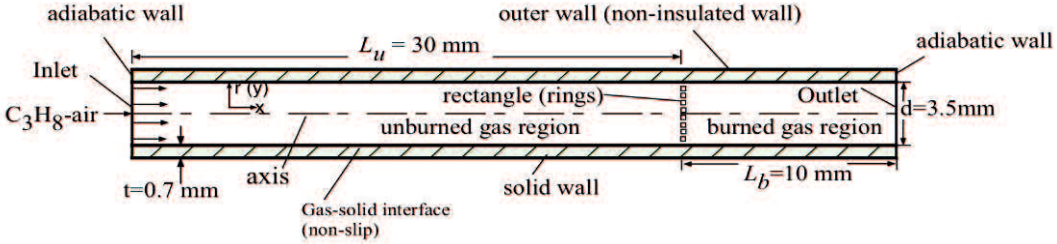

Fig. 1 Schematic of the computational domain (not to scale)

parameters is made. It is widely known that the flame holder prolongs the residence time in the reaction zone that leads to the stable flame. The gap between the rings is set to 0.10 mm to enable the fluid flows and passes through this gap. The fuel type used is propane (C_3H_8)-air mixture. The schematic of the computational domain for this simulation is illustrated in Fig. 1.

In this work, Dufour, gas radiation effects and the work done by pressure and viscous force are assumed to be negligible. Norton and Vlachos (2003) have shown that the gas phase radiation has minimal effect on the combustion reactions. Ideal gas law is assumed for the gas density and the specific heat for all the species is calculated using a piecewise-polynomial fit of temperature. The thermodynamics and transport data are obtained from the Fluent internal database (ANSYS Inc, 2012) and Myer (1998).

Meanwhile, reduced one-step propane combustion with five species as suggested by Westbrook and Dryer (1981) is employed as the combustion chemistry,

$$C_3H_8 + 5O_2 \rightarrow 3CO_2 + 4H_2O \quad (1)$$

The species involved are C_3H_8, O_2, N_2, CO_2 and H_2O.

It should be noted that a detailed kinetics mechanism is compulsory if simulations are performed to evaluate flame or emission characteristics. However, since the focus of this study is to examine the trend pattern of the effect of wall thermal conductivity on the combustion stability, the single step mechanism is sufficient. A non-uniform mesh element size is utilized where high mesh concentration is applied in the area surrounding the rings due to the small gap between these rings. The total number of elements is 19482 and employed for all cases. A grid dependent test was performed and revealed that greater number of elements yields no significant advantage in terms of results accuracy.

Boundary conditions are specified as proposed by Norton and Vlachos (2004) and Li et al. (2009) No-slip boundary type condition is applied at the interface between the fluid and the solid wall. The heat flux at this interface is calculated using Fourier's law. Heat transfer by means of convection at the outer surface of the wall is given by:

[DOI: 10.1299/jtst.2015jtst0008]

$$q" = h\,(T_W - T_{amb}) \quad (2)$$

where h is the convective heat transfer coefficient, T_W is the outer wall temperature and T_{amb} is the ambient temperature, which is set to 300 K for all cases. The convective heat transfer coefficient (h) is fixed to be at 5 W/m^{2}K, which represents a weak natural convection (Li, et al., 2009).

A thermal insulation (zero heat flux boundary) is applied at both left and right wall edges of the combustor. The wall thermal conductivity for both the unburned gas region (k_u) and the burned gas region (k_b) of the solid wall is varied from 1.0 W/m/K to 1000 W/m/K. The solid zone of k_u and k_b can be established by defining two separate cell zones of the solid wall in the ANSYS-Fluent. In a practical application, this region can be separated by using two composite tubes for the unburned and burned gas region. These tubes can be adhered together using special ceramic adhesive as demonstrated by Mikami et al. (2013). For the outlet boundary condition, a fixed pressure is used while a far-field condition is applied for the species normal to the outlet. This means that a zero diffusive flux of species is assumed at the outlet. An axis boundary condition is established at the centerline so that the calculation can be performed only in the half of the domain. Table 1 below summarizes the numerical model setup while Fig.2 shows the results of grid dependent test with different number of elements.

Table 1 Summary of the model setup

Parameters	Model setup
Solver	Pressure-based, steady-state and axisymmetric
Species model	Laminar finite-rate with stiff chemistry solver
Pressure-velocity coupling	SIMPLE
Spatial discretization	First-order upwind scheme
Density	Ideal gas law
Mixture specific heat	Mixing law
Species specific heat	Piecewise polynomial
Convergence criteria for the scaled residuals	1 x 10^{-3} for continuity, 1 x 10^{-3} for velocity 1 x 10^{-6} for energy and 1 x 10^{-3} for species equation

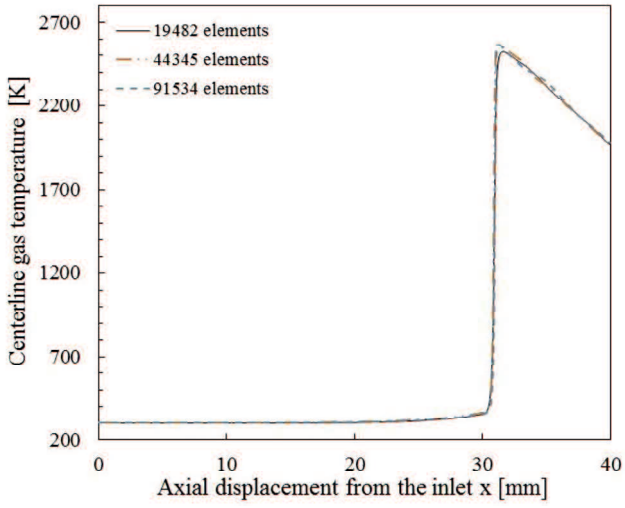

Fig. 2 Centerline gas temperature distribution along the axial displacement with different number of elements with k_u=1 W/m/K and k_b= 1 W/m/K for U 0.30 m/s and ϕ=1.0

A laminar flow of U with a flat velocity profile is applied at the inlet while the inlet feed temperature is maintained at 300 K. At first, the value of U is set to 0.20 m/s and the equivalence ratio (ϕ) of the mixture is initialized to 1. A technique that is called as “cold flow” is employed where the momentum and continuity equation is first solved.

[DOI: 10.1299/jtst.2015jtst0008]

Then, by patching a high temperature around an area that can be defined as patch zone, the energy and species equations are then solved. This patch zone is located at 2 mm from the outlet and should not be placed too close to the outlet since it can result to a reverse gas flow, which negatively affects the ignition process. A sufficiently high temperature of 1700 K is applied on the patch zone to ensure that the fuel-air mixture can be ignited. Once ignited, the flame propagated to the upstream and eventually stabilized near the rings. To obtain the blowout limit, the value of ϕ is first fixed and the value of U is gradually stepped up with 0.01 m/s interval. The corresponding U value that causes the flame to propagate away from the rings and subsequently blown off the tube is considered as the blowout limit. The whole process starting from the cold flow step is repeated to obtain the blowout limits for different values of ϕ.

3. Results and Discussion

3.1 Flame propagation and stabilization

Flame propagation in a narrow channel is a broad subject matter. Investigation of flame propagation characteristics in a narrow channel tube combustor is indeed a formidable task. In order to numerically study the phenomenon of flame propagation inside a meso-scale tube combustor, a detailed kinetics reaction mechanism is required that can lead to a higher computational cost. As mentioned in Section 2, this investigation is mainly on the effect of wall thermal conductivities on the combustion of this type of combustor. Therefore, results shown in Fig. 3 are only limited to demonstrate the capability of the concentric rings.

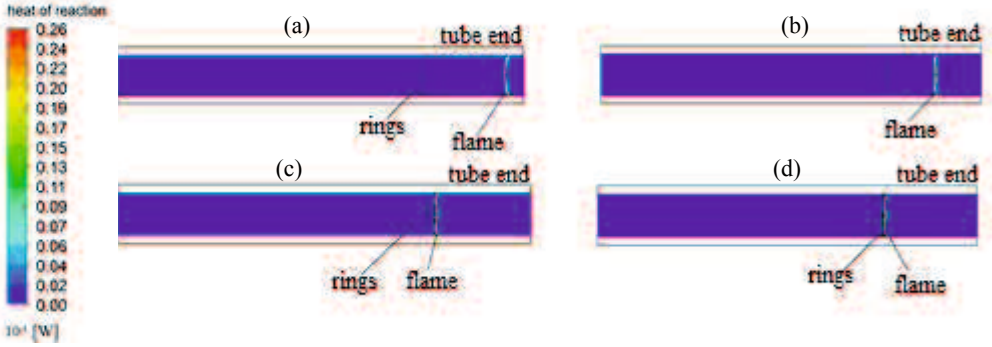

Fig. 3 Heat of reaction contours with different values of iteration number for k_u=1 W/m/K and k_b=1 W/m/K, ϕ =1.0 and U=0.20 m/s, (not to scale; for easier visualization, reflection of axis is used in all figures (a) iteration number=185; (b) iteration number= 385; (c) iteration number=755; (d) solution converged

The ignition was attained by applying a sufficiently high temperature on the patch zone. This ignition method replicates the experimental condition reported by Mikami et al. (2013). The inlet velocity was set to U=0.20 m/s while the equivalence ratio (ϕ) was fixed to 1.0. Since the flame burning velocity is faster than the inlet velocity, the flame propagated towards the inlet once it was ignited. As shown in Fig. 3, the flame stopped to propagate when it reached the rings and stabilized there until a converged solution was achieved. This condition is defined as a stable flame. The concentric rings act as a flame holder by which the flame can be stabilized at a fixed location.

3.2 Flame, gas and wall surface temperature profile

In micro combustors, flame, inner and outer wall temperatures are interdependent to each other. These characteristics are essentially important in a micro power generation research. Yang et al. (2012) suggest that a good combustor for micro power generation application should have a sufficiently high and uniform outer wall surface temperature. As for this simulation study, the wall thermal conductivity values for both the unburned (k_u) and burned (k_b) gas region were varied at 1 W/m/K, 10 W/m/K, 100 W/m/K and 1000 W/m/K. The effect of wall thermal conductivity on the temperature contours of the combustor is shown in Fig.4 while Fig. 5 illustrates the corresponding gas centerline temperature distribution. The flame temperature can be defined as the highest gas temperature recorded along the axial displacement. Figure 4 suggests that the variation of the wall thermal conductivity has a minimal effect on the flame temperature. As the value of k_u and k_b is increased to 10 W/m/K, 100 W/m/K and 1000 W/m/K respectively, there is notably better uniformity of gas and wall temperature distributions in the unburned gas region.

[DOI: 10.1299/jtst.2015jtst0008]

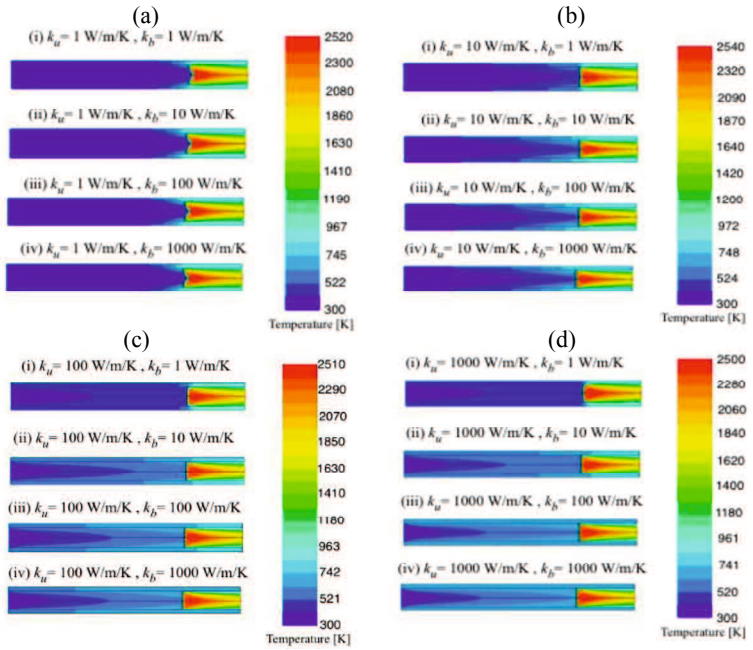

Fig. 4 (a)-(d) Temperature contours with different values of k_u and k_b for U=0.30 m/s and ϕ=1.0 (not to scale; for easier visualization, a reflection of the axis is used in all figures)

Meanwhile, Fig. 5 shows that there is a direct relationship between k_u values and the gas temperature in the unburned gas region particularly from x=3 mm onwards. This change is due to the role of the combustor wall as a heat

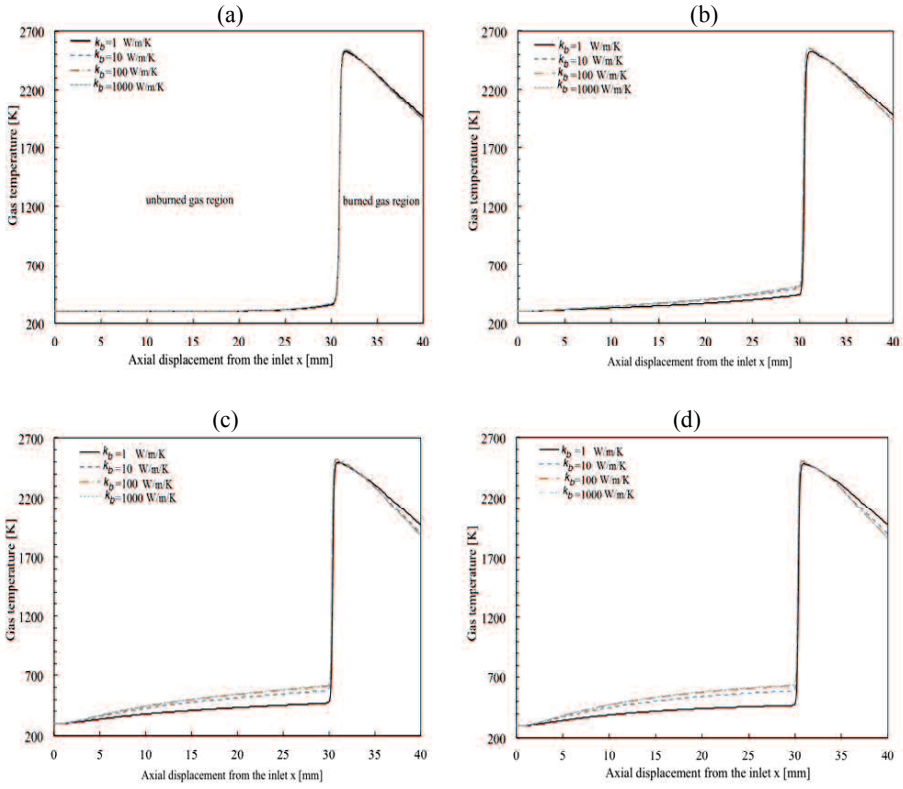

Fig. 5 Temperature distribution of gas at the centerline along the axial displacement with different values of k_u and k_b for U=0.30 m/s and ϕ=1.0: (a) k_u=1 W/m/K; (b) k_u=10 W/m/K; (c) k_u=100 W/m/K; (d) k_u=1000 W/m/K

conductor. The main method of transferring the heat from the hot burned gas to the unburned reactants in this type of combustor is by the wall conduction. The process of heating up the unburned gas prior to the combustion starts from the inner wall. Thus, the intensity of this process depends on the value of k_u. Figure 6 shows the temperature distribution of inner wall and gas inside the combustor with two different values of k_u and a fixed k_b value. For k_u=10 W/m/K, higher inner wall temperature is obtained in the unburned gas region up to x=29.0 mm as more heat energy is

[DOI: 10.1299/jtst.2015jtst0008]

distributed to the unburned gas region. Generally, this trend is repeated with a further increment of the k_u value. Nonetheless, using k_u=1000 W/m/K is no longer effective in boosting up the unburned gas temperature. The next important criterion for meso and micro scale combustion is the outer wall temperature distribution, which is presented in Fig. 7. Obviously, it is shown in the figure that the combination of low wall thermal conductivities in the unburned and burned gas region leads to steeper temperature gradients.

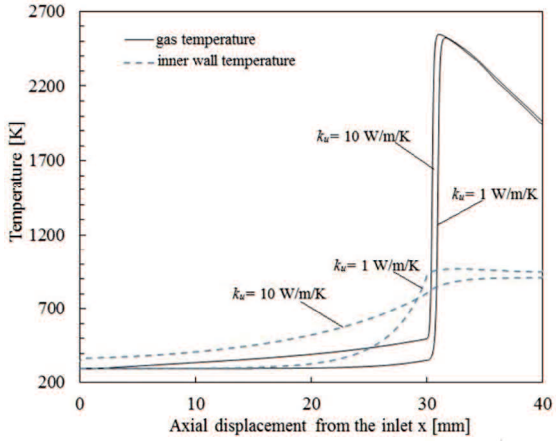

Fig. 6 Temperature distribution of the inner wall and gas at the centerline along the axial displacement from the inlet with k_u=1 W/m/K and k_u=10 W/m/K for k_b=10 W/m/K, U=0.30 m/s and ϕ=1.0

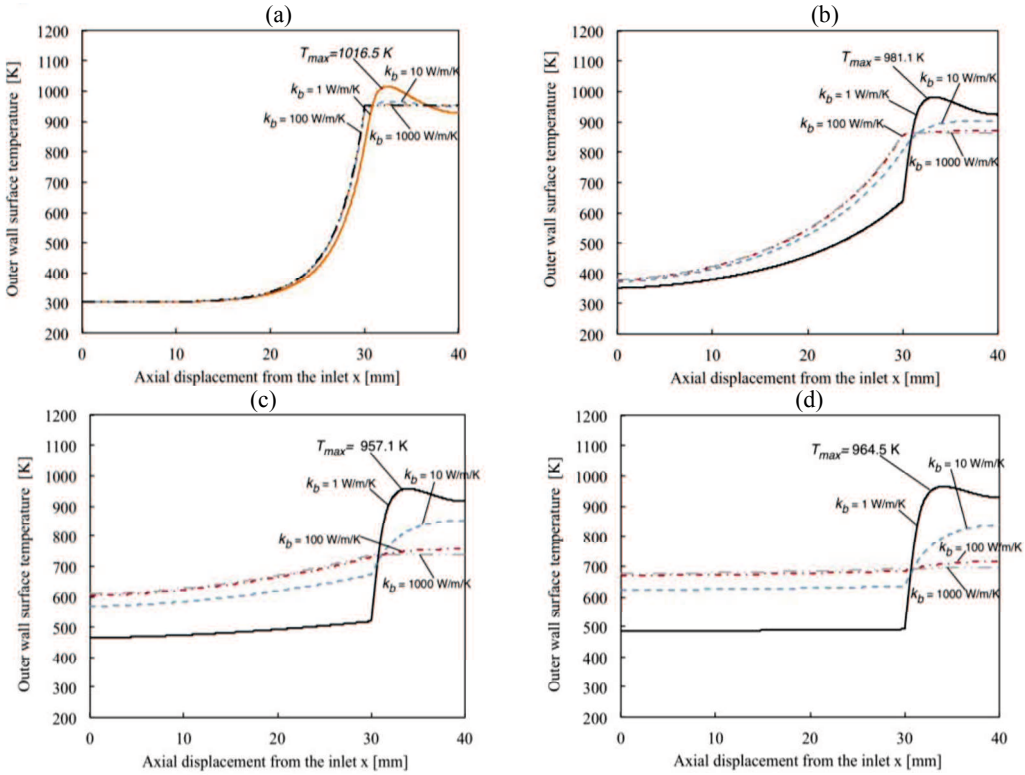

Fig. 7 Outer wall surface temperature distribution along the axial displacement from the inlet with different values of k_u and k_b for U=0.30 m/and ϕ = 1: (a) k_u=1 W/m/K; (b) k_u=10 W/m/K; (c) k_u=100 W/m/K; (d) k_u=1000 W/m/K

According to Norton & Vlachos (2003), such large temperature gradients can significantly reduce the material lifespan. In severe cases, melting of the combustor material might occur. Therefore, to avoid such a problem, a uniform outer wall temperature distribution is desired. This uniform temperature can be achieved by using a high wall thermal conductivity in the unburned (k_u) and burned gas region (k_b). However, it is noted that by utilizing a high value of k_u and k_b, the maximum wall temperature is dramatically reduced. For instance, with k_u=1000 W/m/K and k_b=1000 W/m/K, the maximum wall temperature is only at 694.7 K. This reduction is mainly due to the heat energy being

[DOI: 10.1299/jtst.2015jtst0008]

distributed to a wider range of area. A lower wall temperature means a reduction of the combustor efficiency in converting heat to electrical energy. As such, a proper consideration is necessary in order to balance between the need of a high performance combustor and a durable combustor.

3.3 Effects of the inlet velocity and equivalence ratio

According to Park et al. (2012), the efficiency of a micro combustor in converting the heat produced from combustion to electrical energy is significantly affected by the inlet velocity. This fact is due to the temperature variation with respect to the inlet velocity. With the elevation of the inlet velocity, more reactant mixture is delivered to the burned region that eventually escalates the reaction rate. Consequently, there is a surge of flame temperature that results to a greater outer wall surface temperature distribution.

Figure 8 depicts the outer wall temperature distribution along the axial displacement with different values of inlet velocity (U) and equivalence ratio (ϕ). As shown in Fig. 8 (a), the increment of the inlet velocity escalates the wall

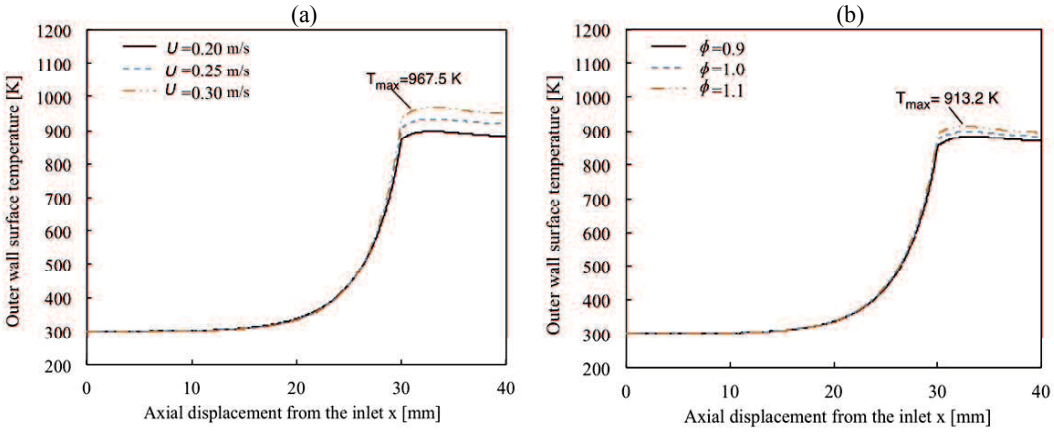

Fig. 8 Outer wall surface temperature distribution along the axial displacement from the inlet with different U and ϕ for k_u=1 W/m/K and k_b=10 W/m/K: (a) for different values of U with constant ϕ=1.0; (b) for different values of ϕ with constant U=0.20 m/s

temperature particularly in the burned gas region. This pattern is also valid for larger values of k_u where the increase of wall temperature is more noticeable in the unburned gas region. It is important to note that the process of obtaining a higher outer wall temperature distribution by applying a higher inlet velocity should be prudently performed as blowout might occur.

The other way to elevate the wall temperature without adjusting the inlet velocity is by increasing the equivalence ratio (ϕ). Figure 8(b) clearly shows that a richer fuel-air ratio can result to an increase in the wall temperature due to greater reaction rate. Nevertheless, considering the environment where micro power generators are utilized, combustion of fuel mixture with below the stoichiometric ratio is preferred.

3.4 Effects of the wall thermal conductivity on the flame stability and combustion efficiency

In meso and micro-scale combustors, the wall thermal conductivity plays a significant role in determining the flame stability. The axial heat conduction from the burned gas region promotes the pre-heating of the unburned gas that eventually enhances the flame stability. One of the indicators of flame instability in a micro combustor is blowout. In general, blowout occurs when the combustor exit velocity is higher than flame burning velocity (Turns, 2003). It is important to determine the blowout limits for meso and micro-scale combustors so that the operative range can be ascertained.

In this study, the determination of blowout limits is as follow. Firstly, a stable flame is established in the combustor. For all cases, a stable flame can be achieved with the inlet velocity (U) of 0.20 m/s regardless of the equivalence ratio (ϕ) value. Then, the value of U is gradually stepped up with 0.01 m/s interval and further calculation is conducted until a converged solution is achieved. For instance, if increasing the value of U from 0.25 m/s to 0.26 m/s

[DOI: 10.1299/jtst.2015jtst0008]

causes the flame to propagate away from the rings toward the outlet, then U=0.25 m/s is considered as the blowout limit. This step is repeated for each case of ϕ and both wall thermal conductivities (k_u and k_b). Figure 9 shows the flame image with a blowout condition while Fig. 10 summarizes the blowout limits with respect to all variable parameters. As depicted in Fig.9, with the value of U increased to 0.42 m/s, the flame is blown out to the tube end resulting to the

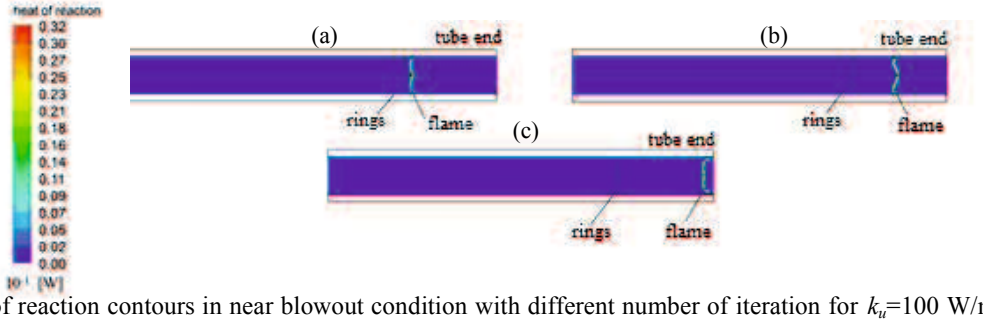

Fig. 9 Heat of reaction contours in near blowout condition with different number of iteration for k_u=100 W/m/K, k_b=100 W/m/K, ϕ=1.0. This phenomenon of blowout occurs when U was increased from 0.41 m/s to 0.42 m/s: (a) iteration number=100; (b) iteration number=7000; (c) iteration number=9500(not to scale, for easier visualization, reflection of axis is used)

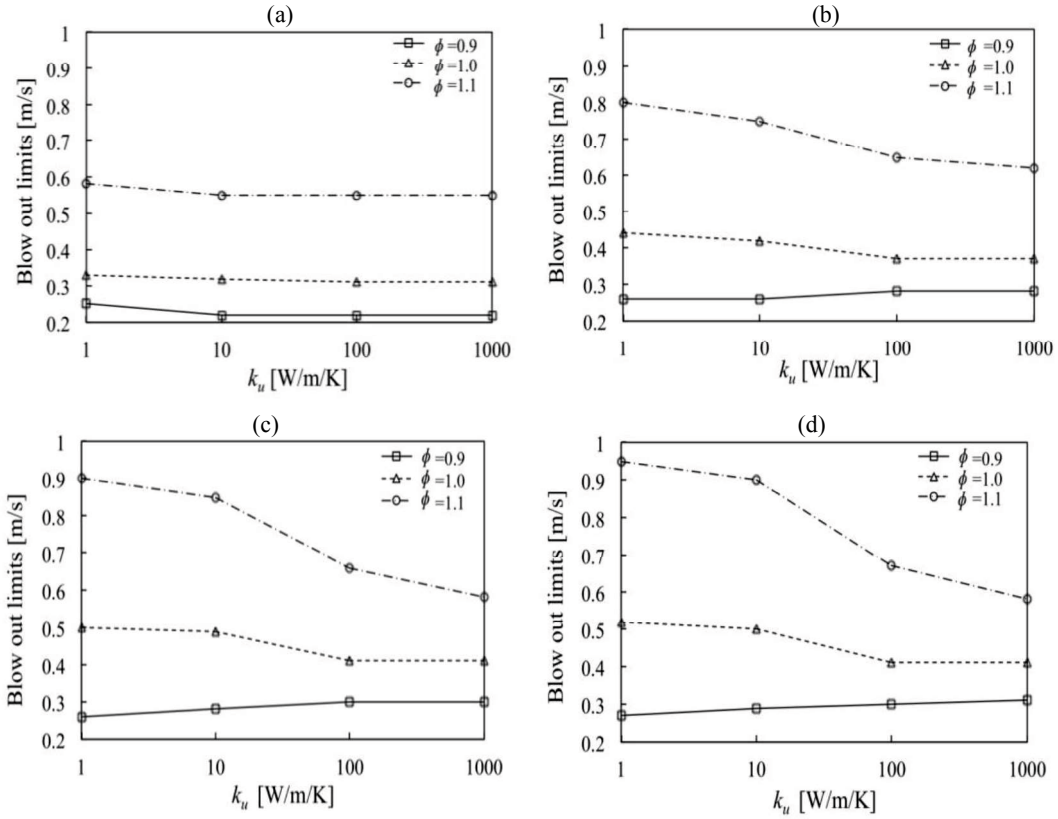

Fig. 10 Blowout limits with different values of k_u, k_b and ϕ (a) k_b=1 W/m/K; (b) k_b=10 W/m/K; (c) k_b=100 W/m/K; (d) k_b=1000 W/m/K

flame extinction. Meanwhile, Figure 10 indicates that as k_b is increased from 1 W/m/K to 100 W/m/K, the flame stability is enhanced. In overall, the combustion of mixture that is rich in fuel significantly improves the blowout limits as Mikami et al. (2013) experimentally showed for meso-scale quartz tube combustors with wire mesh. However, there is only a slight improvement in the limit with the use of k_b=1000 W/m/K. It is also shown that there is an inverse relationship between the value of k_u and the blowout limits except for ϕ=0.90 as indicated in Fig. 10 (b) to (d). This reduction of limit is probably due to the variation of pre-heating effect that occurs in the unburned gas region.

Figure 11 presents the temperature distribution along the inner wall with different values of k_u and k_b. It can be seen from the figure that the inner wall temperature at x=29.5 mm for k_u=1 W/m/K is the highest. This maximum inner

[DOI: 10.1299/jtst.2015jtst0008]

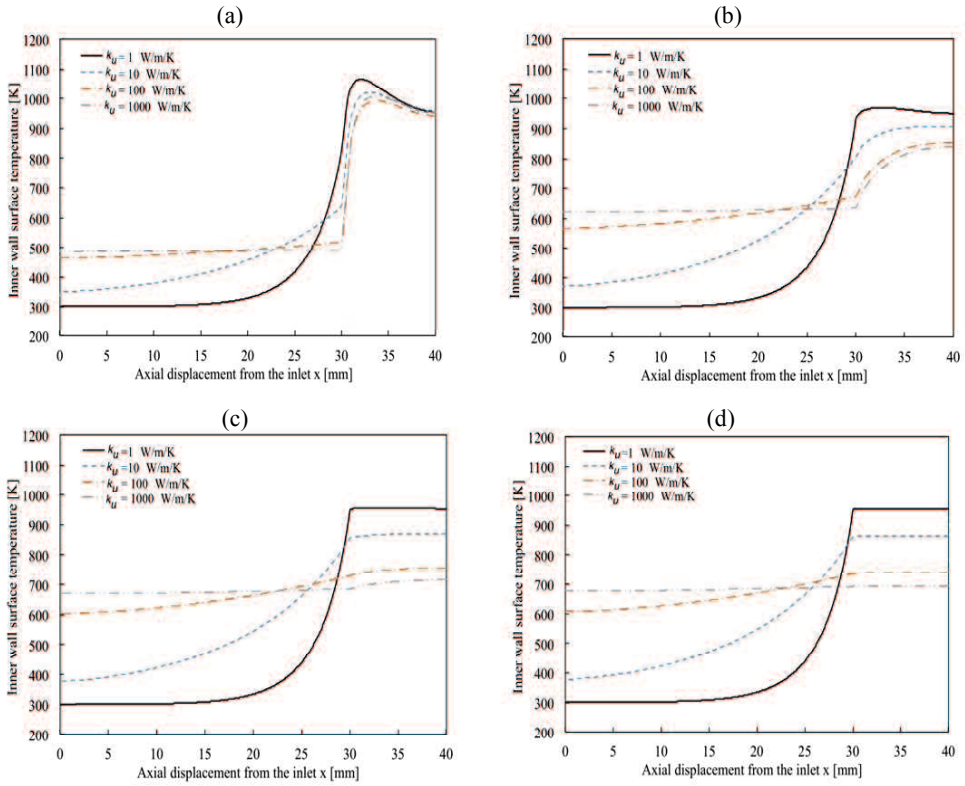

Fig. 11 Inner wall temperature with different values of k_u for U=0.30 m/s and ϕ=1.0; (a) k_b=1 W/m/K; (b) k_b=10 W/m/K; (c) k_b=100 W/m/K; (d) k_b=1000 W/m/K

wall temperature is still within the unburned gas region. Figure 12(a) depicts the numerical value of inner wall temperature at x=29.5 mm while Fig. 12(b) shows the blowout limits for ϕ=1.0. The highest inner wall temperature is recorded to be 848.7 K while the maximum blow out limits is 0.52 m/s. Clearly, Fig. 12 suggests that the blowout limits is affected by the inner wall temperature, particularly in the small area just before the ring position. The increased inner wall temperature at such a position conceivably increases the local burning velocity at the flame attachment region. The use of a bigger k_u value can result to a lower temperature in this area. Consequently, the blowout limit is decreased. However, it is observed from the results that for the combustor with k_b=1 W/m/K, the blowout limit does not change dramatically with the increase of k_u. It is important to note that at near blowout conditions, the flame is slightly displaced towards the downstream. For the combustor with k_u=1 W/m/K and k_b=1 W/m/K, the flame is located at 32.2 mm from the inlet when U is increased to 0.32 m/s (the blowout limit is 0.33 m/s). There is possibility that the elevation of the inner wall temperature has no effect on the flame stability at this near blowout condition.

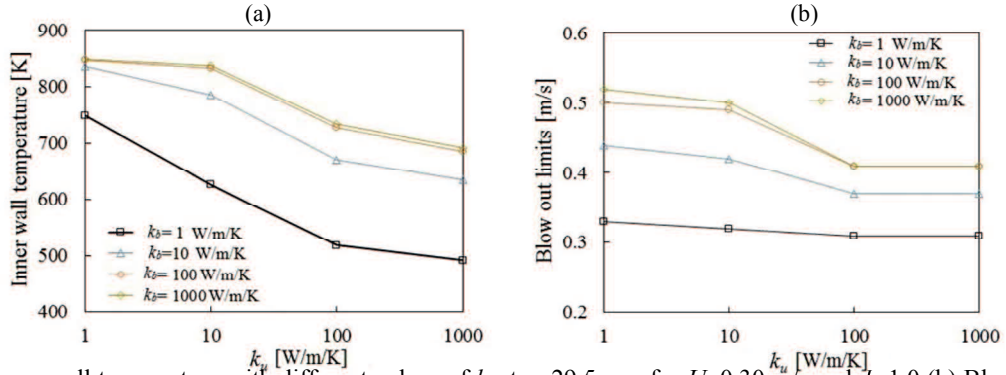

Fig. 12 (a) Inner wall temperature with different values of k_b at x=29.5 mm for U=0.30 m/s and ϕ=1.0 (b) Blowout limits with different values of k_b for ϕ=1.0.

Meanwhile, the combustion efficiency with respect to the wall thermal conductivity is presented in Fig. 13. The combustion efficiency for the combustor with wall thermal conductivity k_b of 1000 W/m/K is not shown in the graph as it has the same tendency as the combustor with k_b=100 W/m/K. It can be seen from the figure that there is an inverse

[DOI: 10.1299/jtst.2015jtst0008]

relationship between the wall thermal conductivity k_u and the efficiency. Jianlong et al. (2012) stated that the combustion efficiency for a micro combustor depends on the inlet velocity, heat losses and flame temperature. Thus, this variation of combustion efficiency is mainly due to the transverse heat loss to the ambient air with the use of higher wall thermal conductivity. Nevertheless, the efficiency change is relatively small.

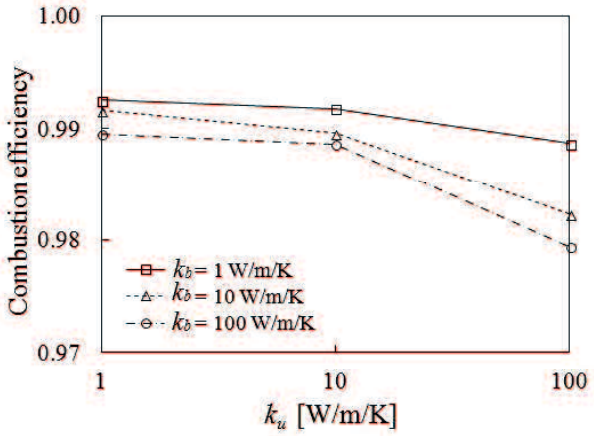

Fig. 13 Combustion efficiency with different values of k_u and k_b for U=0.20 m/s and ϕ= 0.90

4. Conclusions

The numerical simulation of combustion of propane-air mixture in meso-scale tube combustors with concentric rings has been successfully demonstrated. The function of the concentric rings is to stabilize the flame at a fixed location. With the use of these rings, it is possible to vary the wall thermal conductivity in the two different regions.

In this type of combustor, the wall and gas temperature distribution in the unburned gas region is tremendously affected by the value of wall thermal conductivity. However, the use of a high value of k_u or k_b in which for this case k=1000 W/m/K produces no observable effect on both the wall and gas temperature profile. It is demonstrated that the flame temperature is independent to the wall thermal conductivity. On the other hand, the inlet velocity and the equivalence ratio have a significant impact on the flame temperature, which in turn affects the wall and gas temperature distribution.

It is a well-known fact that the utilization of low wall thermal conductivity values leads to the high temperature gradients that eventually contributes to hot spot related problems. Thus, by establishing the two separate regions of wall thermal conductivity, the problems related to the high thermal stress could be minimized without compromising the combustor efficiency.

Lastly, the blowout limits greatly depend on the wall thermal conductivity. The blowout limits are significantly affected by the inner wall temperature particularly in the area just before the ring position. The increased inner wall temperature at such a position conceivably increases the local burning velocity at the flame attachment region. The use of higher wall thermal conductivity in the unburned gas region brings down the value of the inner wall temperature in the area just before the ring position. As a result, the blowout limits are also reduced. It is also demonstrated that the combustion efficiency is influenced by the variation of the wall thermal conductivity k_u. The use of a combustor with a low value of k_u can improve the combustion efficiency. However, other critical factors such as the outer wall temperature and the blowout limits should also be considered before selecting the appropriate wall thermal conductivity.

Acknowledgment

The authors would like to express heartiest gratitude to Universiti Teknologi Malaysia (UTM) for providing the software. This research was partly subsidized by JSPS KAKENHI Grant-in-Aid for Challenging Exploratory Research

[DOI: 10.1299/jtst.2015jtst0008]

(26630443). The first author would like to the Malaysian Ministry of Education (MOE) and Universiti Teknikal Malaysia Melaka (UTeM) for the study scholarship.

References

ANSYS Inc., ANSYS Fluent Tutorial Guide, ANSYS Inc., Canonsburg PA, (2012).

Brambilla, A., Frouzakis, C.E., Mantzaras, J., Bombach, R., Boulouchos, K., Flame dynamics in lean premixed CO/H_2 /air combustion in a mesocale channel, Combustion and Flame, (2013), *In press*.

Chen, M., Buckmaster, J., Modelling of combustion and heat transfer in 'Swiss roll' micro-scale combustors, Combustion Theory and Modeling, Vol. 8, (2004), pp. 701-720.

Feng, L., Liu, Z., Li, Y., Numerical study of methane and air combustion inside a small tube with an axial temperature gradient at the wall, Applied Thermal Engineering, Vol. 30, (2010), pp. 2804-2807.

Hua, J., Wu, M., Kumar, K., Numerical simulation of the combustion of hydrogen–air mixture in micro-scaled chambers Part II: CFD analysis for a micro-combustor, Chemical Engineering Science, Vol. 60, (2005), pp.3507-3515.

Jejurkar, S.Y., Mishra, D.P., Effects of wall thermal conductivity on entropy generation and exergy losses in a H_2-air premixed flame microcombustor, International Journal of Hydrogen Energy, Vol. 36, (2011), pp. 15851-15859.

Jianlong, W., Aiwu, F., Maruta, K., Hong, Y., Wei, L., Experimental and numerical investigation on combustion characteristics of premixed hydrogen/air flame in a micro-combustor with a bluff body, International Journal of Hydrogen Energy, Vol. 37, (2012), pp. 19190-19197.

Kaisare, N.S., Vlachos, D.G., A review on microcombustion: Fundamentals, devices and applications, Progress in Energy and Combustion Science, Vol. 38, (2012), pp. 321-359.

Kurdyumov, V.N., Pizza, G., Frouzakis, C.E., Mantzaras, J., Dynamics of premixed flames in a narrow channel with a step-wise wall temperature, Combustion and Flame, Vol. 156, (2009), pp. 2190-2200.

Li, J., Chou, S.K., Yang, W.M., Li, Z.W., A numerical study on premixed micro-combustion of CH4–air mixture: Effects of combustor size, geometry and boundary conditions on flame temperature, Chemical Engineering Journal, Vol. 150, (2009), pp. 213-222.

Maruta, K., Micro and mesoscale combustion, Proceedings of the Combustion Institute, Vol. 33, (2011), pp. 125-150.

Miesse, C., Masel, R., Short, M., Shannon, M., Experimental observations of methane–oxygen diffusion flame structure in a sub-millimetre microburner, Combustion Theory and Modeling, Vol. 9, (2005), pp. 77-92.

Mikami, M., Maeda, Y., Matsui, K., Seo, T., Yuliati, L., Combustion of gaseous and liquid fuels in meso-scale tubes with wire mesh, Proceedings of the Combustion Institute, Vol. 34, (2013), pp. 3387-3394.

Myer K., Mechanical Engineers Handbook Second Edition (1998), John Wiley & Sons.

Norton, D.G., Vlachos, D.G., Combustion characteristics and flame stability at the microscale: a CFD study of premixed methane/air mixtures, Chemical Engineering Science, Vol. 58, (2003), 4871-4882.

Norton, D.G., Vlachos, D.G., A CFD study of propane/air microflame stability, Combustion and Flame, Vol. 138, (2004), pp. 97-107.

Park, J.H, Lee, S.I., Wu, H., Kwon, O.C.,Thermophotovoltaic power conversion from a heat-recirculating micro-emitter, International Journal of Heat and Mass Transfer, Vol. 55 (2012), 4878–4885

Raimondeau, S., Norton, D., Vlachos, D.G., Masel, R.I., Modeling of high temperature microburners, Proceedings of the Combustion Institute, Vol. 29, (2002), pp. 901-907.

Suenaga, Y., Kitano, M., Yanaoka, H., Development of Ultra-Micro Combustor Using Cylindrical Flames, Journal of Thermal Science and Technology, Vol. 6, (2011), pp. 406-415.

Turns, S., R., An Introduction to Combustion Concepts and Applications 2nd Edition (2003), p.298, McGraw-Hill.

Westbrook, C.K., Dryer, F.L., Simplified Reaction Mechanism for the Oxidation of Hydrocarbon Fuels in Flames, Combustion Science and Technology, Vol. 27, (1981), pp. 31-43.

Yang, W.M., Jiang, D.Y., Chou, S.K., Chua, K.J., Karthikeyan, K.H., Experimental study on micro modular combustor for micro-thermophotovoltaic system application, International Journal of Hydrogen Energy, Vol. 37, (2012), pp. 9576-9583.

[DOI: 10.1299/jtst.2015jtst0008]

IMPROVEMENT OF COMBUSTION STABILITY IN NARROW TUBES WITH WIRE MESH

F.A. MUNIR[1], N. HATAKEDA[1], T. SEO[1] and M. MIKAMI[1]

[1] Graduate School of Science and Engineering, Yamaguchi University
2-16-1 Tokiwadai, Ube, Yamaguchi, 755-8611, Japan

ABSTRACT

Micro combustion system is one of potential solutions that provides better energy requirement for small-scale devices as compared to conventional batteries. In recent years, numerous works have been conducted to enhance the combustion stability of meso and micro-scale combustors. In this study, an approach to enhance the stability of propane/air premixed combustion inside narrow tubes with stainless steel wire mesh was experimentally investigated. Cylindrical quartz tubes with inner diameter of 3.5 mm and different unburned and burned gas region lengths were used as the combustor. The wire mesh was located between the unburned and burned gas regions of the tubes. A part of the tubes was heated by an external source to simulate heat recirculation from the burned gas to the unburned gas. The equivalence ratio and mixture flow velocity were varied and the effects on the combustion characteristics were observed. The wall temperature at the unburned gas area was also measured using a thermography camera. The results show that heating the unburned mixture of propane/air has significant effects on stabilizing the flame in a narrow tube with stainless steel wire mesh. In other words, the flame can be stabilized near the mesh with better range of equivalence ratios.

INTRODUCTION

Dwindling energy resources and the strong demand for better power sources as compared to conventional batteries have sparked research interest in micro power generation [1-3]. The invention of state of the art electronics devices requires more energy capacity, shorter charging period and lightweight, characteristics which batteries lack [4]. Therefore, in recent years micro power generation systems have been seen as potential alternatives to batteries due to the higher energy densities of hydrocarbon fuels [5].

Micro and meso scale combustion phenomena are key components in micro power generation. However, the difficulty of sustaining a stable flame for a micro combustor due to its high surface to volume ratio is one of the major issues in micro combustion [6-8]. This high surface to volume ratio causes large portion of heat loss from flame to wall. Thus, a substantial number of numerical and experimental works to enhance the performance of micro combustors have been conducted. The effects of reduced size of combustor to the flame stability, flame temperature and flame propagation have been thoroughly investigated [9, 10]. The outcome results of these studies demonstrate that the performance of a micro combustor can be significantly affected by wall thickness and combustor geometry.

In addition to that, various methods of improving the performance of meso and micro combustors have been highlighted. For example, flame stabilization in a meso-scale quartz tube with stainless steel wire mesh for both gas and liquid hydrocarbon fuels has been successfully demonstrated [11]. According to their study, the presence of the wire mesh enhanced the heat recirculation in the combustor. Consequently, the combustion stability was significantly improved.

Apart from that, a Swiss-roll burner was successfully used to improve flammability limits, enhance flame stability and reduce quenching distance [12]. This type of burner utilizes the concept of excess enthalpy principle of which the unburned mixture is heated by its own generated heat. Previous studies pertaining to utilization of heat recirculation and excess enthalpy principle in tube shape combustors have been reported by several researchers [13-15]. Their results show that better combustion stability can be achieved by preheating the incoming cold reactants.

In this research, the effect of geometry and heating the unburned gas region on the combustion of propane fuel inside a narrow tube with steel wire mesh was experimentally investigated. The combustion stability in term of flame stabilization limit under different operational conditions was recorded and analyzed.

EXPERIMENTAL SETUP

In this experiment, narrow cylindrical quartz tubes with stainless steel wire mesh were used. The mesh type was 60 mesh/in with wire diameter of 0.14 mm. The inner diameter of the tube was 3.5 mm with wall thickness of 0.7 mm. The length from the mesh to the upstream part of the tube was varied at 10 mm, 30 mm and 160 mm. This length can be defined as the unburned gas region length L_{ub}. On the other hand, L_{bu} is defined as the burned gas region length which is the length between the mesh to the downstream part of the tube. L_{bu} was varied at 5 mm, 10 mm and 30 mm for this investigation. The ambient temperature was 295 K which was maintained at 100 mm away horizontally from the combustor wall. Propane (C_3H_8) and air was mixed and supplied into the tube with equivalence ratio ϕ and the cross-sectional-area mean flow velocity U. Each flow rate of air and propane was controlled by a mass flow controller.

A ceramic heater (WATLOW 220W) was used to heat up the unburned mixture region of the combustor. This condition simulates the excess enthalpy combustors such as Swiss-roll burner where heat recirculation mechanism exists. The heater inner temperature T_h was set to 673 K during experiment. A thermocouple type-K was used to measure the heater inner temperature. It was placed as near as possible to the heater inner wall. A Proportional-Integral-Derivative (PID) controller was employed in order to control the temperature. In addition, this temperature setting of T_h is determined based on the measured exhaust gas

temperature at the downstream area of the tube. Meanwhile, the narrow quartz tube was set up horizontally and connected to a copper tube with 4.5 mm inner diameter and 0.90 mm wall thickness which supplied propane/air mixture. The connection was done using a thermal- resistant cellophane tape. Since the outer diameter of the quartz tube is smaller than the copper tube outer diameter, it was necessary for the connecting part of the quartz tube to be covered by cellophane tape. This is to ensure that both quartz and copper tube can be perfectly fitted together. By doing this, gas leaking can also be avoided. The width of the tape on the quartz tube was fixed to 4 mm.

The quartz tube was inserted L_{in} into the heater using a traverse system. L_{in} is defined as the insertion length which was measured between the downstream of the quartz tube to the heater opened end. L_{in} was consecutively varied at 26 mm and 36 mm in this experiment. Figure 1 summarizes all the parameters involved in the experiment.

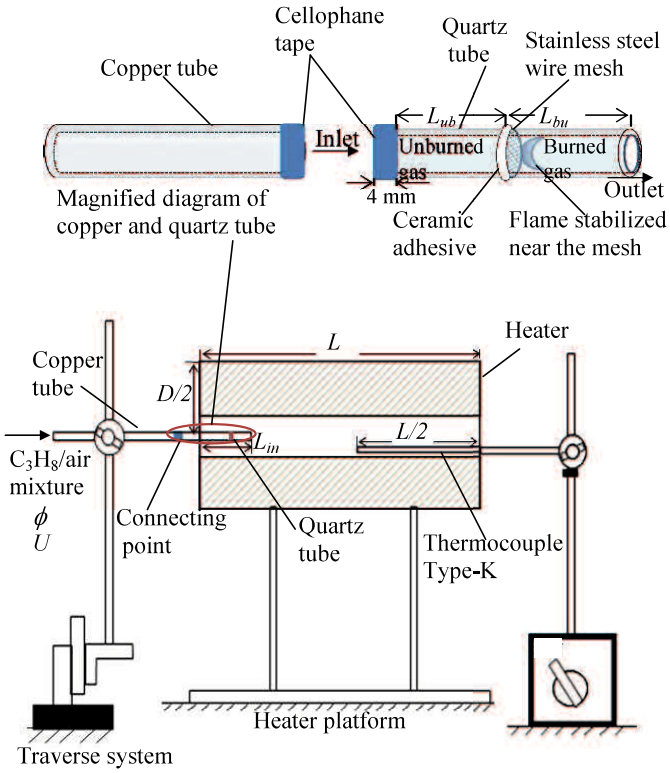

Figure 1. Parameters involved in the experimental setup

Before the quartz tube was inserted into the heater, the temperature inside the heater was measured with respect to the axial distance. A thermocouple type-K which was placed at the center of heater was used for this purpose. Figure 2 depicts the temperature distribution of the heater inner area with respect to the axial distance. Due to heat losses at both ends of the heater, there were temperature variations along the axial distance. Therefore, to reduce the heat losses to the ambient, fiber glass insulator sheets were placed at the heater opened end where the quartz tube was inserted as depicted in Fig. 3. In order to observe flame stabilization inside the tube, no fiber glass insulator sheet was placed at the other heater end. As depicted in Fig. 2, with the presence of the fiber glass insulator, heat loss to the ambient can be reduced. Consequently, higher surrounding temperature can be achieved with the same corresponding distance.

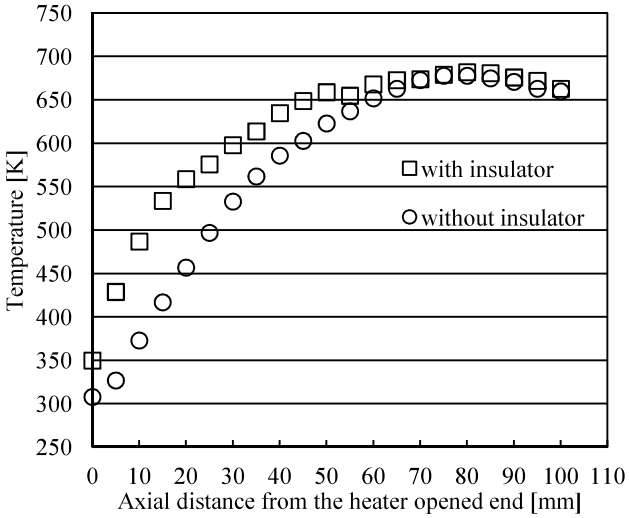

Figure 2. Temperature distribution inside the heater for setting temperature of T_h=673 K

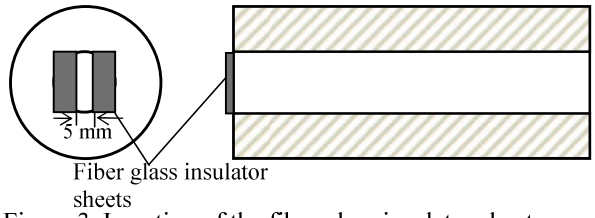

Figure 3. Location of the fiber glass insulator sheet

For the temperature measurement of the outer wall of quartz tubes, a thermography (AVIO InfReC R300R) was used. For the case of heating effect condition of which tube with L_{ub}= 30 mm was used, the tube was totally inside the heater when heating took place. Thus it was necessary to remove the heater quickly so that the wall temperature of the tube (with heating effect) could be measured. Wall temperature was taken as soon as the whole tube was outside of the heater.

RESULTS AND DISCUSSION

Effects of tube lengths on flame stabilization limit

At the initial stage of the experiment, the effect of tube lengths with respect to the unburned and burned gas region on the combustion stability was investigated. For this investigation, the tube was not inserted into the heater. At first, the burned gas region lengths were varied at 5 mm, 10 mm and 30 mm whereas the unburned gas region length L_{ub} was maintained at 10 mm. The results in term of flame stabilization limit for different burned gas region lengths L_{bu} are presented in Fig. 4.

The flame stabilization limit in this work is defined as limit where the flame is stabilized near the mesh inside the combustor. Beyond these limits, the phenomenon of blow off or quenching may occur. For example, in Fig. 4 for the tube with burned gas region length L_{bu} of 10 mm and equivalence ratio of unity, the maximum mean flow velocity is 46 cm/s just before the flame is blown off. As for the minimum mean flow velocity, the flame starts to quench when the velocity is 12 cm/s. As further explained in Fig. 4, there is no significant change in term of flammability limit for all the three types of tube. This suggests that the burned gas region length may not influent the combustion stability for narrow quartz tubes with wire mesh.

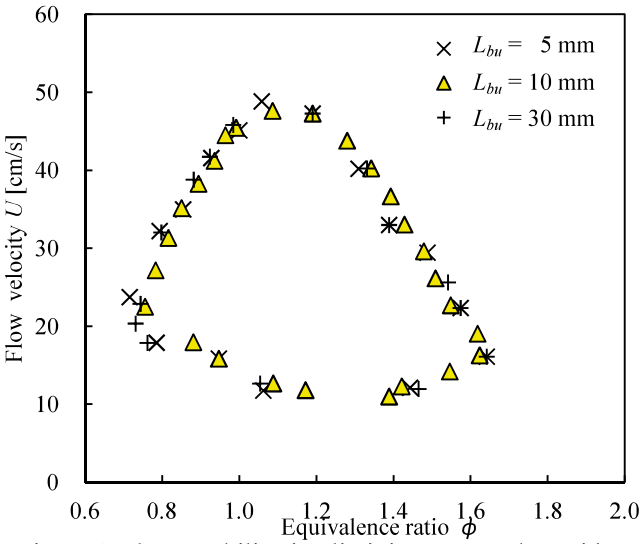

Figure 4. Flame stabilization limit in narrow tubes with wire mesh with L_{ub}= 10 mm for different burned gas region lengths L_{bu} (without heating effect)

Next, Fig. 5 demonstrates the flame stabilization limit for tube with different unburned gas region lengths. The burned gas region length L_{bu} was fixed to 10 mm. On the same graph, flame stabilization limit obtained from the previous research [11] for tube with L_{ub} = 10 mm was plotted as well. The results show that the longer the unburned gas region length is, the smaller the flame stabilization limit is. For instance, the flammability limit for tube with L_{ub}= 160 mm is the smallest as compared to the other two tubes. The reduction is considerable especially in lean and rich conditions. This significant change indicates that combustion stability might be affected by the unburned gas region lengths. The possible cause for this behavior is further explained in the wall temperature section.

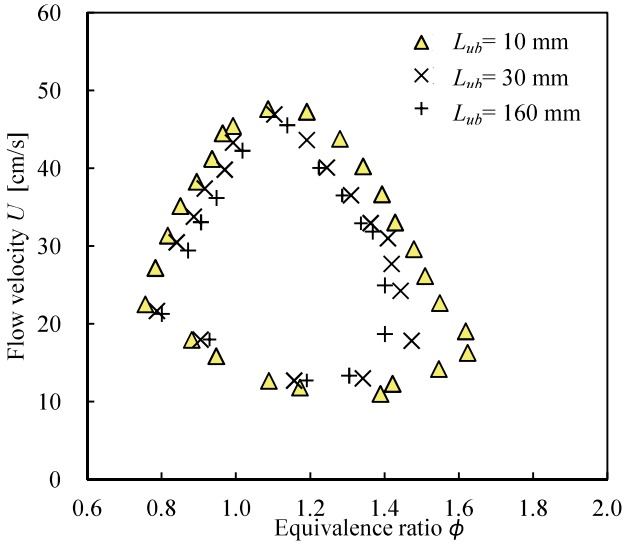

Figure 5. Flame stabilization limit in narrow tubes with wire mesh with L_{bu}= 10 mm for different unburned gas region lengths L_{ub} (without heating effect)

Heating effect on flame stabilization limit

It is predicted that combustion stability can be effectively enhanced by utilizing the heat generated from the combustion products. In a heat recirculation type of combustor, heat is transferred from the burned gas to the unburned gas region to preheat the incoming cold reactants. As a result, the total reactant enthalpy of the cold reactants is escalated. This excess enthalpy combustion leads to better combustion stability. In this experiment, the same mechanism was implemented. The temperature inside the heater was intentionally set to 673 K. This value is determined based on the results obtained in an experiment where the temperature of the exhaust gas was measured using a thermocouple type-R (Fig. 6). For lean condition of which the equivalence ratio ϕ is 0.85, the minimum exhaust gas temperature was 500 K. On the other hand, for rich condition (ϕ=1.25), the minimum temperature measured was 565 K. Both of these minimum temperatures were measured at the quartz tube end. Thus, by considering heat losses, the setting temperature of heater was set to 673 K in order to sufficiently simulate the condition of a heat recirculation combustor.

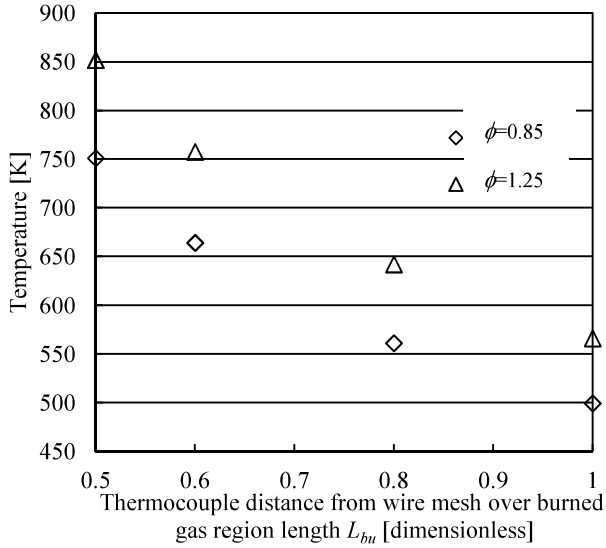

Figure 6. Exhaust gas temperature distribution in the burned gas region with L_{bu}=30 mm (for lean and rich condition)

Next, Fig. 7 illustrates the flame stabilization limit for tube with heating effect and with different insertion lengths L_{in}. The results suggest that the flame stabilization limit is significantly expanded with the presence of heating especially in lean and rich conditions. However, there is only small change in term of minimum flow velocity for all tubes. Apart from that, the flammability limit for the tube with L_{in}= 36 mm is wider than the tube with L_{in}=26 mm. This is possibly due to the temperature variation at different axial distance inside the heater which was previously measured. For instance, at L_{in}=26 mm, the maximum temperature surrounding the tube unburned gas region was 503 K. As the tube was inserted 10 mm further into the heater, the maximum temperature for the same condition was recorded to be 553 K. Hence, it is likely that this increase in temperature leads to a better flame stabilization limit.

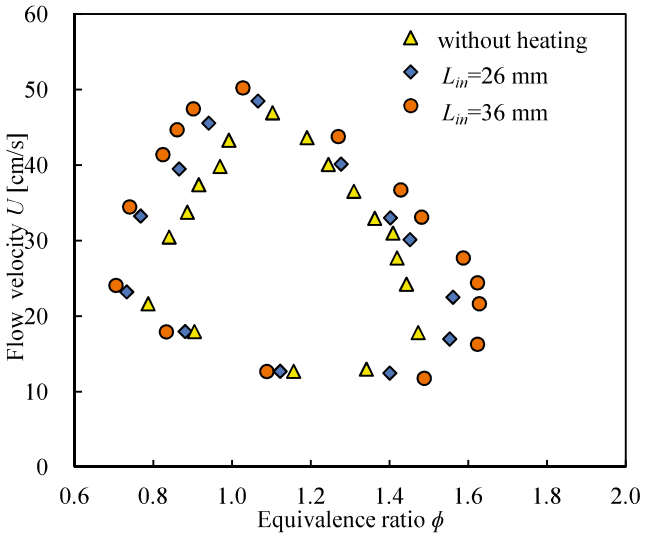

Figure 7. Flame stabilization limit in a narrow tube with wire mesh for tube with L_{ub}=30 mm and L_{bu}=10 mm for different insertion lengths L_{in}

Wall temperature

The wall temperature for the tube with unburned gas region length of L_{ub}= 30 mm with and without heating effect is shown in Fig. 8 below. As depicted in Fig. 8, the wall temperature at the area of the unburned gas region for the tube with heating effect is higher than the tube without heating effect. Clearly, this finding provides evidence of the positive effect of heating to the enhancement of flame stabilization limit.

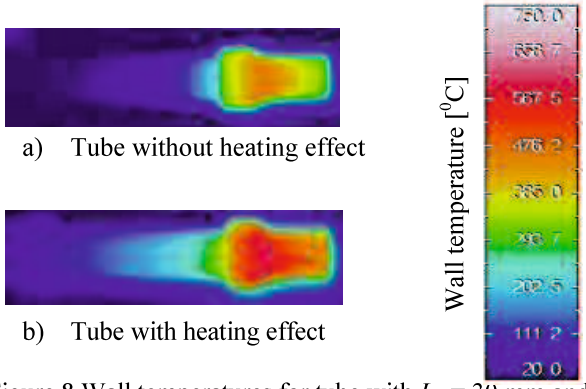

Figure 8.Wall temperatures for tube with L_{ub}= 30 mm and L_{bu}= 10 mm with heating effect of which the insertion length L_{in}= 36 mm and without heating effect

Next, the wall temperature of tubes without heating effect and for different unburned gas region lengths L_{ub} is depicted in Fig. 9. The maximum wall temperature recorded for the tube with L_{ub}= 10 mm was 791 K. For the tube with L_{ub}= 30 mm, on the other hand, the maximum wall temperature was 749 K. Since this maximum wall temperature was recorded near the flame location, this indicates that the flame temperature for the tube with L_{ub}= 10 mm is higher than the tube with L_{ub}= 30 mm. One of the potential causes for this wall temperature difference is heat losses from the tube non-insulated wall to the ambient. These heat losses occurred through convection and radiation. Nonetheless, since there is similarity in term of experimental conditions and type of tube used, the amount of heat losses to surrounding might be the same for both tubes. In other words, the value of convective heat transfer coefficient and the emissivity was made constant for all conditions. Therefore, this suggests that the potential cause for better flame stabilization limit in the tube with L_{ub}= 10 mm is the effect of heat recirculation.

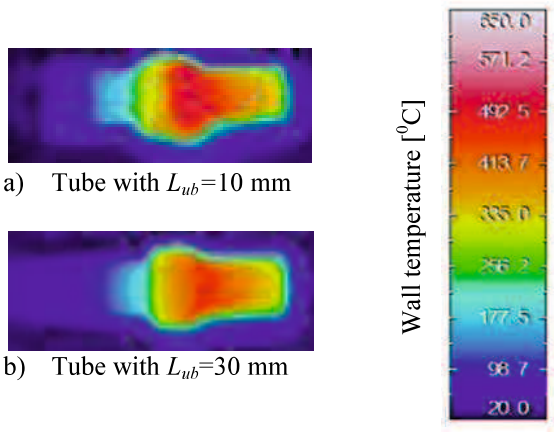

Figure 9. Wall temperatures for tube with L_{bu}= 10 mm and for different unburned gas region lengths L_{ub} (without heating effect)

Even if the tube is not surrounded by the burned gas, heat recirculation occurs from the burned gas to the unburned gas by thermal conduction in the wall and the mesh [11]. In Fig. 9, it appears that heat recirculation is better for the tube with shorter unburned gas region length. This fact is supported by the minimum wall temperature recorded at the area of the unburned gas region. The minimum wall temperature at the unburned gas region for the tube with L_{ub}= 10 mm is higher than the tube with L_{ub}= 30 mm. This suggests that in the tube with L_{ub}= 10 mm, more heat was transferred from the burned gas region to the unburned gas region. This enhancement of heat recirculation may be partly contributed by the distance from the mesh to the copper tube which has higher thermal conductivity than quartz. Obviously, the tube with L_{ub}= 10 mm has shorter distance from the flame to the connecting point (point where the quartz and copper tube were connected). Therefore, there is strong possibility that higher amount of heat is conducted from the burned gas to the copper tube through the quartz tube wall and then from the copper tube to the unburned gas region. As a result, there is wider range of distance where the incoming reactants are heated up before being combusted. Hence, better combustion stability is achieved as demonstrated in the results.

CONCLUSIONS

The combustion stability of propane/air mixture inside narrow quartz tubes with stainless steel wire mesh was experimentally investigated. By heating the unburned gas region of the quartz tube, the combustion stability in term of flammability limits can be significantly improved. Moreover, the enhancement is higher in lean and rich conditions. However, there is almost no change in term of minimum flow velocity recorded.

Apart from that, there is strong possibility that the unburned gas region length L_{ub} may influence the combustion stability in a narrow quartz tube with stainless steel wire mesh. The results show that there is inverse relationship between the L_{ub} to the flame stabilization limit. On the other hand, there is no solid evidence that combustion stability is affected by the burned gas region length L_{bu} .

As for the effect of the unburned gas region length, there is possibility that the use of copper tube that was connected to the quartz tube in the unburned gas region enhanced the effect of heat recirculation from the burned to the unburned gas by thermal conduction in the wall. Thus, by replacing the copper with a quartz tube, any effect due to differences in thermal conductivity between the quartz and the copper tube can be dismissed.

ACKNOWLEDGEMENT

This research was partly subsidized by A-STEP (Adaptable and Seamless Technology Transfer Program through target-driven R & D) Exploratory Research.

NOMENCLATURE

L = Axial length of the heater, mm
L_{ub}= Length of the unburned gas region, mm
L_{bu}= Length of the burned gas region, mm
ϕ = Equivalence ratio, dimensionless
U = Cross-sectional area flow velocity, cm/s
T_h = Setting temperature of the heater inner area, K
L_{in}= Insertion length of combustor in the heater, mm

REFERENCES

(1) Kaisare, N.S., Vlachos, D.G. (2012): "A Review on microcombustion: Fundamentals, devices and applications". *Progress in Energy and Combustion Science*, Vol. 38, pp. 321-359.
(2) Maruta, K. (2011): "Micro and mesoscale combustion". *Proceedings of the Combustion Institute* , Vol. 33, pp. 125-150.
(3) Wang, Y., Zhou, Z., Yang, W., Zhou, J., Liu, J., Wang, Z., Cen, K. (2011): "Instability of flame in micro-combustor under different external thermal environment". *Experimental Thermal and Fluid Science*, Vol. 35, pp. 1451-1457.
(4) Chou, S.K., Yang, W.M., Chua, K.J., Li, J., Zhang, K.L. (2011):" Development of micro power generators A review". *Applied Energy,* Vol. 88, pp. 1-16.
(5) Ju, Y., Maruta, K. (2011): "Review Microscale combustion : Technology development and fundamental research". *Progress in Energy and Combustion Science*, Vol. 37, pp. 669-715.
(6) Yuliati, L., Seo, T., Mikami, M. (2012): " Brief communications liquid-fuel combustion in a narrow tube using an electrospray technique". *Combustion and Flame*, Vol. 159, pp. 462-464.
(7) Benedetto, A.D., Sarli,V.D., Russo, G. (2009): "A novel catalytic-homogeneous micro-combustor". *Catalysis Today*, Vol. 147S, pp. S156-S161.
(8) Chia, L.C., Feng, B. (2007): "Review The development of a micropower (micro-thermophotovoltaic) device". *Journal of Power Sources* , Vol. 165, pp. 455-480.
(9) Junwei, L., Beijing, Z. (2008): " Experimental investigation on heat loss and combustion in methane/oxygen micro-tube combustor". *Applied Thermal Engineering,* Vol. 28, pp. 707-716.
(10) Jejurkar, S.Y., Mishra, D.P. (2011): "Flame stability studies in a hydrogen-air premixed flame annular microcombustor". *International Journal of Hydrogen Energy*, Vol. 36, pp. 7326-7338.
(11) Mikami, M., Maeda, Y., Matsui, K., Seo, T.,Yuliati L. (2013): "Combustion of gaseous and liquid fuels in meso-scale tubes with wire mesh". *Proceedings of the Combustion Institute*, Vol. 34, pp. 3387-3394.
(12) Bei-Jing, Z., Jian-Hua, W. (2010): "Experimental study on premixed CH_4 / air mixture combustion in micro Swiss-roll combustors". *Combustion and Flame*, Vol. 157 pp. 2222-2229.
(13) Maruta, K., Parc, J.K., Oh, K.C., Fujimori,T. Minaev,S.S., Fursenko,R.V. (2004): "Characteristics of combustion in a Narrow Heated Channel", *Combustion , Explosion and Shock Waves*, Vol. 40, pp. 2429-2436.
(14) Maruta, K., Kataoka, T., Kim, N.I., Minaev, S., Fursenko, R. (2005): "Characteristics of combustion in a narrow chanel with temperature gradient". *Proceedings of the Combustion Institute*, Vol. 30, pp. 516-523.

(15) Zhou, J., Wang, Y., Yang, W., Liu, J. , Wang, Z., Cen, K. (2009): "Improvement of micro-combustion stability through electrical heating". *Applied Thermal Engineering*, Vol. 29, pp. 2373-2378.

Modeling of Propane-air Combustion in Meso-scale Tubes with Wire Mesh

Fudhail Abdul Munir & Masato Mikami
Yamaguchi University
Ube, Yamaguchi, Japan

1 Abstract

The prime motivation to the renewed interest in meso and micro-scale power generation is the limited energy resources and the strong demand of long-lasting power sources for electronics devices. It is essential to fully understand the underlying factors that affect the combustion stability in meso and micro-scale combustors. Due to the small scale of micro combustors, numerical simulations can be utilized to investigate vital parameters that affect the combustion characteristics. This paper demonstrates a symmetrical three-dimensional steady state numerical simulation of propane-air combustion in meso-scale cylindrical quartz tube combustors with a stainless steel wire mesh. The inner diameter of the tube and the thickness of the wall are set to 3.5 mm and 0.7 mm, respectively. The wire mesh with a thickness of 0.2 mm is placed between the unburned and burned gas region. The material of the wire mesh is stainless steel. The main function of this wire mesh is to act as a flame holder where a stable flame can be easily established. The results in terms of gas, inner wall and the wire mesh surface temperature distributions are analyzed and presented. Flame stabilization limits at a fixed equivalence ratio were also numerically determined. Experiments were performed to compare these limits. A simulation with geometrical disconnection between the wire mesh and the inner wall was also performed to examine the effect of thermal path between the wire mesh and the inner wall on the blowout limit. The results show that the proposed numerical model can sufficiently represent the propane-air combustion in the meso-scale tube combustor. It is also demonstrated that the wire mesh has a significant impact on the flame stabilization limit.

2 Introduction

Meso and micro-scale combustion phenomena are the key components in micro power generation. An experimental study has shown that flame stabilization in a confined space or a narrow channel is achievable [1]. However, the difficulty of sustaining a stable flame for a micro combustor due to its high surface to volume ratio is a major issue in micro combustion [2]. This high ratio causes a large portion of heat loss from the flame to the wall, which leads to thermal quenching[3, 4]. In recent years, numerical simulation has been utilized as a prominent method to study the combustion feasibility in meso and micro-scale channels. By performing the verification, any newly designed of micro combustors can be thoroughly studied and optimized.

As early as in 2000s, Computational Fluid Dynamics (CFD) has been utilized to numerically investigate the flame propagation in micro-burners [5]. In order to provide a better understanding to the underlying fundamentals of the combustion of gaseous hydrocarbon fuels like propane (C_3H_8) and methane (CH_4) in micro-burners, numerical simulations using commercial software were conducted. For instance, FLUENT software with one-step irreversible reaction mechanism was employed to investigate the effect of wall conductivity, burner dimensions and external heat losses on combustion characteristics in meso-scale burners [6]. A more detailed reaction mechanism with 25 reversible reactions was utilized to model methane-air combustion in narrow cylindrical tubes [7].

It is essentially important to have a stabilized flame in meso and micro tube combustors. The use of catalysts have been successfully demonstrated by many researchers [8, 9]. Nevertheless, due to the complexity and high cost of catalytic combustors, the use of alternative flame stabilization method is desirable. Backward facing step combustor and bluff body insertion are the examples of ways to stabilize the flame in non-catalyst micro scale combustors [10, 11]. The idea of using a flame holder in meso-

Correspondence to: s505wc@yamaguchi-u.ac.jp

scale cylindrical tube combustors was first proposed by Mikami et al. [12]. In their experimental work, a stainless steel wire mesh is placed between the burned and unburned gas region. The experimental results show that the flame can be stabilized for both gas and liquid fuel. In fact, it was also demonstrated that the flame could be even stabilized in a tube with a diameter below than the classical quenching distance. However, due to the scale of the combustor, vital parameters such as the wire mesh surface temperature contours and combustor inner wall temperature could not be established. Thus, a numerical simulation is required.

In this study, a three-dimensional (3-D) numerical simulation of propane-air combustion in meso-scale cylindrical tubes with stainless steel wire mesh is presented. A two-dimensional (2-D) model is not suitable as the conductive heat transfer from the center of the wire mesh to the outer wall of combustor could not be represented. The gas, inner wall and wire mesh temperature were investigated. The flame stabilization limits were also determined. Experiments have been performed to compare the flame stability limits obtained by the simulation. The surface reaction is excluded in the analysis since there are materials that can resist radical quenching. The main purpose of this study is to demonstrate the capability of the wire mesh and to investigate its effect on the flame stabilization in the tube combustor.

3 Numerical Setup

A three-dimensional (3-D) steady-state numerical simulation was performed using ANSYS Release 14.0 with Fluent 6.3 [13]. The inner diameter of the combustor is 3.5 mm and the wall is 0.7 mm thick. The wall thickness is modeled as a solid phase where only the energy equation is solved. The total length of the combustor is set to 40.2 mm. The combustor is divided into two parts namely the unburned and burned gas region by a stainless steel wire mesh. The location of the wire mesh is 30 mm, which is measured from the center of the combustor inlet to the left side of the wire mesh. This value is chosen to ensure that the flow will be fully developed before passing through the wire mesh. Three-dimensional (3-D) conductive heat transfer is assumed on the wire mesh with the value of wall thermal conductivity *(k)* is set to 20 W/m/K, which represent the typical value of *k* for stainless steel [8]. To enable the fluid flows and passes through the wire mesh, a number of square-shaped holes with length of 0.28 mm are created. The fuel type used is propane (C_3H_8)-air mixture. The schematic of the computational domain for this simulation is illustrated in Fig. 1.

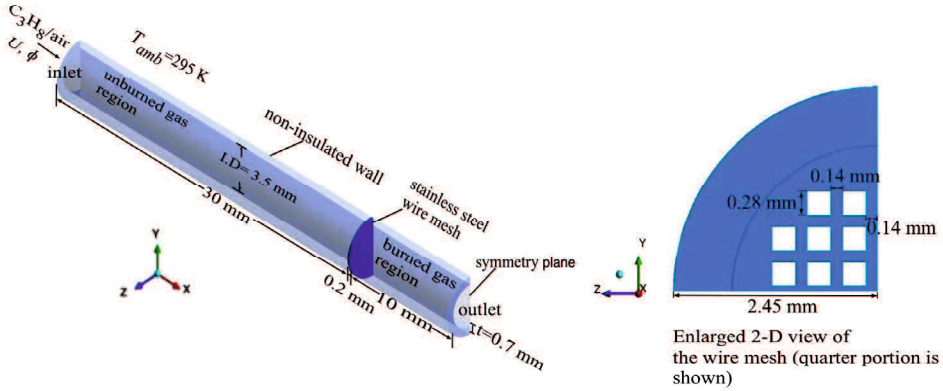

Figure 1. Numerical Setup (the figures size is not to scale)

In this work, Dufour, gas radiation effects and the work done by pressure and viscous force are assumed to be negligible. Norton and Vlachos [14] have shown that the gas phase radiation has minimal effect on the combustion reactions. Ideal gas law is assumed for the gas density and the specific heat for all the species is calculated using a piecewise-polynomial fit of temperature. Meanwhile, the specific heat and the thermal diffusion coefficient of the gas mixture are calculated based on the mixing law and

kinetic theory. A reduced one-step propane combustion with five species is employed as the combustion chemistry [15],

$$C_3H_8 + 5O_2 \rightarrow 3CO_2 + 4H_2O \quad (1)$$

The species involved are C_3H_8, O_2, N_2, CO_2 and H_2O. It should be noted that a detail kinetics mechanism is compulsory if simulations are performed to evaluate flame or emission characteristics.

However, since the focus this study is to examine the flame stabilization mechanism in this type of combustor, the single step mechanism is sufficient. A non-uniform grid element size is utilized where high grid concentrations are applied in the area surrounding the wire mesh. The total number of elements is 43548 and employed for all cases. A grid dependent test was performed and revealed that greater number of elements yields no significant numerical advantage.

Boundary conditions that have been successfully demonstrated by the previous researchers are used [7]. No-slip boundary type condition is applied at the interface between the fluid and the solid wall. The heat flux at this interface is calculated using Fourier's law. Heat transfer per unit area by means of convection at the outer surface of the combustor wall is given by:

$$q_{loss} = h_{conv}(T_{wall} - T_{amb}) + \varepsilon\sigma\left(T_{wall}^4 - T_{amb}^4\right) \quad (2)$$

where h is the convective heat transfer coefficient, T_{wall} is the wall temperature of the combustor and T_{amb} is the ambient temperature. The value of T_{amb} is initilized to 295 K. The convective heat transfer coefficient (*h)* is fixed to be at 5 W/m^{2}K, which represent a weak natural convection [7]. The external emissivity (ε) for the outer wall of the combustor and the wire mesh is set to 0.90 and 0.70 respectively. The value of Stefan-Boltzmann constant (σ) used is $5.67 \times 10^{-8}\mathrm{W/m^2K^4}$. A thermal insulation (zero heat flux boundary) is applied at both left and right wall edge of the combustor. The value of *k* for the tube combustor is set to 1.6 W/m/K, which represents the typical value of *k* for a quartz tube. For the outlet boundary condition, a fixed pressure inlet is applied. A symmetrical boundary condition is established at the origin of z-plane so that the calculation can be performed only in half of the domain.The thermodynamic properties and gas transport data are obtained from Kutz [16] and Fluent internal database [13].

A laminar flow of *U* with a flat velocity profile is applied at the inlet while the inlet feed temperature is initialized at 295 K. No swirl flow of velocity is applied. To ignite the propane-air mixture in the combustor, the value of *U* is first set to 0.20 m/s and the equivalence ratio (ϕ) is fixed to 1. A technique that is called as "cold flow" is employed where the momentum and continuity equation is first solved. Then, by patching a high temperature around an area that can be defined as patch zone, the energy and species equations are then solved. This patch zone is located at 2.5 mm from the outlet and should not be placed too close to the outlet since it can result to a reverse gas flow that negatively affects the ignition process. A sufficiently high temperature of 1500 K is applied in the patch zone to ensure that the fuel- air mixture can be ignited. Once ignited, the flame propagated to the upstream and eventually stabilized near the wire mesh. To obtain the blowout limits, the *U* value is gradually stepped up with 0.05 m/s interval. If the new value of *U* causes the flame to propagate to the outlet, then the process is started again with the previous *U* value. The increment is then reduced to 0.01 m/s interval until the flame is blown out of tube. The maximum value of *U* before the flame is blown out is considered as the blowout limit. As for determining the extinction limit, the value of *U* is gradually reduced with 0.01 m/s interval. The lowest value of *U* before the flame extincts is defined as the extinction limit.

4 Results and Discussion

4.1 Combustion in tube combustors with stainless steel wire mesh

Flame propagation in a narrow channel is a broad subject matter. Investigation of flame propagation characteristics in a narrow channel tube combustor is indeed a formidable task. In order to numerically study the phenomenon of flame propagation inside a meso-scale tube combustor, a detailed kinetics reaction mechanism is required that can lead to higher computational cost. Therefore, results shown in Fig. 2 are only limited to demonstrate the capability of the wire mesh. The ignition was attained by applying a sufficiently high temperature on the patch zone. This ignition method replicates the

experimental condition reported by Mikami et al. [12]. Since the flame burning velocity is faster than the inlet velocity, the flame propagated towards the inlet once it was ignited. As shown in Fig. 2 (b), the flame stopped to propagate when it reached the wire mesh and stabilized there until a converged solution was achieved. This condition is defined as a stable flame. The wire mesh act as a flame holder by which

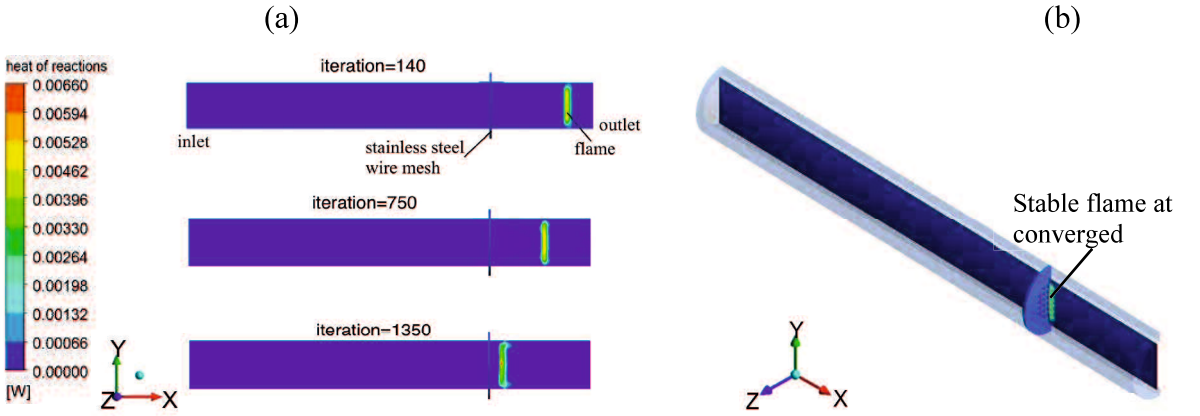

Figure 2. (a) Heat of reaction contours with different values of iteration number for ϕ=1.0 and U=0.20 m/s, taken at z-plane=0.28 mm (b) 3-D view of the stabilized flame (not to scale)

the flame can be stabilized at a fixed location.

Meanwhile, Fig. 3 shows the temperature for gas, inner wall and wire mesh for inlet velocity U= 0.20 m/s and ϕ=1.0 at various locations. It is shown in the figure that the inner wall temperature becomes higher than the gas temperature in the unburned gas region starting from x= 20 mm onwards. This elevation suggests that the heat is conducted from the hot burned gas to the unburned gas region via both the inner wall and the wire mesh. The higher temperature at center of the wire mesh than the

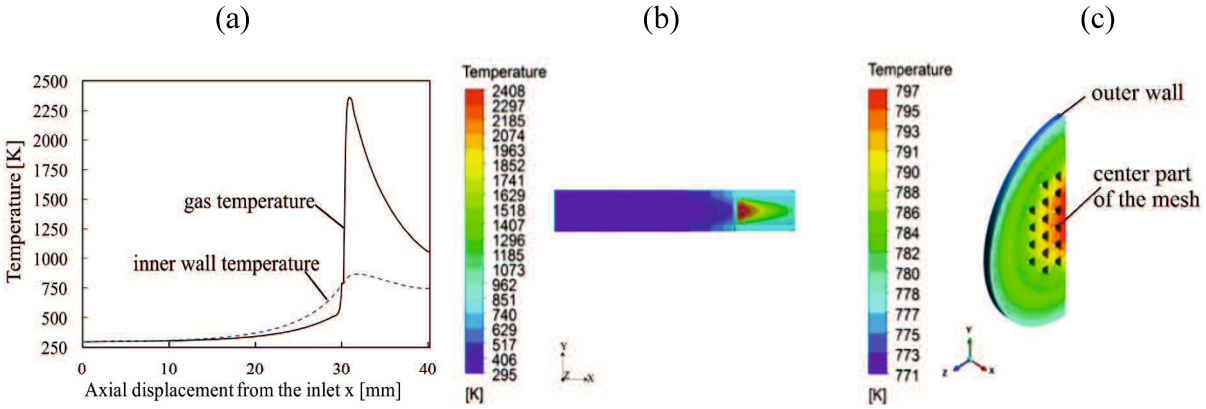

Figure 3. (a) Gas and inner wall temperature distributions along the x-axial displacement (coordinate line y=0 mm & 1.75 mm, z=0 mm & 0.875mm) for ϕ=1.0 and U=0.20 m/s (b) Temperature contours of the combustor 2-D view for ϕ=1.0 and U=0.20 m/s (c) Surface temperature contours of the wire mesh for ϕ=1.0 and U=0.20 m/s

outer mesh wall as shown in Fig. 3(c) indicates that the preheat zone of the flame is in contact with the wire mesh. The corresponding maximum heat release rate for this condition is located at 0.21 mm from the wire mesh. Note that this maximum heat release rate occurs in the reaction zone of the combustion.

Flame stabilization limits are also numerically examined. Blowout and extinction limits are examples of flame stabilization indicators in meso and micro-scale tube combustors. Both limits for this type of combustor are presented in Fig. 4(a). In order to ensure that the numerical model is credible, experiments were also conducted to determine the stability limits. The similar experimental configuration as reported in [12] was utilized. The results obtained from the experiment are plotted on

the same graph as shown in Fig. 4(a). The predicted value of the blowout limit is U=0.46 m/s, which is higher than the experimental result. On contrary, a reverse pattern is recorded for the extinction limit. These notable differences are mainly due to the reduced one-step propane reaction that has over predicted the flame temperature. Figure 4(b) illustrates the surface temperature of the wire mesh for different values of U. It can be seen from the figure that at U=0.10 m/s and U=0.20 m/s, the wall temperature at the center part of the wire mesh is higher than the outer mesh wall. Consequently, the

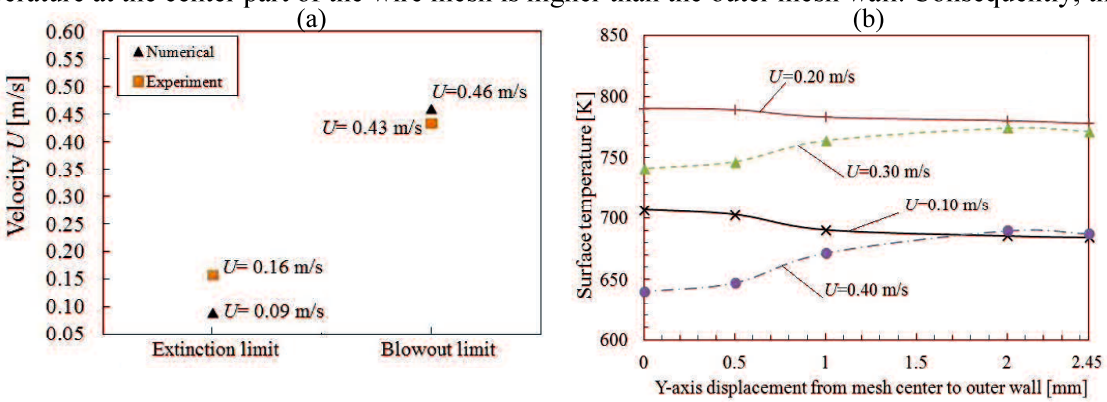

Figure 4. (a) Flame stabilization limits for the tube combustor with ϕ=1.0 (b) Surface temperature of the wire mesh along the y-axis line (coordinate is x=30.2 mm, z=0 mm) for different values of U with ϕ=1.0

transfer of heat from the hot burned gas to the ambient air via the wire mesh is intensified. A further reduction of U could potentially lead to the flame extinction. On the other hand, as the value of U is increased to 0.30 m/s and 0.40 m/s respectively, the opposite trend occurs. A sufficiently high inlet velocity causes the stable flame to slightly displace away from the wire mesh. For instance, for U=0.30 m/s, the maximum heat reaction rate is located at 0.5 mm from the wire mesh. As a result, the direct heat transferred from the flame to the wire mesh is reduced. At this condition, the inner wall of the combustor plays the effective role of circulating the heat from the burned gas to the wire mesh and unburned gas region.

4.2 Effect of thermal path between the stainless wire mesh and the inner wall on the blowout limit

In order to investigate the effect of the wire mesh on the blowout limit, the geometry of the wire mesh is slightly modified. The modified wire mesh has a small gap in between the inner wall. This gap is set to 0.20 mm as shown in Fig. 5. The blowout limit for the modified wire mesh is then numerically determined and shown in Fig. 6(a). From the graph, the predicted value of the blowout limit is 0.34 m/s. The corresponding wire mesh temperature with and without modification is shown in Fig. 6(b). As seen in the figure, the drop in temperature surrounding the center part of the wire mesh is one of the reasons for this reduction of limit.

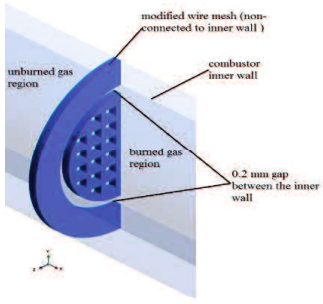

Figure 5. Image of the modified wire mesh (enlarged scale)

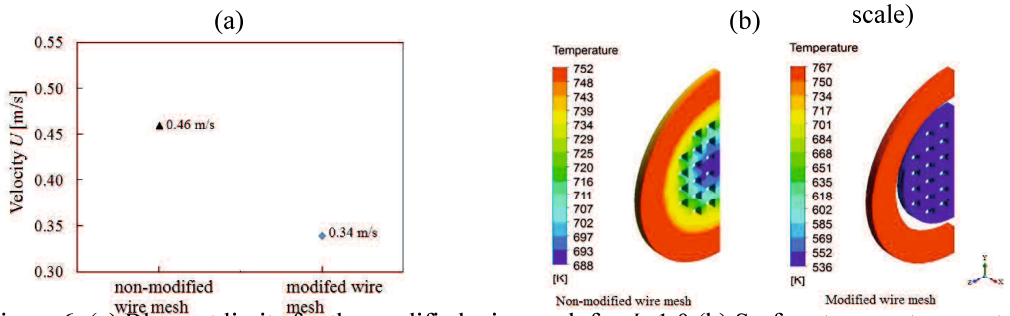

Figure 6. (a) Blowout limits for the modified wire mesh for ϕ=1.0 (b) Surface temperature contours for non-modified and modified wire mesh with U=0.34 m/s and ϕ=1.0

5 Conclusions

The three dimensional (3-D) numerical simulation of combustion of propane-air mixture in meso-scale tube combustors with stainless steel wire mesh has been successfully demonstrated. The presented numerical model can sufficiently represent the propane-air combustion in this type of combustor. At a low inlet velocity, the stabilized flame is located in close proximity to the wire mesh. In fact, the pre-heat zone of the flame is already in contact with the wire mesh. As a result, the transfer of heat from the hot burned gas to the combustor walls and ambient air is intensified. Further reduction of the inlet velocity can potentially lead to the flame extinction.

On the other hand, a sufficiently high inlet velocity but still within the blowout limit slightly shifts the stable flame away from the wire mesh. The pre-heat zone of the flame is no longer in contact with the wire mesh. As such, the inner wall of the combustor dominates the role of recirculating the heat from the hot burned gas to the center part of the wire mesh and the unburned gas region. This heat recirculation enhances the flame stabilization in the combustor. The effect of wire mesh on the flame blowout limit is also numerically investigated. By having a small gap between the inner wall of the combustor and the center part of the wire mesh, the heat from the burned gas region could not be efficiently transferred from the inner wall to the unburned gas region. As a result, the temperature around the center part of the wire mesh decreases. Consequently, the blowout limit is significantly reduced.

Acknowledgment

The first author would like to thank to the Malaysian Ministry of Education and Universiti Teknikal Malaysia Melaka (UTeM) for providing the study scholarship.

References

[1] C.M. Miesse, R.I. Masel, C.D. Jensen, M.A. Shannon, M. Short, AIChE Journal, 50 (2004) 3206-3214.
[2] K. Maruta, Proc. Combust. Inst., 33 (2011) 125-150.
[3] S.K. Chou, W.M. Yang, K.J. Chua, J. Li, K.L. Zhang, Applied Energy, 88 (2011) 1-16.
[4] N.S. Kaisare, D.G. Vlachos, Progress in Energy and Combustion Science, 38 (2012) 321-359.
[5] S. Raimondeau, D. Norton, D.G. Vlachos, R.I. Masel, Proc. Combust. Inst. 29 (2002) 901-907.
[6] D.G. Norton, D.G. Vlachos, Combust. and Flame, 138 (2004) 97-107.
[7] J. Li, S.K. Chou, W.M. Yang, Z.W. Li, Chemical Engineering Journal, 150 (2009) 213-222.
[8] S. Karagiannidis, J. Mantzaras, G. Jackson, K. Boulouchos, Proc. Combust. Inst., 31 (2007) 3309-3317.
[9] Y. Saiki, Y. Suzuki, Proc. Combust. Inst., 34 (2013) 3395-3402.
[10] W.M. Yang, S.K. Chou, C.Shu, Z.W. Li, H. Xue, Applied Thermal Engineering, 2002 (2002) 1777-1787.
[11] J. Wan, A. Fan, K. Maruta, H. Yao, W. Liu, International Journal of Hydrogen Energy, 37 (2012) 19190-19197.
[12] M. Mikami, Y. Maeda, K. Matsui, T. Seo, L. Yuliati, Proc. Combust. Inst., 34 (2013) 3387-3394.
[13] ANSYS. Inc, Canonsburg, PA, 2012.
[14] D.G. Norton, D.G. Vlachos, Chemical Engineering Science, 58 (2003) 4871-4882.
[15] C.K. Westbrook, F.L. Dryer, Combustion Science and Technology, 27 (1981) 31-43.
[16] M. Kutz, in, John Wiley & Sons, USA, 1998.

The 26th International Symposium on Transport Phenomena
27 September –1 October 2015, Leoben, Austria

Approaches to Enhance the Combustion Stability in Meso-scale Cylindrical Tube Combustors

F.A MUNIR[1], T. TOKUMASA[1], T SEO[1] and M. MIKAMI[1]
[1] Graduate School of Science and Engineering, Yamaguchi University
2-16-1 Tokiwadai, Ube, Yamaguchi, 755-8611, Japan

ABSTRACT

The invention of high performing electronics devices has sparked the research interest in micro power generation. Meso or micro scale combustor can be considered as the most important component in a micro power generation system. Flame stabilization in such narrow channel combustors is a considerably challenging task and requires a proper thermal management due to larger heat loss ratio. The utilization of heat recirculation mechanism is one of the approaches to enhance the flame stabilization limits in micro combustors. This paper presents the effective strategies to enhance the combustion in cylindrical quartz tube combustors with stainless steel wire mesh. The inner diameter of the combustor tube is fixed to 3.5 mm while the wall thickness is set to 0.7 mm. The unburned gas mixture of propane and air was pre-heated prior to the combustion and the effect on the combustion was investigated. Two types of pre-heating methods were employed. The first method was performed by varying the wall thermal conductivity of the combustor. For the second method, the combustor was inserted into glass test tubes with specific lengths and inner diameters. The equivalence ratio and mixture flow velocity were varied and results in term of flame stabilization limits were established. Since the scale of the combustor is relatively small, a three dimensional (3-D) numerical simulation was performed to examine the important parameters such as the gas, inner wall and wire mesh temperature of the combustor. The combustion efficiency is also numerically determined. Both numerical and experimental results suggest that significant enhancement of the combustion stability can be achieved by pre-heating the unburned gas mixture.

INTRODUCTION

The scarcity of energy resources and the high demand for better power sources as compared to conventional batteries have sparked research interest in micro power generation [1]. The new state of the art electronics devices require greater energy capacity, shorter charging period and lightweight design, characteristics that batteries lack. Therefore, in recent years micro power generation systems have been seen as potential alternatives to batteries due to the higher energy densities of hydrocarbon fuels [2].

Meso and micro-scale combustion phenomena are the key components in micro power generation. In order to design a reliable micro power generator, it is essential to understand the underlying combustion fundamentals [3]. Flame stabilization in a confined space or a narrow channel is achievable, but it is considerably a great challenge to sustain a stable flame in a micro combustor. This difficulty is partly due to the high surface to volume ratio [4]. This high ratio causes a large portion of heat loss from the flame to the wall that leads to thermal quenching [5].

One of the methods to stabilize the flame in narrow channels is by utilizing the heat produced from the combusted products to pre-heat the unburned reactants. In general there are two types of pre-heating method [3]. Direct method is a condition where heat is transferred from the hot burned gas to the unburned gas region through conduction and radiation. This method is applied in a single channel (SC) micro combustor in which the heat from the burned gas region is axially transferred to the unburned gas region via the combustor wall [6]. As a result, the combustion stability is significantly improved. On the other hand, indirect pre-heating method is an approach where the flow of the burned gas is reversed to pre-heat the unburned reactants. Swiss-roll burner utilizes this concept resulting to a huge improvement of flame stabilization limits as compared to SC combustors. Nevertheless, the geometry of a Swiss-roll combustor is relatively complicated making it difficult to be numerically and experimentally investigated [7]. Thus, a combustor with simpler geometry is preferred.

The idea of using a flame holder in SC meso-scale combustors was first proposed by Mikami et al. [8]. In their experimental work, a stainless steel wire mesh is placed between the burned and unburned gas region. The experimental results show that the flame can be stabilized for both gas and liquid fuel in a cylindrical quartz tube combustor. In fact, it is also demonstrated that flame could be even stabilized in a tube with a diameter below than the classical quenching distance. The wire mesh helps to enhance the flame stabilization limits by distributing the heat from the burned gas to the unburned gas region.

Combustion stability in meso and micro-scale combustors is greatly influenced by a few factors such as the wall thickness and materials. [9, 10]. The effects of wall thermal conductivity on the combustion stability in meso and micro-scale combustors with gaseous hydrocarbon fuels have been thoroughly examined [11, 12]. However, these

studies are limited to combustors without a flame holder. Recently, Fudhail and Mikami [13] numerically investigated the effect of wall thermal conductivity in a combustor with concentric rings. A two-dimensional (2-D) model is proposed and their results suggest that changing the combustor wall thermal conductivity in both the unburned and burned gas region significantly affects the combustion stability. Nevertheless, there is a limitation of the a 2-D numerical model, where it could not effectively simulate the role of stainless wire mesh in enhancing flame stabilization limits as shown in experiment. Thus, a three-dimensional (3-D) numerical model is proposed [14].

This research investigated the effective strategy in enhancing the combustion stability of meso-scale combustors with stainless steel wire mesh. Two methods of pre-heating namely direct and indirect preheating were employed. The combustion stability in terms of flame stabilization limits under different operational conditions was recorded and analyzed. Due to the scale of the combustor, a numerical simulation is performed to establish and examine the vital parameters such as the gas and wire mesh temperature. It is important to investigate these parameters that might have strong influence on the combustion stability and characteristics.

RESEARCH APPROACH

Experimental Setup

In the experiment, meso-scale combustors made of straight cylindrical tube were used. Each type of combustor was made of two-piece tubes. A stainless steel wire mesh was placed in between the two-piece tube dividing between the upstream and the downstream area. The mesh type was 60 mesh/in with wire diameter of 0.14 mm. A heat resistant ceramic adhesive (Ceramabond 569, Aremco Product Inc.) was used to adhere the parts together. The inner diameter of the tube was 3.5 mm with wall thickness of 0.7 mm. The length from the mesh to the upstream part of the tube is set to 30 mm and this area is defined as the unburned gas region. On the other hand, the length from the wire mesh to the downstream of the wire mesh is fixed to 10 mm and this area is named as burned gas region.

The ambient temperature was 295 K, which was maintained at 100 mm horizontally away from the combustor wall. Propane (C_3H_8) and air were mixed and supplied into the combustor with an equivalence ratio of ϕ and a corresponding cross-sectional-area mean flow velocity of U. Propane is preferred since it gives better combustion stability than methane (CH_4). A mass flow controller (SEC-E440J, HORIBASTEC) was used to precisely control the flow rate of the air and fuel. The flame inside the combustor was ignited done by introducing a spark at the exhaust outlet. Once ignited, the flame propagated to the upstream and flame stabilization. The experiment was performed on two types of combustor. The first type of combustor is made of quartz while the later is made of brass tube. A stable flame is defined as a flame that stabilizes near the wire mesh. Initially, the flame stabilization limits for each type of combustor was determined.

To examine the effect of heat being re-circulated from the exhaust gas to the unburned gas region, the combustors are inserted into a glass test tube with 1 mm thickness. The inner diameter of the test tube is 8 mm while the total length is 50 mm. A traverse system is utilized to precisely insert the combustor 48 mm into the glass test tube. The stable flame is visually observed by using a digital video camera (PANASONIC HC-750M). The experimental setup diagram is presented in Fig. 1 while Fig. 2 shows the photography of the sample of brass tube combustor used in the experimental work.

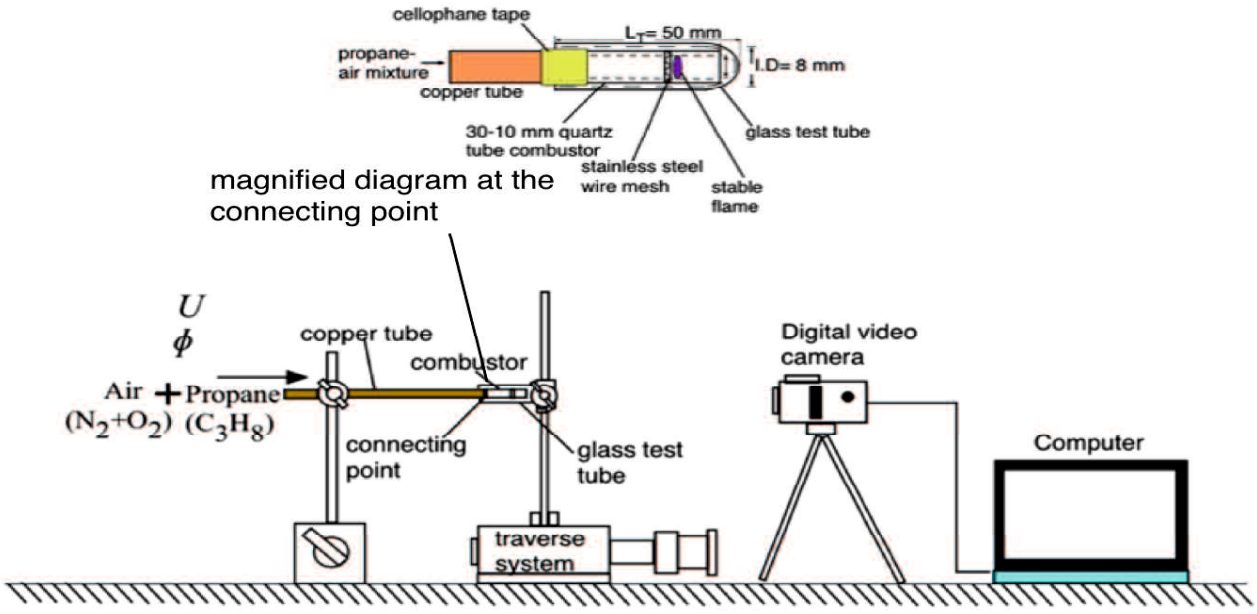

Figure 1 Experimental setup for the heat recirculation effect with a glass test tube

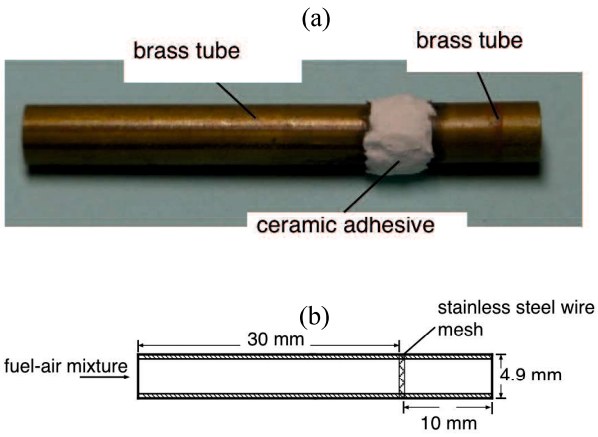

Figure 2 (a) Photography of a brass tube combustor (b) schematic diagram of the combustor

Numerical Setup

A three-dimensional (3-D) steady-state numerical simulation was performed using ANSYS Release 14.0 with Fluent 6.3 [15]. The inner diameter of the combustor is 3.5 mm and the wall is 0.7 mm thick. The wall thickness is modeled as a solid phase where only the energy equation is solved. The similar combustor geometry as the experimental tube combustor is set for the numerical model. A three-dimensional (3-D) conductive heat transfer is assumed on the wire mesh with the value of wall thermal conductivity *(k)* is set to 20 W/m/K, which represent the typical value of *k* for stainless steel [16]. To enable the fluid flows and passes through the wire mesh, a number of square-shaped holes with length of 0.28 mm are created. The fuel type used is propane (C_3H_8)-air mixture. The schematic of the computational domain for this simulation is illustrated in Fig. 3.

In this work, Dufour, gas radiation effects and the work done by pressure and viscous force are assumed to be negligible. Norton and Vlachos [12] have shown that the gas phase radiation has minimal effect on the combustion reactions. Ideal gas law is assumed for the gas density and the specific heat for all the species is calculated using a piecewise-polynomial fit of temperature.

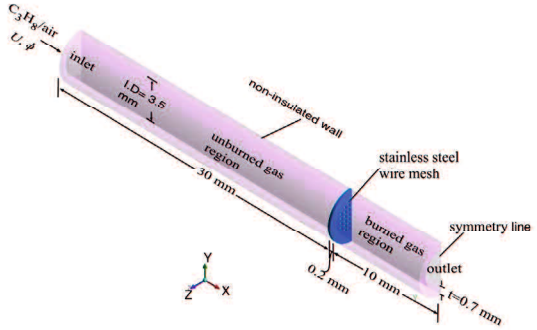

Figure 3 Computational domains

The specific heat and the thermal diffusion coefficient of the gas mixture are calculated based on the mixing law and kinetic theory. A reduced one-step propane combustion with five species is employed as the combustion chemistry. A non-uniform grid element size is utilized where high grid concentrations are applied in the area surrounding the wire mesh. The total number of elements is 43548 and employed for all cases. No-slip boundary type condition is applied at the interface between the fluid and the solid wall. The heat flux at this interface is calculated using Fourier's law. No-slip boundary type condition is applied at the interface between the fluid and the solid wall. The heat flux at this interface is calculated using Fourier's law. No-slip boundary type condition is applied at the interface between the fluid and the solid wall. The heat flux at this interface is calculated using Fourier's law. The heat loss from the non-insulated wall to the ambient is by mean of convection and the equation utilized is as same as in Fudhail and Mikami [14]. The ambient air temperature (T_{amb}) is first initialized to 295 K. The emissivity value (ε) used for the quartz and brass tube is 0.90 and 0.64 respectively [16]. Meanwhile, the wall thermal conductivity for quartz and brass tube is set to 1.6 W/m/K and 100 W/m/K respectively.

A laminar flow of *U* with a flat velocity profile is applied at the inlet while the inlet feed temperature is initialized at 295 K. No swirl flow of velocity is applied. To ignite the propane-air mixture in the combustor, the value of *U* is first set to 20 cm/s and the equivalence ratio *(ϕ)* is fixed to 1. The momentum and continuity equation is first solved. Then, by patching a high temperature around an area that can be defined as patch zone, the energy and species equations are then solved. This patch zone is located at 2.5 mm from the outlet.

A sufficiently high temperature of 1600 K is applied in the patch zone to ensure that the fuel-air mixture can be ignited. Once ignited, the flame propagated to the upstream and eventually stabilized near the wire mesh. To obtain the blowout limits, the *U* value is gradually stepped up with 5 cm/s interval. If the new value of *U* causes the flame to propagate to the outlet, then the process is started again with the previous *U* value. The increment is then reduced to 1 cm/s interval until the flame is blown out of tube. All the other details of the numerical model that are not mentioned in this paper can be obtained from [14]. Blowout limits at a specified equivalence ratio (ϕ) are obtained for each set of combustor setup.

To examine the effect of the heat recirculation on the combustion stability, the ambient air temperature in the numerical model is elevated to 600 K that is selected by considering the experimentally measured value of the exhaust gas.

RESULTS AND DISCUSSION

Role of the wall thermal conductivity in the combustion stability

The wall thermal conductivity of plays an important role in stabilizing the flame in meso and micro scale combustors. Figure 4 presents the experimental results of flame stabilizations limit for quartz tube and brass tube combustor.

There is a significant increase in the limits with the use of brass tube. This notable increment suggests that the high wall thermal conductivity of the brass tube plays an important role in enhancing the flame stability limits. Due to the scale of the combustor, vital parameters such as the gas, inner wall and wire mesh temperature could not be experimentally examined. Thus, a numerical simulation is deemed necessary to investigate the possible cause that contributes to the

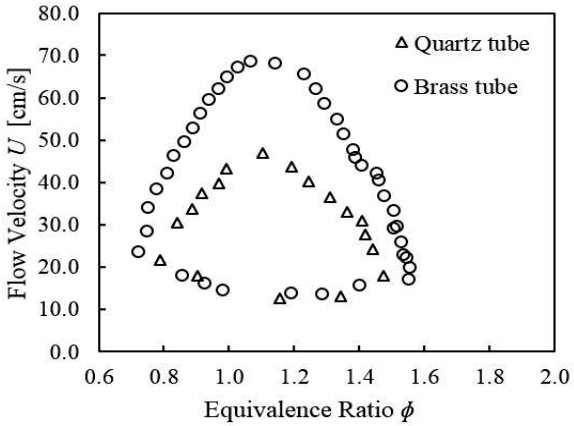

Figure 4 Flame stabilization limits for quartz and brass tube combustor with ϕ=1.0

increase of flame stabilization limits. To validate the numerical model, the blowout limit at equivalence ratio (ϕ) of 1 for both quartz and brass tube combustor model is first determined and compared with the experimental results. The results are shown in Fig. 5. It is seen from the figure that

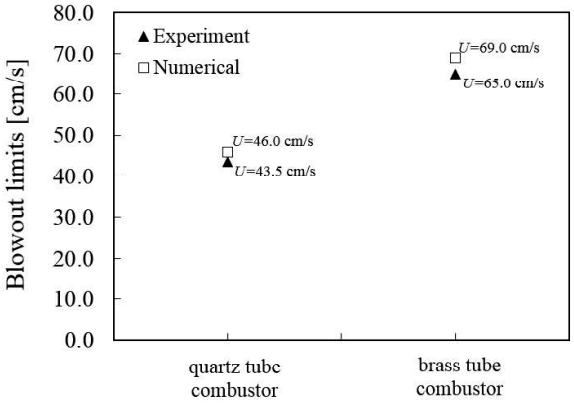

Figure 5 Numerically determined blowout limits in comparison with experimental results for the quartz and brass tube combustor with ϕ=1.0

the numerically determined blowout limit is higher than the experimental results. The use of global one-step reaction mechanism, which over-predicts the flame temperature contributes to this difference. Nevertheless, the tendency of the simulation results is still in coherence with the results obtained from experiments.

The utilization of numerical simulations enables the gas temperatures inside the combustor to be measured as presented in Fig. 6. From the figure, the gas temperature in the unburned gas region for brass tube combustor is significantly higher than the quartz tube combustor. As for an example, the mass-weighted average gas temperature in the unburned gas region for quartz tube combustor is 355 K while it is 561 K for the brass tube combustor. This elevation of gas temperature results to the increase of flame burning velocity. Consequently, the blowout limit is improved.

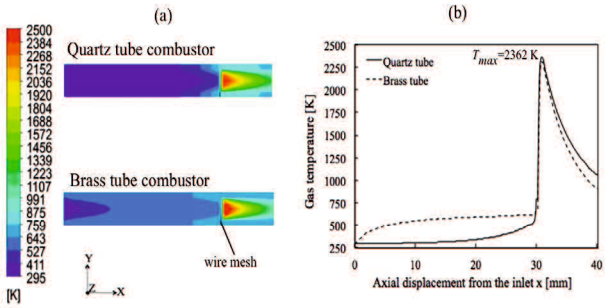

Figure 6 Temperatures for quartz and brass tube combustor with U=20 cm/s and ϕ=1.0 (a) Gas temperature contours (b) Graph of gas temperature along the centerline

The stainless steel wire mesh surface temperature for U=35 cm/s is shown in Fig. 7. For the quartz tube, a near blowout condition occurs at this value of flow velocity (U). In this condition, the flame is slightly displaced away from the wire mesh. As a result, the heat from the hot burned gas region is transferred to the unburned gas region via the inner wall through the wire mesh. That is why the temperature surrounding the outer area of the wire mesh is higher than the area around the center part. In short, at near blowout conditions, the wire mesh plays a major role in enhancing the flame stability for the quartz tube combustor. On the other hand, Fig. 7 also suggests that the temperature especially in the center part of the wire mesh for brass tube combustor is relatively higher than in the quartz tube. This higher temperature has contributed to the increase of blowout limit.

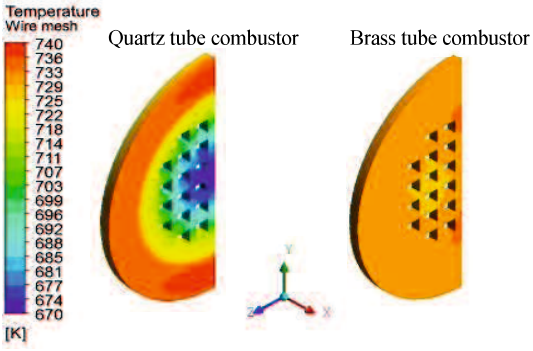

Figure 7 Wire mesh temperature for quartz and brass tube combustor with U=35 cm/s and ϕ=1.0

Meanwhile, the combustion efficiency with ϕ=0.95 for different values of U is presented in Fig.8. It is reasonable to operate within this equivalence ratio value due to the fuel economy benefit. From the figure, the combustion efficiency is first increased with higher flow velocity. However, as the flow velocity is further elevated, the efficiency drops. This trend occurs due to the fluctuation of the flame temperature. Higher flow velocity results to higher reaction rate that leads to the increase of the flame temperature. Nevertheless, after a certain value of inlet flow velocity, the temperature is no

longer escalates. The dilution of mixture at higher flow velocity results to the drop in the combustion efficiency.

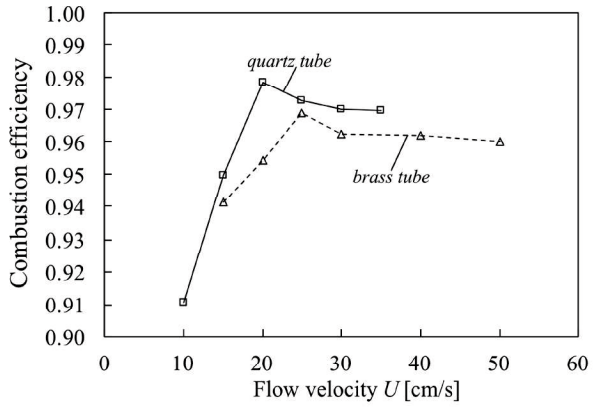

Figure 8 Combustion efficiency with different values of flow velocity (*U)* for ϕ=0.95

Utilization of heat recirculation from the burned gas region

As the combustor is inserted into the glass test tube, the flow of the hot exhaust gas is reversed. Thus, the hot gaseous is being used to pre-heat the unburned reactants. Figure 9 shows the flame stabilization limits obtained from experiments for each type of combustor with and without

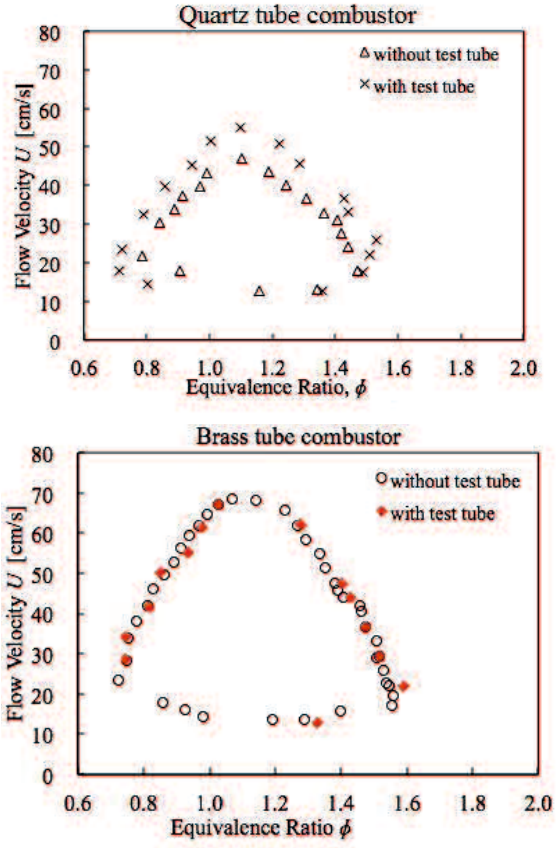

Figure 9 Flame stabilization limits obtained from experiments with and without the test tube

being inserted into the glass test tube. As suggested in the figure, there is a significant expansion of flame stabilization limits for the quartz tube combustor. On the other hand, no notable change of limits is recorded for the brass tube combustor.

In order to precisely determine the potential cause for such pattern change in the flame stabilization limits, numerical simulations were performed. However, due to the high computational cost, the blowout limit is numerically determined only at equivalence ratio (ϕ) of 1. The value of the obtained blowout limits is shown in Table 1 while Fig. 10 depicts the corresponding gas temperature contours. By increasing the ambient temperature (T_{amb}), the blowout limit for both combustors is also improved. However, the percentage improvement of blowout limit is significantly different for each combustor. The quartz tube combustor yields the largest limits increment as compared to its counterpart.

Table 1 Numerical results for the blowout limits with different ambient temperature (T_{amb}) for ϕ=1.0

	Blowout limits		
Type of combustor	T_{amb}=295 K	T_{amb}=600 K	Percentage change (%)
Quartz tube	46.0 cm/s	59.0 cm/s	28.3
Brass tube	69.0 cm/s	75.0 cm/s	8.7

As presented in Fig. 10 and Table 2, there is a considerably increase of the gas temperature in the unburned gas region for the quartz tube combustor. This leads to more reactants being pre-heated before being combusted. In fact, the average temperature in the unburned gas region for the quartz tube has elevated more than 50% (shown in Table 2).

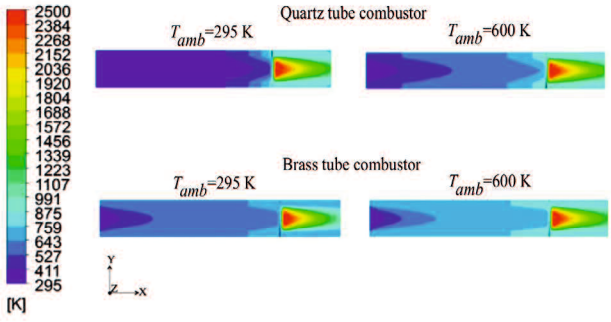

Figure 10 Gas temperature for the simulated quartz and brass tube combustor for *U*=20 cm/s and ϕ=1.0 with different ambient temperature (T_{amb})

However, for the brass tube combustor, the increase of unburned gas temperature is only 15.3 %. Such differences could be the main reason of why utilizing exhaust gas does not result to notable improvement on the combustion stability for the brass tube combustor.

Table 2 Numerically measured of mass-weighted average gas temperature in the unburned gas region measured at U=20 cm/s and ϕ=1.0

Type of combustor	T_{amb}=295 K	T_{amb}=600 K	Percentage change (%)
Quartz tube	355 K	541K	52.5 %
Brass tube	561 K	647 K	15.3 %

Meanwhile, Fig. 11 presents the combustion efficiency with different values of ambient temperature at a fixed equivalence ratio and a flow velocity. The results obviously show that greater combustion efficiency can be achieved with the recirculation of heat from the exhaust gas to the unburned mixture.

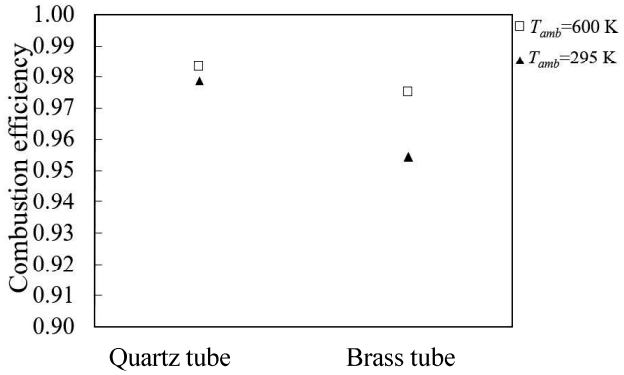

Figure 11 Combustion efficiency with different ambient temperature (T_{amb}) for U=20 cm/s and ϕ =0.95

CONCLUSIONS

The effective approaches of enhancing the combustion stability in a meso-scale cylindrical tube combustor with stainless steel wire mesh have been successfully demonstrated. Both experimental and numerical works show that the effect of pre-heating on the reactants has a strong influence on the combustion stability. Furthermore, the presented numerical model can be sufficiently used to investigate the important parameters that affect the combustion characteristics of the combustors.

The use of a higher wall thermal conductivity leads to better flame stabilization limits, but with a significant reduction of the combustion efficiency. By utilizing the heat generated from the combustion, the flame stabilization limits can be improved. However, the improvement is only notable for the quartz tube combustor.

NOMENCLATURE

ϕ equivalence ratio
ε emissivity
k wall thermal conductivity, W/m/K
U flow velocity, cm/s
T_{amb} ambient temperature, K

ACKNOWLEDGMENT

This research was partly subsidized by Grant-in-Aid for Challenging Exploratory Research (26630443). F.A.M would like to thank the Malaysian Ministry of Education and Universiti Teknikal Malaysia Melaka (UTeM) for providing the study scholarship.

REFERENCES

[1] Maruta K. Micro and mesoscale combustion. Proceedings of the Combustion Institute. 2011;33:125-50.
[2] Ju Y, Maruta K. Microscale combustion: Technology development and fundamental research. Progress in Energy and Combustion Science. 2011;37:669-715.
[3] Raimondeau S, Norton D, Vlachos DG, Masel RI. Modeling of high temperature microburners. Proceedings of the Combustion Institute. 2002;29:901-7.
[4] Yuliati L, Seo T, Mikami M. Liquid-fuel combustion in a narrow tube using an electrospray technique. Combustion and Flame. 2012;159:462-4.
[5] Chou SK, Yang WM, Chua KJ, Li J, Zhang KL. Development of micro power generators – A review. Applied Energy. 2011;88:1-16.
[6] Kaisare NS, Vlachos DG. A review on microcombustion: Fundamentals, devices and applications. Progress in Energy and Combustion Science. 2012;38:321-59.
[7] Lee KH, Kwon OC. Studies on a heat-recirculating microemitter for a micro thermophotovoltaic system. Combustion and Flame. 2008;153:161-72.
[8] Mikami M, Maeda Y, Matsui K, Seo T, Yuliati L. Combustion of gaseous and liquid fuels in meso-scale tubes with wire mesh. Proceedings of the Combustion Institute. 2013;34:3387-94.
[9] Junwei L, Beijing Z. Experimental investigation on heat loss and combustion in methane/oxygen micro-tube combustor. Applied Thermal Engineering. 2008;28:707-16.
[10] Wenming Y, Siawkiang C, Chang S, Hong X, Zhiwang L. Effect of wall thickness of micro-combustor on the performance of micro-thermophotovoltaic power generators. Sensors and Actuators A: Physical. 2005;119:441-5.
[11] Norton DG, Vlachos DG. Combustion characteristics and flame stability at the microscale: a CFD study of premixed methane/air mixtures. Chemical Engineering Science. 2003;58:4871-82.
[12] Norton DG, Vlachos DG. A CFD study of propane/air microflame stability. Combustion and Flame. 2004;138:97-107.
[13] Munir FA, Mikami M. A numerical study of propane-air combustion in meso-scale tube combustors with concentric rings. Journal of Thermal Science and Technology. 2015;10:1-12.
[14] Munir FA, Mikami M. Modeling of Propane-air Combustion in Meso-scale Tubeswith Wire Mesh. 10th Asia Pacific Conference on Combustion (ASPACC 2015). Beijing China, 2015.

[15] ANSYS Fluent Release 14.0. In: Inc A, editor. Canonsburg, PA2012.

REFERENCES

[1] Fernandez-Pello AC. Micropower Generation Using Combustion- Issues And Approaches. Proceedings of the Combustion Institute. 2002;29:883–99.

[2] Li J, Chou SK, Li ZW, Yang WM. A potential heat source for the micro-thermophotovoltaic (TPV) system. Chemical Engineering Science. 2009;64:3282-9.

[3] Kaisare NS, Vlachos DG. A review on microcombustion: Fundamentals, devices and applications. Progress in Energy and Combustion Science. 2012;38:321-59.

[4] Lior N. Sustainable energy development: The present (2009) situation and possible paths to the future. Energy. 2010;35:3976-94.

[5] Dunn-Rankin D, Leal EM, Walther DC. Personal power systems. Progress in Energy and Combustion Science. 2005;31:422-65.

[6] Yuasa S, Oshimi K, Nose H, Tennichi Y. Concept and combustion characteristics of ultra-micro combustors with premixed flame. Proceedings of the Combustion Institute. 2005;30:2455-62.

[7] Fu K, Knobloch AJ, Martinez FC, Walther DC, Fernandez-Pello C, Pisano AP, et al. Design and Experimental Results of Small-Scale Rotary Engines. 2001 ASME International Mechanical Engineering Congress and Exposition. New York2001.

[8] Zhou J, Wang Y, Yang W, Liu J, Wang Z, Cen K. Improvement of micro-combustion stability through electrical heating. Applied Thermal Engineering. 2009;29:2373-8.

[9] Li J, Chou SK, Huang G, Yang WM, Li ZW. Study on premixed combustion in cylindrical micro combustors: Transient flame behavior and wall heat flux. Experimental Thermal and Fluid Science. 2009;33:764-73.

[10] Yang WM, Chou SK, Shu C, Xue H, Li ZW, Li DT, et al. Microscale combustion research for application to micro thermophotovoltaic systems. Energy Conversion and Management. 2003;44:2625-34.

[11] Weinberg FJ, Rowe DM, Min G, Ronney PD. On Thermoelectric Power Conversion From Heat Recirculating Combustion Systems. Proceedings of the Combustion Institute. 2002;2002:941-7.

[12] Chia LC, Feng B. The development of a micropower (micro-thermophotovoltaic) device. Journal of Power Sources. 2007;165:455-80.

[13] Lee SI, Um DH, Kwon OC. Performance of a micro-thermophotovoltaic power system using an ammonia-hydrogen blend-fueled micro-emitter. International Journal of Hydrogen Energy. 2013;38:9330-42.
[14] Yang WM, Jiang DY, Chou SK, Chua KJ, Karthikeyan K, An H. Experimental study on micro modular combustor for micro-thermophotovoltaic system application. International Journal of Hydrogen Energy. 2012;37:9576-83.
[15] Lee KH, Kwon OC. Studies on a heat-recirculating microemitter for a micro thermophotovoltaic system. Combustion and Flame. 2008;153:161-72.
[16] Ju Y, Maruta K. Microscale combustion: Technology development and fundamental research. Progress in Energy and Combustion Science. 2011;37:669-715.
[17] Walther DC, Ahn J. Advances and challenges in the development of power-generation systems at small scales. Progress in Energy and Combustion Science. 2011;37:583-610.
[18] Benedetto AD, Sarli VD, Russo G. Effect of geometry on the thermal behavior of catalytic micro-combustors. Catalysis Today. 2010;155:116-22.
[19] Wang H, Iovenitti P, Harvey E, Masood S, Deam R. Mixing of liquids using obstacles in microchannels. In: William B. Spillman J, editor. BioMEMS and Smart Nanostructures2001.
[20] Maruta K. Micro and mesoscale combustion. Proceedings of the Combustion Institute. 2011;33:125-50.
[21] Guo H, Ju Y, Maruta K, Niioka T, Liu F. Radiation Extinction Limit of Counterflow Premixed Lean Methane-Air Flames. Combustion and Flame. 1997;104:639-46.
[22] Wang Y, Yang ZZW, Zhou J, Liu J, Wang Z, Chen K. Instability of flame in micro-combustor under different external thermal environment. Experimental Thermal and Fluid Science. 2011;35:1451-7.
[23] Lee MJ, Cho SM, Choi BI, Kim NI. Scale and material effects on flame characteristics in small heat recirculation combustors of a counter-current channel type. Applied Thermal Engineering. 2010;30:2227-35.
[24] Turns SR. An Introduction To Combustion Concepts and Applications. Singapore: Mc Graw Hill; 2000.
[25] Feng L, Liu Z, Li Y. Numerical study of methane and air combustion inside a small tube with an axial temperature gradient at the wall. Applied Thermal Engineering. 2010;30:2804-7.

[26] Richecoeur F, Kyritsis DC. Experimental study of flame stabilization in low Reynolds and Dean number flows in curved mesoscale ducts. Proceedings of the Combustion Institute. 2005;30:2419-27.
[27] Maruta K, Parc JK, Oh KC. Characteristics of Microscale Combustion in a Narrow Heated Channel. Combustion, Explosion, and Shock Waves. 2004;40:516-23.
[28] Fan A, Maruta K, Nakamura H, Liu W. Experimental investigation of flame pattern transitions in a heated radial micro-channel. Applied Thermal Engineering. 2012;47:111-8.
[29] Stroock AD, Dertinger SKW, Ajdari A,́ IM, Stone HA, Whitesides GM. Chaotic mixer for microchannels.pdf. Science. 2002;295:647-51.
[30] Hessel V, Löwe H, Schönfeld F. Micromixers—a review on passive and active mixing principles. Chemical Engineering Science. 2005;60:2479-501.
[31] Wong SH, Ward MCL, Wharton CW. Micro T-mixer as a rapid mixing micromixer. Sensors and Actuators B: Chemical. 2004;100:359-79.
[32] Wan J, Fan A, Maruta K, Yao H, Liu W. Experimental and numerical investigation on combustion characteristics of premixed hydrogen/air flame in a micro-combustor with a bluff body. International Journal of Hydrogen Energy. 2012;37:19190-7.
[33] Yang W, Deng C, Zhou J, Liu J, Wang Y, Cen K. Experimental and numerical investigations of hydrogen–air premixed combustion in a converging–diverging micro tube. International Journal of Hydrogen Energy. 2014.
[34] Maruta K, Takeda K, Ahn J, Borer K, Sitzki L, Ronney PD, et al. Extinction Limits of Catalytic Combustion in Microchannels Proceedings of the Combustion Institute. 2002;29:957-63.
[35] Kikas T, Bardenshteyn I, Williamson C, Ejimofor C, Puri P, Fedorov AG. Hydrogen Production in a Reverse-Flow Autothermal Catalytic Microreactor: From Evidence of Performance Enhancement to Innovative Reactor Design. Industrial & Engineering Chemistry Research. 2003;42:6273-9.
[36] Li Y-H, Chen G-B, Wu F-H, Cheng T-S, Chao Y-C. Effects of catalyst segmentation with cavities on combustion enhancement of blended fuels in a micro channel. Combustion and Flame. 2012;159:1644-51.
[37] Hua J, Wu M, Kumar K. Numerical simulation of the combustion of hydrogen–air mixture in micro-scaled chambers Part II: CFD analysis for a micro-combustor. Chemical Engineering Science. 2005;60:3507-15.

[38] Kim KT, Lee DH, Kwon S. Effects of thermal and chemical surface–flame interaction on flame quenching. Combustion and Flame. 2006;146:19-28.
[39] Daou J, M.Matalon. Influence of Conductive Heat-Losses on the Propagation of Premixed Flames in Channels. Combustion and Flame. 2002;128:321-39.
[40] Saiki Y, Suzuki Y. Effect of wall surface reaction on a methane-air premixed flame in narrow channels with different wall materials. Proceedings of the Combustion Institute. 2013;34:3395-402.
[41] V.Shirsat, Gupta AK. A review of progress in heat recirculating meso-scale combustors. Applied Energy. 2011;88:4294-309.
[42] Miesse CM, Masel RI, Jensen CD, Shannon MA, Short M. Submillimeter-scale combustion. AIChE Journal. 2004;50:3206-14.
[43] Law CK. Combustion at a crossroads: Status and prospects. Proceedings of the Combustion Institute. 2007;31:1-29.
[44] Spadaccini CM, Zhang X, Cadou CP, Miki N, Waitz IA. Development of a Catalytic Silicon Micro-combustor for Hydrocarbon-fueled Power Mems. The Fifteenth IEEE International Conference on Micro Electro Mechanical Systems. Las Vegas USA2002.
[45] Ronney PD. Analysis of non-adiabatic heat-recirculating combustors. Combustion and Flame. 2003;135:421-39.
[46] Zamashchikov VV. Brief Communication Experimental Investigation of gas combustion regimes in narrow tubes. Combustion and Flame. 1997;108:357-9.
[47] Sitzki L, Borer K, Schuster E, Ronney PD, Wussow S. Combustion in Microscale Heat-Recirculating Burners. The Third Asia-Pacific Conference on Combustion. Seoul Korea2001.
[48] Bei-Jing Z, Jian-Hua W. Experimental study on premixed CH4/air mixture combustion in micro Swiss-roll combustors. Combustion and Flame. 2010;157:2222-9.
[49] Raimondeau S, Norton D, Vlachos DG, Masel RI. Modeling of high temperature microburners. Proceedings of the Combustion Institute. 2002;29:901-7.
[50] Chou SK, Yang WM, Chua KJ, Li J, Zhang KL. Development of micro power generators – A review. Applied Energy. 2011;88:1-16.
[51] Kim NI, Kato S, Kataoka T, Yokomori T, Maruyama S, Fujimori T, et al. Flame stabilization and emission of small Swiss-roll combustors as heaters. Combustion and Flame. 2005;141:229-40.

[52] Kim NI, Aizumi S, Yokomori T, Kato S, Fujimori T, Maruta K. Development and scale effects of small Swiss-roll combustors. Proceedings of the Combustion Institute. 2007;31:3243-50.
[53] Ju Y, Choi CW. An analysis of sub-limit flame dynamics using opposite propagating flames in mesoscale channels. Combustion and Flame. 2003;133:483-93.
[54] Maruta K, Kataoka T, Kim NI, Minaev S, Fursenko R. Characteristics of combustion in a narrow channel with a temperature gradient. Proceedings of the Combustion Institute. 2005;30:2429-36.
[55] Belmont EL, Schoegl I, Ellzey JL. Experimental and analytical investigation of lean premixed methane/air combustion in a mesoscale counter-flow reactor. Proceedings of the Combustion Institute. 2013;34:3361-7.
[56] Niket S.Kaisare, G.Vlachos D. Extending the region of stable homogeneous micro-combustion through forced unsteady operation. Proceedings of the Combustion Institute. 2007;31:3293-300.
[57] Yang WM, Chua KJ, Pan JF, Jiang DY, An H. Development of micro-thermophotovoltaic power generator with heat recuperation. Energy Conversion and Management. 2014;78:81-7.
[58] Yang W, Chou S, Chua K, An H, Karthikeyan K, Zhao X. An advanced micro modular combustor-radiator with heat recuperation for micro-TPV system application. Applied Energy. 2012;97:749-53.
[59] Akram M, Kumar S. Experimental studies on dynamics of methane–air premixed flame in meso-scale diverging channels. Combustion and Flame. 2011;158:915-24.
[60] Kim GT, Kim NI. Laminar burning velocity predictions by meso-scale flames in an annular diverging tube. Fuel. 2011;90:2217-23.
[61] Sahota GPS, Khandelwal B, Kumar S. Experimental investigations on a new active swirl based microcombustor for an integrated micro-reformer system. Energy Conversion and Management. 2011;52:3206-13.
[62] Deshpande AA, Kumar S. On the formation of spinning flames and combustion completeness for premixed fuel–air mixtures in stepped tube microcombustors. Applied Thermal Engineering. 2013;51:91-101.
[63] S.Kaisare N, G.Vlachos D. Optimal reactor dimensions for homogeneous combustion in small channels. Catalysis Today. 2007;120:96-106.
[64] Junwei L, Beijing Z. Experimental investigation on heat loss and combustion in methane/oxygen micro-tube combustor. Applied Thermal Engineering. 2008;28:707-16.

[65] J.Evans C, C.Kyritsis D. Operational regimes of rich methane and propane/oxygen flames in mesoscale non-adiabatic ducts. Proceedings of the Combustion Institute. 2009;32:3107-14.
[66] Yang WM, Chou SK, Shu C, Li ZW, Xue H. Combustion in micro cylindrical combustors with and without a backward facing step. Applied Thermal Engineering. 2002;2002:1777-87.
[67] Li J, Chou SK, Li ZW, Yang WM. Characterization of wall temperature and radiation power through cylindrical dump micro-combustors. Combustion and Flame. 2009;156:1587-93.
[68] Wenming Y, Siawkiang C, Chang S, Hong X, Zhiwang L. Effect of wall thickness of micro-combustor on the performance of micro-thermophotovoltaic power generators. Sensors and Actuators A: Physical. 2005;119:441-5.
[69] Li J, Chou SK, Li ZW, Yang WM. Experimental investigation of porous media combustion in a planar micro-combustor. Fuel. 2010;89:708-15.
[70] Chou SK, Yang WM, Li J, Li ZW. Porous media combustion for micro thermophotovoltaic system applications. Applied Energy. 2010;87:2862-7.
[71] Jiang LQ, Zhao DQ, Wang XH, Yang WB. Development of a self-thermal insulation miniature combustor. Energy Conversion and Management. 2009;50:1308-13.
[72] Fan A, Wan J, Liu Y, Pi B, Yao H, Liu W. Effect of bluff body shape on the blow-off limit of hydrogen/air flame in a planar micro-combustor. Applied Thermal Engineering. 2014;62:13-9.
[73] Mikami M, Maeda Y, Matsui K, Seo T, Yuliati L. Combustion of gaseous and liquid fuels in meso-scale tubes with wire mesh. Proceedings of the Combustion Institute. 2013;34:3387-94.
[74] Kamijo T, Suzuki Y, Kasagi N, Okamasa T. High-temperature micro catalytic combustor with Pd/nano-porous alumina. Proceedings of the Combustion Institute. 2009;32:3019-26.
[75] Zhang Y, Zhou J, Yang W, Liu M, Cen K. Effects of hydrogen addition on methane catalytic combustion in a microtube. International Journal of Hydrogen Energy. 2007;32:1286-93.
[76] Vlachos DG, Caratzoulas S. The roles of catalysis and reaction engineering in overcoming the energy and the environment crisis. Chemical Engineering Science. 2010;65:18-29.

[77] Li Y-H, Chen G-B, Hsu H-W, Chao Y-C. Enhancement of methane combustion in microchannels: Effects of catalyst segmentation and cavities. Chemical Engineering Journal. 2010;160:715-22.
[78] Federici JA, Norton DG, Brüggemann T, Voit KW, Wetzel ED, Vlachos DG. Catalytic microcombustors with integrated thermoelectric elements for portable power production. Journal of Power Sources. 2006;161:1469-78.
[79] Zhou J, Wang Y, Yang W, Liu J, Wang Z, Cen K. Combustion of hydrogen–air in catalytic micro-combustors made of different material. International Journal of Hydrogen Energy. 2009;34:3535-45.
[80] Wierzbicki TA, Lee IC, Gupta AK. Combustion of propane with Pt and Rh catalysts in a meso-scale heat recirculating combustor. Applied Energy. 2014;130:350-6.
[81] Scarpa A, Pirone R, Russo G, Vlachos DG. Effect of heat recirculation on the self-sustained catalytic combustion of propane/air mixtures in a quartz reactor. Combustion and Flame. 2009;156:947-53.
[82] Li Y-H, Chen G-B, Cheng T-S, Yeh Y-L, Chao Y-C. Combustion characteristics of a small-scale combustor with a percolated platinum emitter tube for thermophotovoltaics. Energy. 2013;61:150-7.
[83] Choi W, Kwon S, Dongshin H. Combustion characteristics of hydrogen–air premixed gas in a sub-millimeter scale catalytic combustor. International Journal of Hydrogen Energy. 2008;33:2400-8.
[84] Di Benedetto A, Di Sarli V, Russo G. A novel catalytic-homogenous micro-combustor. Catalysis Today. 2009;147:S156-S61.
[85] Vican J, Gajdeczko F, Dryer FL, Milius DL, Aksay A, Yetter RA. Development of a microreactor as a thermal source for microelectromechanical systems power generation Proceedings of the Combustion Institute. 2002;29:909-16.
[86] Smyth SA, Christensen KT, Kyritsis DC. Intermediate Reynolds number flat plate boundary layer flows over catalytic surfaces for “micro”-combustion applications. Proceedings of the Combustion Institute. 2009;32:3035-42.
[87] Watson GMG, Bergthorson JM. The effect of chemical energy release on heat transfer from flames in small channels. Combustion and Flame. 2012;159:1239-52.
[88] Park JH, Lee SI, Wu H, Kwon OC. Thermophotovoltaic power conversion from a heat-recirculating micro-emitter. International Journal of Heat and Mass Transfer. 2012;55:4878-85.

[89] Sirignano WA, Pham TK, Dunn-Rankin D. Miniature-Scale Liquid-Fuel-Film Combustor. Proceedings of the Combustion Institute. 2002;29:925-31.
[90] Vijayan V, Gupta AK. Thermal performance of a meso-scale liquid-fuel combustor. Applied Energy. 2011;88:2335-43.
[91] Kyritsis DC, Roychoudhury S, McEnally CS, Pfefferle LD, Gomez A. Mesoscale combustion: a first step towards liquid fueled batteries. Experimental Thermal and Fluid Science. 2004;28:763-70.
[92] Kyritsis DC, Guerrero-arias I, Roychoudhury S, Gomez A. Mesoscale Power Generation By A Catalytic Combustor Using Electrosprayed Liquid Hydrocarbons. Proceedings of the Combustion Institute. 2002;29:965-72.
[93] Kyritsis DC, Coriton B, Faure F, Roychoudhury S, Gomez A. Optimization of a catalytic combustor using electrosprayed liquid hydrocarbons for mesoscale power generation. Combustion and Flame. 2004;139:77-89.
[94] Li Y-H, Chao Y-C, Dunn-Rankin D. Combustion in a Meso-Scale Liquid-Fuel-Film Combustor with Central-Porous Fuel Inlet. Combustion Science and Technology. 2008;180:1900-19.
[95] Sadasivuni V, Agrawal AK. A novel meso-scale combustion system for operation with liquid fuels. Proceedings of the Combustion Institute. 2009;32:3155-62.
[96] Yuliati L, Seo T, Mikami M. Liquid-fuel combustion in a narrow tube using an electrospray technique. Combustion and Flame. 2012;159:462-4.
[97] Kurdyumov VN, Pizza G, Frouzakis CE, Mantzaras J. Dynamics of premixed flames in a narrow channel with a step-wise wall temperature. Combustion and Flame. 2009;156:2190-200.
[98] Lee KH, Kwon OC. A numerical study on structure of premixed methane–air microflames for micropower generation. Chemical Engineering Science. 2007;62:3710-9.
[99] Veeraragavan A, Cadou CP. Flame speed predictions in planar micro/mesoscale combustors with conjugate heat transfer. Combustion and Flame. 2011;158:2178-87.
[100] Nakamura H, Fan A, Minaev S, Sereshchenko E, Fursenko R, Tsuboi Y, et al. Bifurcations and negative propagation speeds of methane/air premixed flames with repetitive extinction and ignition in a heated microchannel. Combustion and Flame. 2012;159:1631-43.
[101] Chen M, Buckmaster J. Modelling of combustion and heat transfer in 'Swiss roll' micro-scale combustors. Combustion Theory and Modelling. 2004;8:701-20.

[102] Sánchez-Sanz M. Premixed flame extinction in narrow channels with and without heat recirculation. Combustion and Flame. 2012;159:3158-67.
[103] Ju Y, Xu B. Theoretical and experimental studies on mesoscale flame propagation and extinction. Proceedings of the Combustion Institute. 2005;30:2445-53.
[104] Norton DG, Vlachos DG. Combustion characteristics and flame stability at the microscale: a CFD study of premixed methane/air mixtures. Chemical Engineering Science. 2003;58:4871-82.
[105] Norton DG, Vlachos DG. A CFD study of propane/air microflame stability. Combustion and Flame. 2004;138:97-107.
[106] Li J, Chou SK, Yang WM, Li ZW. A numerical study on premixed micro-combustion of CH4–air mixture: Effects of combustor size, geometry and boundary conditions on flame temperature. Chemical Engineering Journal. 2009;150:213-22.
[107] Brambilla A, Frouzakis CE, Mantzaras J, Bombach R, Boulouchos K. Flame dynamics in lean premixed /air combustion in a mesoscale channel. Combustion and Flame. 2014;161:1268-81.
[108] Pizza G, Frouzakis CE, Mantzaras J, Tomboulides AG, Boulouchos K. Dynamics of premixed hydrogen/air flames in microchannels. Combustion and Flame. 2008;152:433-50.
[109] Jejurkar SY, Mishra DP. Numerical characterization of a premixed flame based annular microcombustor. International Journal of Hydrogen Energy. 2010;35:9755-66.
[110] Jejurkar SY, Mishra DP. Thermal performance characteristics of a microcombustor for heating and propulsion. Applied Thermal Engineering. 2011;31:521-7.
[111] Hua J, Wu M, Kumar K. Numerical simulation of the combustion of hydrogen–air mixture in micro-scaled chambers. Part I: Fundamental study. Chemical Engineering Science. 2005;60:3497-506.
[112] Stefanidis GD, Vlachos DG. Controlling Homogeneous Chemistry in Homogeneous−Heterogeneous Reactors: Application to Propane Combustion. Industrial & Engineering Chemistry Research. 2009;48:5962-8.
[113] Yan Y, Tang W, Zhang L, Pan W, Yang Z, Chen Y, et al. Numerical simulation of the effect of hydrogen addition fraction on catalytic micro-combustion characteristics of methane-air. International Journal of Hydrogen Energy. 2014;39:1864-73.

[114] Karagiannidis S, Mantzaras J, Jackson G, Boulouchos K. Hetero-/homogeneous combustion and stability maps in methane-fueled catalytic microreactors. Proceedings of the Combustion Institute. 2007;31:3309-17.
[115] Federici JA, Vlachos DG. A computational fluid dynamics study of propane/air microflame stability in a heat recirculation reactor. Combustion and Flame. 2008;153:258-69.
[116] Choi B-i, Han Y-s, Kim M-b, Hwang C-h, Oh CB. Experimental and numerical studies of mixing and flame stability in a micro-cyclone combustor. Chemical Engineering Science. 2009;64:5276-86.
[117] Mikami M, Maeda Y, Matsui K, Seo T, Yuliati L. Combustion of gaseous and liquid fuels in meso-scale tubes with wire mesh. Proceedings of the Combustion Institute. 2013;34:3387-94.
[118] ANSYS® Academic Research R. ANSYS® Academic Research, Release 14.0. In: Inc A, editor. Canonsburg,PA2012.
[119] Westbrook CK, Dryer FL. Simplified Reaction Mechanism for the Oxidation of Hydrocarbon Fuels in Flames. Combustion Science and Technology. 1981;27:31-43.
[120] Chakraborty S, Mukhopadhyay A, Sen S. Interaction of Lewis number and heat loss effects for a laminar premixed flame propagating in a channel. International Journal of Thermal Sciences. 2008;47:84-92.
[121] Kim NI. Effect of an inlet temperature disturbance on the propagation of methane–air premixed flames in small tubes. Combustion and Flame. 2009;156:1332-8.
[122] Bai B, Chen Z, Zhang H, Chen S. Flame propagation in a tube with wall quenching of radicals. Combustion and Flame. 2013;160:2810-9.
[123] Wan J, Fan A, Yao H, Liu W. Effect of thermal conductivity of solid wall on combustion efficiency of a micro-combustor with cavities. Energy Conversion and Management. 2015;96:605-12.
[124] Munir FA, N.Hatakeda, T.Seo, M.Mikami. Improvement of Combustion Stability in Narrow Tubes With Wire Mesh The 24th International Symposium on Transport Phenomena. Yamaguchi Japan2013.
[125] Mikami M, Maeda Y, Matsui K, Seo T, Yuliati L. Combustion of gaseous and liquid fuels in meso-scale tubes with wire mesh. Proceedings of the Combustion Institute2013. p. 3387-94.
[126] Automotive Handbook 7th Edition. Germany: Robert Bosg GmbH; 2007.

[127] Norton DG, Vlachos DG. Combustion characteristics and flame stability at the microscale: a CFD study of premixed methane/air mixtures. Chemical Engineering Science. 2003;58.
[128] Kutz M. Mechanical Engineers Handbook. USA: John Wiley & Sons; 1998.

ACKNOWLEDGEMENT

First and foremost, my gratitude goes to Allah S.W.T. the Creator. His mercy and love have made it possible for me to complete this doctoral course.

This work is dedicated to my family, parents, siblings and parents in-law who have been constantly giving support and prayers during my studies.

Sincere thanks to my academic supervisors, Professor Dr. Masato Mikami and Associate Professor Dr. Takehiko Seo, for the superb guidance and advice. Their profound knowledge and constructive suggestions on the experimental work and computational fluid dynamics simulation have helped me a lot throughout my period of study.

I am also indebted to all ESEL laboratory members especially to the micro combustor research group members for their continuous support. Deepest appreciation to the staff of International Student Support Section of Yamaguchi University for their assistance. Special thanks to Mr Takumi Kadota for his relentless assistance to my family on many official matters throughout our stay in Japan.

Last but not least, to all Malaysian students in Yamaguchi University who have been helping me and my family in many official and personal matters, thank you very much.

Finally, I would like to thank Universiti Teknikal Malaysia Melaka (UTeM) and the Malaysian Government for providing the scholarship for my doctoral study.